Terms and Conditions of Use of Digitised Theses from Trinity College Library Dublin

Copyright statement

All material supplied by Trinity College Library is protected by copyright (under the Copyright and Related Rights Act, 2000 as amended) and other relevant Intellectual Property Rights. By accessing and using a Digitised Thesis from Trinity College Library you acknowledge that all Intellectual Property Rights in any Works supplied are the sole and exclusive property of the copyright and/or other IPR holder. Specific copyright holders may not be explicitly identified. Use of materials from other sources within a thesis should not be construed as a claim over them.

A non-exclusive, non-transferable licence is hereby granted to those using or reproducing, in whole or in part, the material for valid purposes, providing the copyright owners are acknowledged using the normal conventions. Where specific permission to use material is required, this is identified and such permission must be sought from the copyright holder or agency cited.

Liability statement

By using a Digitised Thesis, I accept that Trinity College Dublin bears no legal responsibility for the accuracy, legality or comprehensiveness of materials contained within the thesis, and that Trinity College Dublin accepts no liability for indirect, consequential, or incidental, damages or losses arising from use of the thesis for whatever reason. Information located in a thesis may be subject to specific use constraints, details of which may not be explicitly described. It is the responsibility of potential and actual users to be aware of such constraints and to abide by them. By making use of material from a digitised thesis, you accept these copyright and disclaimer provisions. Where it is brought to the attention of Trinity College Library that there may be a breach of copyright or other restraint, it is the policy to withdraw or take down access to a thesis while the issue is being resolved.

Access Agreement

By using a Digitised Thesis from Trinity College Library you are bound by the following Terms & Conditions. Please read them carefully.

I have read and I understand the following statement: All material supplied via a Digitised Thesis from Trinity College Library is protected by copyright and other intellectual property rights, and duplication or sale of all or part of any of a thesis is not permitted, except that material may be duplicated by you for your research use or for educational purposes in electronic or print form providing the copyright owners are acknowledged using the normal conventions. You must obtain permission for any other use. Electronic or print copies may not be offered, whether for sale or otherwise to anyone. This copy has been supplied on the understanding that it is copyright material and that no quotation from the thesis may be published without proper acknowledgement.

Fibronectin-Binding Protein B Variation in *Staphylococcus aureus*

A thesis submitted for the degree of Doctor in Philosophy

by

Fiona Margaret Burke

Moyne Institute of Preventive Medicine
Department of Microbiology
Trinity College Dublin

December 2010

Declaration

I hereby declare that this thesis has not previously been submitted for a degree at this or any other university and that it is my own work except where it is duly acknowledged in the text.

I agree that this thesis may be lent or copied at the discretion of the Librarian, Trinity College Dublin.

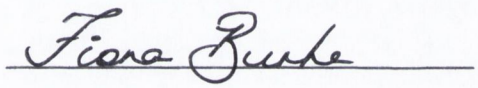

Fiona M. Burke

Acknowledgements

First and foremost I would like to thank my dedicated supervisor Prof. Tim Foster for giving me the privilege of joining his research team. For his guidance, encouragement and enthusiasm throughout my entire period in the Moyne I am forever indebted. Thanks also to the members of my thesis committee for their help and advice. I would like to thank Prof. Pietro Speziale from the University of Pavia and Dr. Ruth Massey from Bath University for their collaboration. Many thanks to all the members of the Massey lab for welcoming me to Bath so warmly. Thanks in particular to Dr. Andrew Edwards for his help, patience and good humour. For financial support during this project I thank both Trinity College Dublin and Science Foundation Ireland.

An enormous thank you to all the members of the TJF lab, "The Fosterettes" both past and present including; Dee, Judy, Fiona, Tony, Maghnus, Rebecca, Helen, Joan, Emma, Tara, Michelle, Marta, Ian, Niamh and Simon. Thank you all for the constant supply of help, moral support, giggles and cake! Special thanks to my conference buddy Emma and also to Joan for being such a marvelous friend and mentor. A big thank you too to all the members of The West Bunker Lab for adopting me so often! Thanks also to the Moyne's office staff, especially Jayne for all the help and friendly chitchat. I would also like to thank the members of the Moyne prep room for all the essential provisions. Thanks in particular to Stephen and Ronan who made me laugh every day.

A special word of thanks to my friends in the Moyne for the many great times we've shared. Thanks especially to Enda, Brian, Alex, Kelly and Fitzy for the madness, the craic and the laughter. A special thank you to my dear friend and comrade Dr. Colin Corcoran- for living this project with me through thick and thin and for all the wonderful memories, cheers buddy. I would also like to thank my other good friends for their encouragement and support. A special thank you to Jen and to Catriona for all the long walks and even longer talks!

Finally, I thank my nearest and dearest. A very special thank you to an old friend who became my best friend- my beloved Finian, thank you for everything. A heartfelt thank you to my sister Caoimhe and to my brother Tomás for their continuous support, understanding and friendship. Many thanks to Pepper for his energy and cheerful company throughout the writing of this thesis. Lastly and most importantly I thank the parents I am blessed with, Tom and Peg. For their unending belief, support and love I am eternally grateful.

Mam and Dad, I dedicate this thesis to you.

Summary

The surface-expressed fibronectin-binding proteins FnBPA and FnBPB of *Staphylococcus aureus* mediate attachment to immobilised fibronectin, fibrinogen and elastin. These proteins are encoded by two closely linked but separately transcribed genes, *fnbA* and *fnbB*. All *S. aureus* strains carry *fnbA* and the majority also carry *fnbB*. Seven different isotypes of FnBPA were previously identified based on divergence in the fibrinogen and elastin-binding N-terminal A domains. This variation creates differences in antigenicity while ligand binding functions are retained. Here, FnBPB variation was examined in both human and bovine isolates and compared to that of FnBPA.

Seven different *fnbB* allelic variants were identified in a genetically diverse collection of human *S. aureus* strains. Some strains that cluster by phylogenetic analysis contain different *fnbB* variants, whereas more divergent strains contain the same *fnb*B variant. This suggests that *fnbB* genes have been horizontally transferred between strains. The phylogeny of *fnbB* alleles does not match the phylogeny of *fnbA* alleles suggesting that *fnbA* and *fnbB* alleles have been inherited independently by horizontal transfer which most likely involved homologous recombination.

It was shown that some FnBPA and FnBPB isotypes that are specified by human *S. aureus* strains are also specified by bovine strains. This provides further evidence of horizontal transfer of *fnb* alleles and indicates that the lack of *fnbB* in the sequenced genome of the bovine strain RF122 is not a defining feature of bovine *S. aureus* isolates.

The seven *fnbB* allelic variants encode seven distinct isotypes of the N-terminal fibrinogen and elastin binding A domain of FnBPB. Variation is confined to the N2N3 subdomains which are 61 to 85 % identical in amino acid sequence. A 3D molecular model of the N2N3 subdomain of FnBPB was generated based on the known structure of ClfA. Like the A domain of ClfA (and FnBPA) it was predicted that the N2N3 subdomain of FnBPB represents the minimal ligand binding region which contains a ligand binding trench between the N2 and N3 subdomains and interacts with ligands by the dock, latch and lock mechanism. Using this model, variant FnBPB N2N3 residues were mapped to the surface of the protein while residues that are predicted to be involved in ligand-binding are highly conserved. Variable FnBPB residues are responsible for the antigenic diversity detected with polyclonal

antibodies and a monoclonal antibody raised against isotype I. It is proposed that antigenic variation in both FnBPA and FnBPB acts as mechanism of immune evasion.

Ligand binding by recombinant FnBPB N2N3 isotypes was compared by ELISA-based solid phase assays and surface plasmon resonance. Each isotype bound to immobilised fibrinogen, elastin and fibronectin dose-dependently and saturably with similar affinities. This confirms that like the A domains of ClfA and FnBPA, the N2N3 subdomain of FnBPB is sufficient for ligand-binding and that the N1 subdomain is not required. These results are consistent with the predicted location of variant residues on the surface of the protein and not in regions predicted to be involved in ligand binding. Binding of recombinant FnBPB N2N3 proteins to fibronectin was surprising because this region of FnBPB does not contain any known motifs that mediate binding to fibronectin. This raised the possibility that the A domain of FnBPB contains a novel fibronectin binding motif that binds fibronectin by a novel mechanism.

The mechanisms of fibrinogen and fibronectin-binding by the N2N3 subdomain of FnBPB were analysed and compared. A C-terminal truncate of rFnBPB N2N3 was constructed which lacked the latching peptide predicted to play an important role in ligand binding by dock, lock and latch. This protein was defective in binding to fibrinogen while its ability to bind fibronectin was retained. This suggests that different mechanisms are involved in the binding of the A domain of FnBPB to fibrinogen and fibronectin. A recombinant protein of FnBPB N2N3 was constructed containing substitutions in residues N312 and F314. These residues are predicted to line the ligand-binding trench between subdomains N2 and N3 and were found to be crucial for the interaction with both fibrinogen and fibronectin. This suggests that the predicted trench between subdomains N2 and N3 of FnBPB plays a key role in both the fibrinogen and fibronectin-binding mechanisms.

Expression of a chimeric protein containing the A domain of FnBPB and the cell wall anchoring domain of ClfA promoted bacterial adhesion to immobilised fibronectin. This is further evidence of a binding site for fibronectin in the A domain of FnBPB. Bacterial adhesion to fibronectin promoted by the A domain of FnBPB was weak and did not trigger the subsequent internalization of bacteria into human endothelial cells. While the precise biological consequences of fibronectin-binding by the A domain of FnBPB requires further investigation, these results have implications for the development of vaccines or immunotherapeutics that target FnBPB.

Publications

Provenza, G., Provenzano, M., Visai, L., Burke, F.M., Geoghegan, J., Stravalaci, M., Gobbi, M., Mazzini, G., Arciola, C.R., Foster, T.J., and Speziale, P. (2010) Functional analysis of a murine monoclonal antibody against the repetitive region of the fibronectin-binding adhesins fibronectin-binding protein A and fibronectin-binding protein B of *Staphylococcus aureus* *FEBS* , 227(21):4490-505

Burke, F.M., McCormack, N., Rindi, S., Speziale, P., and Foster, T.J. (2010). Fibronectin-binding protein B variation in *Staphylococcus aureus*. *BMC Microbiology*, 10:160.

Burke, F.M., Speziale, P. and Foster T.J. Molecular characteristaion of region A of fibronectin-binding protein B of *Staphylococcus aureus.* (Manuscript in preparation).

Contents

List of Tables

List of Figures

Key to abbreviations

Single letter amino acid code

A	Alanine
C	Cysteine
D	Aspartic acid
E	Glutamic acid
F	Phenylalanine
G	Glycine
H	Histidine
I	Isoleucine
K	Lysine
L	Leucine
M	Methionine
N	Asparagine
P	Proline
Q	Glutamine
R	Arginine
S	Serine
T	Threonine
V	Valine
W	Tryptophan
Y	Tyrosine

Nucleotides

A	Adenine
T	Thymine
C	Cytosine
G	Guanine

Key to abbreviations

aa	amino acid
bp	base pair(s)
BSA	bovine serum albumin
DNA	deoxyribonucleic acid
dNTP	deoxy nucleoside triphosphate
EDTA	ethylenediaminetetraacetic acid
ELISA	enzyme linked immunosorbent assay
Fg	fibrinogen
Fn	fibronectin
h	hour(s)
Ig	immunoglobulin
kb	kilobase pair
kDa	kilodalton
min	minute(s)
MSCRAMM	microbial surface component recognizing adhesive matrix molocules
OD	optical density
PBS	phosphate buffered saline
PCR	polymerase chain reaction
Phyre	Protein Homology/analogY Recognition Engine
PVDF	polyvinylidene fluoride
rpm	revolutions per minute
SDS	sodium dodecyl sulfate
SDS-PAGE	sodium dodecyl sulfate polyacrylamide gel electrophoresis
sec	second(s)
SPR	surface plasmon resonance

Key to abbreviations

Tris	trishydroxymethylaminomethane
TSA	trypticase soy agar
TSB	trypticase soy broth
v/v	volume per volume
w/v	weight per volume
wt	wild-type

Do mo thuismitheoirí

Chapter 1

Introduction

1.1 Biology of the staphylococci

1.1.1 Classification and identification

Bacteria of the genus *Staphylococcus* are non-motile, facultative aerobic, gram-positive cocci. Under the microscope they appear as grape-like clusters which result from cell division along multiple axes. Taxonomic studies have placed the staphylococci in the *Bacillus-Lactobacillus-Streptococcus* cluster of the *Micrococcaceae* (Ludwig *et al.*, 1985). Staphylococci are most closely related to *Enterococcus*, *Bacillus* and *Listeria*. Their genomes contain DNA of a low G + C content (30 – 40 %). The staphylococci are extremely halotolerant (growing at up to 3.5 M NaCl) and are resistant to desiccation.

There are at least 40 staphylococcal species comprising commensals and pathogens of both humans and animals, 9 of which also contain subdivisions with subspecies designations (Hauschild & Stepanovic, 2008). The main classification of staphylococci is based on the ability to produce coagulase, a zymogen that causes blood-clot formation. Only a few species are cogaulase-positive, namely *Staphylococcus aureus* and the animal pathogens, *S. intermedius*, *S. schleiferi subs. coagulans*, *S. delphini* and some strains of *S. hyicus*. Coagulase-negative staphylococci (CoNS) are considered to be less virulent. However some CoNS species, in particular *S. epidermidis*, *S. lugdunensis* and *S. haemolyticus* can cause serious human infections.

S. aureus is by far the most studied species of staphylococci due to its prevalence as a human and animal pathogen. It forms smooth, entire, raised colonies that contain a gold pigment. *S. aureus* is distinguished from other staphylococci by the ability to ferment mannitol and to express extracellular coagulase, thermostable DNase and clumping factor (the cell wall associated fibrinogen-binding protein, ClfA).

1.1.2 Colonisation and disease

The habitats of staphylococci are the skin, skin glands and mucous membranes of humans and warm-blooded animals. The primary ecological habitat of *S. aureus* in humans is the moist squamous epithelium of the anterior nares. Approximately 20% of the population are permanently colonised while the remainder are colonised intermittently (van Belkum *et al.*, 2009). It is unclear why some individuals are persistent carriers of *S. aureus* and others are not. Host factors may play a role in nasal colonization. Polymorphisms in genes encoding components of the host immune system have been associated with increased or decreased carriage (van Belkum *et al.*, 2007, Emonts *et al.*, 2008). For example, individuals with an interleukin 4 gene promoter polymorphism that is associated with lower IL-4 serum concentrations and reduced mucin have an increased rate of persistent carriage (Emonts *et al.*, 2008).

Staphylococcal infections are initiated when a breach of the skin or mucosal barrier allows bacteria access to adjoining tissues or the bloodstream. Colonisation has been identified as a risk factor for the development of *S. aureus* infections and individuals are usually infected by the isolate they carry (Wertheim *et al.*, 2004, von Eiff *et al.*, 2001). Whether an infection is contained or spreads depends on a complex interplay between *S. aureus* virulence determinants and host defense mechanisms. The most common types of *S. aureus* infection are superficial skin lesions such abscesses, boils and impetigo. If the organism gains access to the bloodstream (bacteraemia), it can cause a wide variety of invasive infections resulting in high morbidity and mortality. Such infections include those of bone (osteomyelitis), joints (septic arthritis), lungs (pneumonia) and heart valves (infective endocarditis) (Lowy, 1998). While many instances of nosocomial *S. aureus* bactereamia are attributable to an endogenous source (von Eiff *et al.*, 2001), it has been noted that bacteraemia-related death was significantly higher in infected non-carriers compared to infected carriers.

This suggests that carriers could be immunologically adapted to the strain of *S. aureus* that they carry (Wertheim *et al.*, 2004). Treatment of invasive *S. aureus* infections relies heavily on the use of antimicrobial agents to which the organism is increasingly developing resistance.

1.2 Genome structure of *Staphylococcus aureus*

S. aureus carries approximately 2600 genes in its chromosome. Its circular genome contains approximately 2.8 Mb AT-rich DNA (average G + C content of 33 %) (Kuroda *et al.*, 2001). The first whole genome sequence of a *S. aureus* strain was completed by random shot-gun sequencing in 2001. Since then the entire genomes of several *S. aureus* isolates have been published. Strains N315 and Mu50 are closely related, hospital-acquired methicillin-resistant *S. aureus* (MRSA) isolates from Japan (Kuroda *et al.*, 2001). The genome sequences of strain MW2 (a community-acquired (CA) MRSA isolate from the USA (Baba *et al.*, 2002) and the closely related, methicillin-sensitive *S. aureus* (MSSA) isolate MSSA476 (Holden *et al.*, 2004) have also been determined. The genome sequences of an early MRSA isolate (strain COL) has been published (Gill *et al.*, 2005) and the sequence of a related MSSA isolate (strain NCTC 8325) is in the public domain (http://www.genome.ou.edu/staph). Finally, the genome sequence of strain MRSA252, which is representative of the highly successful, epidemic EMRSA-16 clone, has also been determined (Holden *et al.*, 2004).

1.2.1 Core genome

DNA microarray analysis of diverse *S. aureus* isolates from different geographical locations indicates that approximately 75 % of the *S. aureus* genome comprises a core component of genes present in all strains (Fitzgerald *et al.*, 2001). This core genome contains genes involved in metabolism and other house-keeping functions, and also contains some genes not essential for growth, such as surface expressed proteins and exoenzymes (Lindsay & Holden, 2004). Subtle differences in the conserved

core genome have been exploited as a means of understanding the structure of the *S. aureus* population. Multilocus sequence typing (MLST) is the main method for analyzing the clonality of *S. aureus* isolates (Feil & Enright, 2004). Other methods for analyzing the population dynamics of *S. aureus* have been utilised. The "gold standard" for epidemiological analysis has been pulsed-field gel electrophoresis (PFGE) where genomic DNA is cleaved with endonucleases that recognize a small number of sites on the chromosome, yielding a distinct pattern of bands upon agarose gel electrophoresis (Trindade *et al.*, 2003). Amplified fragment length polymorphism (AFLP) is a PCR-based method that scans for polymorphisms in selected restriction sites and the nucleotides bordering these sites (Melles *et al.*, 2004). Other typing methods based upon the sequence of selected surface protein genes have been used in some studies (Shopsin *et al.*, 1999, Robinson & Enright, 2003).

1.2.1.1 MLST typing

Typing of *S. aureus* strains by MLST involves the accurate sequencing of DNA fragments (approximately 450 bp) of seven housekeeping genes: *arcC*, *aroE*, *glpF*, *gmk*, *pta*, *tpi* and *yqiL*. These slowly evolving metabolic genes were selected to represent the stable core genome. The sequences obtained are compared to known alleles at each locus (http://www.mlst.net). A single nucleotide change in a sequence is sufficient to define a new allele. The resulting seven-integer allelic profile defines a sequence type (ST) for each strain. Therefore, *S. aureus* strains that share the same ST share identical alleles at all seven MLST loci. Strains that differ at only one allele out of seven are known as single-locus variants (SLV), and this indicates a close genetic relatedness. Isolates can be grouped based on their MLST sequence types into clonal complexes to give an overall picture of the population structure of *S. aureus*. Clonal complexes are defined as groups of STs in which every ST shares at least five out of seven alleles with at least one other ST in the group (Robinson & Enright, 2004,

Feil *et al.*, 2003). Many studies have employed the use of Burst detection algorithms (Burst analysis) to identify the most likely ancestral strain (ST) within a clonal complex (CC). For example, Enright *et al.,* (2002) used BURST analysis to identify a large complex of related MSSA and MRSA clones, CC8. The ancestor of this group was predicted to be ST250. Significantly, almost all of the MRSA isolates from the 1960's were within CC8 and most of these were ST250 suggesting that methicillin resistance first arouse within *S. aureus* ST250 (Enright *et al.*, 2002).

1.2.1.2 Population structure of *S. aureus*

MLST analysis of a large strain collection (n = 334), obtained from the Oxfordshire area in the U.K. revealed that the population structure of *S. aureus* is highly clonal (Feil *et al.*, 2003). Grouping of isolates into clonal complexes based on their MLST genotype showed that 77 % of all tested isolates fall into eight major clonal complexes (Feil *et al.*, 2003). Phylogenetic analysis revealed that the different clonal complexes within this population show significant divergence from each other. Analysis of clonal diversification within individual clonal complexes suggests that alleles are at least 15-fold more likely to change by point mutation rather than by recombination (Feil *et al.*, 2003). This is in contrast to naturally transformable bacteria such as *Neisseria meningitidis* and *Streptococcus pneumonia* in which alleles change between 5- to 10-fold more frequently by recombination than by mutation (Feil & Spratt, 2001). Both *S. aureus* carriage and invasive isolates were evenly distributed among the clonal complexes suggesting there is no link between MLST genotype and the propensity to cause disease (Feil *et al.*, 2003).

The population structure of a large number of *S. aureus* strains (n = 993), isolated either from healthy carriers or from patients with invasive disease in the Netherlands was recently studied using AFLP analysis (Melles *et al.*, 2004). A clonal population structure was identified comprising five major AFLP clusters, which match the major clonal

complexes identified by MLST (Robinson & Enright, 2004, Feil *et al.*, 2003). This suggests that the same clonal clusters have spread successfully in both the U.K and the Netherlands, and probably worldwide. It was found that carriage strains fell into the same main clusters as isolates from invasive disease, and that MRSA strains from international sources grouped in these same clusters (Melles *et al.*, 2004). Some AFLP sub-clusters contained proportionately more invasive isolates than carriage isolates (Melles *et al.*, 2004). This confirms the suggestion that essentially any *S. aureus* strain has the capacity to cause invasive disease (Feil *et al.*, 2003) but strains from some clonal lineages are more virulent than others (Melles *et al.*, 2004). Invasive disease encompasses a very wide range of disease symptoms which is associated with the wide variety of virulence factors expressed by *S. aureus* (see section 1.3). It is suggested that closely related isolates of the same ST may differ in their content of virulence genes and therefore differ in their capacity to cause disease. The presence of seven virulence factors in the strain collection from the U.K., including surface proteins and exotoxins, was associated with invasive disease (Peacock *et al.*, 2000). Some virulence factors or antibiotic-resistance determinants may be carried on mobile accessory genetic elements. This is discussed in section 1.2.2.

The percentage identity of the core genomes of the hospital-acquired isolates N315 and Mu50 suggest that these isolates are closely related (Kuroda *et al.*, 2001). These strains share identical MLST genotypes (ST-5; Figure 1.1). The closely related community acquired strains MW2 and MSSA476 both belong to ST-1. This sequence type represented the ancestral strain of clonal complex 1 in the Oxfordshire study (Feil *et al.*, 2003). Strains NCTC 8325 and COL (both isolated from the same geographical location in the U.K.) belong to different, but closely related, sequence types (ST-8 and ST-250, respectively) (Lindsay & Holden, 2004) (Figure 1.1). Strain MRSA252 is the most divergent of the sequenced *S. aureus* strains (Holden *et al.*, 2004). This is reflected in its MLST profile (ST-36) which clearly separates this strain from the other sequenced isolates

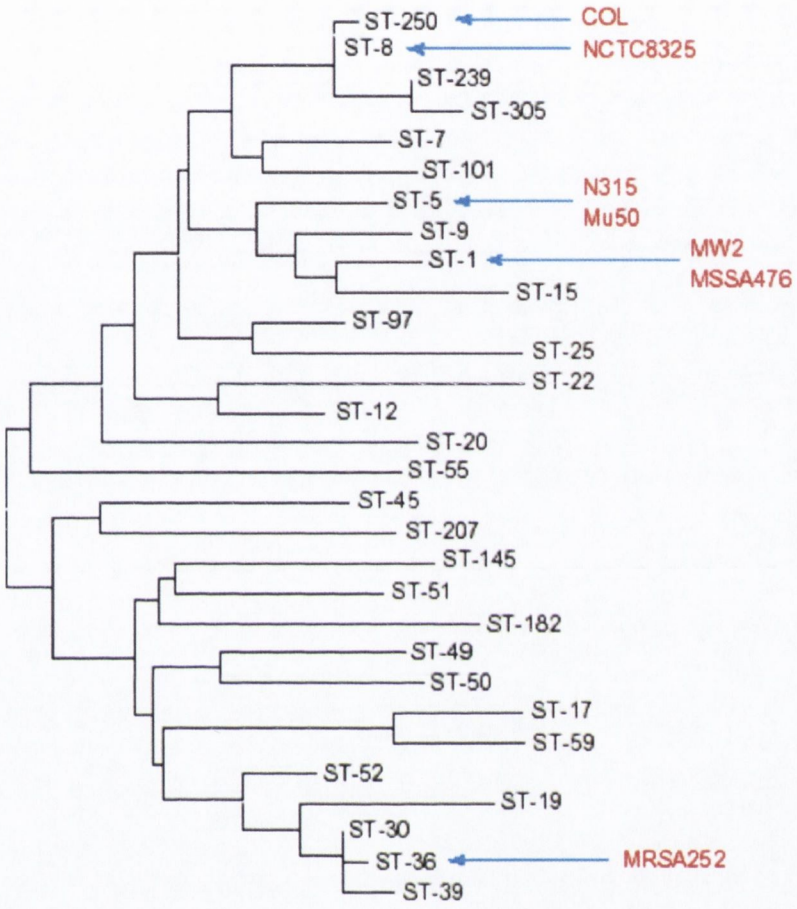

Figure 1.1 Phylogenetic relatedness of *S. aureus* MLST genotypes

A neighbour-joining tree of a representative sample of 30 sequence types (STs) from the *S. aureus* MLST database (http://www.mlst.net). The positions of the seven sequenced *S. aureus* strains are indicated. The sequences of each allele were concatenated to produce 3198-bp of sequence for each ST for construction of the neighbour joining tree.

Adapted from Lindsay and Holden, 2004.

based on phylogenetic analysis (Figure 1.1). This ST is well represented in the major CC30/39 clonal complex found in the U.K. (Feil *et al.*, 2003). The levels of relatedness inferred by MLST correlates well with the overall genomic divergence in the core genomes of the sequenced strains (Lindsay & Holden, 2004). This highlights the suitability of MLST as a means of understanding the evolution and population biology of *S. aureus*.

1.2.2 Accessory genomic elements

It is evident from the available genome sequences and DNA microarray analysis that up to 25 % of any *S. aureus* genome is comprised of dispensable genetic material (Lindsay & Holden, 2004, Fitzgerald *et al.*, 2001). This accessory genome consists mostly of mobile (or once mobile) genetic elements that can be transferred horizontally between different clonal lineages. These elements include bacteriophages, pathogenicity islands, chromosomal cassettes, genomic islands, plasmids and transposons, many of which carry genes associated with virulence or resistance (Holden *et al.*, 2004, Baba *et al.*, 2002). Many of the genes that encode secreted virulence factors, including superantigens, enterotoxins and leukocidins, are found on genomic islands, pathogenicity islands and prophages (Narita *et al.*, 2001, Gill *et al.*, 2005). Perhaps the most striking case of rapid evolution of virulent clones is the acquisition of the genes encoding the Panton-Valentine Leukocidon which is discussed below. Plasmids, transposons and chromosomal cassettes frequently contain genes encoding resistance to antimicrobials and heavy metals (Ito *et al.*, 2003). Selected mobile genetic elements that contribute to the success of *S. aureus* as a pathogen are discussed below.

1.2.2.1 Staphylococcal chromosomal cassette (SCC) *mec*

Acquisition of the staphylococcal chromosomal cassette (SCC) *mec* element in certain clonal lineages of *S. aureus* has resulted in the development of MRSA strains that are endemic in many hospitals in

developed countries and are emerging as invasive pathogens in the community. SCC*mec* elements are mobile genetic cassettes that integrate at the same site near the origin of the *S. aureus* chromosome (Ito *et al.*, 2001). They are defined by the presence of the *mecA* gene encoding a penicillin-binding-protein (PBP2') that has low affinity for methicillin and all other β-lactam antibiotics. PBP2' catalyzes the transpeptidation of cell-wall peptidoglycan in the presence of β-lactams. Strains carrying SCC*mec* (methicillin-resistant *S. aureus*: MRSA) are resistant to this major class of antibiotic (Hartman & Tomasz, 1984). Five classes of SCC*mec* have been characterised. SCC*mec* types I, II and III are large (34-66 kb) and principally found amongst hospital-acquired MRSA strains, whereas community-acquired strains typically contain smaller (20-28 kb) type IV or type V SCC*mec* elements (Katayama *et al.*, 2005, Ito *et al.*, 2004, Ito *et al.*, 2001, Baba *et al.*, 2002). Transposons and insertion sequences carrying resistance determinants (in addition to *mecA*) are often found inserted within SCC*mec* elements from hospital isolates (Kuroda *et al.*, 2001, Holden *et al.*, 2004), resulting in the emergence of strains that are resistant to most classes of antibiotic and, as a result, are more difficult to eradicate. The smaller type IV and type V SCC*mec* elements found in CA-MRSA contain *mecA* as the only resistance determinant (Ito *et al.*, 2004, Baba *et al.*, 2002).

MRSA strains were first identified in 1961, less than 2 years after the introduction of methicillin into clinical use to treat penicillinase-resistant strains (Jevons, 1961). SCC*mec* elements were probably acquired horizontally from coagulase-negative staphylococci such as *Staphylococcus haemolyticus* (Katayama *et al.*, 2001). Acquisition of SCC*mec* in *S. aureus* appears to occur infrequently, and it is proposed that distinct MRSA strains have emerged about 20 times by horizontally acquiring SCC*mec* elements (Robinson & Enright, 2004, Robinson & Enright, 2003). The ability to harbour SCC*mec* appears to be strain dependent, with MRSA strains belonging to five major clonal lineages (Robinson & Enright, 2003,

Katayama *et al.*, 2005). The reason why some strains are permissive for SCC*mec* and others are not is unclear.

While SCC*mec* does not encode any virulence factors *per se*, the expression of β-lactam resistance and other drug resistance determinants associated with SCC*mec* elements confers a survival advantage in rendering infections refractory to treatment with most classes of antimicrobials. Worryingly, isolates containing the enterococcal *vanA* gene are emerging that are fully-resistant to vancomycin (Cosgrove *et al.*, 2004), the last line of defense against multiply-resistant strains. The emergence of *S. aureus* strains that are resistant to all clinically relevant antimicrobials is a real threat.

1.2.2.2 Evolution of virulent clones

The *lukF-PV* and *lukS-PV* genes that encode the bicomponent Panton-Valentine leukocidan (PVL) are found on lysogenic phages in the chromosome of some *S. aureus* strains (Narita *et al.*, 2001, Baba *et al.*, 2002). Approximately 2 % of *S. aureus* strains (carriage and blood-culture isolates) contain the *lukF-PV* and *lukS-PV* genes (Prevost *et al.*, 1995b, Peacock *et al.*, 2002, Melles *et al.*, 2004). Isolates causing abscesses and septic arthritis were found to be significantly enriched (39 %) for *lukF-PV* and *lukS-PV* (Prevost *et al.*, 1995b, Peacock *et al.*, 2002, Melles *et al.*, 2004). PVL has a potent cytolytic activity on human leucocytes, and its expression is strongly associated with severe skin infections such as recurrent furunculosis (Prevost *et al.*, 1995). Recently, PVL-expressing CA-MRSA strains (represented by MW2) have emerged that cause severe necrotizing pneumonia and contagious severe skin infections in previously healthy individuals (Gillet *et al.*, 2002). Strain MW2 was chosen for genome sequencing as it was a highly virulent strain responsible for a community-acquired fatal case of septicaemia and septic arthritis (Baba *et al.*, 2002). MW2 contains a prophage (ΦSa2) encoding PVL that is absent from MSSA476 (Holden *et al.*, 2004, Baba *et al.*, 2002). It was concluded that the

high virulence of MW2 is at least partly due to PVL expression (Baba *et al.*, 2002). The prevalence of PVL-producing *S. aureus* strains in the community is increasing. This is likely due to horizontal transfer of phages carrying this toxin into naïve *S. aureus* MLST types that subsequently spread and cause disease. This is well illustrated by comparison of the genomes of MW2 and MSSA476. Both strains have ST-1 MLST genotypes, a major clone associated with community-acquired disease, and their core genomes are very similar (Lindsay & Holden, 2004, Holden *et al.*, 2004, Baba *et al.*, 2002). However, their differing prophage patterns means that the *lukF-PV* and *lukS-PV* genes are only present in MW2, conferring a heightened pathogenic potential for this strain. This demonstrates the significant role that bacteriophages (and other mobile genetic elements encoding virulence factors) can play in the very short term evolution of *S. aureus*.

In conclusion, the *S. aureus* genome consists of a stable core and accessory elements that are strain specific. The strains that were used for genome sequencing only reflect a fraction of the diversity within the species as a whole. Further sequencing of the genomes of strains from major lineages would likely identify the full range of accessory genes and elements within the species *S. aureus*, and may provide insights on the success of certain clonal lineages.

1.3 *S. aureus* virulence factors

The disease-causing potential of *S. aureus* reflects its ability to produce an arsenal of virulence factors. Adhesins are ligand-binding surface proteins that are attached covalently to the cell wall peptidoglycan and are coordinately expressed to promote binding to components of the host plasma and extracellular matrix (ECM). Expression of these proteins promotes *S. aureus* adhesion to damaged tissue, to the surfaces of host cells and to implanted medical devices. These adhesins have been termed MSCRAMMS (microbial surface components recognizing adhesive matrix molecules) and many have been shown to be critical in the initiation of

infection. Evasins are proteins that help the bacterium to evade the host's immune system. They may be associated with the bacterial cell wall or are secreted into the extracellular environment. Another group of virulence factors are the secreted enzymes, toxins, and proteases which are involved in the later stages of infection and facilitate tissue destruction and spreading. Many virulence factors have multiple functions and contribute to a number of pathogenic processes. Several animal models have been developed to study the function of *S. aureus* virulence factors *in vivo*. However, pathogenicity is a complex phenotype and in most *S. aureus* infections no single factor is responsible.

1.3.1 Cell wall-associated surface proteins

The cell wall is the point of contact between *S. aureus* and its surrounding environment. It acts as a physical barrier and provides a rigid exoskeleton which protects *S. aureus* from the external environment. It consists mainly of peptidoglycan (~ 60%), the remainder comprising wall teichoic acid (WTA), lipoteichoic acid (LTA) and small amounts of protein. *S. aureus* produces a diverse array of ligand-binding proteins on its cell surface that are covalently anchored to the cell wall peptidoglycan. These proteins are collectively known as MSCRAMMs and function in binding to components of the host's extracellular matrix.

MSCRAMMs have many features in common. An N-terminal signal sequence of about 40 amino acids target the proteins to the secretary (Sec) pathway. An 'AXA' motif at the end of the signal is recognised and cleaved by the membrane-anchored signal peptidase enzymes SpsA and SpsB during translocation across the cytoplasmic membrane (Mazmanian *et al.*, 2001, Cregg *et al.*, 1996). C-terminal sequences consist of a wall-spanning region, an LPXTG motif followed by a hydrophobic membrane-spanning domain and a positively charged cytoplasmic tail (Figure 1.2). LPXTG motifs facilitate targeted attachment to the cell wall where they subsequently

become covalently linked to the peptidoglycan layer in a process known as 'sorting'.

1.3.1.1 Sortase-mediated anchoring of cell wall-associated proteins

Covalent attachment of surface proteins to the cell wall petidoglycan is catalysed by the sortase enzymes (Mazmanian *et al.*, 2001). *S. aureus* has two sortase (Srt) enzymes, SrtA and SrtB (Pallen *et al.*, 2001, Mazmanian *et al.*, 2001). SrtA anchors the majority of *S. aureus* surface proteins and recognises the LPXTG motif. SrtB anchors the iron-regulated surface determinant C (IsdC) and recognises the C-terminal NPQTN motif of this protein (Mazmanian *et al.*, 2002). SrtA is a membrane-bound protein with a catalytic domain that is embedded in the petidoglycan layer (Mazmanian *et al.*, 2001). Recognition of LPXTG is highly stringent and amino acid substitutions are not tolerated at positions 1, 2, 4 or 5 (Kruger *et al.*, 2004). X-ray crystal structures of SrtA in complex with an LPETG peptide and NMR analysis of StrA in the presence or absence of ligand provided insight into the detailed action of sortase (Zong *et al.*, 2004, Liew *et al.*, 2004). Cleavage of the LPXTG motif by SrtA occurs between threonine and glycine residues. SrtA covalently attaches the cleaved protein via threonine to glycine in the pentaglycine of the nascent peptidoglycan subunits (Ton-That *et al.*, 2000). The C-terminal membrane-spanning domain and positively charged tail is then released and degraded. The petidoglycan precursor with the attached protein is then linked to the peptidoglycan by a transglycosylation reaction (Ton-That *et al.*, 1997, Navarre *et al.*, 1998) (Figure 1.3).

SrtA plays a crucial role in the correct anchoring of surface proteins, many of which are virulence factors. *S. aureus srtA* mutants, which fail to anchor correctly LPXTG-motif surface proteins, are attenuated in animal infection models of septic arthritis and endocarditis (Weiss *et al.*, 2004, Jonsson *et al.*, 2002).

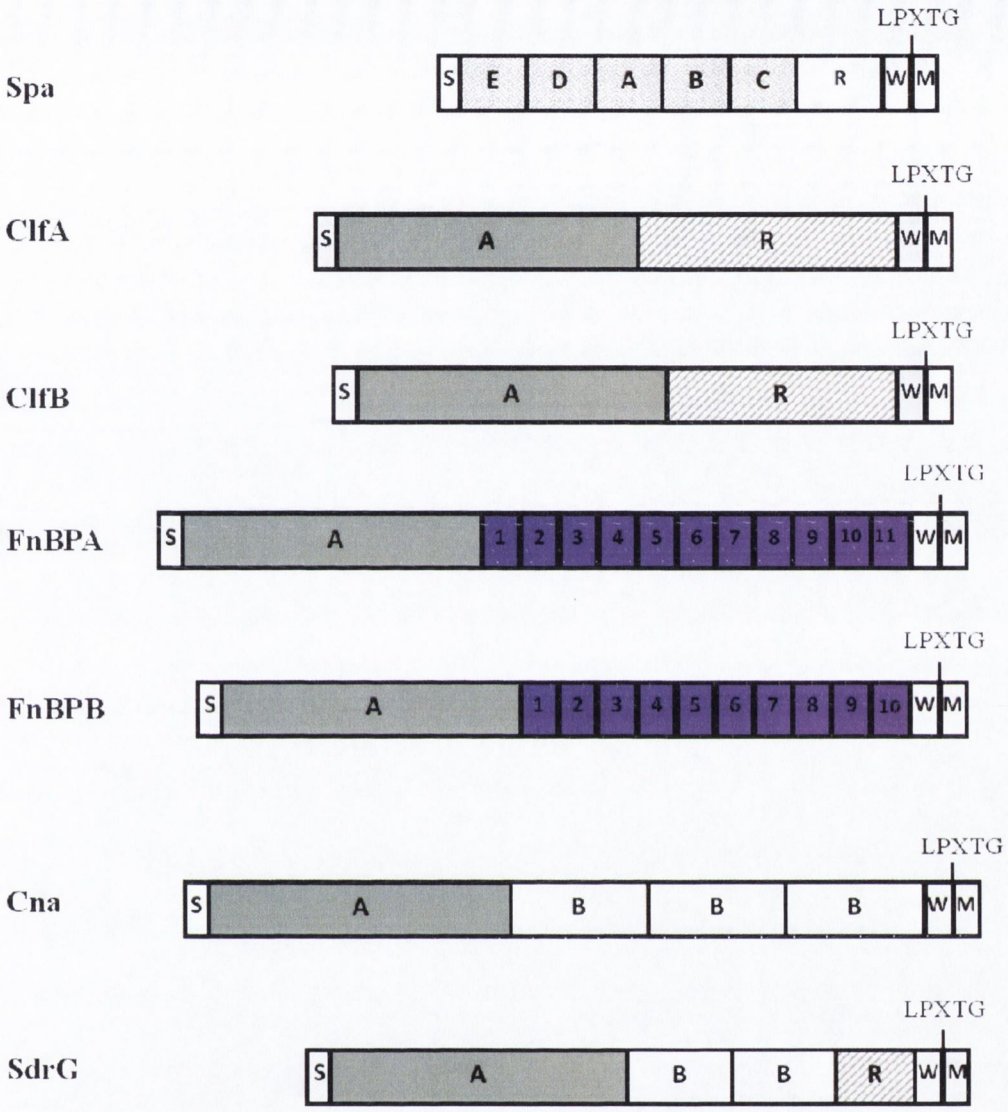

Figure 1.2 Comparative structural organisation of staphylococcal surface proteins

Schematic diagram of the structural organisation found in surface proteins from *S. aureus* (Spa, ClfA, ClfB, FnBPA, FnBPB and Cna) and *S. epidermidis* (SdrG). The signal sequence (S), and wall/membrane spanning regions (WM) are shown. Sortase A recognition motifs (LPXTG) are also indicated. Ligand binding and repeat regions A,B,C, D,E and R are shown. Fbronectin-binding repeats of FnBPA and FnBPB are shown in purple and are numbered.

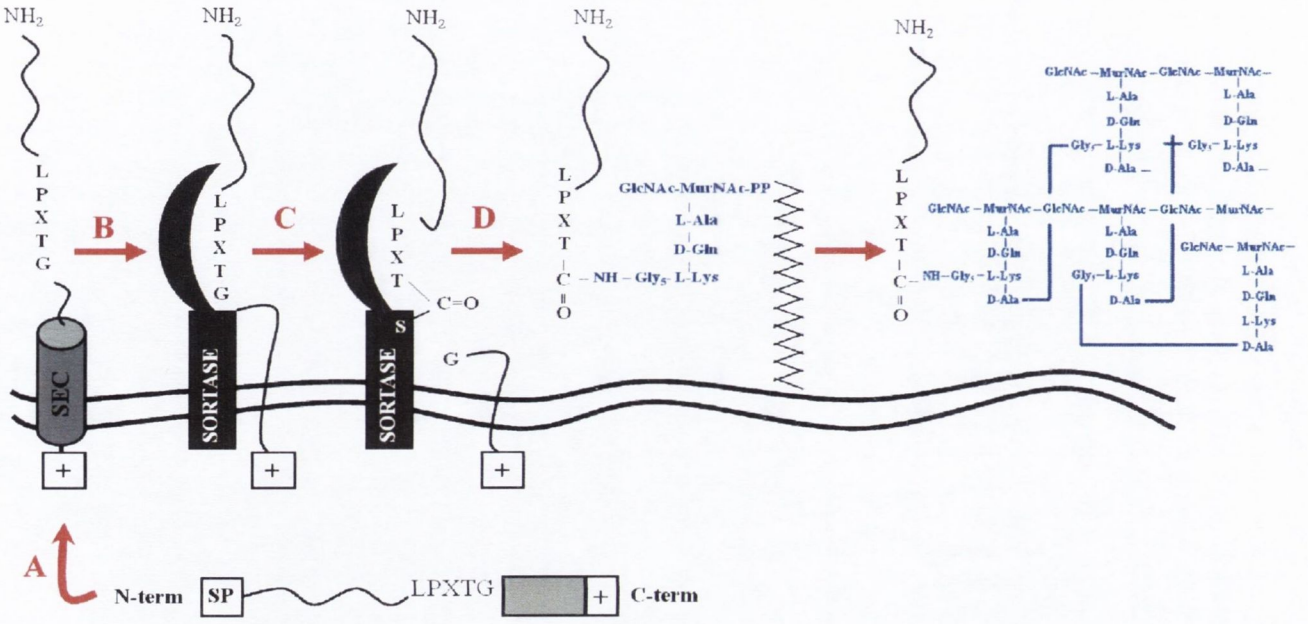

Figure 1.3 Surface protein anchoring in *S. aureus*

(A) Export. Precursor proteins with an N-terminal signal peptide (SP) are initiated into the secretory (Sec) pathway and the signal peptide is removed. (**B**) Retention. The C-terminal sorting signal retains polypeptides within the secretory pathway. (**C**) Cleavage. Sortase cleaves between the threonine and the glycine of the LPXTG motif, resulting in the formation of a thioester enzyme intermediate. (**D**) Linkage. Nucleophilic attack of the free amino group of lipid II by the thioester bond resolves the acyl-enzyme intermediate, synthesizing the amide bond between surface proteins and the pentaglycine cross-bridge and regenerating the active-site sulphydryl. (**E**) Cell wall incorporation. Lipid-linked surface protein is first incorporated into the cell wall via the transglycosylation reaction. The murein pentapeptide subunit with attached surface protein is then cross-linked to other cell wall peptides, generating the mature murein tetrapeptide.

1.3.1.2 Protein A

The first cell wall-associated surface protein of *S. aureus* to be characterised was staphylococcal protein A (Spa). It is expressed on the surface of over 95% of *S. aureus* strains (Forsgren & Nordstrom, 1974) and is a prime example of the multi-functionality shown by *S. aureus* surface proteins. Protein A was first noted for its ability to bind to the Fc region of mammalian IgG in a non-immune reaction (Uhlen *et al.*, 1984, Moks *et al.*, 1986). It was later discovered to bind to the variable region of the Fab heavy chain of V_H3 class antibodies (Hillson *et al.*, 1993). Other ligands for protein A include von Willebrand factor and tumor necrosis factor receptor-1 (TNFR-1) (Hartleib *et al.*, 2000, Gomez *et al.*, 2004). The *spa* gene is transcribed during the mid-exponential phase of growth but expression is repressed as cultures enter stationary phase (Vandenesch *et al.*, 1991).

Protein A is composed of four or five tandem repeats of 58-62 residues, designated E, D, A, B and C domains, followed by a short polymorphic repeat region of variable length (Xr) and a conserved region (Xc) (Uhlen *et al.*, 1984, Moks *et al.*, 1986) (Figure 1.2). Ligand-binding sites are found in each of the five repeat domains and residues important for ligand-binding are highly conserved between domains. Each domain comprises anti-parallel α-helices that pack together to form a compact helical bundle (Gouda *et al.*, 1992).

The crystal structure of domain B of protein A in complex with an Fc fragment has been solved (Deisenhofer, 1981). The Fc-γ binding site spans helices I and II on a single face of the molecule and comprises 11 residues. The binding sites for von Willebrand factor and TNFR-1 have been localised using site-directed mutagenesis and both recognize a region in helices I and II that overlaps the IGg Fc binding site in protein A (O'Seaghdha *et al.*, 2006, Gomez *et al.*, 2006). The crystal structure of the D domain of protein A in complex with a V_H3-Fab shows that it binds to a different face comprising residues in helices II and III (Graille *et al.*, 2000).

Spa residues that form contacts with Fab were confined to helices II and III and are distinct from the Fc-γ binding site.

Protein A has multiple functions in thwarting the host immune response (see Section 1.4.3) and is a virulence factor in murine infection models of subcutaneous infection, sepsis and septic arthritis and staphylococcal pneumonia (Patel *et al.*, 1987, Palmqvist *et al.*, 2005, Gomez *et al.*, 2004). Protein A also possesses immunosuppressive properties. The ability of protein A to bind to the Fab region on V_H3-class IgM on B cells (Sasso *et al.*, 1989, Sasano *et al.*, 1993) causes their activation, proliferation and subsequent apoptotic destruction (Goodyear & Silverman, 2003). A reduction in antibody-secreting cells from the spleen and bone marrow may account for the immunosuppressive activity of Spa (Goodyear & Silverman, 2004).

1.3.1.3 Fibrinogen-binding proteins

Fibrinogen is a blood glycoprotein of 340 kDa produced in the liver by hepatocytes. It is involved in plasma-clot formation through its polymerization to form fibrin and in platelet aggregation at sites of vascular damage. It is also one of the main proteins deposited on implanted prosthesis and medical devices. Fibrinogen is composed of two identical subunits, each of which is formed by an Aα, Bβ and γ polypeptide chains (Doolittle, 1984). These are assembled by their N-termini through a number of disulphide bonds to form a symmetrical dimeric structure. The fibrinogen molecule has four distinct domains, two identical terminal D regions, a central E region, two αC regions and two BβN regions (Figure 1.4). It has long been known that *S. aureus* cells form clumps when suspended in plasma (Much, 1908). It is now known that this reaction is mediated by fibrinogen (Hawiger *et al.*, 1983). Clumping in fibrinogen solution initially was thought to be mediated by cell-bound coagulase (Boden & Flock, 1989) but this has been shown not to be the case (McDevitt *et al.*, 1992).

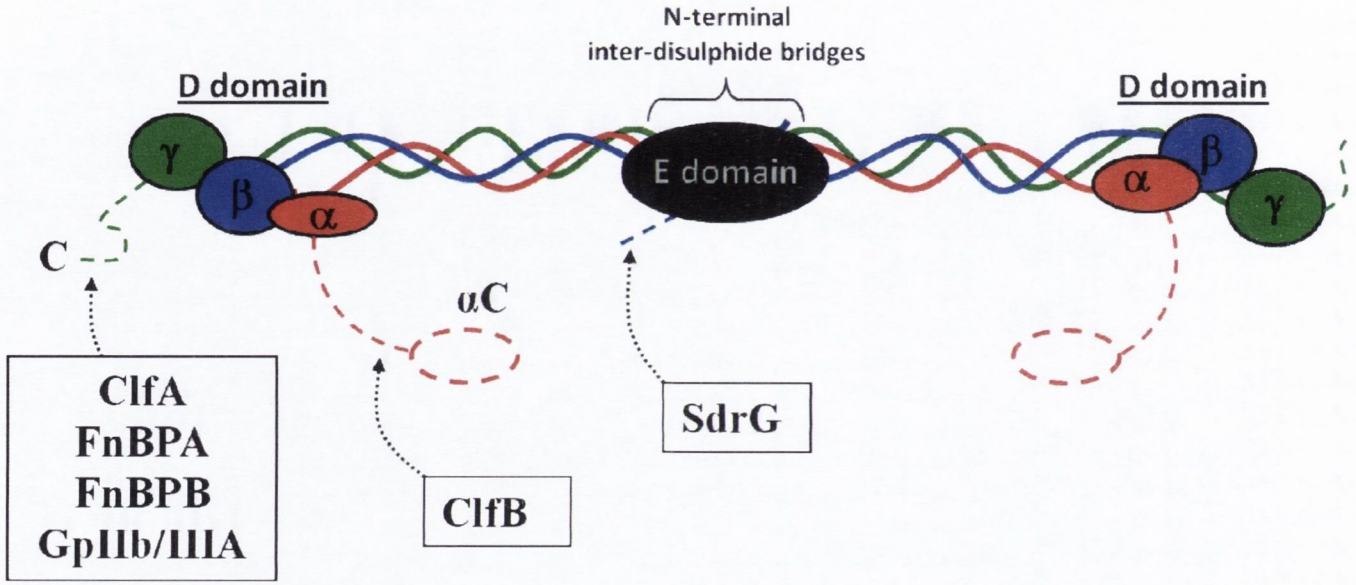

Figure 1.4 Structure of human fibrinogen.

Binding sites for *S. aureus* surface proteins, ClfA, FnBPA, FnBPB and ClfA and the *S. epidermidis* SdrG protein are indicated. The binding site in fibrinogen for ClfA, FnBPA and FnBPB is the same as the GPIIb/IIIa platelet integrin binding site required for platelet aggregation.

S. aureus expresses a collection of proteins that interact specifically with fibrinogen. Several of these are secreted proteins, Eap (Palma *et al.*, 1999) Efb (Palma *et al.*, 2001) and Emp (Hussain *et al.*, 2001). Five cell-surface proteins, ClfA, ClfB, FnBPA, FnBPB and IsdA promote *S. aureus* adhesion to fibrinogen. Closely related fibrinogen binding surface proteins are also found in *S. epidermidis* (SdrG) and *S. lugdunensis* (Fbl). Similarities in amino acid sequences, domains organization and modular design suggest that cell wall-anchored fibrinogen-binding proteins have a risen from a common ancestor. ClfA, FnBPA, FnBPB and Fbl bind to the γ-chain of fibrinogen (Wann *et al.*, 2000, Mitchell *et al.*, 2004, McDevitt *et al.*, 1997), ClfB binds to the α-chain (Walsh *et al.*, 2008) and SdrG binds in close proximity to the thrombin cleavage site of the fibrinogen Bβ-chain (Davis *et al.*, 2001) (Figure 1.4).

1.3.1.3.1 ClfA

Clumping factor A (ClfA) is one of the best characterised MSCRAMMs of *S. aureus*. It promotes the formation of cell aggregates in soluble fibrinogen (clumping) and the adherence of bacterial cells to fibrinogen-coated surfaces (McDevitt *et al.*, 1994). ClfA is expressed at high levels during the stationary phase of growth from a sigma factor B-dependent promoter (Nicholas *et al.*, 1999, Bischoff *et al.*, 2004). Weaker expression of ClfA occurs in the exponential growth phase and is dependent on transcription from a sigma factor 70-dependent promoter (Homerova *et al.*, 2004). The N-terminal 520 aa residue A domain of ClfA contains the fibrinogen binding site that is exposed on the cell surface. It is composed of three subunits, N1, N2 and N3 (Perkins *et al.*, 2001, McDevitt *et al.*, 1997). C-terminal to the A domain is a region consisting of serine-aspartate (SD) dipeptide repeats (McDevitt *et al.*, 1994) (Figure 1.2). The length of this repeat region is variable between different strains (McDevitt & Foster, 1995). The function of the SD repeats is to project the A domain away from the cell surface allowing interaction with fibrinogen (Hartford *et al.*, 1997).

Surface proteins with SD repeats are found in other staphylococci. Four others (ClfB, SdrC, SdrD, SdrE) are present in *S. aureus* and are described in subsequent sections.

The minimum fibrinogen-binding domain of ClfA comprises subdomains N2 and N3. Crystallisation of the N2N3 subdomain of ClfA in the apo-form allowed identification of a hydrophobic trench between N2 and N3 that forms the binding site for the extreme C-terminus of the γ-chain of fibrinogen (Deivanayagam *et al.*, 2002). Substitution of residues around this trench resulted in proteins with markedly reduced affinities for fibrinogen. Solution of subdomain N2N3 of ClfA in complex with the fibrinogen γ-chain peptide indicated that binding occurs by a variation of the dynamic "dock-lock-latch" mechanism (Ganesh *et al.*, 2008) (see Section 1.3.1.3.4). Recent studies have identified a second fibrinogen binding site in the N3 subdomain of ClfA. Amino-acid substitutions within the second binding site reduced fibrinogen-binding but did not affect binding to the γ-chain peptide. This provided evidence for a second binding site for ClfA in fibrinogen (Geoghegan, 2008). Fibrinogen binding by ClfA can be inhibited by millimolar concentrations of Ca^{2+} (O'Connell *et al.*, 1998). The function and structure of subdomain N1 of ClfA is not yet known. It is predicted to be composed mainly of β-sheets and may be organised into more than one subdomain (Deivanayagam *et al.*, 1999).

The ClfA binding site in the γ-chain of fibrinogen is the same as that recognised by the GPIIb/IIIa integrin on platelets which is required for platelet aggregation (Hettasch *et al.*, 1992, Farrell *et al.*, 1992). ClfA has been shown to stimulate platelet activation by forming a fibrinogen bridge between the bacterium and GPIIb/IIa. ClfA-specific immunoglobulin is also required to interact with the platelet immunoglobulin Fc receptor (FcγRIIa) for platelet activation to occur (Loughman *et al.*, 2005). ClfA can also activate platelets by a fibrinogen-independent mechanism that requires complement and specific anti-ClfA immunoglobulin (Loughman *et al.*,

2005). ClfA is anti-phagocytic and protects *S. aureus* from phagocytosis by murine macrophages and by human neutrophils *in vitro* (Palmqvist *et al.*, 2004, Higgins *et al.*, 2006). The anti-phagocytic properties of ClfA are partially dependent on fibrinogen-binding (Higgins *et al.*, 2006). The coating of bacteria with fibrinogen may impair deposition of or access to opsonins. However, bacteria expressing a mutant derivative of ClfA that lacks the ability to bind fibrinogen were still partially protected from opsonophagocytosis (Higgins *et al.*, 2006). Recent studies have indicated that this is due to the ability of ClfA to bind and activate complement control factor I resulting in enhanced degradation of opsonin C3b to iC3b (Hair *et al.*, 2010)

Several studies have reported a role for ClfA in infective endocarditis. *S. aureus clfA* mutants were less infective in endocarditis models than parental strains (Moreillon *et al.*, 1995). Function blocking antibodies to ClfA have been shown to sterilize vegetations on heart valves when administered with vancomycin in experimental endocarditis (Vernachio *et al.*, 2003). ClfA is also a virulence factor in murine models of septic arthritis (Palmqvist *et al.*, 2005, Josefsson *et al.*, 2001). Active immunization with recombinant ClfA or passive immunization with polyclonal anti-ClfA antibodies protected mice from arthritis and sepsis-induced death (Josefsson *et al.*, 2001). ClfA is one of the major factors involved in *S. aureus* adherence to ventricular assist devices (VADs), posing a threat to the survival of patients with congestive heart failure (Arrecubieta *et al.*, 2006). The protein is expressed by almost all *S. aureus* strains tested from healthy blood donors (98%) and in 100% of those with invasive disease (Peacock *et al.*, 2002). This makes ClfA an ideal target for the development of novel immuno prophylactic or therapeutic agents to combat *S. aureus* infections.

1.3.1.3.2 ClfB

Clumping factor B is another cell surface MSCRAMM responsible for the clumping of *S. aureus* cells when suspended in soluble fibrinogen and for adherence to immobilised fibrinogen *in vitro* (Ni Eidhin *et al.*, 1998). In contrast to ClfA which is expressed throughout the growth cycle, ClfB is expressed exclusively during the early exponential phase of growth and its contribution to fibrinogen binding is masked by ClfA (Ni Eidhin *et al.*, 1998, McAleese *et al.*, 2001). ClfB has a similar domain organization to ClfA (Figure 1.2). The N-terminal A domain of ClfB is subdivided into three independently folded subdomains N1, N2 and N3. In common with ClfA, the A domain of ClfB possesses fibrinogen-binding activity which can be inhibited by Ca^{2+} (Ni Eidhin *et al.*, 1998). Sequence alignment of the A domains of ClfA and ClfB shows only 26% amino acid identify. Unlike ClfA, the A domain of ClfB recognizes the α-chain of fibrinogen and can also bind to cytokeratin 10 and cytokeratin 8 (O'Brien *et al.*, 2002, Ni Eidhin *et al.*, 1998, Haim *et al.*, 2010). ClfB is capable of promoting platelet activation by a fibrinogen-dependent and also a complement-dependent mechanism that is similar to but slower than that that of ClfA (Miajlovic *et al.*, 2007).

The ClfB binding site in cytokeratin 10 has been localised to the tail region of cytokeratin 10 which is rich in glycine/serine repeats and is believed to form structures known as Ω loops (Walsh *et al.*, 2004). *Lactococcus lactis* expressing ClfB with amino acid substitutions in the putative ligand-binding trench between subdomains N2 and N3 was defective in adherence to both immobilised fibrinogen and cytokeratin 10. This suggests that both ligands bind to the same or overlapping site(s) in the ClfB trench by a similar mechanism (Walsh *et al.*, 2008).

Cytokeratin 10 is expressed on the surface of desquamated nasal epithelial cells and ClfB can promote adhesion to these cells *in vitro* (O'Brien *et al.*, 2002, Corrigan *et al.*, 2007). ClfB is impotant in nasal

colonization in rodents and humans (Wertheim *et al.*, 2008, Schaffer *et al.*, 2006). Studies using a murine model of nasal colonization demonstrated that immunization (both intranasally and systemically) with recombinant ClfB was protective (Schaffer *et al.*, 2006). In addition, systemic administration of a monoclonal antibody directed against ClfB that inhibited *S. aureus* binding to mouse cytokeratin 10 protected against colonization in naïve mice. The titres of anti-ClfB antibodies have been observed to be higher in non-carriers than in individuals who have *S. aureus* present in their nares (carriers) (Dryla *et al.*, 2005) suggesting that anti-ClfB antibodies may help protect against nasal colonization. ClfB may prove to be a suitable candidate antigen for vaccination against nasal colonization by *S. aureus* as the *clfB* gene was present in all strains examined (Peacock *et al.*, 2002).

1.3.1.3.3 SdrG

The *Staphylococcus epidermidis* surface protein SdrG is a member of the Sdr-Clf protein family characterised by a repeat region (R) made up of SD repeats (McCrea *et al.*, 2000, Hartford *et al.*, 2001). SdrG contains 2-4 B repeats (depending on the strain) in addition to the SD repeat region R (Figure 1.2). The N-terminal A domain of SdrG shares 24% and 23% homology with the A domains of ClfA and ClfB, respectively, and is also divided into subdomains N1, N2 and N3. The N2N3 subdomain is sufficient to promote binding to the Bβ-chain of fibrinogen at a site that overlaps the thrombin cleavage site on fibrinogen (Figure 1.4). SdrG thus prevents thrombin-mediated release of chemotactic fibrinopeptide B which reduces the influx of neutrophils to the site of infection (Davis *et al.*, 2001).

1.3.1.3.4 The dock, lock and latch mechanism for fibrinogen binding binding by surface proteins of staphylococci

The crystal structures of the apo-form of the ligand binding N2N3 subdomains of ClfA, ClfB and SdrG reveals that all three proteins adopt a similar structure (Figure 1.5) comprised of two similarly folded domains

that are a variation of the immunoglobulin (IgG) fold format termed the D E variant IgG (Dev-IgG) fold (Ponnuraj *et al.*, 2003, Deivanayagam *et al.*, 2002). The Dev-IgG fold consists of nine anti-paralleled β-sheets linked by flexible loops. The topology of the Dev-IgG is very similar to that of the C-type IgG fold, but displays variation between the D and E strands on one side (Deivanayagam *et al.*, 2002) (Figure 1.6)

Although the overall structure of the N2 and N3 subdomains of ClfA, ClfB and SdrG are very similar, the position of the C-terminus of the N3 subdomains (coloured pink in Figure 1.5) differs in the crystal structures. The crystal structure of the apo-form of ClfA N2N3 shows the C-terminal residues of N3 wound around the N3 subdomain (Figure 1.5). This may be an artefact of crystallisation since the crystal structures of ClfB and SdrG in the apo-form show the C-terminal residues extending into the solvent (Figure 1.5)

Solution of the crystal structure of the N2N3 domains of SdrG in complex with a synthetic fibrinogen peptide provided information on the structural changes that occur upon ligand binding (Ponnuraj *et al.*, 2003) (Figure 1.7A). The "dock-lock-latch" model was described for SdrG and has been proposed as a common mechanism for fibrinogen binding by staphylococcal surface-associated proteins. Docking of the fibrinogen peptide occurs in the hydrophobic trench that separates the N2 and N3 folded domains. Protein-protein interactions between residues in the trench and the ligand stabilise the docked peptide. Binding triggers structural rearrangements at the C-terminus of the N3 domain (β-strand G″), also known as the latching peptide. Upon ligand docking, the G″ strand undergoes a directional change and crosses over the binding trench. The peptide becomes locked in place by the β-sheet which covers the binding trench and is secured by hydrogen bonding that takes place between the bound fibrinogen peptide and β-strand G′/linker regions. The C-terminal β-strand G″ of the N3 domain then 'latches' in to the neighbouring N2

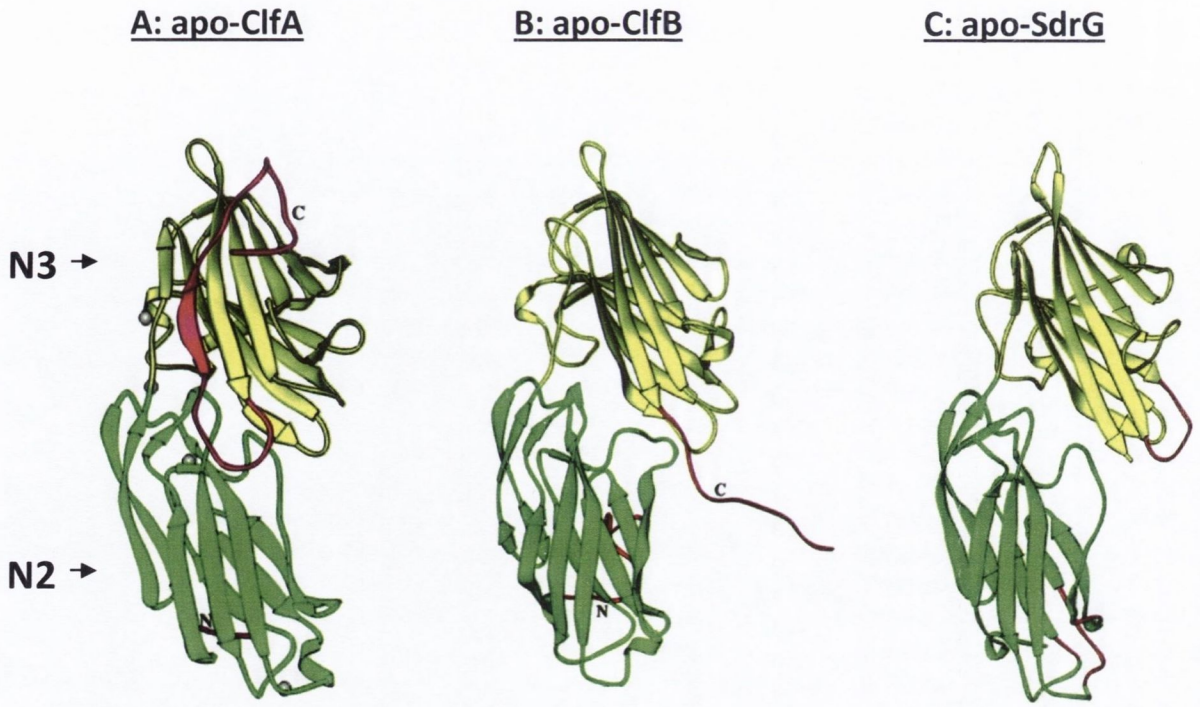

Figure 1.5 Apo structures of domains N2N3 of ClfA, ClfB and SdrG

Ribbon representations of the crystal structure of the apo-forms of ClfA (**A**), ClfB (**B**) and SdrG (**C**) N2N3 subdomains. Regions of poor resolution and the C-terminal extension of subdomains N3 are shown in red. Subdomains N2 (green) and N3 (yellow) are indicated.

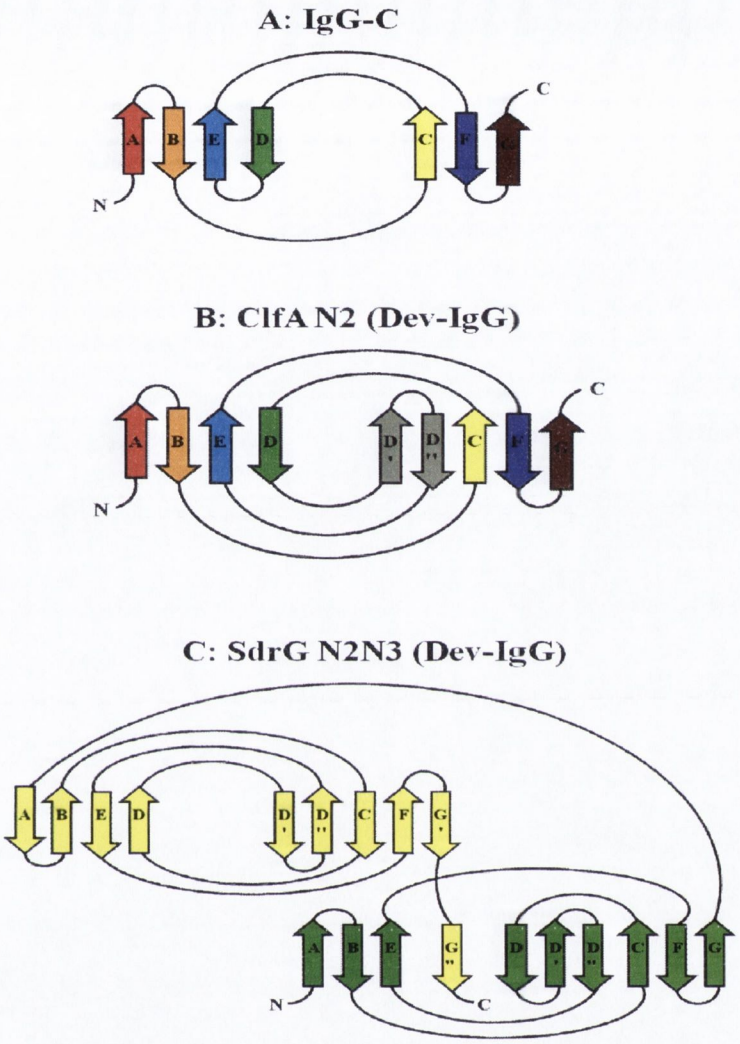

Figure 1.6 Topology of the Dev-IgG fold

(**A**) The immunoglobulinG-C fold.

(**B**) The Dev-IgG fold of the N2 subdomain of ClfA. This variation of the IgG fold contains additional β-strands D' and D" (coloured grey).

(**C**) The N2 and N3 subdomains of SdrG each comprise a Dev-IgG fold similar to that observed for ClfA. Upon ligand binding the latching peptide (G") of the N3 domain (yellow) inserts between strands E and D in the N2 domain (green). The β-strand complementation stabilises the SdrG-fibrinogen interaction. Nomenclature and colouration of the SdrG β-sheets matches that of the SdrG peptide complex in Figure I.7. Modified from Deivanayagam *et al.*, 2002 and Ponnuraj *et al.*, 2003.

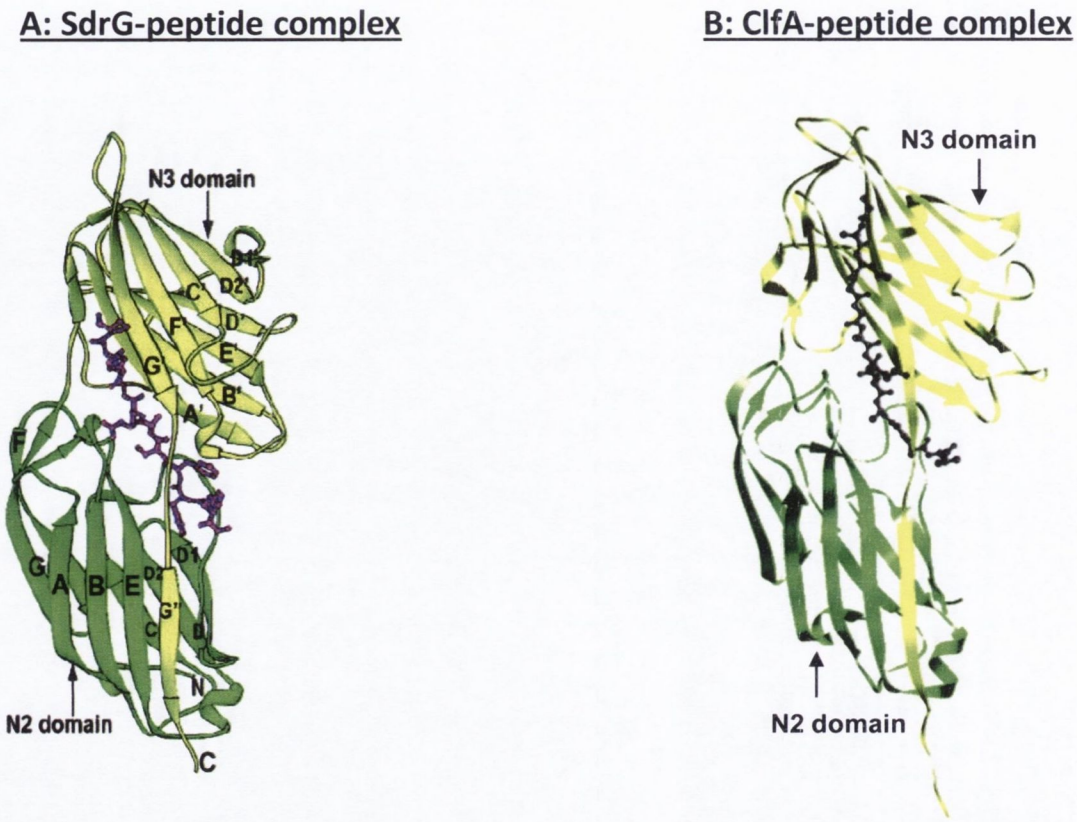

Figure 1.7 Structures of N2N3 subdomains of SdrG and ClfA in complex with fibrinogen peptides
Fibrinogen β-chain (purple) in complex with SdrG (**A**) is shown in ball and stick form. SdrG-peptide complex is taken from Ponnuraj *et al.*, 2003. Fibrinogen γ-chain (black) in complex with ClfA (**B**) is shown in ball and stick form. ClfA-peptide complex is adapted from Vannakambadi *et al.*, 2008.

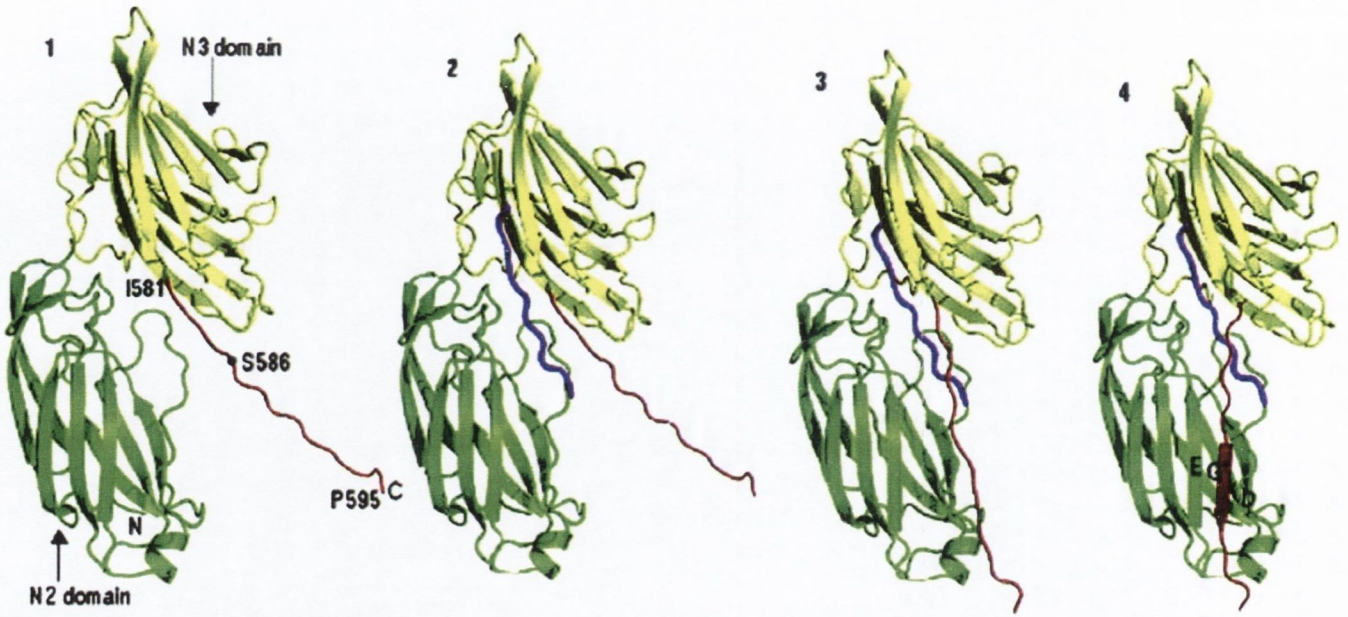

Figure 1.8 The dock, lock and latch ligand-binding mechanism

The N2 subdomain is represented in green, N3 in yellow. The flexible N3 extension is represented by a red line. Apo-SdrG N2N3 (**1**) is in an open conformation. The peptide (represented as a purple line) docks in the trench located between N2 and N3 (**2**). Peptide docking re-directs the N3 extension (**3**). The C-terminal extension crosses over the binding trench and inserts into the N2 subdomain complementing a β-sheet (**4**). Taken from Bowden *et al.*, 2008.

domain, where it inserts between strands E and D (the latching cleft) creating a new β-sheet in the N2 domain. This β-strand complementation stabilizes the overall structure (Ponnuraj *et al.*, 2003) (Figure 1.8). A conserved motif (TYTFTDYVD) at the back of the latching cleft in SdrG, ClfA and ClfB is likely to be involved in binding of the latching peptide to the latching cleft in domain N2 (Ponnuraj *et al.*, 2003).

The importance of the locking and latching steps has been demonstrated experimentally for SdrG. A constrained open form of the protein, where the C-terminal extension is held at the top of the N3 subdomain by a disulphide bond, was unable to bind β-peptide or fibrinogen. The ability of the C-terminal extension to move freely is essential and interfering with its flexibility by substituting residues with prolines prevented movement of the C-terminal strand and abolished β-chain binding (Bowden *et al.*, 2008). Similarly a truncated recombinant SdrG protein lacking the C-terminal extension (latching peptide) was unable to bind (Ponnuraj *et al.*, 2003). A constrained closed form of SdrG where the C-terminus of the N3 subdomain was held at the base of the latching trough by a disulphide bond was unable to bind peptide or fibrinogen because the peptide was unable to penetrate the locked structure (Bowden *et al.*, 2008).

The crystal structure of ClfA N2N3 in complex with the fibrinogen γ-chain peptide (Figure 1.7B) revealed that ClfA binds to the γ-chain by a variation of the dock, lock and latch mechanism (Ganesh *et al.*, 2008). In contrast to SdrG, a closed form of ClfA bound to peptide and fibrinogen. An open form of ClfA is not required because the fibrinogen γ-chain peptide was able to penetrate the closed form of ClfA. Moreover, the closed form of ClfA had increased affinity for the γ-chain peptide compared to the apo-form. Another difference was the direction of the bound peptide; in SdrG the peptide formed an anti-parallel β-sheet with the C-terminal extension of

subdomain N3 while in ClfA the bound peptide formed a parallel β-sheet (Ganesh *et al.*, 2008).

1.3.1.4 Collagen-binding protein

Collagen is a major structural protein of mammals that provides tensile strength to connective tissue such as bone, cartilage and tendon, and to the fibrous matrices of skin and blood vessels. The *S. aureus* collagen-binding protein (Cna) promotes adhesion to collagen substrates and to collagenous tissues (Patti *et al.*, 1992). Expression of the *cna* gene occurs maximally during the exponential phase of growth and is repressed to almost undetectable levels during stationary phase (Gillaspy *et al.*, 1997).

Cna possesses a similar domain organization to that of other *S. aureus* surface proteins (Figure 1.2). The N-terminal A domain contains the collagen-binding activity and is followed by region B which is a tandem array of a 187 residue domain that is repeated one to four times depending on the strain. Region B acts as a stalk to project the A domain from the cell surface (Gillaspy *et al.*, 1998). Based on amino-acid similarity to ClfA, ClfB and SdrG, the A domain of Cna was predicted to comprise three independently folded subdomains, N1, N2 and N3 (Zong *et al.*, 2005). Unlike ClfA, ClfB and SdrG, the high affinity ligand-binding site in Cna is represented by the N1 and N2 subdomains. The crystal structure of Cna N1N2 was solved and the N1 and N2 subdomains were found to each adopt a Dev-IgG fold with a surface trench in one of the β-sheets providing the binding site for the collagen triple helix (Symersky *et al.*, 1997, Deivanayagam *et al.*, 1999). A multi-step 'collagen hug' mechanism for collagen binding by Cna has been proposed (Zong *et al.*, 2005). The collagen triple helix initially interacts with a binding trench on the N2 subdomain. This is a low affinity interaction stabilised by polar and hydrophobic interactions (Symersky *et al.*, 1997). The N1 subdomain then 'hugs' the collagen ligand by folding over it and forming multiple

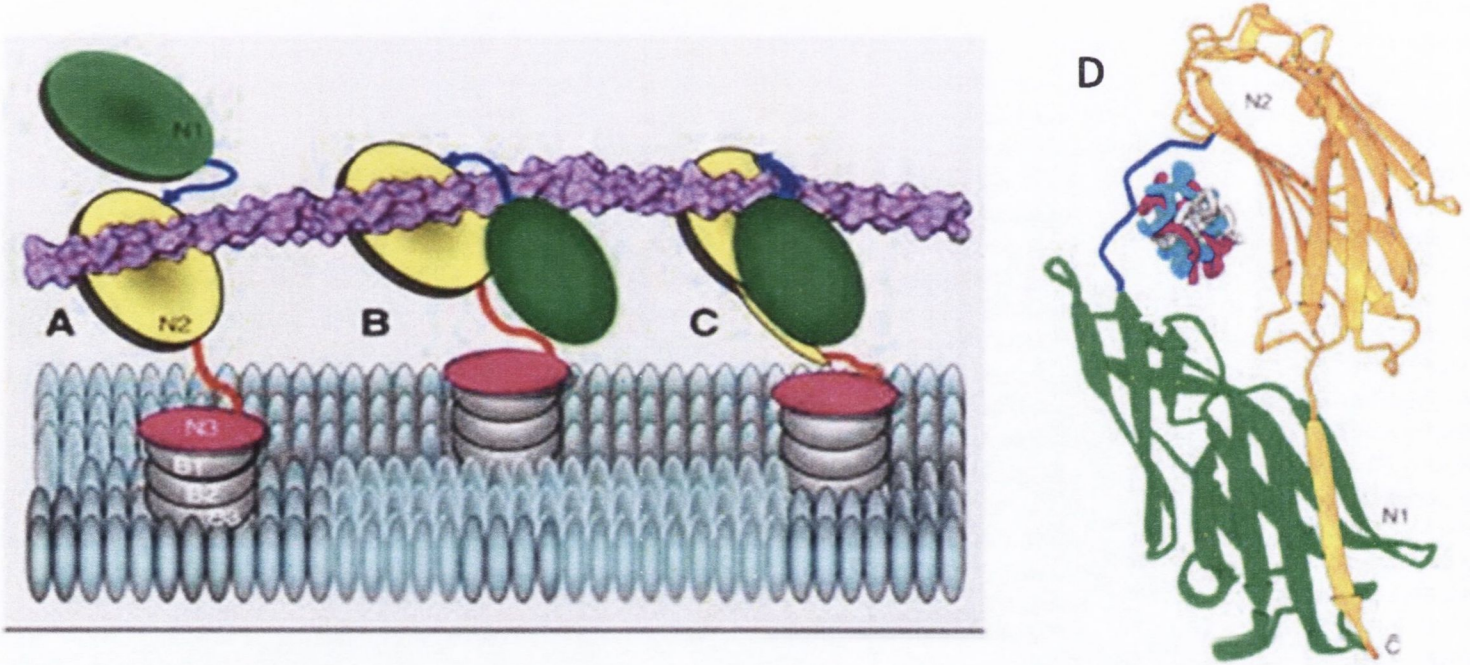

Figure 1.9 The 'Collagen Hug' model

The collagen triple helix initially associates with a trench in the N2 subdomain (**A**) and is then wrapped by the N1-N2 linker and the N1 subdomain (**B**). The N1 subdomain interacts with the N2 subdomain via multiple hydrophobic interactions and finally the C-terminal latch is introduced in the N1 subdomain to secure the ligand in place (**C**).

D. Crystal structure of the collagen peptide in complex with Cna. Taken from Zong *et al.*, 2005.

hydrophobic contacts with the N2 subdomain resulting in a tunnel-like structure that locks the collagen ligand between the two subdomains. The C-terminal extension of subdomain N2 (the latching strand) then reorients itself and inserts into the latching trench on the N1 subdomain by β-strand complementation (Figure 1.9). This event is expected to stabilise the structure (Zong *et al.*, 2005).

The collagen hug model and the dock, lock and latch mechanisms of ligand-binding have several similarities. In both cases, the ligand binding region is situated in between two subdomains containing a Dev-IgG fold; N2 and N3 in SdrG and N1 and N2 in Cna. The ligand-MSCRAMM complex is stabilised by insertion of the extension of the second subdomain into a latching trench in the first subdomain in an inter-domain β-strand complementation. Also, the latching peptide is conserved between MSCRAMMs that are proposed to bind their ligands by dock, lock, latch (SdrG, ClfA, ClfB, FnBPA, FnBPB) and Cna which binds by the collagen hug mechanism.

Cna is a virulence factor in animal models of osteomyelitis, endocarditis and septic arthritis (Patti *et al.*, 1994, Hienz *et al.*, 1996, Elasri *et al.*, 2002). Both active and passive immunisation of mice with a recombinant fragment of Cna and anti-Cna antibodies, respectively, was shown to provide protection against *S. aureus*-mediated septic death (Nilsson *et al.*, 1998). However, the *cna* gene is only present in approximately 30 to 50 % of *S. aureus* isolates (Smeltzer *et al.*, 1997, Peacock *et al.*, 2002, Arciola *et al.*, 2005) and so would not be an ideal vaccine candidate.

1.3.1.5 Fibronectin-binding surface proteins

Fibronectin is a ubiquitous, multi-functional protein, widely dispersed in the body being present on the surface of cells, in the ECM and in all body fluids. There is only one copy of the human fibronectin gene and

targeted inactivation of this gene leads to early embryonic death as a result of defects in fundamental tissue structures such as the mesoderm and neural tube (George *et al.*, 1993). Following the cloning of the gene encoding fibronectin, it was immediately recognised that several splice variants could be generated (Schwarzbauer *et al.*, 1983). At least twenty splice variants are now known of this single fibronectin-encoding gene (ffrench-Constant, 1995). There are two major forms of fibronectin, soluble plasma fibronectin and insoluble cellular fibronectin. Plasma fibronectin is a product of hepatocytes and is found in blood, saliva and other body fluids where it has vital roles in blood-clot formation and wound healing (Midwood *et al.*, 2006, Cho & Mosher, 2006). Cellular fibronectin is secreted by a range of cells including fibroblasts and becomes incorporated at the surface of cells into a fibrillar type matrix (Wierzbicka-Patynowski & Schwarzbauer, 2003, Norton & Hynes, 1990, Mao & Schwarzbauer, 2005).

As a consequence of variation in splicing, fibronectin proteins can come in many molecular guises, including both dimeric and single chain forms (Pankov & Yamada, 2002). In its major forms, fibronectin is a homodimer composed of two splice variant protein chains of between 230 and 270 kDa, linked by disulphide bonds near their C-termini. Each monomer is composed of three distinct types of repeating homologous modules designated type I (F1), type II (F2) and type III (F3) which are separated by connected sequences (Bork *et al.*, 1996) (Figure 1.10). Splicing variation modifies the number of F3 repeats with a minimum of 15 and maximum of 18 in the major plasma and cellular forms. In addition to its functions in cellular adhesion, differentiation and tissue repair after injury, fibronectin also has the capacity to act as a receptor for a variety of molecules including heparin, collagen, fibrin and specific integrins (Potts & Campbell, 1994).

The ability to bind to immobilised fibronectin is a characteristic feature of many *S. aureus* strains (Peacock *et al.*, 2000). Adhesion of *S.*

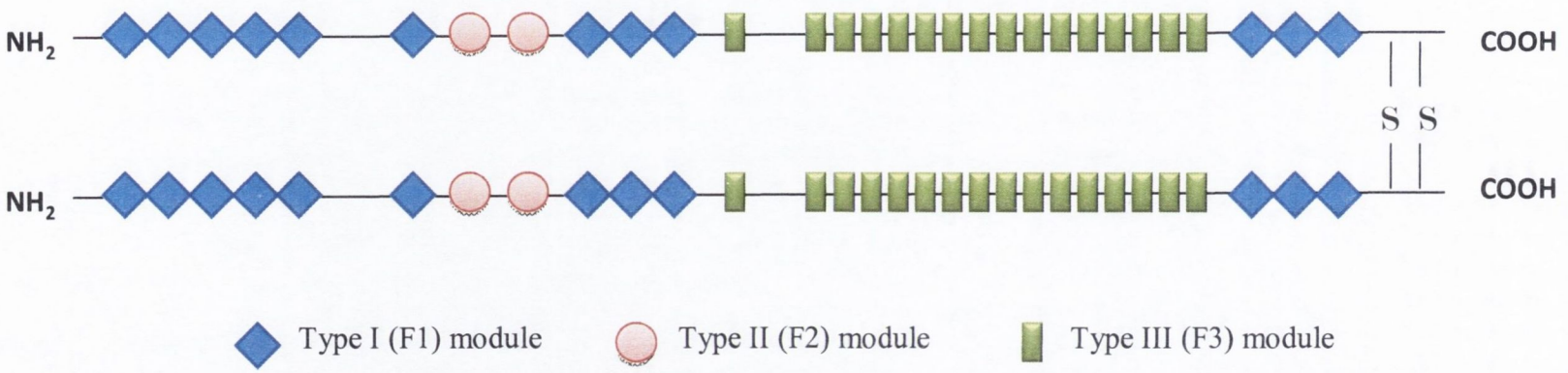

Figure 1.10 Structure of human fibronectin

Schematic diagram of human fibronectin. Fibronectin monomers are linked at their C-termini by a disulphide bond to produce the mature dimer of approximately 500 kDa found in plasma. Each monomer is composed of three different types of proteins modules, F1 (blue), F2 (pink) and F3 (green).

aureus to fibronectin-coated surfaces is mediated by the fibronectin-binding proteins, FnBPA and FnBPB.

1.3.1.5.1 FnBPA and FnBPB

The expression of either FnBPA or FnBPB on the surface of *S. aureus* is sufficient to promote bacterial adhesion to immobilised fibronectin (Greene *et al.*, 1995). The multifunctionality in ligand-binding demonstrated by *S. aureus* MSCRAMMs such as protein A, ClfA and ClfB is also apparent with FnBPA and FnBPB. In addition to binding fibronectin, these proteins also promote adhesion to immobilised fibrinogen and elastin (Wann *et al.*, 2000, Roche *et al.*, 2004). Each FnBP protein also promotes the accumulation of biofilm by MRSA strains growing in glucose-containing media (O'Neill *et al.*, 2008) (see Section 1.4.5).

FnBPA and FnBPB are related cell-wall associated proteins encoded by two closely linked but independently transcribed genes *fnbA* and *fnbB*, respectively, and are expressed predominately in the exponential phase of growth (Signas *et al.*, 1989, Saravia-Otten *et al.*, 1997, Jonsson *et al.*, 1991). FnBPA and FnBPB have considerable organizational and sequence similarity and are composed of a number of distinct domains. Both proteins contain a secretary signal sequence at the N-terminus and a C-terminal LPETG motif required for sortase-mediated anchoring of the proteins to the cell wall peptidoglycan. The N-terminal A domains of FnBPA and FnBPB are exposed on the cell surface and promote binding to fibrinogen and elastin. Located distal to the A domains of FnBPA and FnBPB are unfolded regions which contain multiple, tandemly arranged motifs that mediate binding to fibronectin (Figure 1.11).

1.3.1.5.2 FnBPs binding to fibronectin

The fibronectin-binding regions of FnBPA and FnBPB from *S. aureus* strain 8325-4 share 95 % amino acid identity and consist of eleven and ten tandem repeats, respectively (Figure 1.11). In both cases, each

tandem repeat comprises approximately 40 amino acids, each of which has fibronectin-binding ability (Schwarz-Linek *et al.*, 2003, Meenan *et al.*, 2007). Similar tandem arrays of these fibronectin-binding repeats (FnBRs) have also been found in proteins from several streptococcal species including *Streptococcus dysgalactiae* and *Strep. pyogenes* (Schwarz-Linek *et al.*, 2006). The primary binding site in fibronectin for FnBPs comprises the five N-terminal F1 modules of fibronectin which are involved in the self-association of fibronectin that is necessary for the formation of the fibrils (Figure 1.10). However, another binding site for *S. aureus* FnBPs towards the C-terminus of fibronectin has been reported (Kuusela *et al.*, 1984, Bozzini *et al.*, 1992).

Solution of the crystal structure of the B3 peptide of the Sfbl fibronectin-binding adhesin of *Strep. dysgalactiae* in complex with two N-terminal type I modules of fibronectin provided information about the mechanism of fibronectin-binding employed by bacterial surface proteins. The fibronectin-binding activity of B3 is the result of a 'tandem β-zipper' interaction, where binding motifs in the B3 protein form additional antiparallel β-strands on sequential F1 modules (Schwarz-Linek *et al.*, 2003) (Figure 1.12). Recently, the crystal structures of FnBR-1 and FnBR-5 of *S. aureus* FnBPA, each in complex with four type I modules of fibronectin, have been solved. Structural studies revealed that the FnBRs of FnBPA are disordered and defined a 'tandem β-zipper' model for the interaction between FnBPA and fibronectin in which segments of the FnBR bind to and form an additional strand to the β-sheet of consecutive F1 domains (Bingham *et al.*, 2008) (Figure 1.13). Studies using synthetic peptides have demonstrated that some FnBRs have a high affinity for fibronectin whilst others have a much lower affinity (Meenan *et al.*, 2007). In this model, each of the eleven FnBRs of FnBPA is thought to bind to a string of 3-4 F1 modules in the N-terminal of fibronectin. A similar model has been proposed for the binding of FnBPB to fibronectin except that there is one less binding site in this protein (Meenan *et al.*, 2007). *Borrelia burgdorferi*

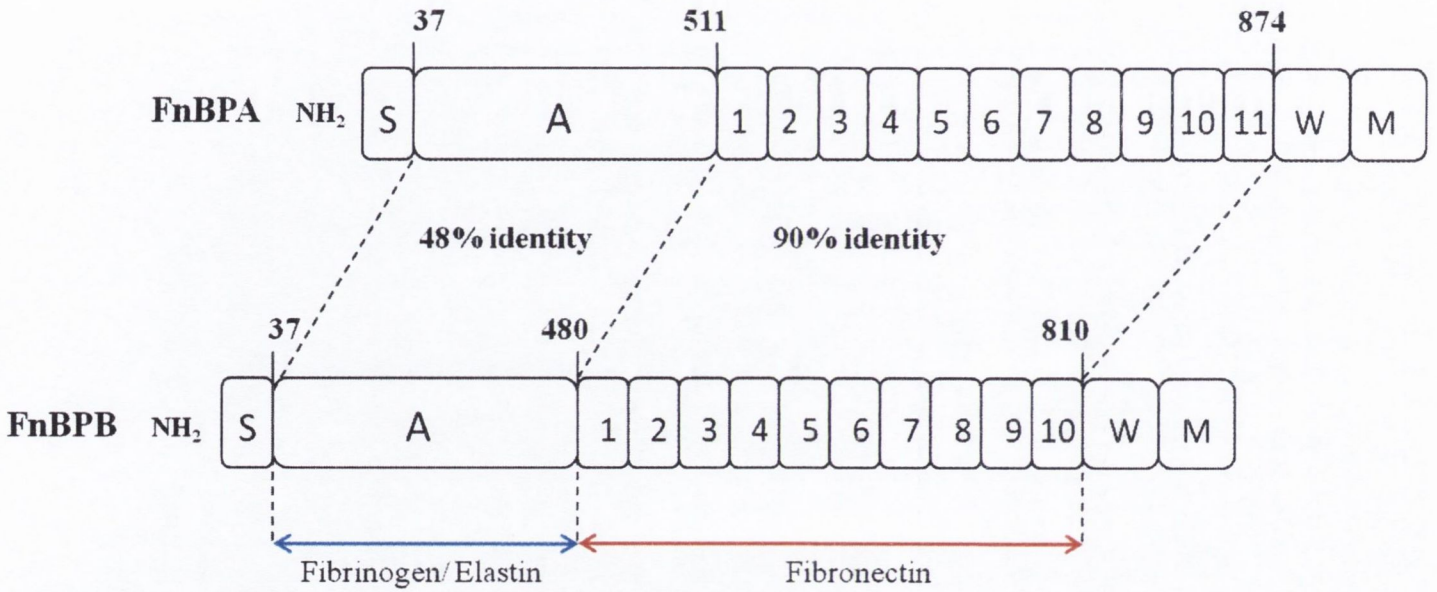

Figure 1.11 Fibronectin-binding proteins A and B of *Staphylococcus aureus* strain 8325-4

Schematic representation of the *S. aureus* fibronectin-binding proteins, FnBPA and FnBPB. Their signal sequences (S), wall/membrane spanning regions (WM) and distinct domains for fibronectin and fibrinogen/elastin- binding and are indicated. Percentage amino acid identities between the binding domains of FnBPA and FnBPB are shown.

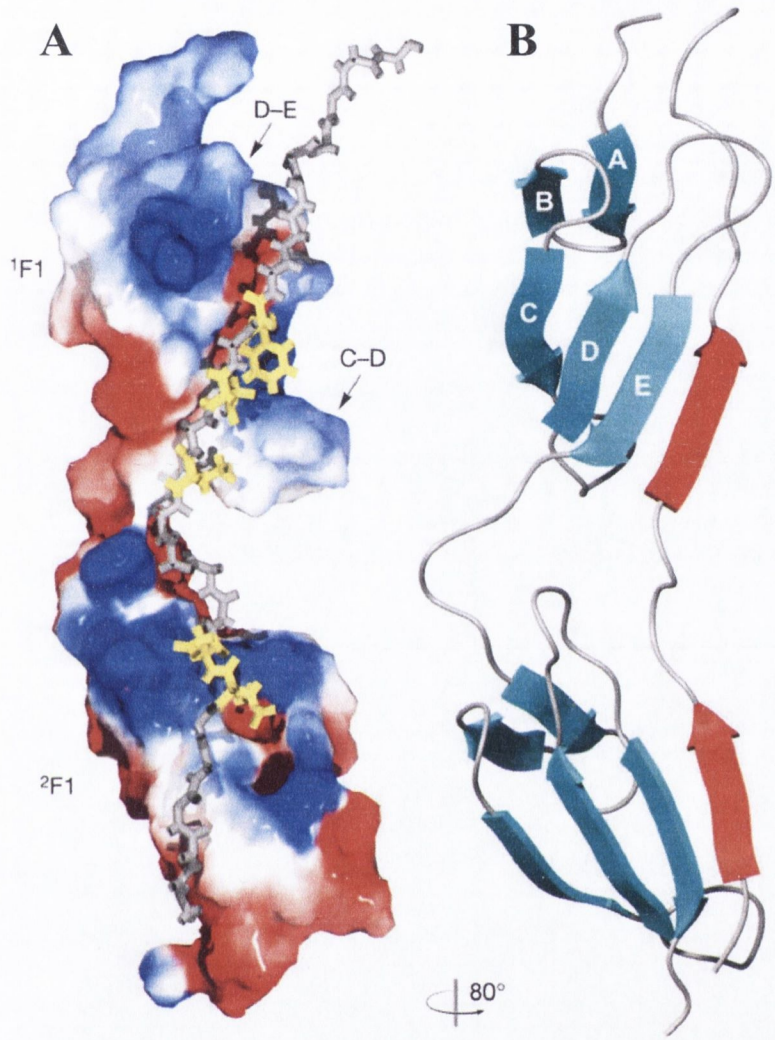

Figure 1.12 Structure of the *Strep. dysgalactiae* B3 peptide in complex with ^{1}F1^{2}F1 type I fibronectin modules

A) Surface potential of ^{1}F1^{2}F1 fibronectin modules with bound B3 peptide (grey). Negatively and positively charged regions of the ^{1}F1^{2}F1 surface are shown in red and blue, respectively. Side chains of hydrophobic and acidic B3 residues are shown in yellow

(B) Ribbon diagram of the lowest-energy β-zipper structure showing strands of the F1 modules (cyan) and the fourth strand formed by B3 (red). The difference in orientation between the two views is indicated.

Adapted from Schwarz-Linek *et al.*, 2003.

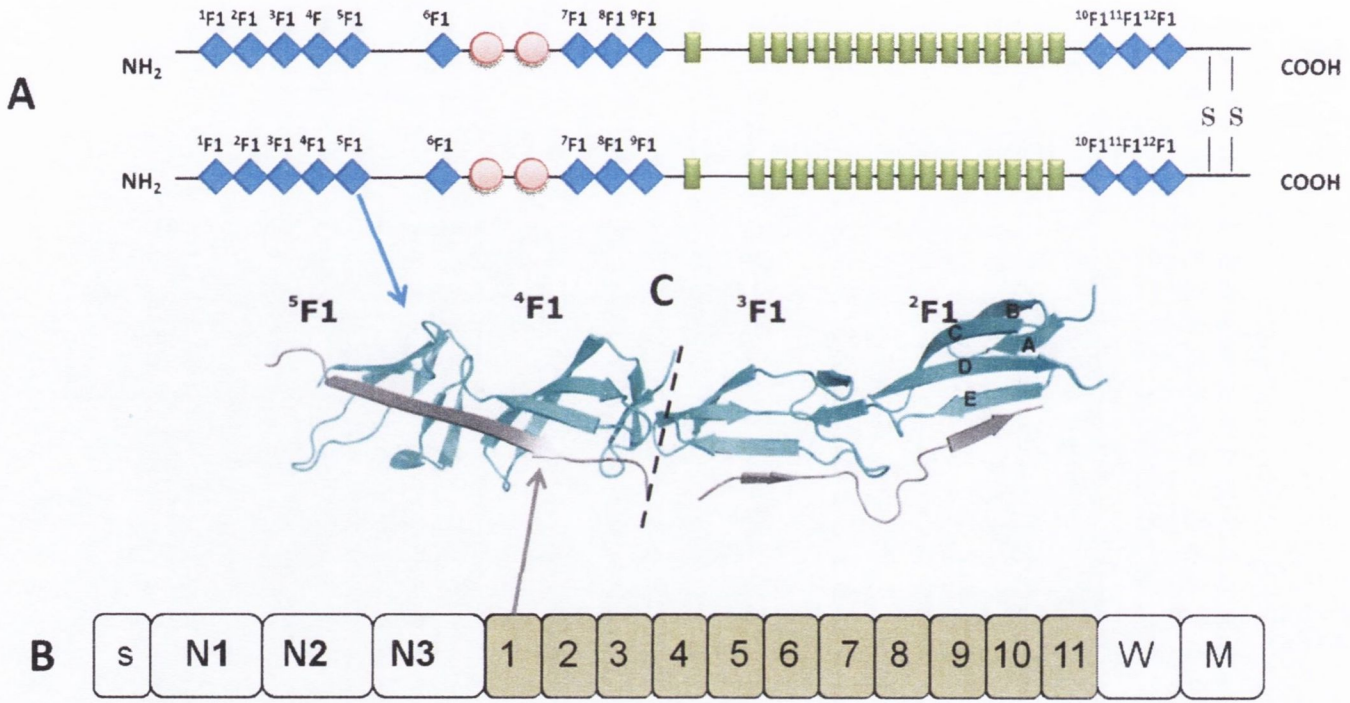

Figure 1.13 Tandem β-zipper mechanism of fibronectin binding by *S. aureus*

(**A**) The N-terminal FI modules of fibronectin each consist of a β-sandwich of two antiparallel β-sheets; a double-stranded sheet (strands A and B) and a triple-stranded sheet (Strands C, D and E). (**B**) The fibronectin-binding domains of FnBPs contain repeated motifs forming β-strands (grey). (**C**). The crystal structure of FnBR peptides from *S. aureus* FnBPA in complex with NTD F1 module pairs from Fn. The structure illustrates a tandem β-zipper mechanism for binding whereby the bacterial peptide contributes a fourth strand to the triple stranded β-sheet of sequential F1 modules. Adapted from Bingham et al., 2008.

also binds fibronectin by the tandem β-zipper mechanism, indicating that it is a common mechanism of fibronectin-binding employed by microorganisms (Raibaud *et al.*, 2005)

The FnBPA-fibronectin crystal structures are in agreement with previous studies which found that the C-terminus of FnBPA lacks discernable secondary structure and only takes on an ordered confirmation upon binding to fibronectin (House-Pompeo *et al.*, 1996). In addition it has been noted that an immune response directed against the C-termini of FnBPs is predominantly against neo-epitopes created when this unfolded region binds fibronectin (Casolini *et al.*, 1998). Recently, however, a monoclonal antibody (15E11) which bound specifically and with high affinity to an epitope shared by FnBR9 and FnBR10 from both FnBPA and FnBPB was isolated and characterised (Provenza *et al.*, 2010). 15E11 effectively inhibited the adherence of *S. aureus* to immobilised fibronectin demonstrating that a function-blocking monoclonal antibody targeting the FnBRs of *S. aureus* can be produced (Provenza *et al.*, 2010).

S. aureus has previously been considered to be an exclusively extracellular pathogen, but it is now clear that this bacterium is a facultative intracellular microorganism that can gain access to the cytoplasm of mammalian cells that are not professional phagocytes. The binding of FnBPs to fibronectin promotes the internalization of *S. aureus* into a number of different cell types including endothelial cells, epithelial cells, osteoblasts and keratinocytes (Lowy, 1998, Kintarak *et al.*, 2004, Hudson *et al.*, 1995, Almeida *et al.*, 1996). Fibronectin acts as a bridging molecule binding N-terminally to *S. aureus* FnBPs and via an RGD motif to the host cell integrin, $\alpha5\beta1$ (Sinha *et al.*, 1999, Massey *et al.*, 2001, Fowler *et al.*, 2000). Indeed the FnBPs have been shown to be sufficient for invasion into endothelial cells (Sinha *et al.*, 2000). Using live-cell imaging, it was shown that FnBPA-mediated uptake of *S. aureus* is relatively slow in comparison to the invasion protein of *Yersinia* (Schroder *et al.*, 2006a). It was proposed that the delay in inducing host cell actin rearrangement and eventual

bacterial internalization was to allow time for *S. aureus* to produce critical amounts of cell damaging toxins (Schroder *et al.*, 2006b). Recent *in vitro* studies have indicated that the number of FnBRs within FnBPA is important for the efficiency of FnBPA-mediated host cell invasion. *S. aureus* expressing FnBPA variants with no or fewer FnBRs either invaded endothelial cells less efficiently or not at all. Furthermore, these strains were significantly less virulent in a murine sepsis model compared to strains expressing FnBPA with the full complement of repeats (Edwards *et al.*, 2010). The uptake of *S. aureus* by mammalian cells may provide a safe harbour for the bacterium from the immune response and most antimicrobials. The FnBPs therefore confer on the bacterium an ability to cross the endothelial lining and to disseminate from the bloodstream to infect other tissues. This may help explain the persistent nature of some *S. aureus* infections.

1.3.1.5.3 FnBPs binding to fibrinogen

The A domains of FnBPA and FnBPB have low sequence identity (~ 48 %) and are antigenically distinct (Loughman *et al.*, 2005). The A domain of each protein shares 25 % amino acid sequence identity to the A domains of ClfA and ClfB. Indeed, the FnBPA and FnBPB A domains bind to the C-terminus of the γ-chain of fibrinogen at the same site as ClfA (Wann *et al.*, 2000) (Figure 1.4). In contract, ClfB binds to the α-chain of fibrinogen (Section 1.3.1.3.2). The integrity of the extreme C-terminus of the fibrinogen γ-chain is important as substitution of the four terminal amino acids from AGDV to VRPE obliterated binding to both ClfA and FnBPA (Wann *et al.*, 2000).

Upon analysis of the N1, N2 and N3 subdomains of ClfA, it was proposed that a similar subdomain organisation exists for region A of FnBPA and FnBPB (Deivanayagam *et al.*, 2002). The primary sequence of the N2N3 subdomain of the A regions of ClfA, ClfB, FnBPA and FnBPB were aligned and predictions of secondary structures showed that A domains

of the FnBPs were likely to contain a variant IgG-like fold similar to ClfA (Deivanayagam *et al.*, 2002) (Section 1.3.2.3.1). It was proposed that ligand-binding occurs through the same dynamic "dock-lock-latch" mechanism that has been predicted for fibrinogen binding to the A domain of ClfA (Section 1.3.1.3.4). Studies of ligand-binding by FnBPA have supported this hypothesis. It has been shown that like ClfA, the N2 and N3 subdomains of FnBPA are sufficient for fibrinogen-binding and that the N1 subdomain is not involved in the interaction. A 3D molecular model of the N2N3 subdomain of FnBPA based on the crystal structure of the equivalent region of ClfA allowed an investigation of residues predicted to be involved in fibrinogen-binding by dock, lock and latch. As with ClfA, residues comprising the predicted latching peptide or lining the predicted ligand-binding trench were identified as being critical for fibrinogen-binding by FnBPA (Keane *et al.*, 2007b)

1.3.1.5.4 FnBPs binding to elastin

Elastin, along with microfibrillar proteins, is a major component of the elastic fibre of the ECM. Elastin is an extensively cross-linked protein. It makes up >90% of the elastic fibres that are found in the ECM and connective tissue, providing elasticity and resilience to tissues (Vrhovski & Weiss, 1998). The elastin protein is found in all vertebrates studied and is amongst the most hydrophobic proteins known. Mammalian tropoeleastin, the soluble monomeric precursor of elastin, is a moderately conserved protein consisting of hydrophobic and hydrophilic crosslinking domains (Boyd *et al.*, 1991). The human genome contains a single elastin gene (Fazio *et al.*, 1991). Expression of tropoelastin mRNA and elastic fibre synthesis is highest during foetal and infant development (Parks *et al.*, 1988).

Unlike ClfA, the A domains of FnBPA and FnBPB can also mediate *S. aureus* adherence to immobilised elastin peptides (Roche *et al.*, 2004). Expression of FnBPs was shown to be crucial for the binding of *S. aureus*

strain P1 to immobilised elastin peptides, a phenotype previously thought to be conferred by the secreted elastin-binding protein, EbpS. In contrast to the LPXTG-anchored surface proteins, EbpS is an integral membrane protein which mediates binding to tropoelastin and to soluble digested elastin fragments (Park *et al.*, 1991, Park *et al.*, 1996). Unlike FnBPA and FnBPB, EbpS is unable to promote *S. aureus* adherence to elastin peptides immobilised on a solid surface (Roche *et al.*, 2004). Thus, EbpS is not an MSCRAMM for elastin. Expression of EbpS was correlated with the ability of cells to grow to a higher density in liquid cultures suggesting that EbpS may have a role in regulating cell growth (Downer *et al.*, 2002).

In addition to elastin peptides, FnBPA can also bind to tropoelastin. As with fibrinogen, the binding site for elastin and tropoelastin has been localised the N2N3 subdomain of FnBPA. Furthermore, recombinant derivatives of the N2N3 subdomain of FnBPA that were deficient in fibrinogen-binding were also unable to bind elastin suggesting that FnBPA binds to both ligands in a similar manner. Thus, based on studies of fibrinogen-binding by FnBPA it is proposed that the dock, lock and latch mechanism is also responsible for the binding of elastin (Keane *et al.*, 2007b). Mutations in the N2N3 subdoman that affected both fibrinogen and elastin-binding had no affect on FnBPA binding to tropoelastin indicating a novel mechanism of ligand-binding by the A domain of FnBPA (Keane *et al.*, 2007a).

1.3.1.5.5 Role of FnBPs in pathogenesis

Most strains of *S. aureus* appear to carry both the *fnbA* gene and the *fnbB* gene although some strains carry only *fnbA*. However, studies with clinical isolates indicated that strains associated with invasive diseases are significantly more likely to have two *fnb* genes (Peacock *et al.*, 2000). Furthermore, 97 % of clinical strains isolated from the airway of cystic fibrosis and pneumonia patients were found to possess both *fnb* genes (Mongodin *et al.*, 2002). Taken together these findings suggest that the

presence of a second FnBP-encoding gene (*fnbB*) enhances the virulence of *S. aureus*. There is also evidence that individuals who have suffered invasive infection contain higher serum anti-FnBP antibody levels than healthy individuals (Dryla *et al.*, 2005) indicating that FnBPs are expressed *in vivo* during infection. Several researchers have studied the role of FnBPA and FnBPB in *S. aureus* pathogenesis with conflicting results (Kuypers & Proctor, 1989, Flock *et al.*, 1996). This can, in part, be explained by the use of FnBP-deficient *S. aureus* laboratory strains such as strain Newman. The sequencing of the genome of *S. aureus* Newman revealed that it contained a point mutation in both the *fnbA* and *fnbB* genes resulting in a premature stop codon (Grundmeier *et al.*, 2004). Strain Newman thus produces truncated FnBP proteins that are secreted rather than anchored to the cell wall peptidoglycan. Due to a small deletion in a positive regulator of sigma factor B (RsbU), *S. aureus* strain 8325-4 produces low levels of FnBPs which results in weak adherence to immobilised fibronectin. The topic is further complicated by the ability of FnBPs to bind several ligands present in host tissue and by the functional redundancy between FnBPs and other *S. aureus* ligand-binding proteins.

Despite this, FnBP expression has been identified as an important *S. aureus* virulence factor in several studies. In a large molecular epidemiological study, adherence to immobilised fibronectin was considerably greater for *S. aureus* isolates associated with orthopedic implant-related arthritis and osteomyelytis (Peacock *et al.*, 2000). FnBP mutants have greatly reduced uptake into host into host cells and antibodies directed against fibronectin reduce staphylococcal internalization (Sinha *et al.*, 1999, Dziewanowska *et al.*, 1999). In fact, FnBPA alone is sufficient for invasion of host cells without the need for staphylococcal cofactors (Sinha *et al.*, 2000). Both FnBPA and FnBPB are potent activators of human platelets (Fitzgerald *et al.*, 2006). The N-terminal fibrinogen and elastin-binding A domains and the C-terminal fibronectin-binding domains of FnBPA and FnBPB are capable of activating platelets in a similar manner to

that described for ClfA and ClfB. Activation is mediated by fibrinogen or fibronectin bridges between the N- and C- termini, respectively, to the low affinity form of the GPIIb/IIIa integrin on resting platelets. Antibodies recognizing the A domain or the complex between the FnBRs and fibronectin bind to the FcγRIIa platelet receptor (Fitzgerald *et al.*, 2006). Bacteria such as *S. aureus* thus exploit circulating anti-MSCRAMM antibodies to cause platelet activation and induce thrombus formation.

Animal models that have been developed to study the role of FnBPs in *S. aureus* infections have focused predominantly on FnBPA. Expression of FnBPA by *S. aureus* was not responsible for the development of experimental septic arthritis, but contributed to systemic inflammation, weight loss and mortality (Palmqvist *et al.*, 2005). A study employing the poorly pathogenic strain *L. lactis* for heterologous expression of *S. aureus* FnBPA showed a positive correlation between expression of FnBPA and the colonisation of damaged heart valves in an experimental model of rats with catheter-induced aortic vegetations (Que *et al.*, 2001). In a later study, *L.lactis* cells expressing ClfA successfully colonised damaged heart valves but were spontaneously eradicated over 48 hours. In contrast, FnBPA-positive lactococci increased bacterial titres and invaded adjacent endothelial cells (Que *et al.*, 2005). It was also demonstrated that binding of fibrinogen was required for initial colonization of thrombi and damaged valves while binding to fibronectin was required for the infection to spread (Que *et al.*, 2005).

1.3.1.5.6 Other fibronectin-binding proteins

In addition to the classical MSCRAMM FnBPs, *S. aureus* possesses several other proteins that have the capacity to bind fibronectin. Ebh is an extremely large (1.1MDa) filamentous protein which is thought to be involved in bacterial cell wall stabilization (Kuroda *et al.*, 2008) and has been demonstrated to bind fibronectin (Clarke *et al.*, 2002). However, it is as yet unclear if this is functionally important to the organism. Extracellular

matrix protein-binding protein (Emp) and extracellular adherence protein (Eap) also bind fibronectin (Hauck & Ohlsen, 2006, Chavakis *et al.*, 2005). Although no structural details are presently known of the mechanisms of interaction of Ebh, Emp and Eap with fibronectin, given the differences in secondary structure of the domains responsible for the interaction, it seems likely that they will turn out to be very different from that of the well studied FnBR mediated tandem β-zipper interactions.

1.3.2 Other surface proteins

The expression of a subset of staphylococcal genes is induced under iron-limiting conditions, which are likely to resemble growth conditions in serum and within the host during infection. The products of four iron-regulated surface determinant (*isd*) genes are involved in iron acquisition. IsdA, IsdB and IsdH each contain the LPXTG sortase A sorting signal, while IsdC appears to be buried in the cell wall and contains an NPQTN motif for sortase B-catalysed cell wall sorting (Mazmanian *et al.*, 2002, Dryla *et al.*, 2003). Collectively these four proteins bind human hemoproteins, remove the heme molecule and transport heme through the cell wall and plasma membrane for accumulation in the bacterial cytoplasm.

In addition to ClfA and CfB, *S. aureus* expresses three other cell wall-anchored surface proteins containing SD dipeptide repeats (Sdr proteins). The *sdrC*, *sdrD* and *sdrE* genes are tandemly arrayed on the *S. aureus* chromosome although some strains do not contain all three (Sabat *et al.*, 2006, Josefsson *et al.*, 1998). The three proteins have a similar structure to ClfA and ClfB, but like SdrG they contain B repeats between the N-terminal region A and the C-terminal region R. SdrC and SdrD promote adhesion of bacteria to an unknown ligand on desquamated nasal epithelial cells (Corrigan *et al.*, 2009). SdrE bears significant homology to the *S. aureus* bone sialoprotein-binding protein Bbp, which may be important in the localization of bacteria to bone tissue and thus might be of relevance in

the pathogenicity of osteomyelitis (Tung *et al.*, 2000). SdrD and SdrE are among the most immunogenic surface proteins (in terms of antibody titre). When used to vaccinate mice, a recombinant SdrD and SdrE together with recombinant IsdA and IsdB (above) gave complete protection against challenge in a murine renal infection model (Stranger-Jones *et al.*, 2006).

Analysis of *S. aureus* genome sequences identified ten putative LPXTG-proteins (Roche *et al.*, 2003a, Mazmanian *et al.*, 2001). These were named *S. aureus* surface (Sas) proteins. SasE, SasI and SasJ have since been renamed IsdA, IsdH and IsdB, respectively, and are described above. SasG promotes bacterial adhesion to desquamated nasal epithelial cells and can also promote biofilm formation (Roche *et al.*, 2003b, Geoghegan *et al.*, 2010, Corrigan *et al.*, 2007) (see Section 1.4.5). In addition, SasG can mask the ability of *S. aureus* surface proteins such as ClfA, ClfB and FnBPs to bind their ligands (Corrigan *et al.*, 2007). Sas A (also known as SraP) can promote *S. aureus* binding to platelets and is a virulence factor in the rabbit endocarditis model (Siboo *et al.*, 2005). SasC was recently found to be involved in cell aggregation and biofilm formation (Schroeder *et al.*, 2009). No functions have been attributed to other Sas proteins (SasD, SasF, SasH, SasK). Antibodies against many Sas proteins have been detected in convalescent sera from patients with documented *S. aureus* infections (Roche *et al.*, 2003b) indicating that expression of these proteins occurs during infection.

1.3.3 Non-covalently attached cell wall proteins

S. aureus also possesses a number of non-covalently attached cell wall-associated proteins that bind to component of the host's ECM. These include the elastin-binding protein EbpS (see Section 1.3.1.4.4) and the second binding protein of immunoglobulin, Sbi. Sbi has two N-terminal domains (D1 and D2) with sequence similarity to the IgG binding domains of Spa which bind the Fc region of IgG in a similar fashion to protein A (Section 1.3.1.2).The protein also contains two domains (D3 and D4) that

each bind to the complement protein C3 and promote its futile consumption (Upadhyay *et al.*, 2008). The C-terminal region of Sbi lacks an LPXTG motif for covalent attachment to peptidoglycan (Zhang *et al.*, 1998). A recent study has indicated that Sbi exists both as an extracellular protein and cell wall-associated protein bound to the cytoplasmic membrane. The same study demonstrated that both cell-associated Sbi and secreted Sbi promote survival of *S. aureus* in human blood (Emma Smith, unpublished data). This is discussed further in Section 1.4.3.

1.3.4 Secreted proteins

More than half of the actual or potential virulence determinants in *S. aureus* are secreted extracellular proteins (Kuroda *et al.*, 2001). Some of these are described in Table 1.1. These include specific proteins that interfere with the host's innate and adaptive immunity. Secreted proteins targeting the innate immune system include those that inhibit complement fixation, proteins that inhibit neutrophil migration and toxins that kill leukocytes.

1.4 Immune evasion by *S. aureus*

When *S. aureus* breaches the body's barriers of skin and mucous membranes through a wound, it encounters the innate and acquired immune system of the host. Infection of the skin by *S. aureus* stimulates a strong inflammatory response causing neutrophil and macrophage migration to the site of infection. The function of these cells is to engulf and dispose of the invading organisms in co-ordination with antibodies and complement present in the host's serum. The complement system comprises proteins and their proteolytic derivatives which function in both innate and acquired immunity to destroy foreign cells or induce other effectors involved in the immune response (Rus *et al.*, 2005). The primary role of complement fixation on *S. aureus* is opsonisation ie, to promote phagocytosis by professional phagocytes (neutrophils and macrophages). Formylated

peptides released by growing bacteria and chemoattractant molecules released during complement activation (C3a and C5a) attract phagocytes to the site of infection. The efficiency of phagocytosis is enhanced by expression of specific receptors on the phagocytes for complement fragments and formylated peptides. Neutrophils also carry specific receptors that can recognize the Fcγ region of IgG and complement proteins bound to the bacterial surface that facilitate efficient uptake and killing.

S. aureus uptake by macrophages initially stimulates the acquired immune response. B cells in the lymph nodes differentiate and secrete antibodies to neutralise toxins and recognise bacterial surface molecules thereby promoting more efficient phagocytosis of bacterial cells. However, *S. aureus* has evolved to overcome the host's immune response. Antibody titres to *S. aureus* antigens already present in all humans rise following infection (Roche *et al.*, 2004, Dryla *et al.*, 2005). Nonetheless, antibody production and immunological memory appear to be inadequate for the prevention of subsequent infections. *S. aureus* has evolved numerous strategies to thwart the host immune response to facilitate its survival and pathogenesis in superficial and invasive disease conditions. Selected examples of such mechanisms are discussed below.

1.4.1 Complement evasion

Complement recruits effector molecules that are deposited on the *S. aureus* cell surface labelling the bacteria for destruction by immune effector cells such as neutrophils. There are three pathways which trigger complement activation and fixation. The alternative and lectin pathways are components of innate immunity whereas the classical pathway is triggered by specific interaction with antibodies that have bound to antigens on the surface of bacterial cells.

Assembly of C3 convertase on the surface of *S. aureus* is a prerequisite for complement activation (Fujita, 2002). C4b2a (classical and

Table 1.1 Extracellular proteins of *S. aureus*

Secreted protein	Effect	Reference
alpha-toxin	Pore forming toxin. Lyses mammalian erythrocytes.	Montoya and Gouaux, 2003
beta-toxin	Sphingomyelinase. Lysis of cells with high content of sphingomyelin in their plasma membranes	Doery, 1963 Walev *et al.*, 1996
gamma-toxin	2-component cytolytic toxin. Lyses mammalian erythrocytes	Kaneko and Kamio, 2004
Panton-Valentine leukocidan	2-component cytolytic toxin highly specific for leukocytes.	Kaneko and Kamio, 2004
CHIPS	Inhibits neutrophil chemotaxis	de Haas *et al.*, 2004 Postma *et al.*, 2004
SCIN	Inhibits complement fixation on bacterium surface	Rooijakkers *et al.*, 2005
Efb	Secreted fibrinogen-binding protein. Inhibitor of complement fixation. Blocks platelet aggregation	Lee *et al.*, 2004 Shannon and Flock, 2004.
Staphylokinase	Plasminogen activator. Binds to and inactivates human defensins.	Sakharov *et al.*, 1996 Jin *et al.*, 2004
Aureolysin	Metalloprotease. Tissue damage Inactivation of antimicrobial peptides	Sieprawska-Lupa *et al.*, 2004
Enterotoxins	Superantigen, food poisoning	Bohach *et al.*, 1990
TSST-1	Superantigen, toxic shock	McCormick *et al.*, 2001
Coagulase	Activates prothrombin, causes clotting of fibrinogen	Boden and Flock, 1992
V8 protease	Serine protease. Modification of *S. aureus* surface proteins	Shaw *et al.*, 2004 McGavin *et al.*, 1997
Staphopain A and B	Cysteine proteases. Cause vascular leakage leading to septic shock	Shaw *et al.*, 2004 Imamura *et al.*, 2005

lectin pathways) and C3bBb (alternative pathway) cleave C3 resulting in the release the C3a chemoattractant peptide and attachment of the opsonin C3b to the bacterium. *S. aureus* secretes a small protein called staphylococcal complement inhibitor (SCIN) which binds to and stabilizes both C4b2a and C3bBb resulting in inhibition of further C3b formation (Rooijakkers *et al.*, 2005). Recent studies have indicated that SCIN blocks the activity of C2 convertases by inducing dimerization of these enzymes (Jongerius *et al.*, 2010). Normally C3 convertases are transiently active and dissociation leaves the bound C4b and C3b to act as cofactors for further cleavage of C2 and factor B, respectively. Stabilisation of the complexes by SCIN blocks the crucial amplification loop and is a potent mechanism for preventing complement activation. Preventing C3b formation ultimately inhibits C5 convertase activity and reduced release of potent neutrophil chemoattractant C5a. SCIN was shown to block phagocytosis and killing of *S. aureus* cells by human neutrophils (Rooijakkers *et al.*, 2005).

Host plasminogen attaches to unknown receptors on the *S. aureus* cell surface. Staphylokinase secreted by *S. aureus* can bind to plasminogen and activate its potent serine protease activity on the cell surface (Bokarewa *et al.*, 2006). This serves to cleave surface-bound C3b and IgG molecules resulting in reduced phagocytosis by neutrophils (Rooijakkers *et al.*, 2005)

The *S. aurues* MSCRAMM ClfA can also interfere with complement by binding to and activating complement factor I. This leads leading to enhanced degredation of C3b and a reduction in phagocytosis of *S. aureus* by human neutrophils (Visai *et al.*, 2009, Hair *et al.*, 2010).

1.4.2 Inhibition of neutrophil migration

Invading bacteria generate chemoattractants that stimulate the migration of neutrophils to the site of infection to engulf and destroy the invading organism. To counter these attractants, *S. aureus* secretes several proteins that block neutrophil receptors and inhibit neutrophil activation and

migration. The secreted chemotaxis inhibitory protein of *S. aureus* (CHIPS) is expressed by 60% of clinical isolates (de Haas *et al.*, 2004). The protein contains two distinct domains which facilitate binding to receptors for complement fragment C5a (C5aR) and the formylated peptide receptor (FPR) on neutrophils. This blocks the cognate agonists from binding and results in potent inhibition of chemotaxis. (de Haas *et al.*, 2004).

The cell adhesion molecule P-selectin is present on the endothelial cell surface during inflammation. The P-selectin receptor (PSGL-1) on circulating neutrophils binds P-selectin and initiates the process of neutrophil rolling. Staphylococcal superantigen-like 5 (SSL5) is a secreted protein that binds PSGL-1 and prevents neutrophil rolling on activated endothelial cells (Bestebroer *et al.*, 2007).

The β2 integrins Mac-1 and leucocyte function associated antigen -1 (LFA-1) on leucocytes both interact with the counter-receptor intercellular adhesion molecule-1 (ICAM-1) on endothelial cells to allow neutrophil adhesion to endothelial cells before transmigration across blood vessels. The extracellular adhesion protein Eap can bind to ICAM-1 to block the interaction with LAF-1 and reduces neutrophil attachment to and transmigration through endothelial cells (Chavakis, *et al.*, 2002).

1.4.3 Resistance to phagocytosis

S. aureus expresses several anti-opsonic surface proteins. Protein A and Sbi bind IgG in a non-immune manner (Section 1.3.1.2) inhibiting phagacytosis. Binding of the Fc-region of IgG to protein A and/or Sbi results in the coating of bacteria with IgG molecules in the incorrect orientation to be recognised by neutrophil Fc-receptors.

ClfA also displays anti-phagocytic properties (Palmqvist *et al.*, 2004). Bacteria expressing a non-fibrinogen binding ClfA mutant were phagocytosed more efficiently *in vitro* than bacteria expressing the wild-type protein. Other *S. aureus* fibrinogen-binding surface proteins (ClfB,

FnBPA and FnBPB) may exhibit similar anti-phagocytic properties. The ability of ClfA to bind and activate complement factor I also contributes to the anti-phagocytic effects as discussed above (Section 1.4.1), *S. aureus* secretes a number of proteins that interfere with complement fixation on the bacterial cell surface and thus also inhibit phagocytosis by neutrophils.

Capsular polysaccharide (CP) is produced by a majority of *S. aureus* clinical isolates (Roghmann *et al.*, 2005, O'Riordan & Lee, 2004). Expression of CP serotypes 5 and 8 is associated with increased virulence in animal infection models (Thakker *et al.*, 1998, Nilsson *et al.*, 1998, Luong & Lee, 2002, Lee *et al.*, 1997, Baddour *et al.*, 1992) and may mask *S. aureus* surface adhesins. In a recent study expression of capsule inhibited *S. aureus* clumping factor A-mediated binding to fibrinogen and platelets (Risley *et al.*, 2007). Capsule inhibits binding of antibodies to *S. aureus* cell surface components which hinders opsonisation (Thakker *et al.*, 1998). It also obstructs access of phagocyte complement receptors to complement components assembled beneath the capsule layer (Cunnion *et al.*, 2003).

1.4.4 Superantigens

Clinical *S. aureus* isolates often express several superantigens. Superantigens have the ability to bind the exterior of the major histocompatibility (MHC) class II protein on the surface of antigen-presenting cells and link it to T-cell receptors on the surface of a T helper cell (Proft & Fraser, 2003). When expressed at high levels, superantigen toxins cause the unrestricted expansion of T-cells and massive release of cytokines from macrophages and T cells. This cytokine release mediates toxic shock, causing tissue damage and multi-organ dysfunction (Kappler 90). Superantigen-mediated T cell activation is antigen-independent and the resultant inflammation does not serve to fight staphylococcal infection, but rather overwhelms the host immune system leading to toxic shock, multiple organ system failure and death. Low-level expression of superantigen toxins can cause immune suppression by the local depletion of T cells. The

binding of protein A to the VH3 domains of IgM on B-lymphocytes also induces a similar mitogenic response leading to depletion of a significant proportion of the repertoire of potential antibody-secreting B cells in the spleen and bone marrow (Goodyear & Silverman, 2004).

1.4.5 Biofilm

S. epidermidis and *S. aureus* possess the ability to form biofilms (Mack *et al.*, 2004), a multilayered dense structure that protects bacteria from the host immune system. Staphylococcal biofilm formation first came to prominence in infections associated with indwelling medical devices but may also be important in conventional staphylococcal infections. The initial attachment phase of biofilm formation is mediated by bacterial adhesion to naked plastic or metal surfaces by a surface component such as the major autolysin Atl (Biswas *et al.*, 2006). Alternatively, adhesion to surfaces that have been conditioned with fibronectin and fibrinogen from host plasma is mediated by surface proteins such as ClfA, FnBPA and FnBPB of *S. aureus* or SdrG of *S. epidermidis*.

Until recently, the accumulation phase of biofilm formation by *S. epidermidis* and *S. aureus* was attributed solely to the ability to synthesize an extracellular polysaccharide called polysaccharide intercellular adhesin (PIA), which is composed of partially deacetylated poly-*N* acetylglucosamine (Vuong *et al.*, 2004, Mack *et al.*, 2004). However, some clinical staphylococcal isolates from device-related infection form biofilm *in vitro* but do not express PIA. Here, surface proteins such as the accumulation-associated protein (Aap) of *S. epidermidis* and the related protein SasG from *S. aureus* promote biofilm accumulation (Hussain *et al.*, 1997, Corrigan *et al.*, 2007).

Aap and SasG are typical LPXTG-anchored multidomain cell wall-associated proteins. Each protein contains an N-terminal A domain followed by several homologous B-repeats. Aap is cleaved by a protease to remove

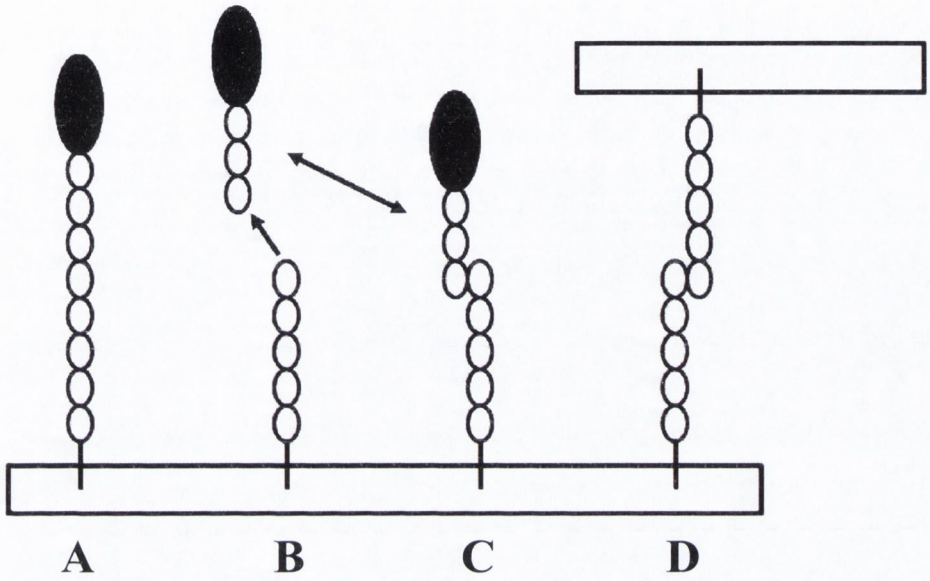

Figure 1.14 Model for *S. aureus* SasG-mediated biofilm formation
The smaller open circles represent the B domains of SasG, while the large black circle is the N-terminal A domain. (**A**) The full-length SasG protein is attached to the *S. aureus* cell wall peptidoglycan by sortase. (**B**) Cleavage in the B region results in detachment of the N-terminal A region with some B-repeats. (**C**) The released fragment can reattach to the cell wall-anchored B domain in a Zn^{2+}-dependent manner. (**D**) Cell-cell interactions occur by exposed B domains dimerizing in a Zn^{2+}-dependent manner during the accumulation phase of biofilm formation. Modified from Geoghegan *et al.*, 2010.

the N-terminal A domain which exposes the B-repeat region allowing the cell to cell binding required for biofilm formation involving protein-protein interactions (Hennig *et al.*, 2007). In contrast to Aap, SasG on the cell surface is processed within the B domains to a limited degree resulting in cleaved proteins of various lengths being released into the supernatant. Some of the released molecules associate with the surface-exposed B domains that remain attached to the cell (Geoghegan, *et al.*, 2010) (Figure 1.14). Recombinant B repeats of Aap and SasG form homodimers in the presence of Zn^{2+}. In both cases, B repeats appear to associate by a 'zinc zipper' mechanism for B repeat-mediated intercellular adhesion in staphylococcal biofilm (Conrady *et al.*, 2008)

Another PIA-independent mechanism of biofilm formation by *S. aureus* occurs in some MRSA isolates where biofilm formation is mediated by the expression of FnBPA and FnBPB (O'Neill *et al.*, 2008). While expression of either FnBPA or FnBPB is sufficient for promoting MRSA biofilm, MRSA isolates from device-related infections that carry both *fnbA* and *fnbB* genes produce significantly more biofilm than isolates with either gene alone (O'Neill *et al.*, 2009). Studies involving FnBPA deduced that it is the N-terminal fibrinogen and elastin-binding A domain of FnBPA and not its C-terminal fibronectin-binding repeats that promotes biofilm formation. Additionally, the expression of a fibrinogen-binding deficient mutant of FnBPA did not affect biofilm indicating that *S. aureus* biofilm promoted by FnBP-expression is independent of known ligand-binding activities (O'Neill *et al.*, 2008). Like SasG-mediated biofilm, the formation of biofilm that is mediated by *S. aureus* FnBPs is dependent on pH and the presence of a physiological level of concentration of Zn^{2+} (J.Geoghegan, unpublished data).

1.4.6 Virulence factor variation

Sequence variation in genes encoding important *S. aureus* virulence factors can result in the generation of isoforms that are antigenically distinct.

Thus, virulence factor variation may represent another mechanism of immune evasion by *S. aureus*.

1.4.6.1 Coagulase variation

Coagulase is a highly variable secreted *S. aureus* virulence factor (Cheng *et al.*, 2010). It is a zymogen that binds to human prothrombin in a 1:1 molar ratio to form a complex called staphylothrombin which converts fibrinogen to fibrin resulting in blood-clot formation. The coagulase molecule consists of two independently folded α-helical N-terminal domains, a C-terminal repeat region and a highly conserved central domain. The N-terminal domains contain the prothrombin-binding and activation sites and the C-terminal repeat regions can bind fibrinogen (Friedrich *et al.*, 2003, Boden & Flock, 1989). The ability to bind both prothrombin and fibrinogen simultaneously may be involved in bringing coagulase-activated prothrombin into close proximity with fibrinogen, allowing the formation of fibrin.

Ten different serotypes of staphylococcal coagulase have been identified to date. Variation is confined to two regions (D1 and D2) in the N-terminus of coagulase with amino acid identities of 52.8% and 60.2% respectively (Watanabe *et al.*, 2005). The flanking regions of *coa* genes are highly conserved indicating that the gene could be transmitted to *S. aureus* while sections of it, responsible for variable antigenicicty, may have evolved independently (Watanabe *et al.*, 2009). It is proposed that antigenic variation in coagulase may be useful to evade the host's immune response and/or adapt to the different coagulase-prothrombin binding sites of mammalian species.

1.4.6.1 FnBPA variation

FnBPA is a highly variable *S. aureus* cell wall-anchored multifunctional MSCRAMM that promotes adhesion to immobilised fibronectin, fibrinogen and elastin (see Section 1.3.1.4.1). The N2N3

subdomain of the N-terminal fibrinogen and elastin-binding A domain of FnBPA contains the minimum ligand-binding site. Recent studies have shown that the N2 and N3 subdomains of FnBPA have undergone considerable amino-acid sequence divergence. There are at least seven distinct isotypes of FnBPA N2N3.The amino acid differences do not affect ligand-binding and it is predicted that variant residues occur primarily on the surface of the protein. FnBPA A domain residues involved in ligand-binding by dock, lock and latch are conserved in all isotypes (Loughman *et al.*, 2008). The same study demonstrated that FnBPA isotypes differ antigenically and exhibit limited immuno cross-reactivity suggesting a role for FnBPA variation in immune evasion (Loughman *et al.*, 2008).

1.5 Rationale for this study

Most *S. aureus* strains can express two distinct fibronectin-binding proteins, FnBPA and FnBPB. While most strains carry both the *fnbA* and *fnbB* genes, some strains contain only *fnbA*. Studies with site-specific *fnbA* and *fnbB* insertion mutants have shown that either FnBPA or FnBPB can mediate *S. aureus* adherence to immobilised fibronectin, but there was no difference in adherence between wild type strains and single *fnb* mutants, indicating functional redundancy. However, *S. aureus* isolates associated with invasive diseases are significantly more likely to have two *fnb* genes. Taken together these studies imply that expression FnBPB enhances the virulence of *S. aureus* through a function that is independent of ligand-binding.

Seven variants of FnBPA were recently identified based on divergence in the minimal ligand-binding N2N3 subdomain. Each FnBPA isotype retains ligand-binding activity but is antigenically distinct suggesting that FnBPA variation plays a role in immune evasion by *S. aureus*. Given its functional, organizational and sequence similarity with FnBPA, it was hypothesised that FnBPB may display a similar pattern of antigenic variation. The initial aim of this study was to determine the extent

of FnBPB variation and its relevance to avoidance of immune responses during infection.

The A domain of FnBPB promotes adhesion to immobilised fibrinogen and elastin. It shares significant homology with the A domains of ClfA and FnBPA which each bind to the same region of fibrinogen as that recognised by FnBPB. Fibrinogen binding by ClfA and FnBPA has been well characterised. ClfA binds fibrinogen by a variation of the dock, lock and latch mechanism. The same mechanism has been predicted for fibrinogen binding by FnBPA. Another aim of this study was to characterize the molecular mechanism of fibrinogen binding employed by FnBPB with an analysis based on previous studies of ClfA and FnBPA.

When the functionality of recombinant FnBPB A domain protein was tested, it was noted that the N2N3 subdomain of FnBPB bound immobilised fibronectin while the equivalent region of FnBPA did not. This was surprising because the N2N3 subdomain of FnBPB does not contain any known fibronectin-binding motifs. This study aimed to characterize the molecular mechanism of fibronectin binding by the A domain of FnBPB. Finally, the biological significance of fibronectin binding by the A domain of FnBPB was explored in this study. The ability of the A domain of FnBPB to promote bacterial adhesion to immobilised fibronectin and the subsequent invasion of human endothelial cells was tested.

Chapter 2

Materials and Methods

2.1 Bacterial strains and growth conditions

Escherichia coli, *Staphylococcus aureus* and *Staphylococcus epidermidis* strains are listed in Table 2.1. *E. coli* was routinely grown on Luria (L) agar or in L-broth (Difco) at 37°C. *E.coli* carrying plasmids were grown in L-broth supplemented with ampicillin (100 μg/ml) at 37°C. *S. aureus* and *S. epidermidis* were grown on Trypticase Soy agar (TSA, Oxoid) or broth (TSB) at 37° C for liquid cultures. Chloramphenicol (10 μg/ml) was incorporated into TSB where appropriate. *E. coli, S. aureus* and *S. epidermidis* broth cultures were grown in an orbital shaker at 200 rpm at 37°C. For expression studies and adherence assays exponential phase cultures of *S. epidermidis* were inoculated 1:100 from overnight starter cultures. Cells were washed in phosphate buffered saline and grown to the required optical density. Stocks of bacterial strains were made by supplementing broth cultures with 20 % (v/v) glycerol and snap-freezing in liquid nitrogen.

2.2 Plasmids

All plasmids and derivatives are listed in Table 2.2.

2.3 DNA manipulation

DNA manipulation techniques were performed using standard methods (Sambrook & Russell, 2001). Restriction enzymes were purchased from Promega and were used according to the manufacturers' instructions. *E. coli* transformants were screened for the presence of recombinant plasmids using the rapid colony screening procedure developed by Le Gouill and Dery (1991). Recombinant plasmids isolated from *E. coli* were established in *S. epidermidis* by electroporation. All confirmatory DNA sequencing was performed by GATC Biotech. Chemicals were purchased from Sigma Chemical Co.

2.3.1 Isolation of plasmid and genomic DNA

Plasmid DNA was purified using Promega Wizard SV Plus Minipreps DNA purification system as recommended by the supplier. Preparation of genomic DNA was performed using the Genomic DNA purification kit (Edge Biosystems) as per the supplier's protocol, except that *S. aureus* cells were treated with 200 μg lysostaphin (AMBI, New York) for 20 min at 37°C to digest the cell-wall peptidoglycan.

2.3.2 Polymerase chain reaction

Polymerase chain reaction (PCR) amplification was carried out in a DNA thermal cycler (Techne). Plasmid DNA (10 ng) or *S. aureus* genomic DNA (100 ng) was used as a template. Primers were purchased from Sigma-Aldrich and are listed in Table 2.3. DNA fragments for cloning were amplified using the high fidelity polymerase Phusion® (Finnzymes) according to the manufacturer's instructions. Reaction mixtures (50μl) contained forward and reverse primers (1 μM), 10mM dNTPs, template DNA and 1 U of Phusion® polymerase in a standard Phusion® polymerase buffer (Finnzymes). Amplification was carried out with an initial denaturation step at 98°C for 30 sec. This was followed by 30 cycles of denaturation for 10 sec, annealing for 30 sec at a temperature dependent on the melting temperature of the primers and extension at 72°C, allowing 30 sec/kb for genomic DNA or 15 sec/kb for plasmid DNA templates. Alternatively, DNA fragments were amplified using *Taq* DNA polymerase (Roche) according to the manufacturer's instructions. Reaction mixtures (100 μl) contained forward and reverse primers (100 pmol), 2.5 mM dNTPs, 1.5 mM $MgCl_2$, template DNA and 1.25 U *Taq* polymerase in a standard Roche *Taq* reaction buffer. Amplification was carried out with an initial denaturation step at 94°C for 1 min before addition of the enzyme. This was followed by 30 cycles of denaturation for 30 sec, annealing for 1 min at a temperature dependent on the melting temperature of the primers and extension at 72°C, allowing 1 min/kb of DNA being amplified. DIG-labeled

Table 2.1 Bacterial strains

Strain	Relevant characteristics	Source/ Reference
E. coli		
XL-1 Blue	Propagation of plasmids	Stratagene
Topp3	Protease deficient strain. Used for recombinant protein expression	Stratagene
S. aureus		
8325-4	NCTC 8325-4 cured of prophages	Novik, 1967
N315	Hospital-acquired MRSA strain	Kuroda *et al.*, 2001
MSSA476	Community-acquired MSSA strain	Holden *et al.*, 2004
P1	Rabbit virulent strain. Strong adhesion to extracellular matrix proteins	Sheretz *et al.*, 1993
2	Human clinical isolate	Feil *et al.*, 2003
19	Human clinical isolate	Feil *et al.*, 2003
114	Human clinical isolate	Feil *et al.*, 2003
116	Human clinical isolate	Feil *et al.*, 2003
138	Human clinical isolate	Feil *et al.*, 2003
162	Human clinical isolate	Feil *et al.*, 2003

Table 2.1 Bacterial strains, continued

Strain	Relevant characteristics	Source/ Reference
S. aureus		
233	Human clinical isolate	Feil *et al.*, 2003
304	Human clinical isolate	Feil *et al.*, 2003
316	Human clinical isolate	Feil *et al.*, 2003
402	Human clinical isolate	Feil *et al.*, 2003
563	Human clinical isolate	Feil *et al.*, 2003
617	Human clinical isolate	Feil *et al.*, 2003
863	Human clinical isolate	Feil *et al.*, 2003
964	Human clinical isolate	Feil *et al.*, 2003
3015	Human clinical isolate	Feil *et al.*, 2003
3077	Human clinical isolate	Feil *et al.*, 2003
3084	Human clinical isolate	Feil *et al.*, 2003
3089	Human clinical isolate	Feil *et al.*, 2003
3110	Human clinical isolate	Feil *et al.*, 2003

Table 2.1 Bacterial strains, continued

Strain	Relevant characteristics	Source/ Reference
S. aureus		
3132	Human clinical isolate	Feil *et al.*, 2003
RF122	Bovine virulent strain	Fitzgerald *et al.*, 2000
RF26	Bovine isolate	Fitzgerald *et al.*, 2000
RF79	Bovine isolate	Fitzgerald *et al.*, 2000
RF283	Bovine isolate	Fitzgerald *et al.*, 2001
PSA5	Bovine isolate	Fitzgerald *et al.*, 2001
DS35	Bovine isolate	Smyth *et al.*, 2009
DS36	Bovine isolate	Curcarella *et al.*, 2001
DS37	Bovine isolate	Curcarella *et al.*, 2004
DS40	Bovine isolate	Smyth *et al.*, 2009
DS42	Bovine isolate	Smyth *et al.*, 2009
DS70	Bovine isolate	Smyth *et al.*, 2009
MSA17.1	Bovine isolate	Fitzgerald *et al.*, 2001

Table 2.1 Bacterial strains, continued

Strain	Relevant characteristics	Source/ Reference
S. aureus		
MSA915	Bovine isolate	Smyth *et al.*, 2005
MSA1006	Bovine isolate	Smyth *et al.*, 2005
MSA1007	Bovine isolate	Smyth *et al.*, 2005
MSA1011	Bovine isolate	Fitzgerald *et al.*, 2001
MSA1047	Bovine isolate	Fitzgerald *et al.*, 2001
MSA1363	Bovine isolate	Fitzgerald *et al.*, 2001
MSA1468	Bovine isolate	Fitzgerald *et al.*, 2001
MSA1547	Bovine isolate	Fitzgerald *et al.*, 2001
S. epidermidis		
TU3298	Transformable strain. Poor adhesion to extracellular matrix proteins.	Allgator *et al.*, 1986

Table 2.2 Plasmids

Plasmid	Features	Marker(s)	Source/ Reference
pBluescript KS+	High copy number plasmid for *E. coli*. Used for general cloning	Amp^R	Stratagene
pBluescript::*fnbB* P1	pBluescript plasmid containing a 2.0 kb *Bam*HI PCR generated fragment of the *fnbB* gene from *S. aureus* P1	Amp^R	This study
pBluescript::*fnbB* 2	pBluescript plasmid containing a 2.0 kb *Bam*HI PCR generated fragment of the *fnbB* gene from *S. aureus* 2	Amp^R	This study
pBluescript::*fnbB* 114	pBluescript plasmid containing a 2.0 kb *Bam*HI PCR generated fragment of the *fnbB* gene from *S. aureus* 114	Amp^R	This study
pBluescript::*fnbB* 138	pBluescript plasmid containing a 2.0 kb *Bam*HI PCR generated fragment of the *fnbB* gene from *S. aureus* 138	Amp^R	This study
pBluescript::*fnbB* 304	pBluescript plasmid containing a 2.0 kb *Bam*HI PCR generated fragment of the *fnbB* gene from *S. aureus* 304	Amp^R	This study
pBluescript::*fnbB* 304	pBluescript plasmid containing a 2.0 kb *Bam*HI PCR generated fragment of the *fnbB* gene from *S. aureus* 304	Amp^R	This study
pBluescript::*fnbB* 563	pBluescript plasmid containing a 2.0 kb *Bam*HI PCR generated fragment of the *fnbB* gene from *S. aureus* 563	Amp^R	This study
pBluescript::*fnbB* 3077	pBluescript plasmid containing a 2.0 kb *Bam*HI PCR generated fragment of the *fnbB* gene from *S. aureus* 3077	Amp^R	This study
pBluescript::*fnbB* 3110	pBluescript plasmid containing a 2.0 kb *Bam*HI PCR generated fragment of the *fnbB* gene from *S. aureus* 3110	Amp^R	This study

Table 2.2 Plasmids, continued

Plasmid	Features	Marker(s)	Source/ Reference
pBluescript::*fnbB* 233	pBluescript plasmid containing a 2.0 kb *Bam*HI PCR generated fragment of the *fnbB* gene from *S. aureus* 3110	Amp^R	This study
pQE30	*E. coli* vector for the expression of hexa-histidine tagged recombinant proteins	Amp^R	Quiagen
pQE30::rFnBPB$_{163-480}$ / rN2N3 isotype I	pQE30 derivative encoding the N2N3 subdomain of FnBPB isotype I from *S. aureus* 8325-4	Amp^R	This study
pQE30::rN2N3 isotype II	pQE30 derivative encoding the N2N3 subdomain of FnBPB isotype II from *S. aureus* N315	Amp^R	This study
pQE30::rN2N3 isotype III	pQE30 derivative encoding the N2N3 subdomain of FnBPB isotype III from *S. aureus* MSSA476	Amp^R	This study
pQE30::rN2N3 isotype IV	pQE30 derivative encoding the N2N3 subdomain of FnBPB isotype IV from *S. aureus* P1	Amp^R	This study
pQE30::rN2N3 isotype V	pQE30 derivative encoding the N2N3 subdomain of FnBPB isotype V from *S. aureus* 2	Amp^R	This study
pQE30::rN2N3 isotype VI	pQE30 derivative encoding the N2N3 subdomain of FnBPB isotype VI from *S. aureus* 3077	Amp^R	This study
pQE30::rN2N3 isotype VII	pQE30 derivative encoding the N2N3 subdomain of FnBPB isotype VII from *S. aureus* 233	Amp^R	This study
pQE30::rFnBPB$_{37-480}$	pQE30 derivative encoding residues the full length A domain (N1N2N3) of FnBPB from strain 8325-4	Amp^R	This study

Table 2.2 Plasmids, continued

Plasmid	Features	Marker(s)	Source/ Reference
pQE30::rFnBPB$_{163-463}$	pQE30 derivative encoding residues 163-463 of FnBPB from strain 8325-4	Amp^R	This study
pQE30::rFnBPB$_{163-308}$	pQE30 derivative encoding subdomain N2 (residues 163-308) of FnBPB from strain 8325-4	Amp^R	This study
pQE30::rFnBPB$_{309-480}$	pQE30 derivative encoding subdomain N3 (residues 309-480) of FnBPB from strain 8325-4	Amp^R	This study
pQE30::rFnBPB$_{163-480}$ N312A/F314A	pQE30 derivative encoding the N2N3 subdomain of FnBPB from strain 8325-4 with mutations encoding the changes N312A and F314A	Amp^R	This study
pQE30::rFnBPB$_{163-480}$ S224A	pQE30 derivative encoding the N2N3 subdomain of FnBPB from strain 8325-4 with mutations encoding the change S224A	Amp^R	This study
pQE30::rFnBPB$_{163-480}$ Y3244A	pQE30 derivative encoding the N2N3 subdomain of FnBPB from strain 8325-4 with mutations encoding the change Y324A	Amp^R	This study
pCU1	Derivative of pC194 and pUC19. Shuttle vector	Amp^R in *E. coli* Cm^R in *S. epidermidis*	Augustin *et al.*, 1992
pCF77	pCU1 derivative containing an entire copy of the *clfA* gene	Amp^R in *E. coli* Cm^R in *S. epidermidis*	Hartford *et al.*, 1997

Table 2.2 Plasmids, continued

Plasmid	Features	Marker(s)	Source/ Reference
p*fnbB*A::R*clfA*	pCF77 derivative encoding chimeric protein FnBPBA::RClfA	Amp^R in *E. coli* Cm^R in *S. epidermidis*	This study
p*fnbB*	p*fnbB*A::R*clfA* derivative containing an entire copy of the *fnbB* gene from strain 8325-4	Amp^R in *E. coli* Cm^R in *S. epidermidis*	This study

^{R} Resistance

Table 2.3 Primes

Primer	Sequence (5'-3') [a,b]	5' Restriction site
FnBPB A F	CCGGGATCCAAGAAAACACAAATTGGGAGC	*Bam*HI
FnBPB A R	CCGGGATCCACATGAATAGAATCTTCTTCAG	*Bam*HI
FnBPA A F	CCGGGATCCGTGAAAAACAATCTTAGGTAC	*Bam*HI
FnBPA A R	CCGGGATCCTATCAATAGCTGATGAATCCG	*Bam*HI
FnBPB probe I F	CTGGTCAAGTAACTAAAGG	
FnBPB probe I R	GTATAATAATAGTTATAATATC	
FnBPB probe II F	ACTGGTCAAGTAACATCTG	
FnBPB probe II R	GTAGTATTTATGATATCCTGA	
FnBPB probe III F	TAAAGGTGGATTGTATACAG	
FnBPB probe III R	TAATAGTAATAACCGTAATTAG	
FnBPB probe IV F	ACTGGTCAAGTAACATCTG	
FnBPB probe IV R	AGTAATAGTTATAATAACCTTG	
FnBPB probe V F	CTGGTCAAGTAACATCTGG	
FnBPB probe V R	GGATAATATGGGTAATAATAGT	
FnBPB probe VI F	GCTAATAAGCCAACAGTCAAAG	
FnBPB probe VI R	CTCGTATATCCAGTTCAATTAACTTG	
FnBPB probe VII F	ATATAAACACATTGGTTCAGATG	
FnBPB probe VII R	TCTCCACTGGAGGCTCAGATTTAATGTC	
FnBPB probe I F	AAAGGTAGTAATCAAATGG	

Primer	Sequence (5'-3') [a,b]	5' Restriction site
FnBPB probe I R	GTTAAGGTATATCCTCTATC	
FnBPB probe II F	GATAGTGTTACTGTAACGG	
FnBPB probe II R	TAGCGATTTTCAGGGTATC	
FnBPB probe III F	TAGTAATTTAGCTGGTGGAC	
FnBPB probe III R	GATATCCCCCATAAACATAG	
FnBPB probe IV F	CAAAGCAAATGGAAATGCTC	
FnBPB probe IV R	AGTTGGTATCCCAAATGAG	
FnBPB probe V F	GAAAGGTAGCAACTCTAATG	
FnBPB probe V R	TGTTAATGTATAGCCGTGG	
FnBPB probe VI F	CTCAGGGAAGTAATCCAAATG	
FnBPB probe VI R	CCATTATCCCAAGTTAATTGAT	
FnBPB probe VII F	CTTAACACAAGGCAGTAATG	
FnBPB probe VII R	ACTAAGCCATTATCCCAAG	
FnBPB N2 I F	GGGGGATCCGGTACAGATGTAACAAATAAAG	*Bam*HI
FnBPB N3 I R	AATCCCGGGTTACTTTAGTTTATCTTTGCCG	*Sma*I
FnBPB N2 II F	GGGGGATCCGGTACAGATGTAACAAATAAAG	*Bam*HI
FnBPB N3 II R	GCGCCCGGGTTATTTGGTTTATCTTTACCATG	*Sma*I
FnBPB N2 III F	CCTGGATCCGGTACAGATGTAACAAGTAAAGTG	*Bam*HI

Primer	Sequence (5'-3') [a,b]	5' Restriction site
FnBPB N3 III R	AATCCCGGGTTAATTTGGCTTATCTTTACCGTCG	*Sma*I
FnBPB N2 IV F	CCTGGATCCGGTACAGATGTAACAAATAAAGTG	*Bam*HI
FnBPB N3 IV R	ATTCCCGGGTTAATTTGGCTTATCTTTGCCGTC	*Sma*I
FnBPB N2 V F	TAAGGATCCGGTACAGATGTAACAAGTAAAG	*Bam*HI
FnBPB N3 V R	ATTCCCGGGTTAATTTGGTTTATCTTTACCGTCG	*Sma*I
FnBPB N2 VI F	AATGGATCCGGCTCAGATGTAACAAGTAAAG	*Bam*HI
FnBPB N3 VI R	TCTCCCGGGTTAATTGGGCTTATCTTTGCCGT	*Sma*I
FnBPB N2 VII F	CTAGGATCCGGTACAGATGTAACAAGTAAAG	*Bam*HI
FnBPB N3 VII R	AATCCCGGGTTTCTTCGATTGTACCATTC	*Sma*I
FnBPB N1 I F	CGGGGATCCGCATCGGAACAAAACAATAC	*Bam*HI
FnBPB N2 I R	CTCCCCGGGCTATTGAATATTAAATATTTTGCTAA	*Sma*I
FnBPB N3 I F	CCCGGATCCTATTTAGGTGGAGTTAGAGATAAT	*Bam*HI
FnBPB N3ΔL R	ATTCCCGGGTAATTTTTCCAAGTTAAATTACTTG	*Sma*I
FnBPB N312A F	GAATTATCTTTA**GC**TCTA**GC**TATTGATCC	
FnBPB F314A R	GGATCAATA**GC**TAGA**GC**TAAAGATAATTC	
FnBPB S224A F	CTAACAACCAGTCGTTA**GC**CTCTGTGACAGTAACTG	
FnBPB S224A R	CAGTTACTGTCACAGAG**GC**TAACGACTGGTTGTTAG	
FnBPB Y324A F	CACACCTTTTTGGA**GC**TTATAACTATTATTATAC	
FnBPB Y324A R	GTATAATAATAGTTATAA**GC**TCCAAAAAGGTGTG	

Primer	Sequence (5'-3') [a,b]	5' Restriction site
FnBPB UPR F	GCAGAATTCGTCGGCTTGAAATACGCTG	*Eco*RI
FnBPB N3 R2	AATGGATCCTTACTTTAGTTTATCTTTGCCG	*Bam*HI
FnBPB FnBRs F	CCCAAGCTTGATGATGTCAGC	*Hind*III
FnBPB FnBRs R	CCCAAGCTTGAACGCCTTCATAGTGTC	*Hind*III

[a] Restriction sites used for cloning are underlined [b] Nucleotides changed for site-directed mutagenesis are indicted in boldface type.

probes were constructed by PCR using Taq polymerase as described above but using DIG DNA labeling mix (10 μl, Roche) in place of dNTPs.

In both cases, PCR products were purified either directly or from an agarose gel using the Wizard SV GEL and PCR Clean-Up System purification kit (Promega).

2.4 Cloning of *fnbB* gene fragments into pBluescript

Generic primers FnBPB A F and FnBPB A R (Table 2.3) corresponding to conserved DNA encoding the signal sequence and fibronectin binding domain 2, respectively, were designed from conserved sequences in *fnbB* genes from publicly available *S. aureus* genomes. PCR products were cleaved at *Bam*HI restriction sites incorporated into the primers, ligated to *Bam*HI-cleaved pBluescript DNA and transformed into chemically competent *E. coli* XL-1 Blue cells (Section 2.7). Transformants were screened for the presence of recombinant plasmids using the rapid colony screening procedure developed by Le Gouill & Dery, 1991 and validated by DNA sequencing.

2.5 DNA hybridisation using *fnbA and fnbB* isotype-specific probes

DIG-labelled isotype-specific probes were synthesised by PCR. Primers were designed to amplify a small region of DNA (~300 bp) in the N3 subdomain of FnBPB isotypes I-VII or FnBPA isotypes I-VII (Loughman *et al.*, 2008). The PCR products were labeled by incorporating DIG-labeled dNTPs (Roche). Five ng of DNA encoding the A domain of FnBPA or FnBPB from clinical or bovine isolates was spotted onto positively charged nylon membranes (Roche) and allowed to air-dry. Membranes were incubated for 5 min on blotting paper soaked in denaturation solution (1.5 M NaCl, 0.5 M NaOH), 5 min in neutralization solution (1.5 M NaCl, 1 M Tris-HCl, pH 7.4), and finally for 15 min on blotting paper soaked with 2x SSC solution (300 mM NaCl, 30 mM tri-sodium citrate). DNA was fixed on the membranes by incubation at 120°C

for 30 min. Membranes were incubated for 2 h at 68°C in pre-hybridization solution (5x SSC, 0.1 % w/v N-lauroylsarcosine, 0.02 % w/v SDS and 1x Blocking Reagent (Roche). DIG-labeled probes were denatured by heating at 95°C for 10 min, diluted in pre-hybridization solution and incubated with nylon membranes for 18 h at 68°C. Following hybridization, the membranes were washed twice with 2x SSC / 0.1 % w/v SDS at room temperature followed by two washes with 0.5x SSC / 0.1 % w/v SDS at 68°C for 20 min. Membranes were equilibrated for 30 min in maleic acid buffer (100 mM maleic acid, 150 mM NaCl, pH 7.5), and bound DIG-labeled probes were detected by incubation for 30 min with alkaline phosphatase-conjugated anti-DIG antibody (Roche) diluted 1:10,000 in maleic acid buffer. After washing twice with maleic acid buffer containing 0.3 % v/v Tween 20, the chemiluminescence substrate CSPD (Roche) was used to detect bound anti-DIG antibodies and membranes were exposed to X-OMAT UV Plus Film (Kodak) and visualised using a Kodak X-OMAT 1000 Processor developing machine.

2.6 Cloning of FnBPB truncates into pQE30 and isolation of mutants

Gene fragments encoding FnBPB protein truncates were amplified by PCR using specific primer pairs (Table 2.3). Forward primers incorporated a *Bam*HI restriction site while reverse primers contained a *Sma*I restriction site and included a 3` stop codon.

2.6.1 rFnBPB $_{163-480}$ / rN2N3 isotype I

Primers FnBPB N2 I F and FnBPB N3 I R were designed to amplify DNA encoding the N2N3 subdomain (residues 163-480) of FnBPB isotype I from the genomic DNA of *S. aureus* strain 8325-4. *Bam*HI and *Sma*I-cleaved DNA was ligated with pQE30 DNA cleaved with the same enzymes to generate plasmid pQE30 rFnBPB$_{163-480}$ for the production of rN2N3 isotype I.

2.6.2 rN2N3 isotypes II-VII

The equivalent N2N3 regions of FnBPB isotypes types II-VII were amplified using the relevant primer pairs (Table 2) and genomic DNA templates from strains N315, MSSA476, P1, 2, 3077 and 233. Each *Bam*HI and *Sma*I-cleaved PCR product was ligated with pQE30 DNA cleaved with the same enzymes to generate plasmids pQE30 rN2N3 II-VII.

2.6.3 rFnBPB$_{37-480}$

Primers FnBPB N1 I F and FnBPB N3 I R were used to amplify DNA encoding residues 37-480 (subdomains N1, N2 and N3) of FnBPB from strain 8325-4 using genomic DNA as the template. *Bam*HI and *Sma*I-cleaved DNA was ligated with pQE30 DNA cleaved with the same enzymes to generate plasmid pQE30 rFnBPB$_{37-480}$.

2.6.4 rFnBPB$_{163-463}$

The gene fragment encoding residues 163-463 of FnBPB from *S. aureus* strain 8325-4 was amplified using primer pair FnBPB N2 I F and FnBPB N3ΔL R and plasmid pQE30::rFnBPB$_{163-480}$ as the template. *Bam*HI and *Sma*I-cleaved DNA was ligated with pQE30 DNA cleaved with the same enzymes to generate plasmid pQE30 rFnBPB$_{163-480}$.

2.6.5 rFnBPB$_{163-308}$ (rN2)

Primers FnBPB I N2 F and FnBPB N2 I R were used to amplify DNA encoding residues 163-308 (subdomain N2) of FnBPB from strain 8325-4 using pQE30::rFnBPB$_{163-480}$ as the template. *Bam*HI and *Sma*I-cleaved DNA was ligated with pQE30 DNA cleaved with the same enzymes to generate plasmid pQE30 rFnBPB$_{163-308}$.

2.6.6 rFnBPB$_{309-480}$ (rN3)

Primers FnBPB N3 I F and FnBPB N3 I R were used to amplify DNA encoding residues 309-480 (subdomain N3) of FnBPB from strain 8325-4 using pQE30::rFnBPB$_{163-480}$ as the template. *Bam*HI and *Sma*I-cleaved DNA was ligated with pQE30 DNA cleaved with the same enzymes to generate plasmid pQE30 rFnBPB$_{309-480}$.

2.6.7 Site-directed mutagenesis of pQE30rFnBPB$_{163-480}$

The pQE30 expression plasmid containing the *S. aureus* 8325-4 DNA sequence encoding rFnBPB$_{163-480}$ was subjected to site-directed mutagenesis by the Quickchange method (Stratagene) (Figure 2.1). Two complementary primers, each containing the desired nucleotide changes, were extended during thermal cycling creating a mutated plasmid with staggered DNA nicks. The resulting PCR products were digested with *Dpn*I at 37°C for 1 h to remove parental methylated wild-type DNA and then transformed into competent cells of *E. coli* strain XL-1 Blue. Transformants were screened by restriction analysis and verified by DNA sequencing. Plasmids containing the correct codon changes were transformed into *E. coli* strain Topp3 for protein expression and purification as described in Section 2.8.

2.7 Transformation of *E.coli* cells with plasmid DNA

Competent *E. coli* cells were prepared by the $CaCl_2$ method (Sambrook & Russell, 2001). Competent cells (200 μl) were incubated on ice for 30 min with 2 ng plasmid or 20 ng DNA ligation reactions. The mixture was then incubated at 42°C for 2 min followed by a further 2 min on ice. Next, 1 ml L-broth was added and the mixture was incubated with shaking for 1 h at 37°C. 100 μl of the mixture was plated on L-agar plates containing ampicillin and incubated for 16-24 h. Transformants were screened for the presence of recombinant plasmids using the rapid colony screening procedure developed by Le Gouill and Dery (1991).

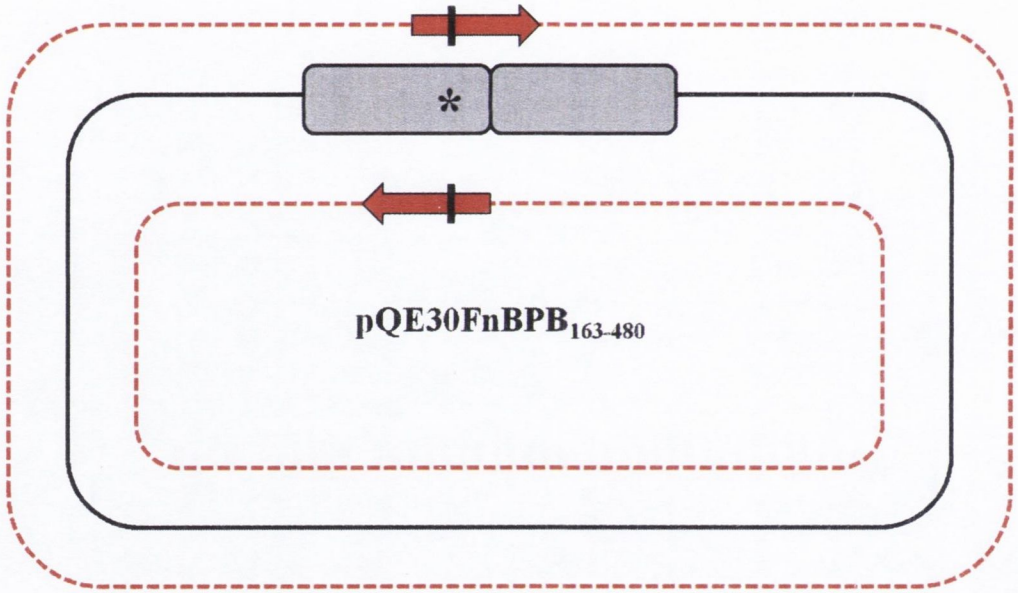

Figure 2.1 Site-directed mutagenesis of the N2N3 subdomain of FnBPB

A plasmid containing the coding sequence for rFnBPB163-480 was used as a template for PCR with mutagenic primers containing the desired codon changes(s). These primers anneal to both DNA strands surrounding the target site for mutation (*) and are extended by DNA polymerase to generate daughter plasmids that are circular but nicked. The resulting PCR product is treated with *Dpn*I to digest the original parental plasmid DNA which is methylated. The remaining plasmids are transformed into *E. coli* where nicked strands are repaired and plasmid replication can take place.

2.8 Expression and purification of His-tagged recombinant proteins

Recombinant His-tagged proteins were purified by immobilised nickel-chelate affinity chromatography. Proteins expressed from pQE30 contained an N-terminal hexahistidine tag. Expression was induced by the addition of 1mM IPTG to exponentially growing cells. After 4 h cells were harvested by centrifugation and resuspended in 30 ml binding buffer (0.5 M NaCl, 20 mM Tris-HCl, 20 mM imidazole, pH7.9) containing protease inhibitors (Complete EDTA-free, Roche). Cells were lysed in a French pressure cell and the lysate was cleared by high-speed centrifugation. DNAse was added to the supernatant which was filtered through a 0.45 μm Sartorius filter.

A HiTrap Chelating HP column (GE Healthcare) was charged with 150 mM Ni^{2+} and equilibrated with binding buffer. The cleared lysate was applied to the column and the column was then washed with binding buffer. Bound protein was eluted in fractions with a continuous linear gradient of imidazole (5-100 mM) in 0.5 M NaCl, 20 mM Tris-HCl (pH 7.9). Samples were analysed by SDS-PAGE and fractions containing protein of the correct molecular weight were pooled and dialysed against PBS for 16 h at 4 °C. Protein concentrations were determined by measuring the absorbance at 280 nm according to the Beer-Lambert Law (A_{280} = E.c.l)

2.9 Construction of shuttle plasmids encoding FnBPB constructs

2.9.1 p*fnbB*A::R*clfA*

Shuttle plasmid pCF77 was described previously (Hartford *et al.*, 1997). It carries the entire *clfA* gene from strain 8325-4 together with 1300bp of upstream sequence containing both the sigma factor 70-dependent and sigma factor B-dependent *clfA* promoters. pCF77 DNA was cleaved with *Eco*RI and *Bam*HI to remove DNA encoding the fibrinogen-binding A domain of ClfA and upstream promoter region which is contained within a 3 kb *Eco*RI-*Bam*HI fragment of the plasmid. Primers FnBPB UPR

F and FnBPB N3 R2 were designed to amplify 1.9 kb of *fnbB* DNA from strain 8325-4 genomic DNA which encodes the entire A domain of FnBPB and contains the upstream *fnbB* promoter. The PCR product was cleaved with *Eco*RI and *Bam*HI at restriction sites incorporated into the primers and ligated to pCF77 DNA cleaved with the same enzymes to generate plasmid p*fnb*BA::R*clf*A for the expression a chimeric protein containing the A domain of FnBPB and the stalk (Region R) and cell wall anchoring domain of ClfA.

2.9.2 p*fnbB*

Primers FnBPB FnBRs F and FnBPB FnBRs R were designed to amplify DNA encoding FnBPB residues 388-980 using genomic DNA from strain 8325-4 as a template. The PCR product was cleaved with *Hind*III at restriction sites incorporated into the primers and ligated to p*fnbB*A::R*clfA* DNA cleaved with the same enzyme to generate plasmid p*fnb*B for the expression of full length wild-type FnBPB.

2.10 Preparation and transformation of electrocompetent *S. epidermidis*

Electrocompetent *S. epidermidis* cells were prepared by a protocol based on the method described by Lofblom *et al.*, (2007). *S. epidermidis* strain TU3298 grown in Basic Medium (1% casein hydrolysate, 2.5% yeast extract, 0.5% glucose, 0.5% NaCl and 0.1% K_2HPO_4, pH7.4) was diluted 1/100 in fresh BM. Bacterial cells were grown at 37°C with shaking to an OD600 of 0.5-0.6. Cells were harvested by by centrifugation at 3000 g for 10 min and washed in ice cold 10% glycerol. A further two washes were carried out before final resuspension in 2 ml of ice cold glycerol. Electrocompetent cells were aliquoted, snap frozen and stored at -70°C.

Thawed electrocompetent cells (90 μl) were incubated with 2-4 μg of plasmid DNA for 20 min at room temperature. Electroporation was carried out in 0.1 cm electrode gap cuvettes (Flowgen) which were pulsed at 2 kV, 25 μF capacitance and 100 Ω resistance. Cells were immediately added to 1

ml of Basic Medium and incubated at 37°C for 1 h with shaking. Following recovery, cells were plated on TSA with selective antibiotic.

2.11 Antibodies to *S. aureus* FnBPB

Antibodies to *S. aureus* FnBPB were a gift from Prof. P. Speziale, University of Pavia, Italy. Polyclonal and monoclonal antibodies raised against the isotype I N2N3 domain of FnBPB were generated by immunising rabbits and mice, respectively, with $rFnBPB_{163-480}$ from *S. aureus* 8325-4. For ELISA and immunoblotting experiments, antibodies were generally diluted between 1/500 and 1/2000 in 1-10 % milk in PBS or TS buffer.

2.12 Protein electrophoresis and immunoblotting

2.12.1 SDS-PAGE

Proteins for sodium dodecyl sulphate-polyacrylamide gel electrophoresis (SDS-PAGE) were adjusted to specific final concentrations in PBS and diluted 2-fold in final sample buffer (10 % (v/v) glycerol, 5 % (v/v) β-mercaptoethanol, 3 % (w/v) SDS, 0.01 % bromophenol blue in 62.5 mM Tris-HCl, pH 6.8). 20 μl volumes were separated by SDS-PAGE (Laemmli, 1970) using 4.5 % stacking and 10 % separating acrylamide gels, except in the case of cell wall-associated proteins, which were separated through 7.5 % separating acrylamide gels. Prestained protein molecular weight markers were purchased from New England Biolabs or Invitrogen. Protein samples were electrophoresed at 130 V. After separation, proteins were either visualised using Coomassie blue stain or electroblotted onto PVDF membranes (Roche) for 1 h at 100 V using a wet transfer cell (BioRad) for detection.

2.12.2 Western immunoblotting

Non-specific binding to PVDF membranes was blocked by incubation for 2-18 h in 10% (w/v) skimmed milk powder (Marvel) in TS

buffer (10 mM Tris-HCl, 0.9% NaCl, pH 7.4). Blots were probed with polyclonal anti-FnBPB antibodies diluted 1:500 in 10% skimmed milk (Marvel) in TS buffer. The blots were then washed three times with gentle agitation for 15 min in TS-Tween (10 mM Tris-HCl, 0.9% NaCl, pH 7.4, 0.05 % (v/v) Tween 20 (Sigma) to remove unbound antibodies. Bound antibodies were detected using goat anti-rabbit antibodies conjugated to horseradish peroxide (Dako) according to the manufacturer's instructions. Reactive bands were visualised using the LumiGLO Reagent and peroxide detection system (Cell Signalling Technology) as recommended by the manufacturer, exposed to X-Omat autoradiographic film (Kodak) and visualised using a Kodak X-OMAT 1000 Processor developing machine.

2.12.3 Whole cell and recombinant protein dot immunoblotting.

For whole cell dot immunoblotting, *S. epidermidis* cells were grown to exponential phase (OD_{600} nm of 0.4-0.5), washed twice in PBS and adjusted to an OD_{600} nm of 2.0 in PBS. For recombinant protein dot immunoblotting, $rFnBPB_{163-480}$ was diluted from 2 μg to 0.156 μg/ ml in PBS. 5 μl of each cell suspension or protein dilution to be analysed was applied to a nitrocellulose membrane (Protran, Schleicher & Schull) and allowed to dry. Membranes were blocked for 2 h in TS buffer (10mM Tris-HCl, 0.9% NaCl, pH 7.4) containing 10% (w/v) skimmed milk powder (Marvel). Rabbit polyclonal antibodies specific for *S. aureus* surface proteins were diluted to a suitable concentration in 10 % milk in TS buffer and incubated with the membrane for 1.5 h with shaking. Membranes were washed three times in TS buffer to remove unbound antibody. Membranes were then incubated with goat anti-rabbit antibodies conjugated to horseradish peroxidase (Dako) diluted 1:2000 in 10 % milk in TS buffer for 1.5 h. Membranes were then washed three times in TS buffer to remove unbound antibody. The membrane was developed in the dark using the chemiluminescent substrate LumiGlo (New England BioLabs) as described above.

2.13 Enzyme linked immunosorbent assays (ELISA)

2.13.1 Antibody ELISA

Recombinant FnBPB proteins, diluted to various concentrations in PBS, were coated onto microtitre plates (Nunc) in sodium carbonate buffer (pH 9.6) for 18 h at 4°C. The plates were washed three times with PBS and blocked with 5% (w/v) skimmed milk powder (Marvel) in PBS for 2 h at 37°C. Wells were washed again and appropriate dilutions of mouse monoclonal anti- 6xHis antibody (7E8), mouse monoclonal anti-FnBPB isotype I antibody (2E11) or polyclonal rabbit anti-FnBPB isotype I antibodies were added to the wells and incubated for 1 h at room temperature with shaking. After three washes with PBS, the appropriate HRP-conjugated secondary antibody was added to the wells and the plate was incubated for 1h at room temperature with shaking. After three further washes with PBS, bound HRP-conjugated antibodies were detected by the addition of 100 μl of 3,3',5,5'-tetramethylbenzidine (TMB) (0.1 mg/ml) (Sigma) prepared in 0.05 M phosphate citrate buffer (pH5.0) containing 0.006% (v/v) hydrogen peroxide. Plates were then developed for 10 min. The reaction was stopped by the addition of 50 μl of 2 M H_2SO_4 to each well. The absorbance at 450 nm was measured with an ELISA plate reader (Multiskan EX, Labsystems).

2.13.2 Ligand ELISA

Human fibrinogen (Enzyme Research Labs; 10 μg/ml in PBS) and fibronectin (Calbiochem; 10 μg/ml in PBS) were coated onto microtitre plates (Sarstedt) in 100 μl volumes and kept at 4°C for 18 h. rGST and rGST γ-chain (gifts from Dr.Joan Geoghegan, Trinity College Dublin) were diluted to 10 μg/ml in sodium carbonate buffer (pH9.6), coated onto microtitre plates (Nunc) in 100 μl volumes and incubated for 18 h at 4°C. Human aortic elastin (Elastin Products Company; 20 μg/ml) was immobilised onto microtiter wells (Nunc) in 50 μl volumes and air dried

under UV light (366 nm) at room temperature for 18 h. All wells were subsequently blocked with 5% skimmed milk in phosphate buffered saline (PBS) for 2 h at 37°C. Following three washes with PBS containing 0.05 % v/v Tween 20 (PBST) various concentrations of purified rFnBPB proteins in PBS were added and incubated at 37°C for 2 h. After three washes with PBST, bound protein was detected by incubation with a 1:500 dilution of monoclonal antibody 7E8 that recognizes the N-terminal hexahistidine fusion tag. After 1h incubation with shaking at room temperature, the wells were washed three times with PBST followed by 100 µl per well of goat anti-mouse IgG antibodies conjugated to horseradish peroxidase (HRP) diluted 1:2000. After incubation for 1 h at room temperature, wells were washed three times with PBST, and bound HRP-conjugated antibodies were detected with 100 µl per well of 3,3',5,5'-tetramethylbenzidine (TMB; Sigma) in 0.05 M phosphate-citrate buffer containing 0.006% (v/v) hydrogen peroxide. After incubation at room temperature for 10 min the reaction was stopped by adding 50 μl of 2 M H_2SO_4. The absorbance at 450 nm was measured with an ELISA plate reader (Multiskan EX, Labsystems).

ELISA-type binding graphs shown throughout this thesis are graphs of individual experiments that are representative of three independent experiments. Each plot in such graphs represents the average of triplicate wells.

2.14 Surface plasmon resonance (SPR)

2.14.1 Surface plasmon resonance analysis of rFnBPB proteins binding to immobilised ligands

Surface plasmon resonance (SPR) was performed using the BIAcore X100 system (GE Healthcare). Human fibrinogen, fibronectin, aortic elastin (as above) and rGST γ-chain were covalently immobilised on CM5 sensor chips using amine coupling. This was performed using 1-ethyl-3-(3-dimethylaminopropyl) carbodiimide hydrochloride (EDC), followed by *N*-

hydroxysuccinimide (NHS) and ethanolamine hydrochloride, as described by the manufacturer. Fibrinogen, fibronectin, aortic elastin and rGST γ-chain were dissolved in 10 mM sodium acetate at pH 4.5 (50 μg/ml) and then immobilised onto separate chips at a flow rate of 30 μl/min in PBS (Gibco) to give response levels of 4500, 8000, 5000 and 3000 response units (RU), respectively. As a negative control, each chip contained a second flow cell which was uncoated to provide a reference flow cell for these studies. Concentrations of recombinant proteins were flowed over immobilised ligands and the reference cell in PBS for 180s at a flow rate of 5 μl/min. Next, PBS was passed over the surface for 300s to allow dissociation. This was followed by a regeneration step, passing 1M NaCl over the chip for 1 min at a flow rate of 5 μl/min. All sensorgram data presented were subtracted from the corresponding data from the blank cell. The response generated from injection of buffer over the chip was also subtracted from all sensorgrams. Rate constants for association (k_a) and dissociation (k_d) and the equilibrium dissociation constant (K_D) were obtained by locally fitting the data using the BIAevaluation software version 3.0 using the Langmuir 1:1 binding model. Alternatively, a plot of the level of binding (RU) at equilibrium against concentration of analyte was used to determine the overall affinity (K_D).

Sensorgrams shown throughout this thesis are representative of three independent experiments which were carried out using separate ligand-coated chips.

2.14.2 Surface plasmon resonance analysis of the inhibition of binding of rFnBPB$_{163\text{-}480\ to}$ immobilised rGST γ-chain by divalent cations

For inhibition assays, rFnBPB$_{163\text{-}480}$ (1 μM) was pre-incubated with doubling dilutions of $MgCl_2$, $NiCl_2$ or $CaCl_2$ for 1 h at room temperature. These solutions were then passed over the surface of rGST γ-chain coated-chips as described in Section 2.14.1 above. The level of binding (RU) at equilibrium was plotted against cation concentration. The graph shown in

this thesis is representative of three independent experiments which were carried out using three different rGST γ-chain coated-chips.

2.15 Bacterial adherence to immobilised ligands

2.15.1 Bacterial adherence to immobilised fibrinogen and fibronectin

Microtitre plates (Sarstedt) were coated with doubling dilutions of human fibrinogen and fibronectin in PBS. Control wells contained PBS only. Plates were incubated overnight at 4°C and blocked for 2 h at 37°C with 5 % (w/v) bovine serum albumin (BSA). 100 μl of washed exponential phase *S. epidermidis* cultures at an OD_{600} of 2.0 in PBS were added and incubated for 2 h at 37°C. After three washes with PBS, adherent cells were fixed with formaldehyde (25 % v/v) for 15 min and then stained with crystal violet (0.5 % w/v) for 1 min. The wells were extensively washed with PBS to remove excess stain. Cell-bound crystal violet was solubilised using acetic acid (5 % v/v) and the absorbance at 570 nm was measured using an ELISA plate reader (Multiskan EX, Labsystems).

2.15.2 Bacterial adherence to immobilised elastin

Microtitre wells (Povair) were coated with various concentrations of human aortic elastin and air-dried under UV light (366 nm) at room temperature overnight. Control wells contained PBS only. Plates were washed three times with PBS and the remaining protein sites were blocked with BSA (5 % w/v) for 2 h at 37°C. *S. epidermidis* cultures were grown to exponential phase, washed in PBS and resuspended to an $OD_{600\ nm}$ of 2.0. Bacterial cell adherence was measured using a nucleic acid binding probe, SYTO-13 (Molecular Probes) supplied as a 5mM stock solution which was diluted 1:10 in 10 mM Tris-HCl (pH 7.5) to give a working dilution of 0.5 mM. Washed bacterial cultures were were incubated with SYTO-13 at a final concentration of 2.5 μM at room temperature for 15 min in the dark. Elastin-coated wells were washed three times in PBS. Stained bacterial cells were added to the wells and incubated in the dark at room temperature for

1.5 h. After incubation, wells were washed three times with PBS and the amount of cells bound was determined using a LS-50B florescent spectrophotometer with excitation at 488 nm and emission at 509 nm.

Adherence graphs shown throughout this thesis are graphs of individual experiments that are representative of three independent experiments.Each plot in such graphs represent the average of triplicate wells.

2.16 Endothelial cell culture

The cell line EA. hy926, established by the fusion of human umbilical endothelial cells (HUVEC) and the permanent lung epithelial carcinoma cell line A549 (Edgell *et al.*, 1983) was cultured in Dulbecco's Modified Eagle's medium (DMEM; Invitrogen) supplemented with foetal bovine serum (FBS; 10%) and L-glutamine (2 mM) at 37°C and 5% CO_2. Pooled primary HUVECs were purchased from Lonza (Basel, Switzerland) and cultured in endothelial basal medium supplemented with 2% fetal bovine serum, bovine brain extract (including heparin), human endothelial growth factor, hydrocortisone and GA-1000 (Gentamicin & Amphotericin B) at 37°C and 5% CO_2 according to manufacturer's instructions (Lonza). Endothelial cells were cultured in T75 flasks to approximately 95% confluency, liberated with trypsin-EDTA, resuspended in the relevant culture medium and added to 24-well plates containing thermanox glass coverslips (Massey *et al.*, 2001). Plates were incubated for 48 h as described above before the coverslips were removed, dip-washed in PBS and added to new 24-well plates containing fresh medium and bacteria (Massey *et al.*, 2001).

2.17 Endothelial cell adhesion and invasion assays

Cultured cells were dissociated from plastic flasks using trypsin-EDTA solution (Invitrogen) and approximately 5 x 10^5 (in 0.5 ml medium) were seeded into each well of 24-well plates (Nunc) containing 13 mm

plastic Thermanox cover slips (Fisher) and allowed to attach for 48 h (37°C, 5% CO_2). Coverslips were dip-washed once in PBS and placed in the well of a new 24-well plate containing 450 μl of DMEM containing 10% FBS. To each well, 50 μl of washed bacteria were added (approximately 2 x 10^6 CFU *S. epidermidis*) and incubated for 30–120 min at 37°C in 5% CO_2. To measure the total number of bacteria associated with the cells (adherent and internalised), coverslips were dip-washed 3 times in PBS and added to wells containing 500 μl 0.5% Triton X-100. Wells containing coverslips were agitated by pipetting to fully lyse the cells and CFU were enumerated by serial dilution and plating onto TSA agar plates and incubated overnight at 37°C in 5% CO_2.

For invasion assays, the bacterial suspension was removed and replaced with 500 μl DMEM containg 10% FBS supplemented with 200 μg/ml gentamicin and incubated at 37°C in 5% CO_2 for 60 min to allow killing of bacterial cells that were unable to invade the endothelial cells. Coverslips were washed three times in PBS, lysed and plated for CFU as described for the adhesion assay above.

2.18 Bioinformatic and phylogenetic analysis of FnBPB A domain isotypes

Complete *S. aureus* genome sequences (strains COL, N315, Mu50, MW2, MSSA476 and MRSA252) were searched for proteins displaying homology to FnBPB from *S. aureus* 8325-4. All strains except MRSA252 contained both an FnBPA-like and an FnBPB-like protein. Strain MRSA252 contained a single FnBP that was more similar to $FnBPA_{8325\text{-}4}$ than to $FnBPB_{8325\text{-}4}$, and was designated as FnBPA in this analysis. DNA encoding the A domain of FnBPB from *S. aureus* strain P1 was cloned and sequenced as described in Section 2.4. Subdomains of FnBPBs from the sequenced strains and strain P1 were defined based on amino acid alignments with the FnBPs from strain 8325-4 (Signäs *et al.*, 1989, Jönsson *et al.*, 1991). Pairwise alignments of FnBPs were performed the ExPasy

SIM-alignment tool (http://us.expasy.org/), and the percentage of identical amino acids between the aligned proteins was noted. Multiple alignments of FnBP proteins were performed using the Clustal W tool (http://www.ebi.ac.uk/). The concatenated MLST allele sequences of *S. aureus* strains were downloaded from the MLST database (http://saureus.mlst.net/). A phylogenetic analysis of concatenated MLST allele sequences was conducted using MEGA version 4 (Tamura *et al.*, 2007).

2.19 Generation of a 3D structural model for the N2N3 subdomain of FnBPB

A theoretical model of the structure of subdomains N2 and N3 of region A of FnBPB was obtained by submitting the amino acid sequence for this segment of the protein to the Protein homology recognition engine (Phyre) service of the 3D-PSSM website (http://www.sbg.bio.ic.ac.uk/phyre/). This web-based tool models the structure of this sequence based on the known crystal structures of similar proteins. The resulting hits are scored based on the estimated precision of the prediction. The highest score for the N2N3 subdomain of FnBPB was structure based on the equivalent domains of the apo-form of *S. aureus* clumping factor ClfA. The accuracy of the structural prediction was estimated to be very high (e 1.2^{-33}). The pdb file supplied by the Phyre service was downloaded and viewed by the user-sponsored molecular visualization system pyMOL (http://www.pymol.org).

Chapter 3

Analysis of the diversity and phylogeny of *fnbB* alleles

3.1 Introduction

S. aureus is a very important and versatile human pathogen. Much research has been focused on the virulence factors that are important in the initiation of staphylococcal infections. This depends on the ability of the bacterium to adhere to the host's extracellular matrix (ECM) via surface-expressed ligand-binding proteins termed Microbial Surface Components Recognising Adhesive Matrix Molecules (MSCRAMMs). These proteins have evolved to recognize specifically distinct constituents of the host plasma and extracellular matrix in an attempt to evade the host's immune system and establish a focus of infection (Foster & Höök, 1998). The importance of *S. aureus* MSCRAMMs is suggested by the fact that genes encoding these proteins are present in most invasive isolates of *S. aureus* (Peacock *et al.*, 2002).

The fibronectin-binding proteins (FnBPs) A and B of *S. aureus* are multifunctional MSCRAMMs which recognise fibronectin, fibrinogen and elastin (Wann *et al.*, 2000, Roche *et al.*, 2004, Jonsson *et al.*, 1991). FnBPA and FnBPB are encoded by two closely linked but separately transcribed genes, *fnbA* and *fnbB* (Signas *et al.*, 1989, Jonsson *et al.*, 1991). Transcription of the *fnb* genes is restricted to the early exponential phase of growth (Greene *et al.*, 1995) under the control of the global regulators, Agr and SarA (Wolz *et al.*, 2000, Saravia-Otten *et al.*, 1997). While some clinical isolates (~34%) only contain *fnbA*, the majority of strains (~66%) carry both *fnbA* and *fnbB* (Peacock *et al.*, 2000). The ability to adhere to immobilised fibronectin does not vary in relation to the number of *fnb* genes present (Peacock *et al.*, 2000). However, studies with clinical isolates suggest that strains associated with invasive diseases are significantly more likely to have both *fnbA* and *fnbB* genes (Peacock *et al.*, 2000). Also, the percentage of strains carrying both the *fnbA* and the *fnbB* gene was high as 91% in a study of MRSA isolates (Rice *et al.*, 2001).

FnBPA and FnBPB have considerable organization and sequence similarity and are composed of a number of distinct domains (Jonsson *et al.*, 1991) (Figure 3.1). Starting from the N-terminus, each FnBP contains a signal sequence followed a ligand-binding A domain. The A domains of FnBPA and FnBPB mediate binding to the C-terminus of the fibrinogen γ-chain and to elastin peptides (Wann *et al.*, 2000, Roche *et al.*, 2004). Both A domains are predicted to comprise three separately folded subdomains (N1, N2, and N3) similar to the fibrinogen-binding A domains of *S. aureus* ClfA and *S. epidermidis* SdrG (Ponnuraj *et al.*, 2003, Deivanayagam *et al.*, 2002). The X-ray crystal structure of the N2N3 subdomains of ClfA and SdrG have been solved and show striking similarities to each other, despite the fact that they are only ~20% identical at the amino acid level (Ponnuraj *et al.*, 2003, Deivanayagam *et al.*, 2002) (Figure 1.5). The crystal structures reveal that subdomains N2 and N3 are independently folded in a novel type of immunoglobulin fold (DEv-IgG). The A domains of FnBPA and FnBPB each share 25% amino acid sequence similarity with the A domain of ClfA which binds to the same region of fibrinogen as the FnBPs. However, unlike ClfA, the A domains of FnBPA and FnBPB also bind elastin (Roche *et al.*, 2004). Sequence alignments of the A domains of FnBPA, FnBPB and ClfA indicates a similar domain architecture. The minimal ligand-binding site in the A domain of ClfA and FnBPA has been localised to the N2N3 subdomains (McDevitt *et al.*, 1997, Keane *et al.*, 2007b) (Figure 3.1).

Located distal to the A domains of FnBPA and FnBPB are multiple tandemly arranged fibronectin-binding repeats (FnBRs) which mediate binding to the N-terminal type I modules of fibronectin by a tandem β-zipper mechanism (Schwarz-Linek *et al.*, 2003) (Figure 1.13). These regions are unfolded and do not contain any discernable secondary structure (House-Pompeo *et al.*, 1996). Studies of FnBPA from strain 8325-4 indicated that the fibronectin-binding moiety is organised into 11 tandem repeats, each capable of interacting with the N-terminal domains of fibronectin (Meenan *et al.*, 2007). Based on amino acid sequence alignments, it has been

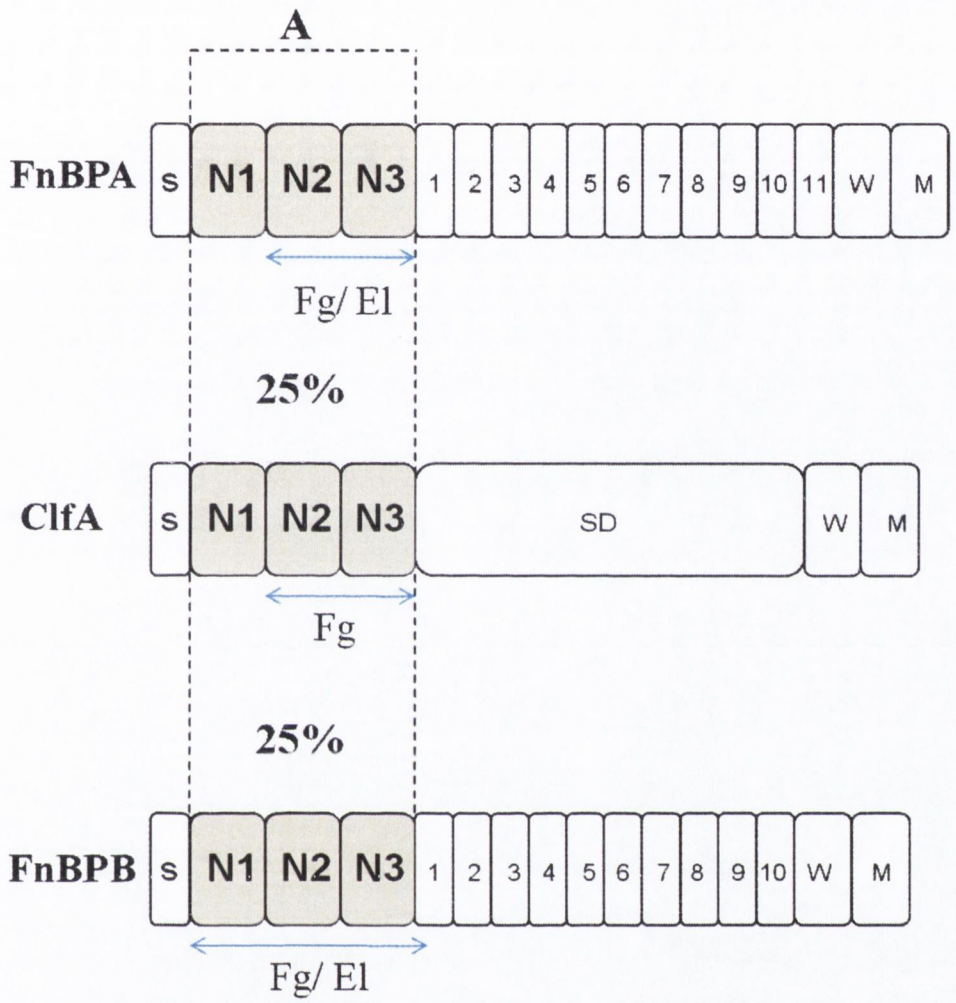

Figure 3.1 Domain organisation of FnBPA, FnBPB and ClfA of *S. aureus*

The A domain of ClfA is divided into three individual subdomains N1, N2 and N3 as indicated. The percentage amino acid identity between the A domains of ClfA and the FnBPs is shown. Based on this homology, it is proposed that the A domain of FnBPA and FnBPB shares a similar structural organisation. The A domain of ClfA bind to the same region of fibrinogen (Fg) as the FnBPs which also bind elastin (El). The minimal ligand-binding site in the A domains of FnBPA and ClfA has been localised to subdomains N2 and N3. Signal sequences (S) and wall/membrane spanning regions are indicated. The serine-aspartate repeat region of ClfA (SD) is shown and the fibronectin-binding repeats of FnBPA and FnBPB are numbered.

predicted that FnBPB from strain 8325-4 contains 10 rather than 11 repeats. (Meenan *et al.*, 2007) (Figure 3.1). In both FnBPA and FnBPB, the FnBRs are followed by C-terminal features required for cell wall anchoring such as a transmembrane domain, an LPXTG motif and a short cytoplasmic domain (Signas *et al.*, 1989, Jonsson *et al.*, 1991). The *fnbA* and *fnbB* genes were originally cloned from *S. aureus* strain 8325-4 (Signäs *et al.*, 1989, Jönsson *et al.*, 1991). The fibronectin-binding repeats of FnBPA (residues 512-874) and FnBPB (residues 481-810) are highly homologous, sharing 90 % identical residues. By contrast, the A domains of FnBPA (residues 37-511) and FnBPB (residues 37-480) are far more divergent and share only 48 % amino acid identity (Figure 1.11). Polyclonal antibodies raised against the A domain of FnBPA of strain 8325-4 do not react with the A domain of FnBPB from same strain, and vice-versa (Loughman, 2006).

Studies of *S. aureus* FnBPs have focused largely on the FnBPs expressed from strain 8325-4. However, the presence of a defective sigma factor (SigB) means that the level of FnBPs expressed by this strain is low (Bischoff *et al.*, 2004). By contrast, *S. aureus* strain P1 expresses high-levels of FnBPs on it's cell surface as indicated by the high-level of adherence of the strain to immobilised fibronectin and elastin as well as the it's potent ability to promote platelet activation (Roche *et al.*, 2004, Peacock *et al.*, 2000, Fitzgerald *et al.*, 2006) (see Section 1.3.1.5.5). The elimination of FnBP expression in a P1*fnbAfnbB* mutant correlated with impaired fibronectin and elstin-binding and delayed platelet aggregation (Fitzgerald *et al.*, 2006). It was observed in a previous study that polyclonal antibodies raised against the recombinant A domains of FnBPA and FnBPB from strain 8325-3 did not efficiently recognize the native FnBPs expressed by strain P1 (Loughman, 2006). Immunoblotting experiments were carried out which involved cell wall extracts from *S. aureus* strains P1, a P1*fnbAfnbB* mutant and P1*fnbAfnbB* complemented with plasmids over expressing FnBPA or FnBPB from strain 8325-4. Anti-FnBPA A domain and anti-FnBPB A domain antibodies showed a strong reaction with their cognate

antigen in either complemented strain but failed to react detectably with FnBPs expressed by wild type P1 (Loughman, 2006). These results raised the possibility that differences in amino acid sequences of the A domains was responsible for the difference in antibody reactivity.

The *fnb* genes have undergone greater sequence divergence than other surface protein genes such as *clfB* and *clfA* (Kuhn *et al.*, 2006). That study investigated the divergence of 17 *S. aureus* genes in a collection of 60 *S. aureus* strains. The genes included ten genes encoding surface proteins (*clfA*, *clfB*, *fnbA*, *fnbB*, *spa*, *ebpS*, *map*, *sdrC*, *sdrD* and *sdrE*) which were compared to seven housekeeping genes routinely used in multilocus sequence typing (MLST) (*arcC*, *aroE*, *glpF*, *gmk*, *pta*, *tpi* and *yqiL*). All of the surface protein-encoding genes had undergone a higher degree of nucleotide diversity compared to housekeeping genes. Interestingly, the amount of diversity varied, ranging from 2-fold for *spa* to greater than 10-fold for *fnbA* and *fnbB* (Kuhn *et al.*, 2006). These findings, together with the results of the immunoblotting experiments with strain P1, prompted our group to examine more closely the A domains of FnBPs. Initially, the region of *fnb*A encoding the A domain of FnBPA of *S. aureus* P1 was cloned, sequenced and compared to the A domain of the 8325-4 FnBPA (Keane *et al.*, 2007b). The N1 domains of FnBPA from 8325-4 and P1 were highly homologous (91.4% identical) compared to domains N2 (78.3% identical) and N3 (59.2% identical) (Keane *et al.*, 2007b). In the same study, variant FnBPA A domain residues were studied in the context of a predicted 3D model of domains N2 and N3 of strain 8325-4. This model was based on the crystal structure of the equivalent domain of ClfA (Deivanayagam *et al.*, 2002). Most of the variant residues were predicted to be located on the surface of the protein. Residues identified by mutagenesis to be important in ligand binding were largely conserved. Using recombinant forms of the N2N3 domains of FnBPA from strain P1 and 8325-4, it was shown that sequence variation results in a reduced ability of polyclonal and monoclonal antibodies raised against the 8325-4 protein to bind to the P1 protein while

the ability to bind to fibrinogen and elastin was retained (Keane *et al.*, 2007b). Subsequently, seven variants (isotypes I-VII) of FnBPA were later identified based on divergence in the minimal ligand-binding N2N3 subdomain (Loughman *et al.*, 2008). Each recombinant FnBPA N2N3 retained ligand-binding function but was antigenically distinct. Modelling the 3D structures showed that the amino acid variation occurred in surface-exposed residues and not in those involved in ligand-binding (Loughman *et al.*, 2008).

The purpose of this study was to determine if, like FnBPA, divergence in the A domain of FnBPB is a common feature amongst *S. aureus* strains. To facilitate this, an investigation including FnBPBs from a variety of clonal types was required. Using a genetically diverse collection of *S. aureus* strains that had been characterised by MLST, *fnbB* sequences encoding FnBPB A domains were analysed. The phylogeny of *fnbB* alleles was demonstrated and compared to the phylogenetic relatedness of the strains as determined by MLST.

3.2 Results

3.2.1 Cloning and sequencing analysis of DNA encoding the A domain of FnBPB from *S. aureus* strain P1.

It has been demonstrated previously that the FnBPA A domain from strain P1 differs substantially from that of FnBPA from strain 8325-4, sharing only 73.5 % identical amino acids. This was sufficient to create differences in surface-exposed epitopes which affected immuno-crossreactivity, while ligand binding activity was conserved (Keane *et al.*, 2007b). Previous immunoblotting experiments with proteins released from whole cells indicated that, like FnBPA, the FnBPB protein of *S. aureus* strain P1 reacted weakly with polyclonal antibodies raised against the A domain of FnBPB from strain 8325-4 (Loughman, 2006). It was predicted that similar to FnBPA, amino acid variation in the A domain of FnBPB is responsible for the reduced ability of anti- $FnBPB_{(8325\text{-}4)}$ antibodies to cross react with FnBPB expressed by strain P1.

In order to verify this, the region of the P1 *fnbB* gene encoding the A domain of FnBPB was amplified using 8325–4-based primer pairs homologous to the more conserved flanking sequences. The resulting PCR product was cloned, sequenced and the deduced amino acid sequence compared to that of domain A of FnBPB from strain 8325-4 by pairwise alignment (Figure 3.2). The overall amino acid sequence identity was 80 % but closer examination indicated that the greatest divergence occurred in subdomains N2 and N3. As was found with the FnBPA proteins from these two strains, the N1 subdomains of FnBPBs from 8325-4 and P1 were very similar (90.9% identical) compared to domains N2 (74.5% identical) and N3 (78.5% identical). This suggested that like FnBPA, the low reactivity of the anti-$FnBPB_{(8325\text{-}4)}$ antibodies against cell wall extracts of *S. aureus* P1 is the result of the presence of different epitopes on the P1 FnBPB protein.

3.2.2 *fnbB* gene variation in *S. aureus* genome sequences.

The A domain sequences of FnBPB from *S. aureus* strain P1 and those deduced from analysis of published *S. aureus* genomes were compared to determine if diversity in this domain is widespread. All of the sequenced strains except strain MRSA252 and the bovine strain RF122 contain genes encoding both FnBPA and FnBPB. Strains MRSA252 and RF122 both encode the FnBPA protein only. The amino acid sequences of the A domains of FnBPB from *S. aureus* strains 8325-4, COL, USA300, Mu50, MSSA476, N315, MW2 and P1 were aligned in pairwise combinations and the identities were calculated. These strains can be grouped according to their MLST types.

The FnBPB proteins of strains COL, USA300 and 8325-4 have identical A domains which were classified here as isotype I. These three strains belong to MLST clonal complex 8 (CC8; Enright *et al.*, 2002), indicating a close phylogenetic relationship. Two ST-5 strains (N315, Mu50) belonging to CC5 containe novel *fnbB* genes specifying A domain proteins that are identical to one another, but are only 78% identical in amino acid sequence to isotype I and were called A domain isotype II. ST-1 strains (MSSA476, MW2; belonging to CC1) specify identical FnBPB A domains that share 70.9% and 72.2% amino acid identity with isotypes I and II, respectively, and were called isotype III. The FnBPB A domain from *S. aureus* strain P1 (a novel single-locus variant of ST-133), is divergent from isotypes I, II and III and was called isotype IV.

Variation between A domain isotypes I-IV was largely confined to the N2N3 subdomains while the N1 subdomains are more conserved with identities of 94%-100% between different isotypes. In FnBPA, the N2 and N3 subdomains represent the minimal ligand binding region while subdomain N1 is not required for binding to fibrinogen or elastin (Keane *et al.*, 2007b). Based on its homology with FnBPA, it is predicted that the N2 and N3 subdomains of FnBPB are also sufficient to promote binding to

Figure 3.2 Amino acid Sequence alignment of region A of FnBPB from *S. aureus* strains 8325-4 and P1

Amino acid alignment of region A of FnBPB from *S. aureus* strain 8325-4 (37-480) and P1 (37-481) showing the extent of residue diversity along subdomains N1 (black), N2 (red) and N3 (blue). * indicates an identical residue while : and . indicate conserved and semi-conserved substitutions, respectively.

these ligands. For this reason, FnBPB isotypes were defined based on the highly variable N2N3 subdomain amino acid sequences.

The divergent N2N3 subdomains of isotypes I-IV share between 61.1% and 80.6 % identify in any pairwise alignment (Table 3.1). By contrast, the C-terminal fibronectin-binding motifs of FnBPB isotypes I-IV were highly conserved indicating that the FnBPB A domains alone, in particular the N2N3 subdomains, are subject to variation.

3.2.3 DNA hybridisation analysis using *fnbB* isotype-specific probes.

To determine the distribution of FnBPB A domain isotypes I-IV in *S. aureus* strains of different MLST types and to identify novel A domain isotypes, DNA hybridization was used with isotype-specific probes homologous to DNA segments encoding a portion of most highly divergent N3 subdomain. DNA encoding the entire A domain was amplified by PCR using generic A domain flanking primers. The resulting PCR products were spotted onto membranes and hybridised with the DIG-labelled isotype-specific probes. The results of hybridization experiments with probes I-IV is shown in Figure 3.3. The probes were shown to be FnBPB isotype-specific because each probe only hybridised to the appropriate control *fnbB* fragment (top row of blots). The FnBPB isotype / *fnbB* allelic variant was predicted without having to sequence the A domain-encoding region of the *fnbB* genes. As shown in Figure 3.3, *fnbB* gene fragments from each strain only hybridised to one probe. The isotyping data is summarised in Table 3.2. *fnbB* DNA from *S. aureus* strains 2 (ST7),114 (ST39), 233 (ST45), 304 (ST39), 138 (ST30), 563 (ST37), 3077 (ST17) and 3110 (ST12) did not hybridise to probes I-IV indicating that they may specify novel FnBPB isotypes or lack the *fnbB* gene .

3.2.4 Identification of novel FnBPB isotypes (Types V, VI and VII).

The *fnbB* gene fragments amplified from *S. aureus* strains 2 (ST7), 114 (ST39), 233 (ST45), 304 (ST39), 138 (ST30), 563 (ST37), 3077 (ST17)

and 3110 (ST12) did not hybridise to probes specific for FnBPB isotypes I-IV. The *fnbB* gene fragments from these strains were cloned, sequenced and the deduced A domain amino acid sequences were compared to the sequences of A domains isotypes I-IV. The amino acid identities were calculated and are shown in Table 3.3. *S. aureus* strains 2 (ST7) and 3110 (ST12) specify a novel FnBPB A domain called isotype V (N2N3, 68.8 – 73.3 % identical to isotypes I – IV). The A domains of strains 3077 (ST17) and 233 (ST45) are also different and were called isotype VI (N2N3, 66.0–76.6 % identical to types I – V) and isotype VII (N23, 66.2% - 85% identical to types I-VI), respectively. Strains 114, 563, 138 and 304 specify an identical A domain which is 92% identical to isotype II and was called isotype II* (Table 3.2).

3.2.5 Phylogenetic analysis of FnBPB A domain isotypes I-VII in strains of different MLST types

Figure 3.4 shows a neighbour-joining phylogenetic tree which was constructed based on the concatenated sequences of the seven housekeeping genes used for MLST analysis. As MLST reflects the evolution of the stable core genome (Lindsay & Holden, 2004) this tree describes the phylogenetic relatedness of the *S. aureus* strains studied here. It is separated into two major clusters as was also shown previously in a detailed phylogenetic analysis of thirty diverse *S. aureus* isolates(Cooper & Feil, 2006). The FnBPB A domain isotypes specified by each genotype (as predicted by DNA hybridisation or sequencing) are indicated. The phylogeny of *fnbB* alleles illustrated here does not correspond to that of the core genome which is reflected by MLST. For example, two strains that cluster together in Group 1 (ST49 and ST52) carry *fnbB* genes encoding isotype II, as do distantly related strains from Group 2 (ST5 and ST18). Conversely, clustered strains such as ST8 and ST97 from Group 2 contain *fnbB* genes encoding isotypes I and IV, respectively. Isolates belonging to the same ST (ST45) were found to specify different FnBPB isotypes (II and

Table 3.1 Percentage amino acid identities of FnBPB A domain isotypes I – IV

The region of the *fnbB* gene encoding the A domain was cloned from amplified from genomic DNA of *S. aureus* strain P1, cloned and sequenced. The deduced amino acid sequences were compared to the equivalent region of the *fnbB* gene present in the sequenced *S .aureus* genomes. Strains belonging to the same clonal complex (CC) were found to share identical A domains. Based the sequences of the most diverent N2 and N3 domains, four isotypes (I-IV) of FnBPB were identified.

		CC8 8325-4 COL USA300	CC5 N315 Mu50	CC1 MSSA476 MW2	CC133 P1
FnBPB Type I	8325-4 COL USA300	100 %	72.6 %	61.1 %	77.1 %
FnBPB Type II	N315 Mu50	72.6 %	100 %	65.5 %	80.6 %
FnBPB Type III	MSSA476 MW2	61.1 %	65.5 %	100 %	65.5 %
FnBPB Type IV	P1	77.1 %	80.6 %	62.2 %	100 %

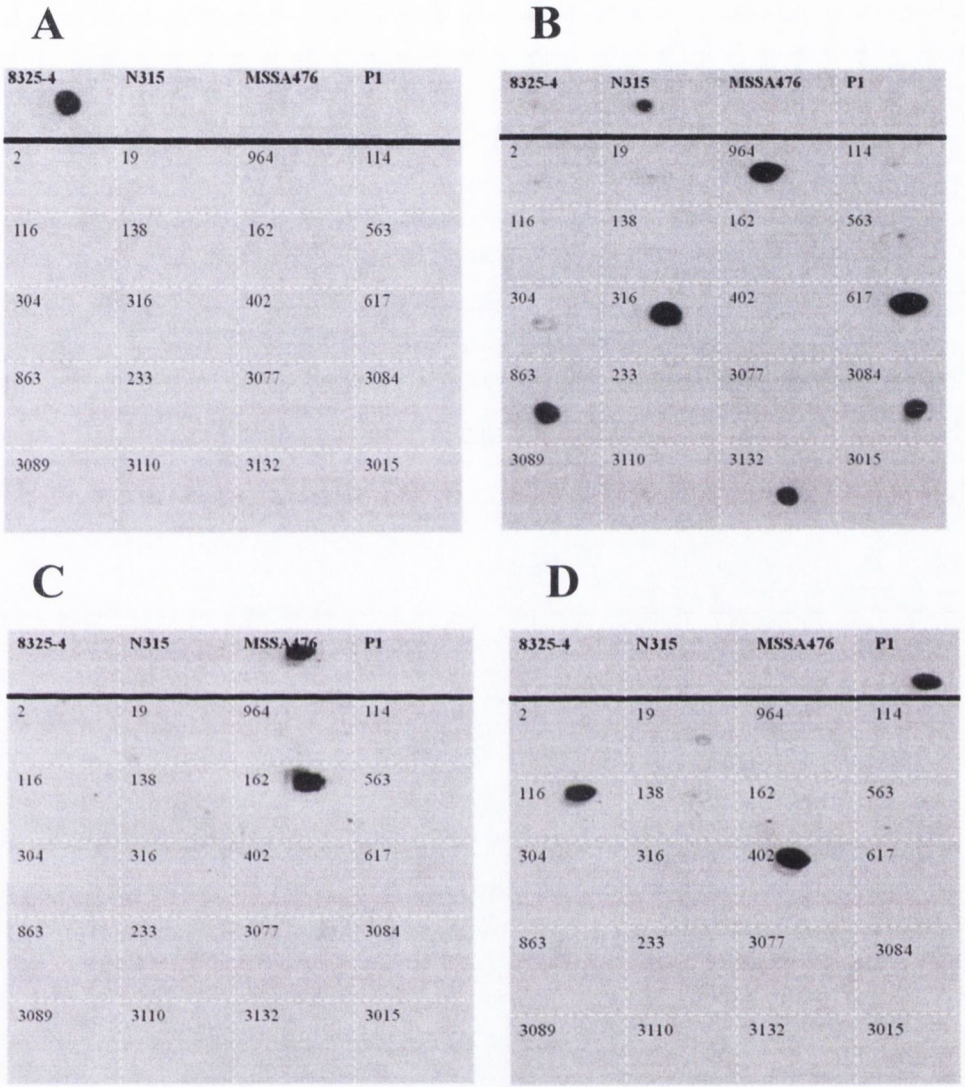

Figure 3.3 FnBPB A domain isotyping of human *S. aureus* strains by dot blot hybridisation

DNA fragments coding for the entire A domain of FnBPB were amplified by PCR from human *S. aureus* isolates. PCR products were spotted onto nitrocellulose membranes and probed with DIG-labelled probes specific for FnBPB isotypes (**A**) I, (**B**) II, (**C**), III and (**D**) IV. *fnbB* DNA from strains 8324-5, N312, MSSA476 and P1 was used as a control (top row of blots).

Table 3.3 Percentage amino acid identities of FnBPB A domain isotypes I – VII

	I	II	III	IV	V	VI	VII
I	100 %	72.6 %	61.1 %	77.1 %	68.8 %	76.6 %	74.4 %
II	72.6 %	100 %	65.5 %	80.6 %	76.4 %	73.5 %	82.0 %
III	61.1 %	65.5 %	100 %	65.5 %	60.7 %	66.0 %	66.2 %
IV	77.1 %	80.6 %	62.2 %	100 %	78.3 %	73.1 %	73.7 %
V	68.8 %	76.4 %	60.7 %	78.3 %	100 %	71.2 %	71.8 %
VI	76.6 %	73.5 %	66.0 %	73.1 %	71.2 %	100 %	85.0 %
VII	74.4 %	82.0 %	66.2 %	73.7 %	71.8 %	85.0 %	100 %

Table 3.2 FnBPB A domain (N2N3) isotype distribution in human *S. aureus* strains

A diverse collection of *S. aureus* strains representing different MLST types were screened for *fnbB* alleleic variants. The FnBPB A domain isotype specified by each strain was determined by either DNA hybridisation using isotype-specific probes (I-IV) homologous to a portion of the highly divergent N3 sub-domain or by sequencing.

Strain	ST	FnBPB	Method of detection
8325-4	8	I	Genome sequence (Signas *et al.*, 1989)
N315	5	II	Genome sequence (Kuroda *et al.*, 2001)
MSSA476	1	III	Genome sequence (Holden *et al.*, 2004)
P1	973	IV	*fnbB* gene sequence (This study)
2	7	V	*fnbB* gene sequence (This study)
19	10	IV	DNA hybridization
114	39	II*	*fnbB* gene sequence (This study)
116	9	II	DNA hybridization
138	30	II*	*fnbB* gene sequence (This study)
162	1	III	DNA hybridization
304	39	II*	*fnbB* gene sequence (This study)
316	49	II	DNA hybridization
402	13	IV	DNA hybridization
563	37	II*	*fnbB* gene sequence (This study)
617	45	II	DNA hybridization
863	20	II	DNA hybridization
964	18	II	DNA hybridization
3015	123	IV	DNA hybridization
3077	17	VI	*fnbB* gene sequence (This study)
3084	52	II	DNA hybridization
3089	97	IV	DNA hybridization
3110	12	V	*fnbB* gene sequence (This study)
3132	2	II	DNA hybridization
233	45	VII	*fnbB* gene sequence (This study)

Figure 3.4 Neighbour-joining tree based upon concatenated sequences of MLST alleles from human *S. aureus* strains

MLST allele sequences representing each clinical strain studied here were used to generate a neighbour joining tree using MEGA 4. The A domain isotypes carried by strains of each MLST genotype, determined by sequencing and hybridization analysis, are indicated. The dashed line indicates the separation of the MLST genotypes into Groups 1 and 2, which is based on sequence data from MLST alleles and other unlinked loci (Cooper and Feil, 2006). The percentage of replicate trees in which the associated taxa clustered together in the bootstrap test (500 replicates) are shown next to the branches (Kumar *et al.*, 2004; Takezaki *et al.*, 2004). The phylogenetic tree was linearized assuming equal evolutionary rates in all lineages (Takezaki *et al.*, 2004). The evolutionary distances were computed using the Maximum Composite Likelihood method (Tamura *et al.*, 2007) and are in the units of the number of base substitutions per site.

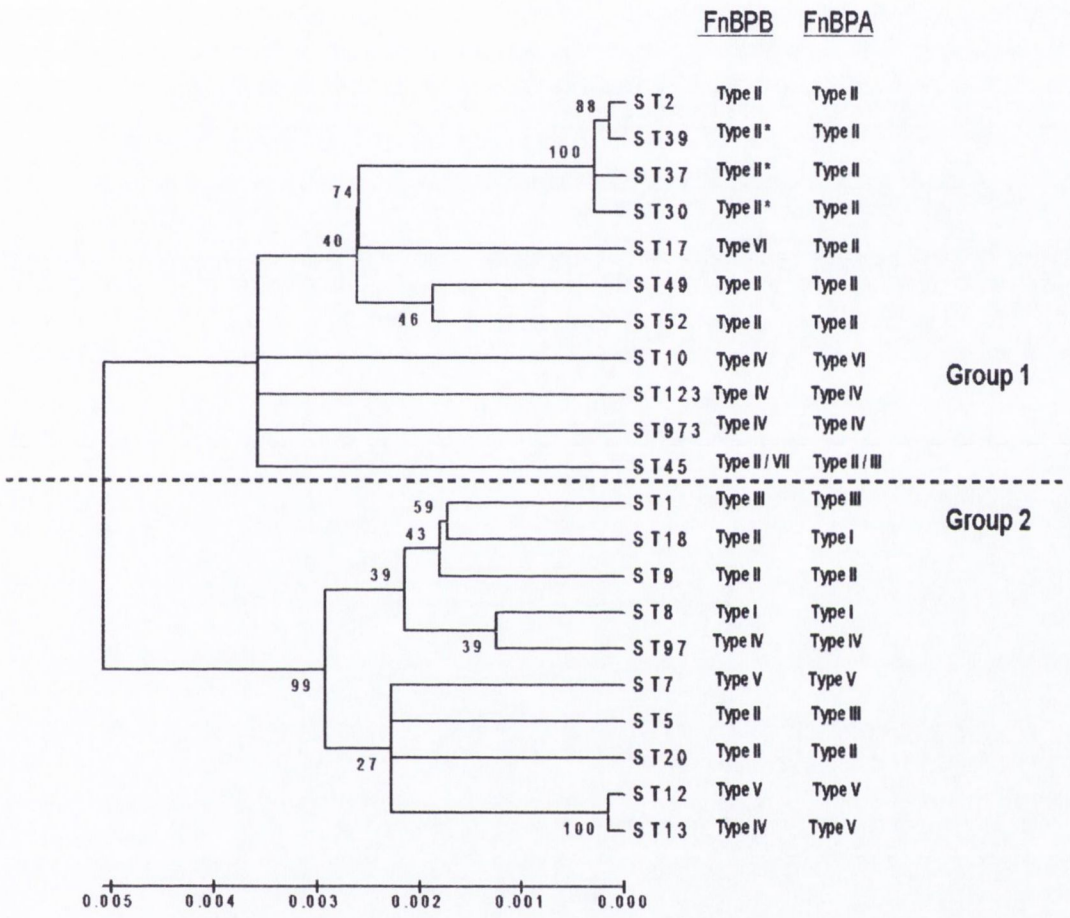
FnBPB
FnBPA
ST2 Type II Type II
ST39 Type II* Type II
ST37 Type II* Type II
ST30 Type II* Type II
ST17 Type VI Type II
ST49 Type II Type II
ST52 Type II Type II
ST10 Type IV Type VI
ST123 Type IV Type IV
ST973 Type IV Type IV
ST45 Type II / VII Type II / III
ST1 Type III Type III
ST18 Type II Type I
ST9 Type II Type II
ST8 Type I Type I
ST97 Type IV Type IV
ST7 Type V Type V
ST5 Type II Type III
ST20 Type II Type II
ST12 Type V Type V
ST13 Type IV Type V
88
100
74
40
46
59
43
39
39
99
27
100
Group 1
Group 2
0.005
0.004
0.003
0.002
0.001
0.000

VII). These results suggest that *fnbB* alleles have dispersed by horizontal transfer, most likely by homologous recombination.

The results of previous isotyping experiments involving FnBPA reported that strains 116 (ST9) and 3077 (ST17) specify an identical FnBPA A domain called isotype II (Loughman *et al.*, 2008). In this study, the same strains were found to specify different FnBPB A domains, isotypes II and VI, respectively (Figure 3.4). This indicates that the phylogeny of *fnbB* alleles does not match that of *fnbA* alleles despite the two genes being closely linked.

3.2.6 Occurrence of FnBPB isotypes I – VII in bovine *S. aureus* strains

The investigation into FnBP variation was further expanded in this study to include FnBPs from a variety of bovine *S. aureus* strains. Nineteen bovine isolates representing genetically unrelated strains were screened to determine if they specified the same FnBPA/B isotypes as human strains. This strain collection included strain RF122, the genome of which has been sequenced (Guinane *et al.*, 2008). RF122 contains only one *fnb* gene encoding FnBPA.

DNA encoding *fnbA* was amplified by PCR from the genomic DNA of each strain using generic A domain flanking primers. These PCR products hybridised to FnBPA probes specific for isotypes I, II, III or IV. Similarly *fnbB* DNA was amplified by PCR from the genomic DNA of all strains except RF122. These PCR products hybridised to FnBPB probes specific for isotype I, II, III, IV or V. The hybridisation data for experiments involving bovine *S. aureus* isolates is shown in Figures 3.5 and 3.6 and is summarised in Table 3.4. These results indicate that the FnBPA/B isotypes that are expressed by human strains are also specified by bovine strains. Furthermore, the results of this study suggest that the lack of *fnbB* in the genome of strain RF122 is not characteristic of all bovine strains. None of the bovine strains tested specify FnBPA isotypes V, VI or VII or FnBPB

isotypes VI or VII. Figure 3.7 shows a neighbour-joining phylogenetic tree which was constructed based on MLST data as described above. The FnBPA and FnBPB A domain isotypes specified by each genotype are included. The distribution of *fnbB* and *fnbA* variants does not correlate with the genetic relatedness of the strains as determined by MLST. The phylogeny of *fnbA/B* alleles carried by bovine *S. aureus* isolates is therefore very similar to that of human strains.

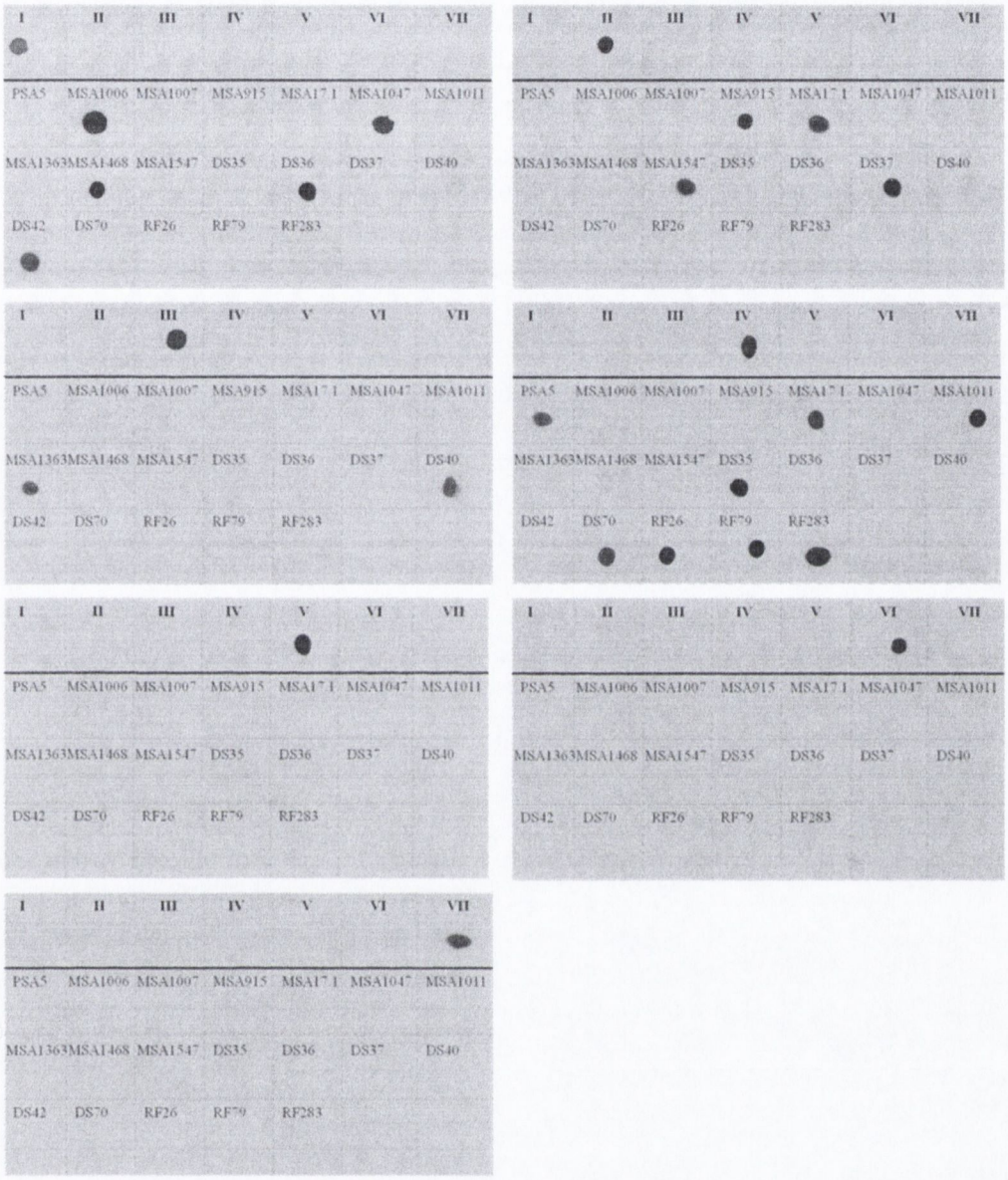

Figure 3.5 FnBPA A domain isotyping of bovine *S. aureus* strains by dot blot hybridisation

DNA fragments coding for the entire A domain of FnBPA were amplified by PCR from bovine *S. aureus* isolates. PCR products were spotted onto nitrocellulose membranes and probed with DIG-labelled probes specific for FnBPA isotypes I-VII. *fnbA* DNA from strains 8325-4, MRSA252, MSSA476, P1, 3110, RF122 and 3153 (top row of blots) was used a control for FnBPA isotypes I-VII, respectively.

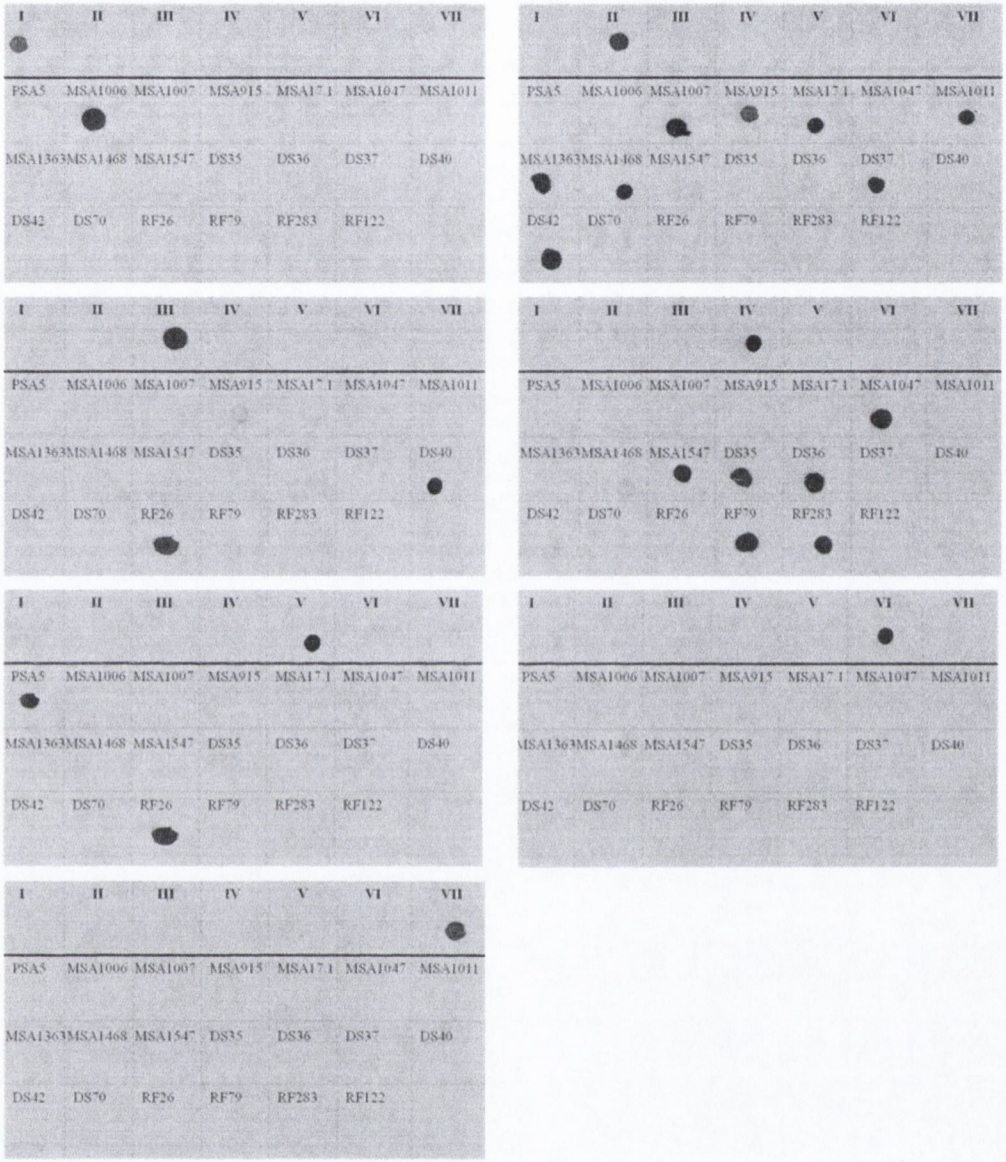

Figure 3.6 FnBPB A domain isotyping of bovine *S. aureus* strains by dot blot hybridisation

DNA fragments coding for the entire A domain of FnBPB were amplifiesd by PCR from bovine *S. aureus* isolates. PCR products were spotted onto nitrocellulose membranes and probed with DIG-labelled probes specific for FnBPB isotypes I-VII. *fnbB* DNA from strains 8325-4, N312, MSSA476, P1, 2, 3110, 3077 and 233 (top row of blots) was used a control for FnBPAB isotypes I-VII, respectively.

Table 3.4 FnBPA and FnBPB A domain isotype distribution in bovine *S. aureus* strains

Using generic primers, the *fnbA* genes were amplified from the genomic DNA of nineteen bovine strains representing different *S. aureus* MLST types. Likewise, the *fnbB* gene was amplified from the genomic DNA of the same strains, except strain RF122 which contains only *fnbA*. To determine the FnBPA/B isotypes specified by each strain, the *fnbA* and *fnbB* PCR products were subsequently probed with DNA probes specific for A domain isotypes specified by human *S. aureus* strains.

Strain	ST	FnBPA	FnBPB	Method of detection
PSA5	698	IV	V	DNA hybridization
RF79	71	IV	IV	DNA hybridization
MSA1007	708	III	II	DNA hybridization
DS37	20	II	II	DNA hybridization
DS40	1	III	III	DNA hybridization
DS42	479	I	II	DNA hybridization
MSA915	115	II	II	DNA hybridization
MSA1547	699	II	IV	DNA hybridization
MSA1047	350	I	IV	DNA hybridization
DS70	697	IV	II	DNA hybridization
MSA1363	25	III	II	DNA hybridization
RF26	97	IV	III	DNA hybridization
DS35	696	IV	IV	DNA hybridization
MSA1006	8	I	I	DNA hybridization
MSA17.1	693	IV	II	DNA hybridization
MSA1011	352	IV	II	DNA hybridization
RF283	133	IV	IV	DNA hybridization
MSA1468	694	I	II	DNA hybridization
DS36	126	I	IV	DNA hybridization
RF122	151	VI	absent	DNA hybridisation/ Genome sequence (Guinane *et al.*, 2008)

Figure 3.7 Neighbour-joining tree based upon concatenated sequences of MLST alleles from bovine *S. aureus* strains.

MLST allele sequences representing each bovine-specific strain studied here were used to generate a neighbour joining tree using MEGA 4. The A domain isotypes carried by strains of each MLST genotype, as determined by hybridization analysis, are indicated. A gene encoding FnBPB is absent from the genome of strain RF122 (ST155). The percentage of replicate trees in which the associated taxa clustered together in the bootstrap test (500 replicates) are shown next to the branches (Kumar et al., 2004). The evolutionary distances were computed using the Maximum Composite Likelihood method (Tamura *et al.*, 2007). and are in the units of the number of base substitutions per site.

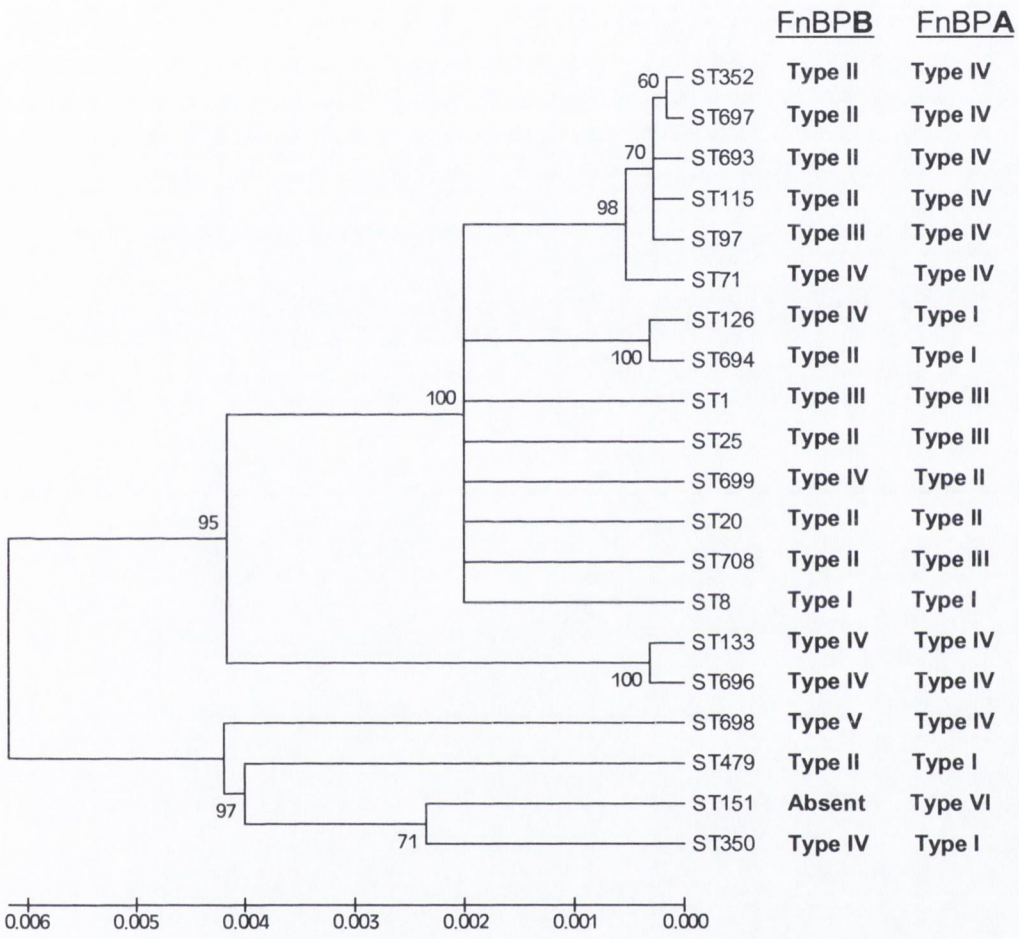
FnBPB
FnBPA
60
ST352
Type II
Type IV
ST697
Type II
Type IV
70
ST693
Type II
Type IV
98
ST115
Type II
Type IV
ST97
Type III
Type IV
ST71
Type IV
Type IV
ST126
Type IV
Type I
100
ST694
Type II
Type I
100
ST1
Type III
Type III
ST25
Type II
Type III
ST699
Type IV
Type II
95
ST20
Type II
Type II
ST708
Type II
Type III
ST8
Type I
Type I
ST133
Type IV
Type IV
100
ST696
Type IV
Type IV
ST698
Type V
Type IV
ST479
Type II
Type I
97
ST151
Absent
Type VI
71
ST350
Type IV
Type I
0.006
0.005
0.004
0.003
0.002
0.001
0.000

3.3 Discussion

An important factor in bacterial pathogenesis is the ability of the invading organism to colonise host tissue. *S. aureus* possesses on its cell surface a family of adhesion proteins known as MSCRAMMs which promote binding of the organism to components of the host extracellular matrix and play an important role in virulence. Belonging to the *S. aureus* MSCRAMM family are two fibronectin-binding proteins, FnBPA and FnBPB. These proteins are encoded by two closely linked genes, *fnbA* (Signäs *et al.*, 1989) and *fnbB* (Jönsson *et al.*, 1991). Both *fnb* genes appear to be carried by most *S. aureus* strains (Peacock *et al.*, 2000). These include the lab strain 8325-4 and the wild-type virulent strain P1 (Jonsson *et al.*, 1991, Fitzgerald 2006). Strain P1 expresses high levels of FnBPs that are responsible for its ability to bind elastin and fibronectin strongly and to promote platelet aggregation (Roche *et al.*, 2004, Fitgerald *et al.*, 2006). However, antibodies raised against the A domains of FnBPA and FnBPB from strain 8325-4 did not recognize the FnBPs expressed by *S. aureus* P1 (Keane *et al.*, 2007b).

DNA encoding the A domains of FnBPA and FnBPB was subsequently cloned, sequenced and their deduced amino acid sequences determined. FnBPA and FnBPB from strain P1 were found to be 73.5 % and 80.6 % identical to the A domains of *S. aureus* 8325-4 FnBPA and FnBPB, respectively (Keane *et al.*, 2007b; this study). Similar levels of diversity were found in the FnBPA/B A domains from the genome sequences of *S. aureus* strains. (Loughman *et al.*, 2008; this study). By contrast, the A domains of ClfA from the sequenced *S. aureus* genomes did not display such diversity and were greater than 90 % identical in any pairwise alignment. Likewise, the fibronectin-binding repeats of FnBPA and FnBPB encoded in the sequenced genomes did not display any significant differences either and were also greater than 90 % identical. This suggests a specific selective advantage in variation in the A domains of the FnBPs.

An assessment of the variation within the A domains of FnBPB from sequenced *S. aureus* strains and strain P1 indicates that the variability of this domain has a very distinct pattern. Interestingly, the differences were not spread evenly. N1 was more highly conserved while N3 was the most divergent. This is consistent with the pattern of variation in the A domain of FnBPA which was described previously (Loughman *et al.*, 2008). By comparing the FnBPB sequences specified by sequenced *S. aureus* strains and strain P1, four FnBPB variants (isotypes I-IV) were identified based on divergence in N2N3 subdomains, which are 66-76% identical to one another. In order to determine the distribution of FnBPB isotypes I-IV and to identify novel isotypes, type-specific probes were generated and used to screen *fnbB* DNA from a variety of clonal types using a well characterised strain collection of human origin and human isolates where genomes have been fully sequenced (Feil *et al.*, 2003). Three novel FnBPB isotypes were identified (isotypes V, VI and VII) which are 61.1% - 85% identical to isotypes I-IV. Phylogenetic analysis of FnBPB isotypes indicated that, similar to the phylogeny of *fnbA* alleles (Loughman *et al.*, 2008), the phylogeny of *fnbB* alleles does not correlate with that of the core genome which is reflected by MLST. This is consistent with results of the study by Kuhn *et al* (2006) in which *fnbB* alleles from MRSA strains belonging to CC1, CC5, CC8, and CC45 were sequenced and all had *fnbB* genes encoding I, II, III and VII, respectively. This matches the distribution of *fnbB* allelic variants reported here.

The evolution of *S. aureus* has been predominantly clonal where alleles are 5- to 10-fold more likely to diversify by point mutations than by recombination (Feil *et al.*, 2003). The distribution of *fnbA* and *fnbB* alleles amongst different *S. aureus* lineages suggests, however, that recombination has been involved. Horizontal transfer by homologous recombination is likely to be responsible for the dispersion of genes encoding the same FnBPA/B isotypes across strains of different phylogenies and for different *fnbA* or *fnbB* alleles in closely related strains (e.g. ST-45) which was

reported here and previously (Loughman *et al.*, 2008). Similarly, the distribution of staphylocoagulase serotypes amongst *S. aureus* strains is also likely to have occurred by recombination because the phylogenetic relationship of *coa* alleles did not match that of MLST alleles (Watanabe *et al.*, 2005). Further evidence for the role of recombination in the evolution of *S. aureus* comes from the genome structures of ST239 strains which are composed of 557 kb of ST8 DNA spliced into 2,220 kb of an ST30 strain (Robinson & Enright, 2004).

The distribution of *fnbA* alleles described in the study by Loughman *et al* (2008) does not match the distribution of *fnbB* alleles described here. Different combinations of FnBPA and FnBPB isotypes are specified by strains that cluster phylogenetically. For example, strains belonging to ST12 were shown to specify FnBPB isotype V and FnBPA isotype V while closely related strains belonging to ST13 specify FnBPB isotype IV and FnBPA isotype V (Figure 3.4). This suggests that the phylogeny of *fnbB* alleles has evolved independently from that of *fnbA* alleles and has involved separate recombination events despite the genes being closely linked. This is further supported by an analysis of the *fnb* alleles carried by strains belonging to CC30. The ST-36 strain MRSA252 belongs to CC30 and carries only one *fnb* gene, *fnbA* (Lindsay & Holden, 2004, Feil *et al.*, 2003). However, a number of closely related ST-30 strains, which also belong to CC30 (Feil *et al.*, 2003), have been found to carry both the *fnbA* and the *fnbB* genes (Loughman *et al.*, 2008, Kuhn *et al.*, 2006 and this study). This observation indicates that *fnbA* and *fnbB* alleles have evolved separately. It also suggests that the loss or gain of *fnbB* has occurred independently from the evolution of the core genome.

The study of FnBP variation in *S. aureus* was extended in this study to include bovine *S. aureus* strains. The genome of the bovine strain RF122 contains only the *fnbA* gene and lacks *fnbB*. Using generic primers, DNA encoding the A domains of FnBPA and FnBPB was amplified from the

genomic DNA of nineteen bovine *S. aureus* isolates which had been typed previously using MLST (Smyth *et al.*, 2009). The amplification of *fnbB* DNA from these strains indicated that the lack of the *fnbB* gene in strain RF122 is not a common feature of bovine *S. aureus* strains. The *fnbA* and *fnbB* PCR products were subsequently probed with DNA probes specific for A domain isotypes specified by human *S. aureus* strains. It was shown that bovine isolates specify the some of the same isotypes of FnBPA and FnBPB as those specified by human isolates. Sung *et al.*, (2008) demonstrated that the majority of animal-associated *S. aureus* strains clustered into animal-specific lineages using MLST. The fact that strains belonging to bovine-specific lineages were found here to specify some of the same FnBPA and FnBPB isotypes as strains belonging to human-specific lineages provides further evidence to suggest that the phylogeny of *fnbA* and *fnbB* alleles have evolved independently from that of the stable core genome which is reflected by MLST (Lindsay & Holden, 2004).

The distribution of FnBP isotypes across the population of bovine strains tested here was found to be uneven. None of the bovine strains specified FnBPA isotypes V, VI or VII or FnBPB isotypes VI or VII. The majority of these strains were found to specify FnBPA isotype IV and FnBPB isotype II. By contrast FnBPA isotype II was found to predominate in human clinical isolates (Loughman *et al.*, 2008). It could be postulated that this difference in FnBPA isotype frequency reflects the differences in selective pressures posed by these two distinct host immune systems.

The FnBPB isoforms described here were identified based on the sequences of the most divergent subdomains, N2 and N3. It is this region of FnBPB that, based on studies with ClfA and FnBPA, was predicted to form the minimum region required for binding to fibrinogen and, in the case of FnBPA, elastin (McDevitt *et al.*, 1992, Keane *et al.*, 2007b). In contrast to the FnBP A domains, the sequences of the fibronectin-binding repeats (FnBRs) of FnBPA and FnBPB were well conserved in all strains tested

here and previously (Loughman *et al.*, 2008). While the sequences of the FnBRs are well conserved, the number FnBRs present in FnBPA and FnBPB varies between strains (Rice *et al.*, 2001). However, the ability of strains to adhere to immobilised fibronectin does not vary in relation to the number of FnBRs within FnBP molecules (Rice at al., 2001). Any variation in fibronectin-binding by different isolates of *S. aureus* was attributed to the transcriptional activity of the Agr locus and to protease activity (Rice *et al.*, 2001). This is an example of a *S. aureus* MSCRAMM molecule where ligand binding is conserved despite sequence variation.

Another important example of FnBP variation is that which occurs in the A domain of FnBPA. Seven variants (isotypes I-VII) of FnBPA were previously identified based on divergence in the amino acid sequences of the minimal fibrinogen and elastin-binding N2N3 subdomains. The seven recombinant N2N3 isoforms bound to immobilised ligands with similar affinities indicating that the variation in A domain of FnBPA does not compromise it's ligand-binding activity. The variation was, however, sufficient to create differences in surface-exposed epitopes which affected immuno-crossreactivity (Loughman *et al.*, 2008) suggesting that variation in the A domain may be employed by *S. aureus* as a mechanism for avoiding the host immune response to FnBPA.

In this chapter, the amino acid sequence of the A domain of FnBPB from strain P1 was deduced and compared to that of strain 8325-4. The sequences were found to be 20 % divergent which could explain the inability of anti-FnBPB$_{(8325\text{-}4)}$ antibodies to recognise FnBPB expressed by strain P1 is earlier immunoblotting experiments. Seven isotypes of FnBPB were then identified in a diverse collection of *S. aureus* clinical isolates and sequenced strains. The definition of the isotypes was based on the sequences of the most variable region of the A domains, the N2N3 subdomain which is predicted to contain the minimum fibrinogen and elastin-binding sites. Like FnBPA, variation in the A domain of FnBPB was shown to be widespread

among *S. aureus* strains and variation in both FnBP proteins was found to occur in bovine as well as human isolates. Based on the previous study of FnBPA variation, it was proposed that variation in the A domain of FnBPB may similarly affect the antigenicity of this region of the protein. The significance FnBPB A domain variation is investigated in the following chapter where the functionality and antigenicity of FnBPB isoforms I-VII is tested and compared.

Chapter 4

Antigenic and functional analysis of FnBPB A domain isotypes I-VII

4.1 Introduction

The fibronectin binding proteins (FnBPs) A and B of *S. aureus are* encoded by two closely linked but separately transcribed genes, *fnbA* and *fnbB* (Signas *et al.*, 1989, Jonsson *et al.*, 1991). While most strains contain both genes, some strains contain only *fnbA* (Peacock *et al.*, 2000). The gene encoding FnBPB is present significantly more often in invasive isolates than carriage strains (Peacock *et al.*, 2002). In a study of *S. aureus* isolated from the airway of cystic fibrosis and pneumonia patients, 97% of isolates were found to possess both *fnb* genes. (Mongodin *et al.*, 2002). Taken together, these data suggest that both FnBPA and FnBPB contribute to the virulence of *S. aureus* and to the development of invasive infections. However, most investigations into the role of FnBPs in *S. aureus* pathogenesis have focused predominantly on FnBPA. Indeed FnBPA has been shown to be a virulence factor in several models of *S. aureus* infection. Heterologous expression of FnBPA in the poorly pathogenic bacterium *Lactococcus lactis*, increased infectivity 100-fold in a rat endocarditis model (Que *et al.*, 2001). FnBPA expression by *L. lactis* correlated with increased bacterial densities in vegetations and promoted the invasion of adjacent endothelial cells which resulted in enhanced valvular destruction (Que *et al.*, 2005). The role of FnBPA has also been assessed in a mouse model for septic arthritis where it was found to contribute to the induction of systemic inflammation characterised by interleukin-6 secretion, severe weight loss and mortality (Palmqvist *et al.*, 2005). Sera from healthy individuals colonised by *S. aureus* (nasal carrier) and non-carriers contains low levels of antibodies recognising FnBPA (Dryla *et al.*, 2005). Sera obtained from patients with documented *S. aureus* infections have increased anti-FnBPA antibodies, showing that FnBPA is expressed in vivo during infection and suggesting a role for FnBPA as a virulence factor (Dryla *et al.,* 2005).

Analysis of the deduced amino acid sequences of FnBPA and FnBPB from strain 8325-4 revealed that the two proteins share a similar domain organization. Originally, the N-terminal fibrinogen and elastin-binding A domains of FnBPA and FnBPB included residues 37-544 and residues 37-540, respectively (Figure 4.1). Fibronectin-binding activity is contained within the regions C-terminal to the A domains that were initially defined as the CD domains in both FnBPA and FnBPB. As shown in Figure 4.1, FnBPA contains an additional fibronectin-binding region, originally termed the B-repeat domain, which is absent in FnBPB (Signas *et al.*, 1989, Jonsson *et al.*, 1991). The domain organization of $FnBPA_{(8325\text{-}4)}$ was later revised following an examination of the fibronectin-binding domains of FnBP from *Streptococcus dysgalactiae* (Schwarz-Linek *et al.*, 2003). The structure of the B3 peptide from this FnBP in complex with two type I modules of fibronectin was characterised using nuclear magnetic resonance (NMR). The fibronectin-binding activity of B3 is the result of a tandem β-zipper interaction, where binding motifs in the B3 peptide form antiparallel β-strands on sequential type I modules of fibronectin (Shwarz-Linek *et al.*, 2003) (Figure 1.12). In the same study, bioinformatic analysis suggested that a similar mechanism of fibronectin-binding is employed by the *S. aureus* FnBPA protein. Sequence analysis indicated that the C-terminal regions of $FnBPA_{(8325\text{-}4)}$ are arranged into 11 segments (Figure 4.1) such that each (except segment 7) contains putative fibronectin type I module binding motifs stretching from the C-terminus of the A domain to the D-repeats of FnBPA (Schwarz-Linek *et al.*, 2003). The first of these fibronectin-binding repeats (FnBR-1) lies inside the previously defined boundary of the A domain of FnBPA as shown in Figure 4.1. Indeed, rFnBPA(37-544) was later found to be capable of binding fibronectin, demonstrating the presence of a functional fibronectin-binding motif (Keane *et al.*, 2007b). More recently, the crystal structures of FnBR-1 and FnBR-5 of $FnBPA_{(8325\text{-}4)}$, each in complex with four type I modules of fibronectin have been solved and

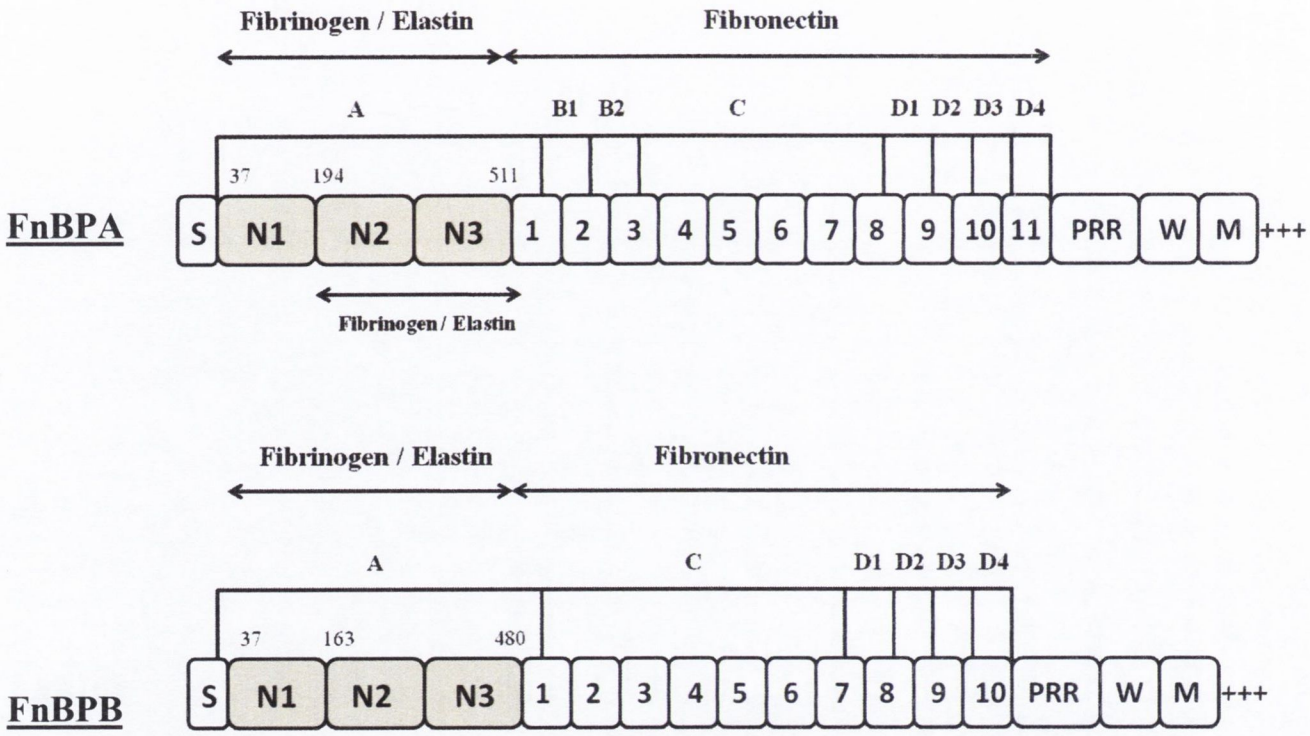

Figure 4.1 Re-defining the A domains of FnBPA and FnBPB from *S.aureus* 8325-4

Mapping of the 11 fibronectin-binding tandem motifs at the C-terminus of FnBPA resulted in the re-defining of the A domain of the protein.C-terminal residues 512-544 of the A domain are actually contained within the first fibronectin-binding motif which spans residues 512-540. The true A domain of FnBPA thus ends at residue 511.The minimum fibrinoegen and elastin binding domain is contained in the N23 subdomain which spans residues 194-511. Sequence analysis indicates the presence of 10 fibronectin-binding motifs at the C-terminus of FnBPB and include residues 480- 510 of the A domain. Based on a sequence alignment with FnBPA, it is predicted that the true A domain of FnBPB ends at residue 480. Signal sequences (S), wall/membrane spanning regions (WM) and the origionally defined ligand-binding domains A,B,C and D are indicted.

confirm the tandem β-zipper mechanism (Bingham *et al.*, 2008) (Figure 1.13). Furthermore, a recombinant FnBPA A domain protein which lacks FnBR-1 did not bind fibronectin but retained the ability to bind fibrinogen and elastin with the same affinity (Keane *et al.*, 2007b).The A domain of FnBPA thus spans residues 37-511 (Figure 4.1). In addition, the revised FnBPA N2N3 subdomain (residues 194-511) was shown to be sufficient for binding to fibrinogen and elastin indicating that the N1 subdomain of FnBPA is not required for ligand binding (Keane *et al.*, 2007b) (Figure 4.1). An alignment of $FnBPB_{(8325\text{-}4)}$ with the FnBRs of $FnBPA_{(8325\text{-}4)}$ indicates that $FnBPB_{(8325\text{-}4)}$ contains 10 rather than 11 FnBRs (Meenan *et al.*, 2007). As with FnBPA, the first FnBR is contained within the C-terminus of the previously defined A domain of FnBPB, spanning residues 37-540. Based on this alignment, it was predicted that the minimum A domain of FnBPB lacking FnBR-1 consists of residues 37-480 (Meenan *et al.*, 2007) (Figure 4.1).

Seven isotypes of the N2N3 subdomain of FnBPA have been identified based on sequence variation in subdomains N2 and N3. The divergent residues were mapped on a three-dimensional model of the FnBPA A domain and were predicted to be surface-exposed, while residues that are known to be important in fibrinogen and elastin binding by the type I A domain were mostly conserved across all isotypes (Keane *et al.*, 2007b, Loughman *et al.*, 2008). Recombinant forms of each FnBPA N2N3 isotype (I-VII) were expressed and were shown to have the same affinity for fibrinogen and elastin indicating that sequence variation does not affect ligand binding. However, antibodies raised against the rN2N3 isotype I protein bound weakly to rN2N3 isotypes II-VII indicating that amino acid variation had resulted in proteins that are antigenically distinct (Loughman *et al.*, 2008). In the previous chapter, seven isotypes of the A domain of FnBPB were similarly identified based on divergence in the revised N2N3 subdomain. This region is predicted, based on studies of the A domains of

ClfA and FnBPA, to contain the minimum ligand-binding site. It was shown in an earlier study that antibodies raised against the original A domain of FnBPB from strain 8325-4 (FnBPB isotype I) did not recognize FnBPB expressed on the surface of strain P1, which was subsequently shown to express FnBPB isotype IV (Loughman, 2006). This suggests that like FnBPA, variation in the A domain of FnBPB effects the antigenicity of the protein.

In this chapter, a 3D structural model of the A domain of FnBPB is studied and variant residues mapped. Antibodies which were raised against a recombinant N2N3 isotype I protein were tested for their ability to recognize recombinant N2N3 isotypes I-VII. The ligand-binding ability of the revised N2N3 subdomain of FnBPB from strain 8325-4 (isotype I) was tested and verified. The affinities of recombinant N2N3 isotypes I-VII for immobilised fibrinogen, elastin and fibronectin was compared by ELISA-type binding assays and by surface plasmon resonance (SPR).

4.2 Results

4.2.1 Three dimensional molecular models of the N2N3 subdomains of FnBPB isotypes.

In Chapter 3, seven isoforms of the N2N3 subdomain of FnBPB were identified which share 61%-80% amino acid identity. In order to study the significance of this variation for antigenicity and functionality, it was important to examine a molecular model of the N2N3 region of FnBPB. The primary sequence of the revised N2N3 subdomain of isotype I FnBPB (residues 126-480) was submitted to the Protein homology/analogy recognition engine (Phyre) from the Imperial College, London (http://www.sbg.bio.ic.ac.uk/~phyre/). This service predicts the 3D structure of the submitted sequence based on the crystal structures of similar proteins. The predictions are graded according to the precision of the predicted structure compared to that on which it is modeled. The highest recommendations for the structure of FnBPB are based on ClfA and SdrG. It was decided to study the ClfA-based structure of FnBPB due to the greater similarity of the two proteins and the fact that they bind to the same region of fibrinogen. The resulting structure was viewed using the user-sponsered pyMOL molecular viewing software (http://www.pymol.org) and can be seen in Figure 4.2. Figure 4.2A shows the independently folded subdomains N2 (yellow) and N3 (green) which are composed largely of anti-parallel β-strands. The C-terminus of the γ-chain of fibrinogen is predicted to dock into the hydrophobic trench, similar to the ClfA-peptide structure (Figure 4.2B). Residues 467-480 of FnBPB comprise the predicted latching peptide and are shown in white in Figure 4.2. Here, the latching peptide is shown wound around domain N3 as predicted in the structure of ClfA in the apo form. This is most likely an artifact. It is more likely that the latching peptide is not bound to N2 or N3 in the apo-form.

Residues that vary between the N2N3 subdomains from FnBPB isotypes I-VII were highlighted in the model structures and are shown in red in Figures 4.2B and 4.2C. Residues lining the predicted ligand binding trench are completely conserved as are the residues that comprise the predicted latching peptide. By contrast, the majority of variant residues were predicted to be exposed on the surface of the protein. When the space filled model of the 3D structure of the protein is viewed, most of the variant residues are visible (Figure 4.2C). Most of the variant residues are surface exposed and may lead to antigenic variation.

4.2.2 Purification of recombinant N2N3 subdomains of FnBPB isotype I-VII

The predicted minimum binding regions comprising subdomains N2 and N3 of each of the seven FnBPB isotypes were expressed in *E. coli* as 6xHis fusion proteins. Primers were designed using the *fnbB* sequences described in Chapter 3. Reverse primers were modified to ensure that the resulting PCR products contained a stop codon immediately 3′ to the last *fnbB* codon. The seven PCR products were cloned into pQE30 between the *Bam*HI and *Sma*I sites (Figure 4.3). Each construct was verified by restriction analysis and PCR. An example of this is shown in Figure 4.4. The seven constructs were finally validated by sequencing using generic primers which flank the multiple cloning site of pQE30. Fusion proteins were expressed in the protease deficient strain Topp3 and purified from lysates by nickel-chelate affinity chromatography. The proteins were analysed by SDS-PAGE and Coomassie blue staining following incubation at 4°C for 18 h (Figure 4.5). Each protein migrates with an apparent molecular mass of approximately 50kDa. This is slightly greater than their molecular masses which are listed in Table 4.1. It is shown here that each recombinant N2N3 protein was purified to homogeneity and is intrinsically stable.

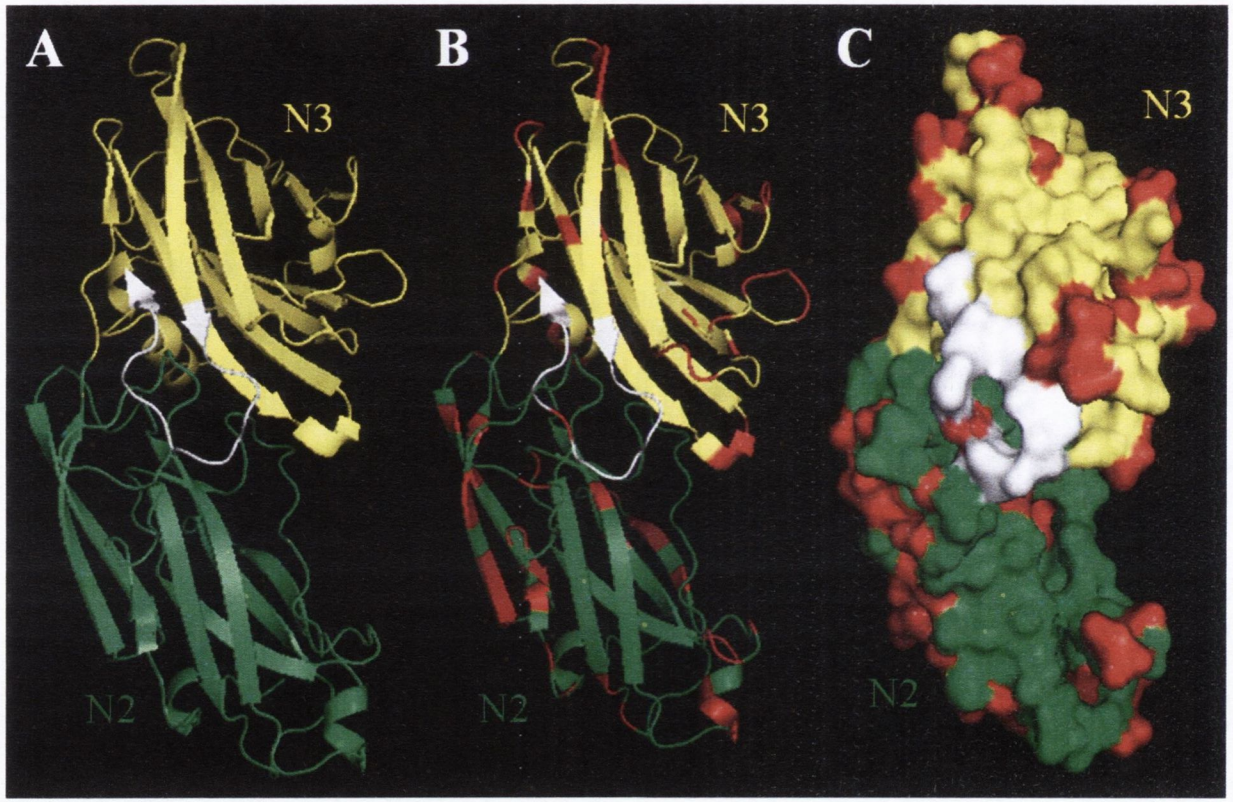

Figure 4.2 Predicted 3D structure of FnBPB isotype I.

Based on the crystal structure of domain A of ClfA, a ligand-binding trench is predicted to form between the N2 (green) and N3 (yellow) domains of FnBPB. The fourteen C-terminal residues that are predicted to form the putative latching peptide are shown in white. Residues that differ in FnBPB types II, III and IV are highlighted in red in the ribbon (**B**) and space fill (**C**) models. Residues that are predicted to form the latching peptide and ligand binding trench are conserved while variant residues are located on the surface.

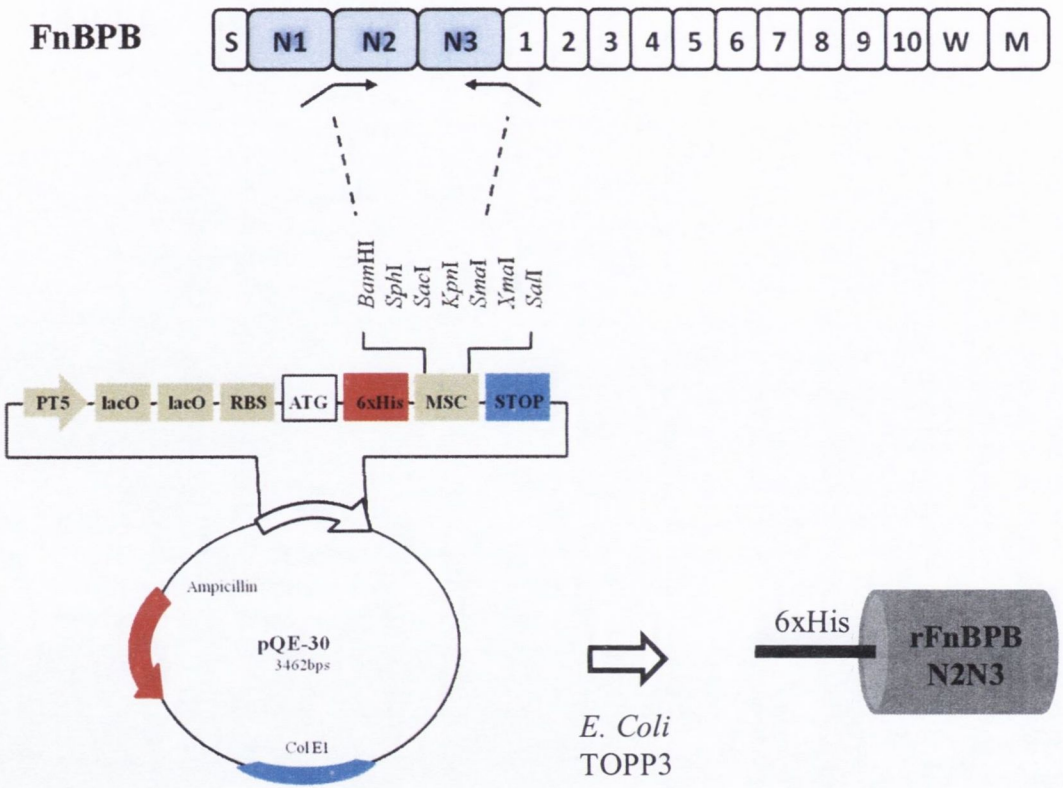

Figure 4.3 Cloning *fnbB* DNA for the expression of rN2N3 proteins

DNA encoding the N2N3 subdomain of FnBPB isotypes I-VII was amplified from the genomic DNA of *S. aureus* strains 8325-4, N315, MSSA476, P1, 2, 304 and 3077 respectively. PCR products were cloned into the *E.coli* expression vector pQE30 using *Bam*HI and *Sma*I restriction sites. pQE30 constructs were transformed into the protease deficient *E. Coli* strain TOPP3 for the expression of recombinant His-tagged FnBPB A domian proteins.

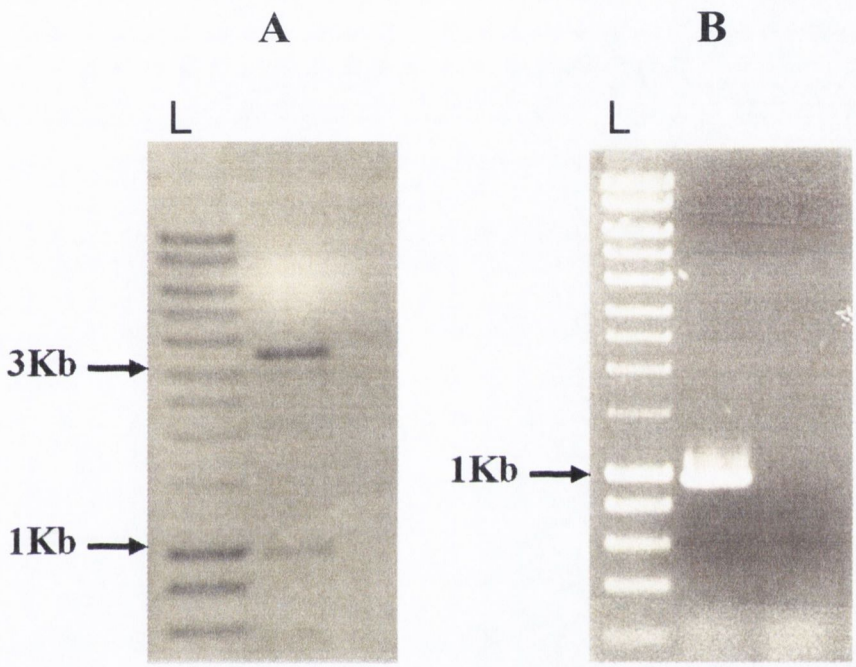

Figure 4.4 Restriction analysis of pQE30N2N3 constructs
The pQE30 plasmid containing the coding region for the N2N3 subdomain of FnBPB isotype I was verified by digestion with *Bam*HI and *Sma*I restriction enzymes (**A**). The double digestion of plasmid DNA yielded two distinct bands correspond to the pQE30 backbone (3 kb) and the N2N3 encoding insert (0.9 kb) as indicated. The uncut plasmid was used as a template for PCR to amplify the 0.9 kb N2N3 encoding insert (**B**). Lanes "L" were loaded with 5 μl of a 1 kb DNA ladder.

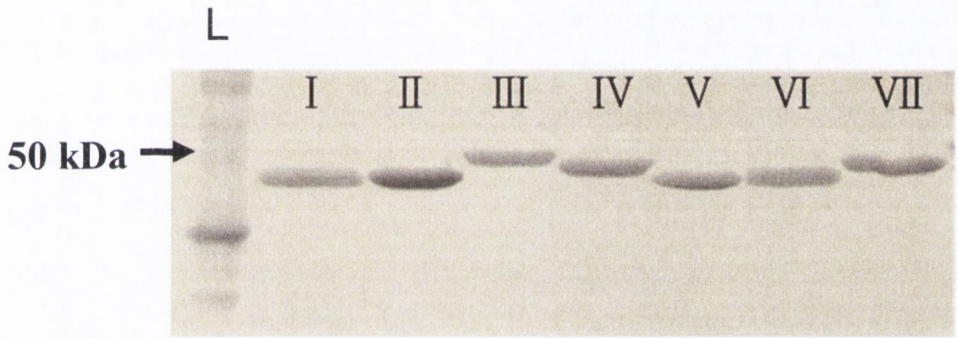

Figure 4.5 SDS-PAGE analysis of rN2N3 isotypes I-VII

Recombinant N2N3 isotype proteins (I-VII) were incubated for 18h at 4°C. Equal amounts (10μM) of each protein was analysed by SDS-PAGE and Coomassie blue staining. Lane "L" was loaded with 5μl of a molecular weight marker

Table4.1 Molecular weights of rFnBPB N2N3 His-tagged proteins (Isotypes I-VII)

FnBPB N2N3 isotype	Number of amino acids	Molecular mass of recombinant 6xHis fusion protein (kDa)
I	318	36.94
II	318	36.94
III	325	38.52
IV	321	37.75
V	319	37.16
VI	320	37.42
VII	326	38.1

4.2.3 Titration of anti-rFnBPB isotype I antibodies

In order to measure the affinities of rabbit polyclonal antibodies and a mouse monoclonal antibody that were raised against rN2N3 isotype I, varying concentrations of the recombinant protein antigen were applied to nitrocellulouse membrane strips and probed with dilutions of antibodies (1:500-1:1600) (Figure 4.6). A relatively weak reaction was observed for both antibodies with high concentrations of each antibody needed to detect nanogram amounts rN2N3 isotype I protein.

4.2.4 Binding of anti-FnBPB A domain antibodies to isotypes I – VII

The majority of variant residues in different FnBPB A domain isotypes types were predicted to be exposed on the proteins' surface. This might create differences in surface-exposed epitopes that affect antigenicity. It was previously demonstrated that polyclonal antibodies raised against FnBPB A domain isotype I from strain 8325-4 bound poorly to FnBPB expressed by strain P1 which expresses FnBPB A domain isotype IV (Loughman, 2005). Here the affinity of polyclonal anti-FnBPB isotype I antibodies and a monoclonal anti-FnBPB isotype I antibody for recombinant FnBPB A domains of different isotypes was measured by ELISA.

A control experiment was preformed to ensure that each protein had coated the microtitre dish equally. This was determined using a monoclonal antibody that recognizes the 6xHis fusion tag at the N-terminus of each protein (Figure 4.7). Polyclonal rabbit anti-FnBPB isotype I antibodies had a 4-9 fold lower affinity at half maximum binding for isotypes II-VII compared to isotype I (Figure 4.8A). This suggests that amino acid variation creates differences in surface-exposed epitopes on the A domain molecule that affect immune-crossreactivity. Mouse monoclonal antibody 2E11 bound efficiently to rN2N3 isotype I but showed little binding to

recombinant N2N3 isotypes II-VII as shown in Figure 4.8B. This suggests that the 2E11 epitope is only present on the isotype I protein.

4.2.5 Testing the binding of FnBPB A domain isotypes I-VII to immobilised ligands by ELISA

The revised N2N3 subdomains of FnBPB were predicted to contain the fibrinogen and elastin-binding sites but lack the ability to bind fibronectin due to the absence of fibronectin-binding motifs. The ability of purified recombinant FnBPB A domain proteins to bind to fibrinogen and elastin was measured in solid-phase binding ELISA-type assays. Microtitre dishes were coated with a single concentration of human fibrinogen or elastin and incubated with rN2N3 proteins ranging in concentration from 0.15 μm to 10 μM. The bound rFnBPB protein was detected using an anti-6xHis monoclonal antibody, thus recognizing a constant feature of each variant protein. Each recombinant N2N3 isotype bound to immobilised fibrinogen and elastin in a dose-dependent and saturable manner as shown in Figure 4.9. The estimated half maximum binding concentrations were 0.5 μM and 0.9 μM, respectively. Binding to fibronectin was also measured. Unexpectedly, each of the seven proteins bound fibronectin dose-dependently and saturably with a half maximum binding concentration of 1μM (Figure 4.10). The recombinant N2N3 subdomain of FnBPA (isotype I) was used as a negative control in these assays. The ability of the rN2N3 FnBPB isotypes to bind fibronectin was somewhat surprising because the amino acid sequences do not contain any known fibronectin-binding motifs.

4.2.6 Comparison of binding of recombinant N2N3 isotypes I-VII using surface plasmon resonance

ELISA-based solid phase binding assays are routinely employed to study protein-protein interactions. However, this method has many limitations. It is a static method which measures the level of binding at a

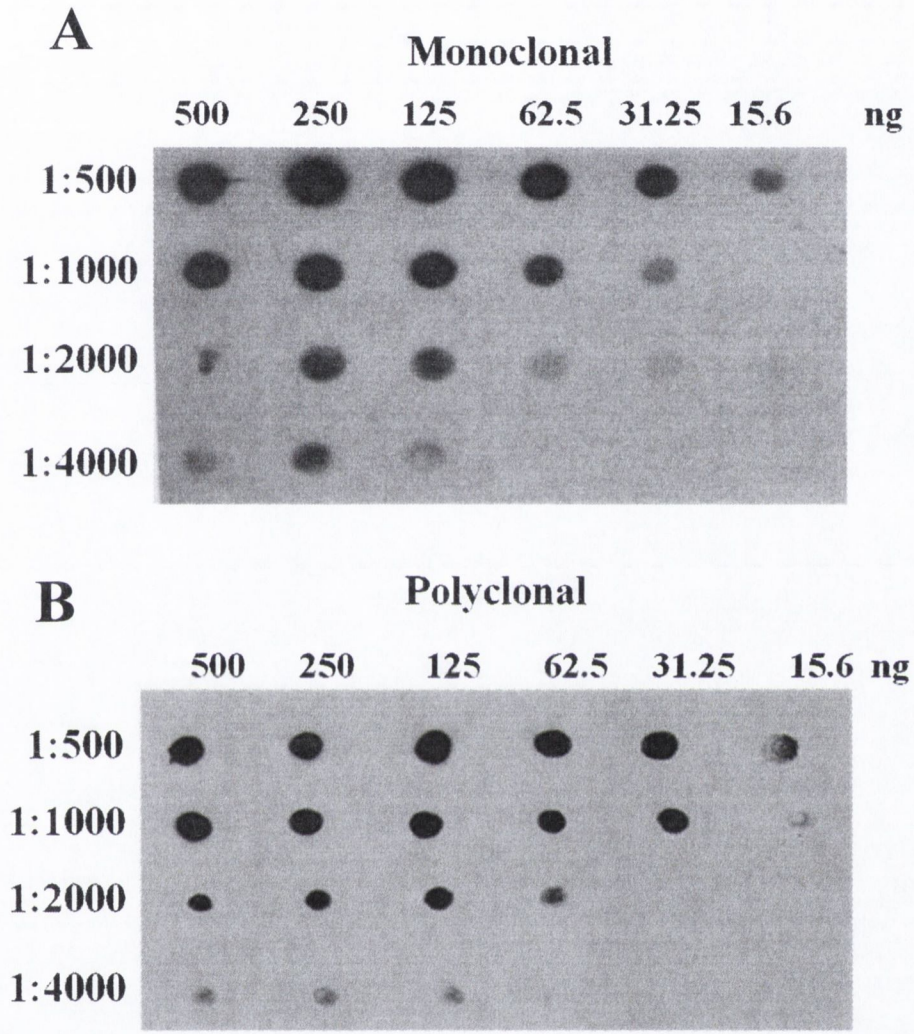

Figure 4.6 Titre of anti-rFnBPB N2N3 isotype I antibodies

Titre of monoclonal mouse anti-FnBPB N2N3 isotype I antibodies (**A**) and a polyclonal rabbit anti-FnBPB N2N3 isotype I antibody (**B**) for their antigen in recombinant form. Dilutions of rN2N3 isotype I ranging from 15.6 ng to 500 ng were dotted onto nitrocellulouse membranes and probed with various dilutions of anti – A domain antibodies followed by detction with rabbit anti-mouse (**A**) or goat anti-rabbit (**B**) HRP

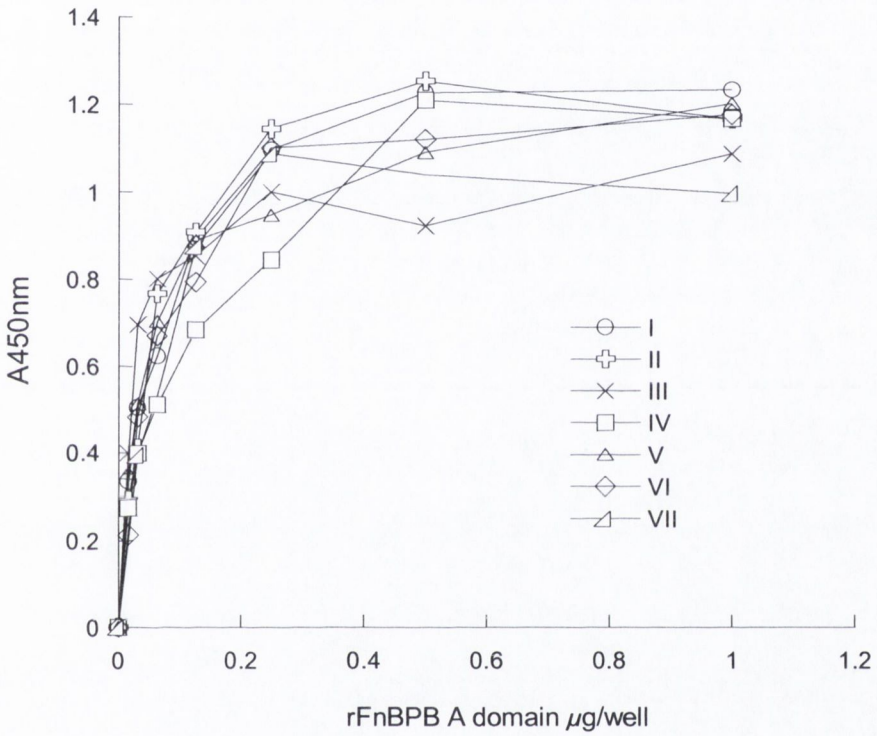

Figure 4.7 Binding of anti-His tag antibodies to rN2N3 isotypes I-VII
Microtitre wells were coated with doubling dilutions of rN2N3 proteins, isotypes I-VII. And probed with anti-hexahistidine mouse monoclonal antibody 7E8 followed by rabbit anti-mouse HRP. Plates were developed with TMB substrate. Data points represent the mean of triplicate wells.

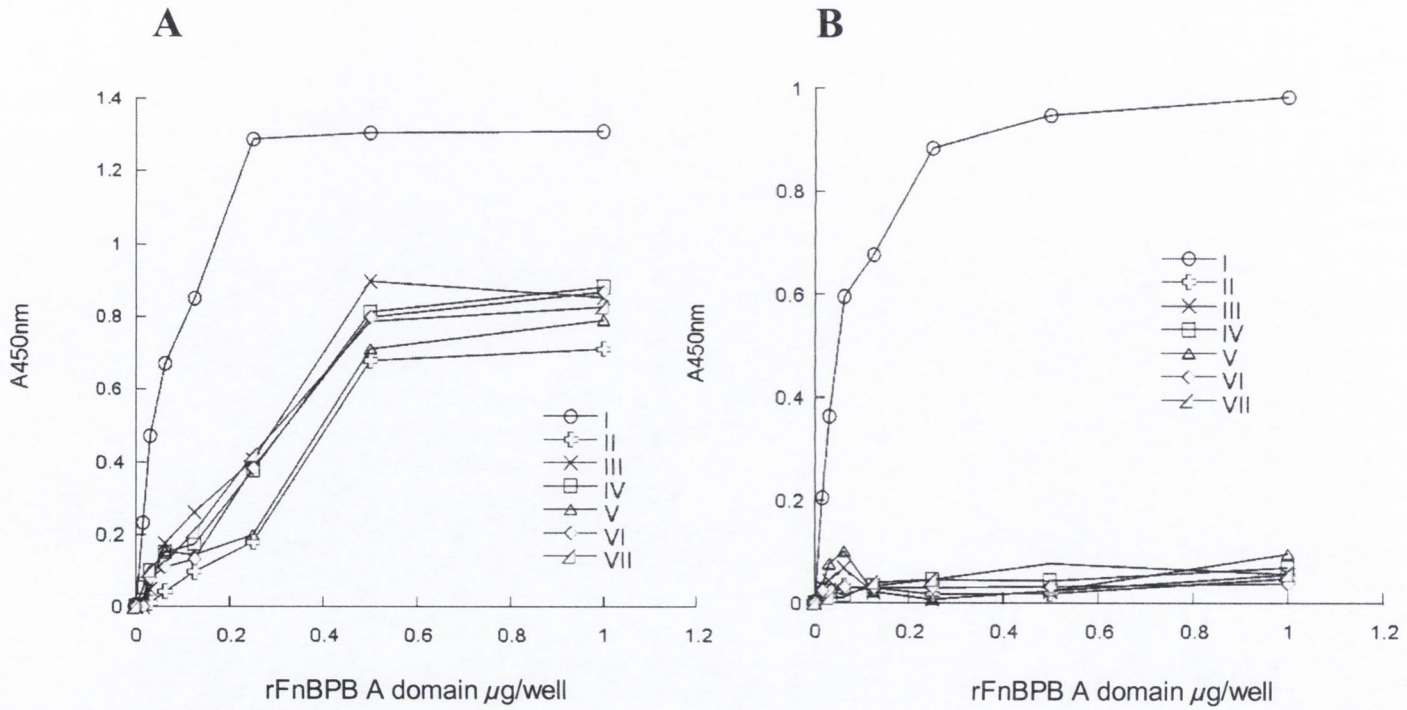

Figure 4.8 Binding of polyclonal and monoclonal anti-isotype I A domain antibodies to recombinant A domain isotypes I – VII

Microtitre dishes were coated with A domains isoype I – VII at the indicated concentrations. Wells were blocked and then incubated with (**A**) polyclonal rabbit anti-isotype I A domain antibodies, or (**B**) mouse monoclonal anti-isotype I A domain antibody 2E11. Bound antibodies were detected with either (**A**) HRP-conjugated goat anti-rabbit IgG antibodies or (**B**) HRP-conjugated goat anti-mouse IgG antibodies followed by TMB substrate. Graphs are representative of three separate experiments.

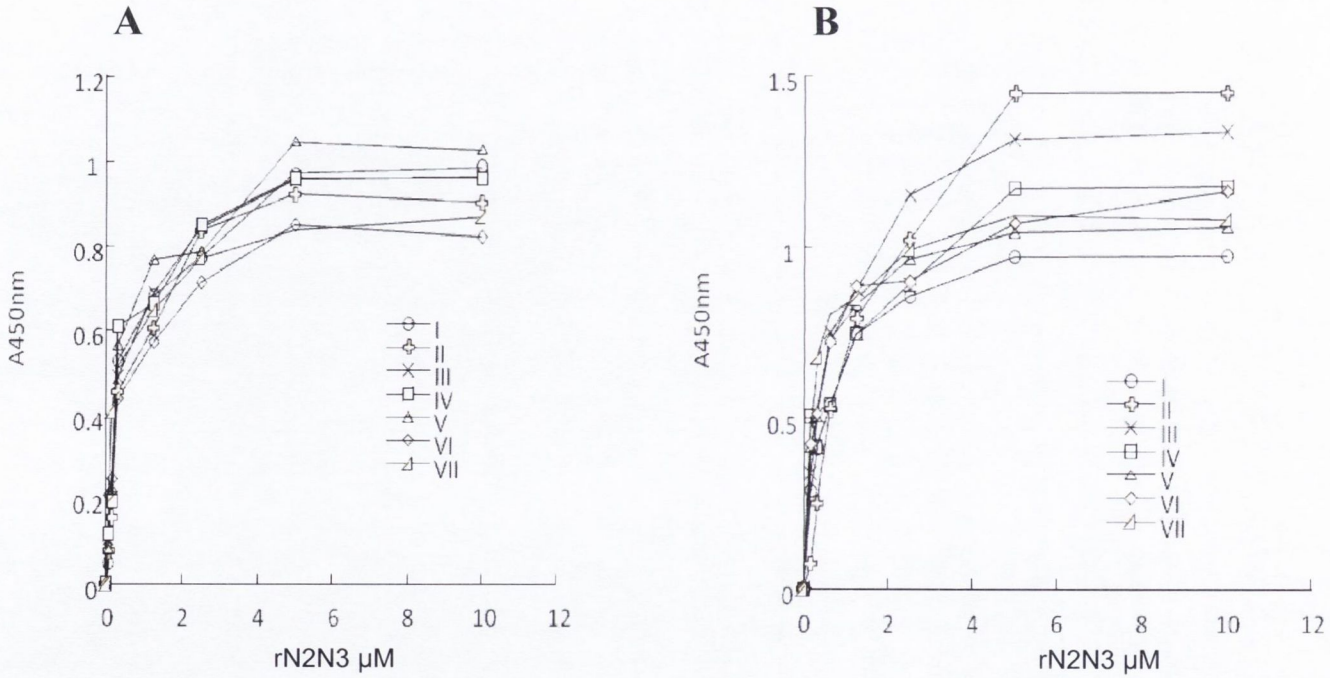

Figure 4.9 Binding of rN2N3 isotypes I-VII to immobilised human fibrinogen and elastin

Microtitre plates were coated with human fibrinogen (**A**) and human aortic elastin (**B**). Increasing concentrations of rN2N3 FnBPB isotypes I-VII were added for 2h at 37^0C. Bound protein was detected with mouse anti-hexahistidine monoclonal antibody 7E8 followed by development with TMB substrate. Graphs are representative of three separate experiments.

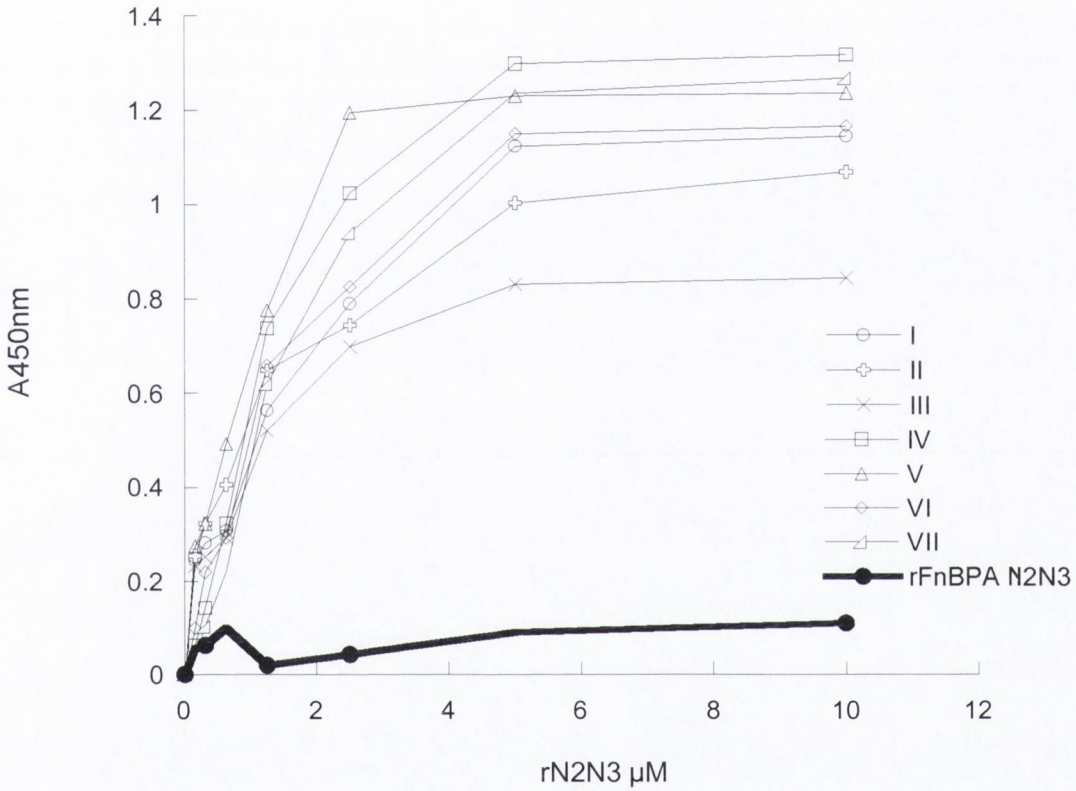

Figure 4.10 Binding of rN23 isotypes I-VII to immobilised human fibronectin

Microtitre plates were coated with human fibronectin. Increasing concentrations of rN2N3 FnBPB isotypes I-VII were added for 2h at 37^{0}C. rN2N3 FnBPA protein was used as a negative control. Bound protein was detected with mouse anti-hexahistidine monoclonal antibody 7E8 followed by development with TMB substrate. Graphs are representative of three separate experiments.

single time point. This sensitive technique is subject to pipetting errors and results depend heavily on the length of the incubation periods and on the potency of the antibody used for detection. To verify the unexpected results of the solid-phase assays described above, it was important to analyse ligand-binding by the rN2N3 proteins using a second method.

Surface Plasmon Resonance (SPR) is an extremely useful technique for measuring biomolecular interactions in real-time. Biacore (GE Healthcare) is the most widely used biosensor. The Biacore instrument comprises an SPR detector, a sensor chip and a flow system. The sensor chip is essentially a glass slide coated with a thin layer of gold which is modified with a carboxymethylated dextran layer and serves as a substrate for attachment for one interacting partner. The analyte is continuously injected into the flow cell and passes over the immobilised ligand. The phenomenon of SPR occurs when polarised light strikes an electrically conducting gold layer at the interface of media with different refractive indices. In Biacore experiments this phenomenon is exploited to detect changes in refractive index (RI) at the interface between the sensor surface and the solution which occurs upon binding of analyte to ligand. The changes in RI are measured in real-time and plotted as a sensorgram. Biacore sensorgrams have four main phases; establishment of a baseline, association, dissociation and regeneration as shown in Figure 4.11. SPR has several advantages over other techniques for studying protein-protein interactions. It is a label-free and automated detection method that provides accurate concentration measurements. The analyte is in solution and although the ligand is essentially immobilised, Biacore conditions closely mimic a fluid environment.

Here, amine coupling was used to immobilize human fibrinogen, elastin or fibronectin onto the surface of dextran chips (Figure 4.12). Equal concentrations (2μM) of each recombinant A domain isotype was passed

over the surface of each chip to compare the level of binding and the sensogram profiles obtained. All seven proteins bound fibrinogen, elastin and fibronectin. In agreement with ELISA, similar levels of binding to each ligand were achieved by each rN2N3 isotype (Figure 4.13).

4.2.7 Measuring the affinity of FnBPB A domain isotype I for fibrinogen, elastin and fibronectin by surface plasmon resonance

Another advantage of using SPR-based biosensors is that they can be used for the detailed characterization of protein-protein interactions in terms of both affinity and kinetics. Biacore experiments to calculate kinetic constants or affinity involve injecting a series of increasing concentrations of analyte over the surface of the chip and recording the sensorgram. To obtain kinetic parameters, sensorgrams may be analysed using one of several binding models provided with the BIAevaluation software. This allows calculation of the association rate constant (k_a) and the dissociation rate constant (k_d) (Figure 4.11). The ratio of the two rate constants (k_a/k_d) can be used to determine the disscociation constant (K_D).

The results of the solid-phase binding assays suggested that the A domain of FnBPB binds fibrinogen, elastin and fibronectin with similar affinity. Estimated half maximal binding concentrations were in the low micromolar range. To verify these results, the recombinant N2N3 isotype I protein was taken as the FnBPB A domain prototype and its affinity for fibrinogen, elastin and fibronectin were measured using SPR. Increasing concentration (0.15μM to 10μM) of the rN2N3 type I protein was passed over the surface of dextran chips which had been coated with human fibrinogen, elastin or fibronectin. The representative sensorgrams shown in Figure 4.14 have been corrected for the response obtained when recombinant protein was flowed over uncoated chips. The association rate constants (k_a) were determined to be less than or equal to 2.42×10^4 $M^{-1}s^{-1}$ indicating fast on-rates in the each interaction. The off rate or dissociation

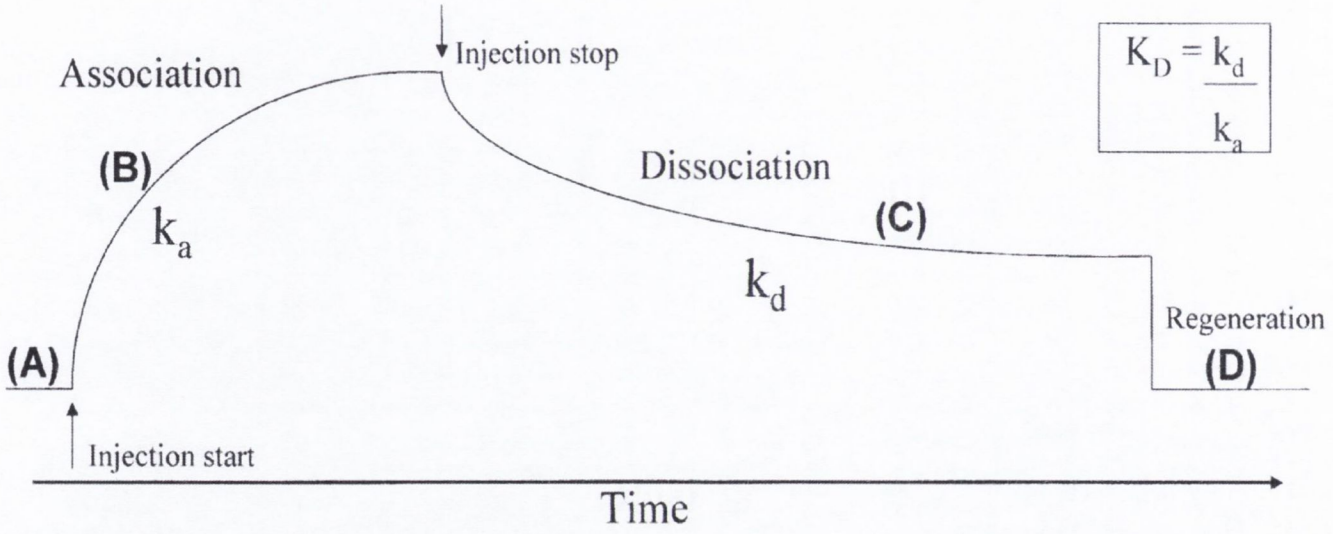

Figure 4.11 Biacore sensorgram

(**A**) Buffer is passed over chip to establish baseline. (**B**) Injection of rFnBPB protein causes a dose-dependent and saturable binding response. The rate of theis association phase is termed k_a. (**C**) Buffer is passed over the system to remove unbound rFnBPB and to investigate the stability of the complex formed between rFnBPB and the immobilised ligand. The rate of the dissociation phase is termed k_d. (**D**) A regeneration buffer is passed over the chip to remove all rFnBPB and return the system to baseline for the next cycel. The final affinity constant K_D is calculated by k_d/k_a.

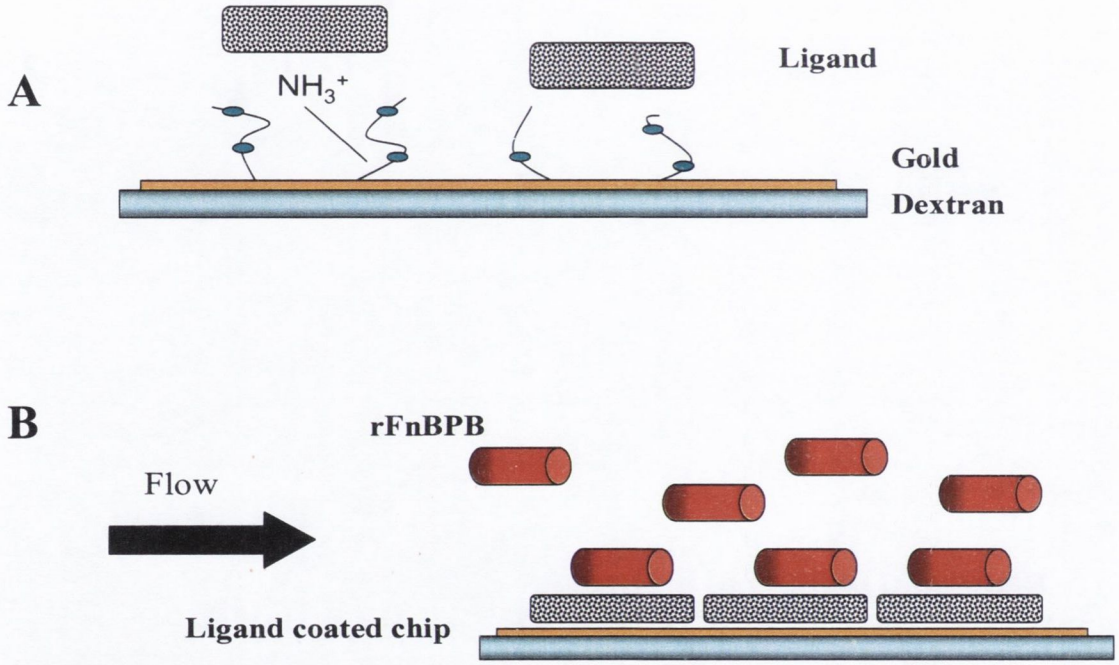

Figure 4.12 Biacore procedure

(**A**) Protein ligands are immobilised onto CM5 sensor chips using amine coupling of the lysine residues of the ligand to the carboxy moieties on the dextran chip. (**B**) Recombinant FnBPB proteins are passed over the surface of the chip to investigate the kinetics of binding of this protein to the immobilised ligand.

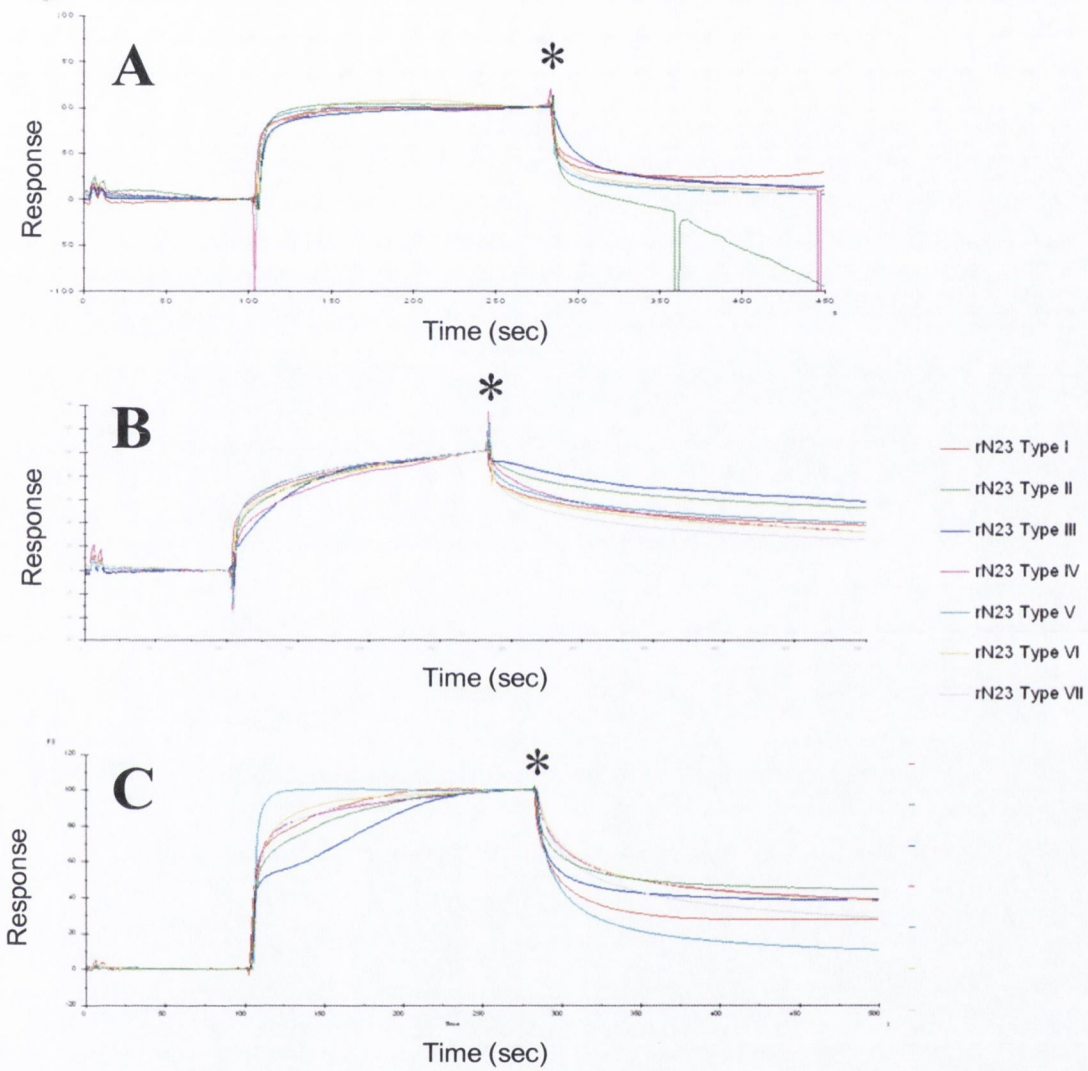

Figure 4.13 Surface plasmon resonance analysis of rFnBPB isotypes I-VII binding to fibrinogen, elastin and fibronectin

Human fibrinogen (**A**), elastin (**B**) and fibronectin (**C**) were immobilised onto the surface of dextran chips. The same concentration of (2μM) of each recombinant protein were passed over the surface of each chip. Injection started at 180s and ended at 420s. The point of maximal binding is indicated with an astrix.

constant (k_d) in each case was relatively slow indicating that the interaction between rN2N3 and each of the three ligands is stable. The overall affinity (K_D) for fibrinogen, elastin and fibronectin was calculated to be 2μM, 3.2μM and 2.5μM, respectively. The rate constants calculated for each of the three interactions are listed in Table 4.2. These experiments were repeated three times on different chips with similar results.

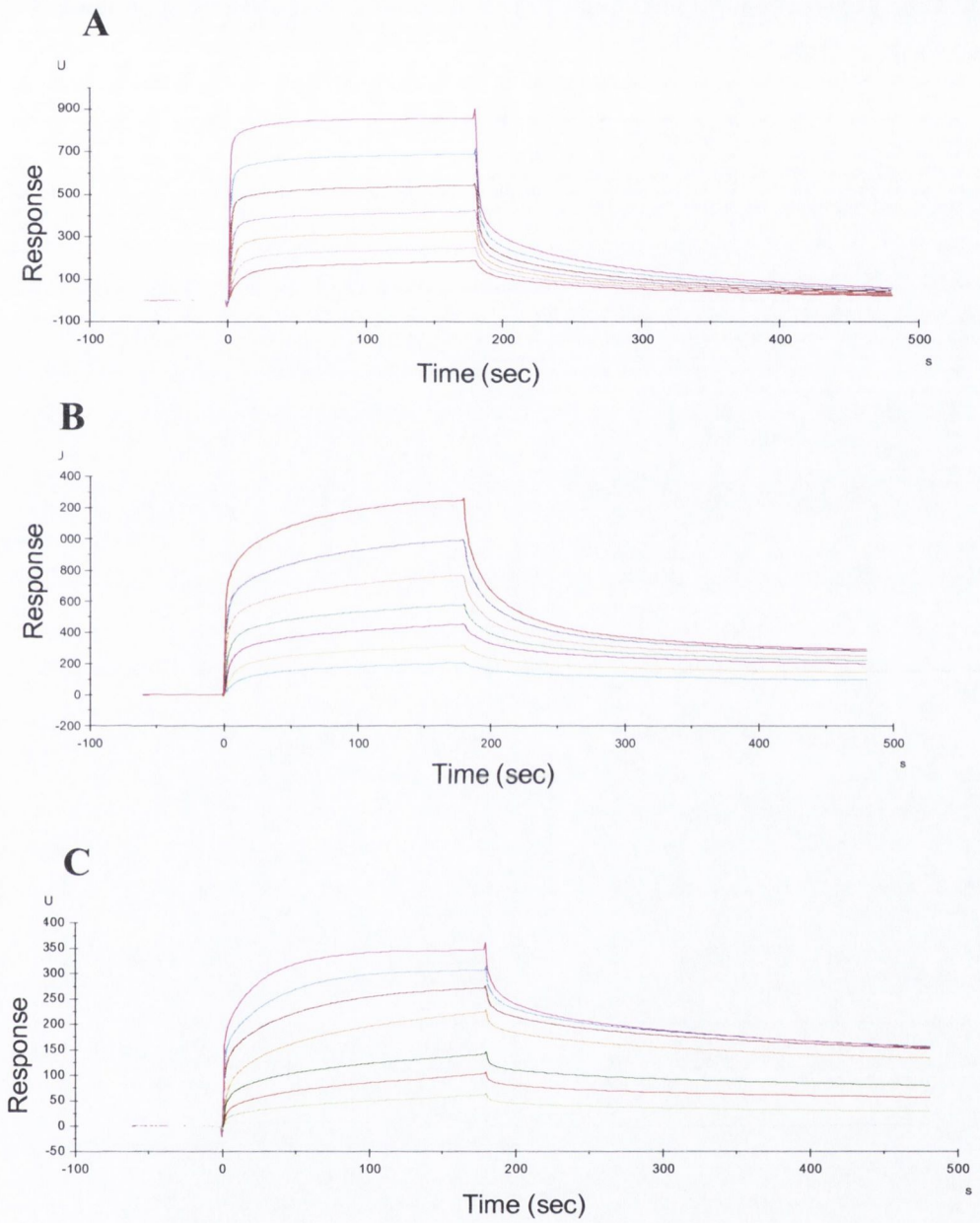

Figure 4.14 Surface plasmon resonance analysis of rN2N3 FnBPB isotype I binding to fibrinogen, elastin and fibronectin

Human fibrinogen (**A**), elastin (**B**) and fibronectin (**C**) were immobilised onto the surface of dextran chips. In each assay, recombinant FnBPB N2N3 isotype I was passed over the surface in concentrations ranging from 0.15μM (lower-most trace) to 10μM (upper-most trace). The phases of association and dissociation are indicated. The representative sensorgrams have been corrected for the response obtained when recombinant FnBPB proteins were flowed over uncoated chips.

Table 4.2 Rate constants for the interaction of recombinant FnBPB N2N3 isotype I with fibrinogen, elastin and fibronectin

Ligand	Association rate constant (K_a) (M)	Dissociation rate constant (K_d) (M)	Equilibrium dissociation constant (K_D) (μM)
Fibrinogen	2.417×10^4	7.675×10^3	2
Elastin	1.096×10^4	3.126×10^3	3.2
Fibronectin	1.027×10^4	1.920×10^3	2.5

4.3 Discussion

An important factor in bacterial pathogenesis is the ability of the invading organism to thwart the host immune responses during colonisation or invasive infection. *S. aureus* possesses on its cell surface a number of proteins, collectively called MSCRAMMs, which promote the binding of the organism to components of the host's plasma and extra cellular matrix. MSCRAMMs promote colonisation of diverse sites and help *S. aureus* to avoid phagocytosis by neutrophils. FnBPA and FnBPB are multifunctional MSCRAMMs that interact specifically with fibrinogen, elastin and fibronectin. Ligand-binding by *S. aureus* FnBPs has been shown to promote platelet activation and aggregation as well as internalisation into host cells (Sinha *et al.*, 1999, Fitzgerald *et al.*, 2006). The expression of FnBPs has been identified as an important virulence factor in the animal models for endocarditis and septic arthritis (Que *et al.*, 2005, Palmqvist *et al.*, 2005).

FnBPA and FnBPB have considerable organization and sequence similarity and are composed of a number of distinct domains (Jonsson *et al.*, 1991). In both proteins, a series of C-terminal tandemly repeated motifs mediate binding to fibronectin while N-terminal A domains bind fibrinogen and elastin. Revision of the coordinates of the fibrinogen and elastin-binding A domain of FnBPA prompted a re-assessment of the A domain of FnBPB. Like FnBPA, seven distinct isotypes of FnBPB A domain were identified (Chapter 3). In this chapter, the significance of variation in this region of FnBPB was examined in terms of the functionality and antigenicity of the protein.

A 3D molecular model of the N2 and N3 domains of FnBPB was generated based on the known structure of ClfA. Like the A domain of ClfA (and FnBPA) it is predicted that the N2N3 subdomain of FnBPB represents the minimal ligand-binding region and that a ligand-binding trench is formed between the N2 and N3 subdomains. Based on this model, it was shown that the majority of variant residues are located on the surface of the

protein while residues that are predicted to be involved in ligand-binding by dock, lock and latch are highly conserved. However, it is important to place this in the context of the entire protein. The structure of the N1 subdomain and the impact that this and the fibronectin-binding domains linked to the C-terminus of the predicted latching peptide might have on the conformation and exposure of residues in subdomains N2 and N3 is not known. It is possible therefore that some residues that are surface-exposed on the 3D structural model of N2N3 of FnBPB, may not be surface-exposed on the full length protein expressed on the surface of the bacterial cell. I has been shown here that at least some of the variant residues in the A domain of FnBPB are surface exposed.

Amino acid sequence variation affected antibody recognition. Polyclonal antibodies against isotype I had reduced affinity for isotypes II – VII while a monoclonal antibody raised against isotype I had little or no affinity for all other isotypes. As with FnBPA isotypes, FnBPB sequence variation has created different epitopes on the A domains that affect immunocross-reactivity. This result is consistent with the predicted location of variant residues on the surface of the protein and not in regions involved in ligand binding. The ligand binding ability of seven recombinant FnBPB N2N3 isotypes was compared by ELISA-based solid phase binding assays and SPR. Each A domain isotype bound to immobilised fibrinogen and elastin with similar affinities indicating that variation in the A domain of FnBPB does not compromise its ligand-binding function. Using the recombinant N2N3 isotype I protein as a prototype, the affinity of FnBPB for fibrinogen and elastin was analysed by SPR. The K_D for both interactions was in the low micro molar range. These results confirm that like the A domains of ClfA and FnBPA, the revised N2N3 subdomain of FnBPB is sufficient for ligand-binding and that the N1 subdomain is not required. The results also suggest that these ligand-binding functions are biologically important and are consistent with the predicted location of

variant residues on the surface of the protein and not in regions predicted to be involved in ligand binding. Together, the theoretical 3D model of the A domain of FnBPB and the results of functional assays described here, hint at the importance of the N2 and N3 domains in ligand binding during dock, lock and latch. This proposed mechanism for ligand-binding is further investigated in Chapter 6.

As discussed in Chapter 3, the variation in both FnBPA and FnBPB is confined to the A domain of each protein. By contrast, the fibronectin-binding repeats of FnBPA and FnBPB were greater than 90% identical in any pairwise alignment. This suggests a selective advantage in variation in the FnBPA/FnBPB A domains, most likely as a mechanism of immune evasion through antigenic variation, while still retaining ligand binding. A similar mechanism of antigenic variation in the fibronectin-binding repeat region would not confer an advantage because the majority of antibodies against this region recognise neo-epitopes formed only upon fibronectin-binding (Casolini *et al.*, 1998). A reduction in the host immune response against the fibronectin-binding repeats might involve a reduction in the affinity of fibronectin-binding repeat regions for fibronectin. This may affect aspects of pathogenesis such as host cell invasion.

Previous studies have indicated that *S. aureus* isolates which are associated with invasive diseases are significantly more likely to carry genes encoding FnBPB as well as FnBPA suggesting that both proteins are important virulence factors (Peacock *et al.*, 2000). Antigenic variation in both FnBPA and FnBPB may be employed by *S. aureus* to thwart the host immune responses during invasive infection. It could be proposed that variation in the A domains of FnBPA and FnBPB helps *S. aureus* evade the immune response in individuals previously exposed to a strain expressing a different FnBPA/FnBPB isotype profile. Carriers of *S. aureus* have an increased chance of developing invasive disease caused by the carriage

strain but have a lower mortality rate than non-carriers that develop *S. aureus* bacteremia (Wertheim *et al.*, 2004, von Eiff *et al.*, 2001). Individuals who carry *S. aureus* in their nares mount an immune response against the superantigens that are specifically expressed by their colonizing strain (Holtfreter *et al.*, 2006). Generation of a strain-specific immune response might explain the improved prognosis of carriers compared to non-carriers (Holtfreter *et al.*, 2006). A similar phenomenon might occur with FnBPs, whereby carriers mount a specific immune response to the FnBPA and FnBPB isotypes expressed by their colonizing strain and prime the immune system to mount a robust anti-FnBPA/FnBPB isotype-specific antibody response during infection. Conversly, FnBP variation may help a strain to infect a persistent carrier of a different FnBPA/FnBPB isotype combination, or a non-carrier previously exposed to a different FnBPA and FnBPB isotypes. It is important to remember that some strains of *S. aureus* only specify FnBPA and lack the gene encoding FnBPB. Colonisation by or exposure to such strains may render a carrier or non-carrier vulnerable to infection by *S. aureus* strains expressing any isotype of FnBPB. Thus, it may be postulated that the expression of a second fibronectin-binding protein, FnBPB, may contribute to the virulence of *S. aureus* by increasing its ability to evade pre-primed anti-FnBP immune responses that are mounted by its host.

At the onset of this study the A domain of FnBPB of strain 8325-4 (isotype I) was predicted to comprise residues 37-480 by comparison with FnBPA and ClfA. Domain N2 and N3 of FnBPB were sufficient for binding fibrinogen and elastin, presumably by dock, lock and atch. Unexpectedly, recombinant FnBPB N2N3 was found to bind to fibronectin despite lacking any fibronectin-binding motifs. In fact, the seven recombinant N2N3 isotypes examined in this study each bound to immobilised fibronectin in solid-phase binding assays and Biacore experiments. Using SPR, rN2N3 isotype I (residues 37-480) bound fibronectin with a K_D in the low micro

molar range. This is similar to the K_D calculated for the binding of the protein to both fibrinogen and elastin. This raises the possibility that the A domain of FnBPB contains a novel fibronectin-binding motif that is conserved despite sequence variation and may bind fibronectin by a novel mechanism. The biological significance of fibronectin-binding by the A domain of FnBPB is assessed in the following chapter and the molecular mechanism for this interaction is examined.

Chapter 5

Analysis of fibrinogen binding by FnBPB

5.1 Introduction

The development of *S. aureus* infections depends in part on the ability of the bacterium to adhere to components of the host's plasma and extra cellular matrix (ECM) via surface expressed ligand-binding proteins termed MSCRAMMs. *S. aureus* expresses several different MSCRAMMs that bind specifically to fibrinogen, a 340kDa glycoprotein found in blood plasma. It is composed of two identical disulphide-bonded subunits, each formed by an Aα, Bβ and γ polypeptide chain (Figure 1.4). The fibrinogen-binding MSCRAMMs of *S. aureus* include ClfA, FnBPA and FnBPB which each bind fibrinogen at the C-terminus of the γ-chain (Wann *et al.*, 2000, McDevitt *et al.*, 1997).

The interaction between ClfA and fibrinogen has been well characterised. The N-terminal A domain of ClfA binds to the C-terminal 15 residues of the fibrinogen γ-chain (McDevitt *et al.*, 1997). The A domain of ClfA is composed of three independently folded immunoglobulin G-like domains, N1, N2 and N3. Subdomains N2 and N3 are sufficient for binding to the fibrinogen γ-chain (Deivanayagam *et al.*, 1999). This region of ClfA has been crystallised both in the apo form and in complex with a peptide corresponding to the C-terminus of the fibrinogen γ-chain (Figures 1.5 and 1.7).These structures indicate that ClfA binds to the fibrinogen γ-chain by a variation of the dock, lock and latch mechanism of ligand-binding whereby the γ-chain peptide binds in a hydrophobic trench lying between the N2 and N3 subdomians (Ganesh *et al.*, 2008, Deivanayagam *et al.*, 2002). ClfA containing substitutions in residues P336 and Y338, which are located within the ligand-binding trench, were found to be defective in fibrinogen-binding (Loughman *et al.*, 2005, Deivanayagam *et al.*, 2002). Upon ligand-binding, the C-terminus of the N3 subdomain of ClfA forms the latching sequence that crosses over the ligand-binding trench and locks the γ-chain peptide into place by insertion between two β-strands in N2 by β-strand

complementation. A recombinant truncate of ClfA lacking the latching peptide is defective in ligand-binding (Geoghegan, 2008). Previous studies have shown that the interaction between ClfA and fibrinogen is inhibited by Ca^{2+} ions. Ca^{2+} ions bind to an inhibitory site within the A domain of ClfA and induce a conformational change that is incompatible with binding to the C-terminus of the γ-chain of fibrinogen (O'Connell *et al.*, 1998).

The A domains FnBPA and FnBPB also bind fibrinogen at the C-terminus of the γ-chain (Wann *et al.*, 2000). Based on their sequence similarity to ClfA, the A domains of FnBPA and FnBPB are predicted to fold into three subdomains N1, N2 and N3. Like ClfA, the N2 and N3 subdomains of FnBPA and FnBPB are sufficient for fibrinogen-binding and are predicted to bind to the γ-chain of fibrinogen by a similar mechanism (Keane *et al.*, 2007b ; Chapter 4). A 3D molecular model of the N2N3 subdomain of FnBPA allowed an investigation of residues predicted to line the ligand-binding trench. Residues N304 and F306 were found to be crucial for binding to fibrinogen (Keane *et al.*, 2007b). The substitution of each residue for an alanine resulted in a recombinant FnBPA A domain protein that showed a large reduction in ligand-binding *in vitro* (Keane *et al.*, 2007b). These residues are located in the equivalent positions residues P336 and Y338 of ClfA.

More recent studies have indicated that ClfA binds fibrinogen at two distinct sites. While the dock, lock and latch mechanism explains how the C-terminal γ-chain peptide binds to the trench between domains N2 and N3, a second in N3 has been identified by mapping the epitope for a function-blocking monoclonal antibody (Geoghegan, 2008). Amino acid substitutions within the epitope which reduced the binding of antibody also reduced fibrinogen binding. However, the mutants bound to the fibrinogen γ-chain peptide with the same affinity as the wild type protein (Geoghegan, 2008). This is consistent with the finding that ClfA has a higher affinity for

fibrinogen than for the γ-chain peptide (Wann *et al.*, 2000, Geoghegan, 2008). Taken together these data support a hypothesis that there is a second binding site for ClfA in fibrinogen and for fibrinogen in ClfA. This could explain the results from earlier studies which suggested that the interaction of ClfA with fibrinogen may be more complex than simply binding to the C-terminal residues of the γ-chain. Wann *et al.* (2000) noted that binding of recombinant ClfA A domain to fibrinogen could only be inhibited to 60-70% by γ-chain peptide, whereas binding of recombinant FnBPA A domain to fibrinogen could be inhibited to 100% by the same peptide. These findings suggest that ClfA recognizes more than one site in fibrinogen while FnBPA binds solely to the C-terminal residues of the γ-chain.

In this chapter, the mechanism by which the A domain FnBPB binds fibrinogen was investigated. Based on studies of ClfA and FnBPA, it was proposed that fibrinogen-binding by the A domain of FnBPB occurs through variation of the dock, lock and latch mechanism. In Chapter 4 it was shown that like ClfA and FnBPA, the N2N3 subdomain of FnBPB is sufficient for ligand-binding and that each recombinant N2N3 isotype (I-VII) bound fibrinogen with a similar affinity. Residues predicted to be involved in fibrinogen-binding by dock, lock and latch are conserved in all isotypes of FnBPB. Here, amino acids likely to be involved in both the latching peptide and the ligand-binding trench of FnBPB were identified using the 3D model of the A domain of FnBPB which is based on the crystal structure of ClfA (Chapter 4). The possibility that FnBPB contains a second fibrinogen-binding site was explored and the effect of divalent cations on the interaction between FnBPB and the fibrinogen γ-chain peptide was assessed.

5.2Results

5.2.1 Purification of rFnBPB$_{37-480}$

The A domain of FnBPB shares 45% sequence identity with the A domain of FnBPA and 25% sequence identity with the A domain of ClfA. It was predicted that, like FnBPA and ClfA, the N2N3 subdomain of FnBPB contains the minimum ligand-binding region and that the N1 subdomain is not involved in the binding of FnBPB to fibrinogen. The N2N3 subdomain of FnBPB from strain 8325-4 consists of residues 163-480. In Chapter 4, a recombinant protein encompassing these residues (rN2N3 isotype I) was shown to be sufficient to promote binding to fibrinogen. However, it was not clear if the N1 subdomain plays any role in the interaction. To analyse more thoroughly fibrinogen binding by the A domain of FnBPB, the full length A domain of FnBPB from strain 8325-4 was expressed. DNA encoding FnBPB residues 37- 480 was amplified by PCR from *S. aureus* 8325-4 genomic DNA and the resulting PCR product was cloned into pQE30 between the *Bam*HI and *Sma*I sites as described in Chapter 4 (Section 4.2.2) The recombinant protein was expressed and purified as described in Section 4.2.2. To compare the size and integrity of rFnBPB$_{37-480}$ and rFnBPB$_{163-480}$, the proteins were analysed by SDS-PAGE (Figure 5.1A). Both rFnBPB$_{37-480}$ and rFnBPB$_{163-480}$ migrated with an apparent molecular weight that is slightly higher than their molecular masses of 50 kDa and 37 kDa, respectively.

5.2.2 Binding of rFnBPB$_{37-480}$ to immobilised fibrinogen

In order to investigate if the N1 subdomain plays any role in the binding of FnBPB to fibrinogen, Surface Plasmon resonance (SPR) was carried out to determine accurately the dissociation constant (K_D) for the interaction between rFnBPB$_{37-480}$ and fibrinogen. SPR was carried out as described in Chapter 4 (Section 4.2.7). Different concentrations of rFnBPB$_{37-480}$ ranging from 0.15μM to 10μM were passed over the surface

of a fibrinogen-coated chip. The same chip was used to analyse the interaction of rFnBPB$_{163-480}$ which is described in Chapter 4 (Section 4.2.7). The representative sensorgram obtained for the interaction involving rFnBPB$_{37-480}$ is shown in Figure 5.2. rFnBPB$_{37-480}$ bound to fibrinogen with a K_D of 2μM. This is identical to that calculated for rFnBPB$_{163-480}$ (Chapter 4). The kinetic rate contants calculated for the two rFnBPB constructs are listed in Table 5.1. These data indicate that the N1 subdomain of FnBPB (residues 37-162) plays no role in fibrinogen-binding. The binding site for fibrinogen within FnBPB$_{(8325-4)}$ is thus located between residues 163-480.

5.2.3 Design and purification of a recombinant A domain truncate of FnBPB lacking C-terminal residues

Based on the molecular model described in Chapter 4, FnBPB residues likely to be involved in fibrinogen-binding by dock, lock and latch were identified. The C-terminal 17 residues of the N3 subdomain of FnBPB are underlined in the amino acid sequence shown in Figure 5.3 and are highlighted in pink in the 3D model shown in Figure 5.4. In the crystal structure of ClfA these residues form the latching peptide that plays a crucial role in the dock, lock and latch mechanism. Since FnBPB is predicted to bind to the fibrinogen γ-chain by the same mechanism, it was proposed that the C-terminal 17 residues of the A domain of FnBPB form the latching peptide and play a similar role in the interaction of FnBPB with fibrinogen. In order to anylyse the role in fibrinogen-binding of residues contained in the predicted latching peptide, a C-terminal truncate of the A domain of FnBPB was created. DNA encoding FnBPB residues 163-463 was amplified by PCR from pQE30 rFnBPB$_{163-480}$ DNA (Chapter 4). The PCR product was cloned into pQE30 between the *Bam*HI and *Sma*I sites as described in Chapter 4 (Section 4.2.2). The resulting construct was verified by restriction analysis and by DNA sequencing. The recombinant FnBPB truncate protein was produced as described in Chapter 4 (Section 4.2.2) and

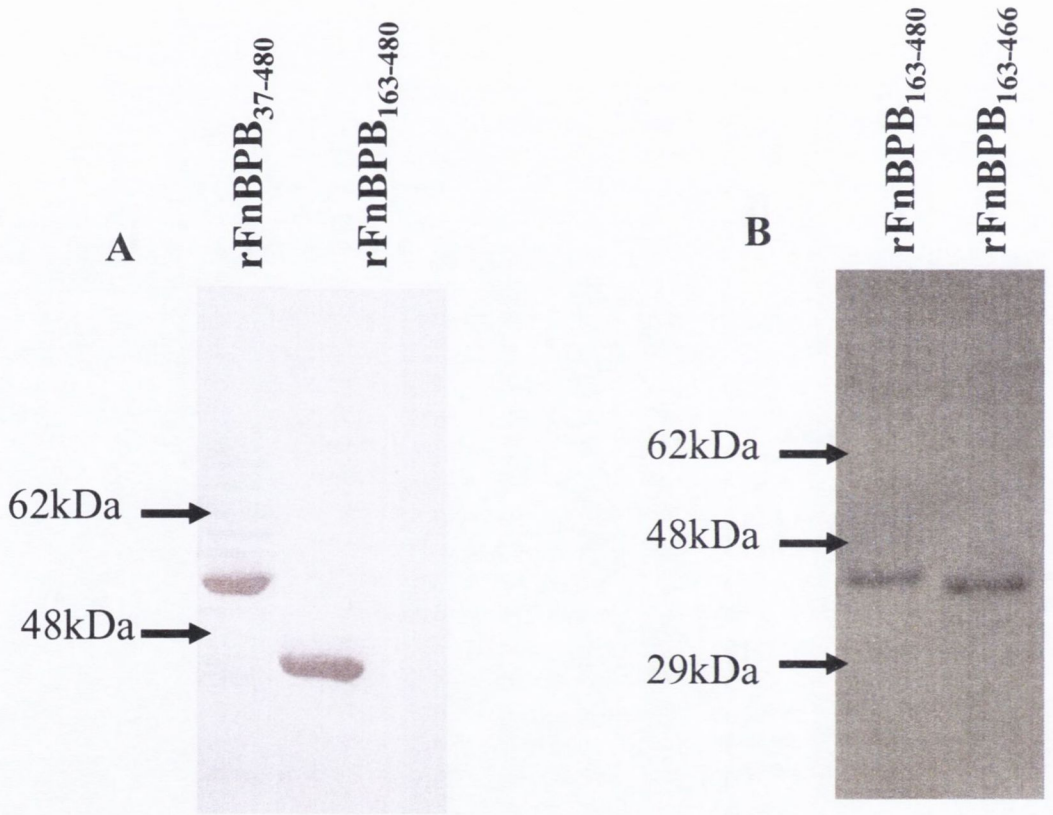

Figure 5.1 SDS-PAGE analysis of rFnBPB A domain truncates

Equal amounts (5μM) of (**A**) $rFnBPB_{37-480}$ and $rFnBPB_{163-480}$ or (**B**) $rFnBPB_{163-480}$ and $rFnBPB_{163-466}$ were analysed by SDS-PAGE and stained with Coomassie blue.

compared with $rFnBPB_{163-480}$ by SDS-PAGE analysis (Figure 5.1). The truncated N2N3 domain protein was purified to homogeneity was intact and migrated with an apparent molecular mass that is ~2kDa lower than that of wild-type protein.

5.2.4 Binding of $rFnBPB_{163-463}$ to immobilised fibrinogen

To investigate the role in fibrinogen binding played by the C-terminal residues in the A domain of FnBPB forming the putative latching peptide, the interaction of $rFnBPB_{163-463}$ with fibrinogen was analysed by SPR as described in Chapter 4 (section 4.2.7.). No detectable interaction was observed when concentrations of $rFnBPB_{163-463}$ (0.15μM- 10μM) were passed over the surface of a fibrinogen-coated chip (Figure 5.5). This experiment was repeated three times with similar results. As a control, the same chips were used when analyzing the interaction $rFnBPB_{163-480}$ with fibrinogen, the results of which are described and discussed in Chapter 4. The result of this section indicates that the C-terminal 17 residues of the A domain, which are predicted to form the latching peptide, are essential for the interaction of FnBPB with fibrinogen and may be important for the "latching" and "locking" steps in the fibrinogen-binding mechanism.

5.2.5 Design and purification of alanine-substituted variants of $rFnBPB_{163-480}$

Residues that line the predicted ligand-binding trench and which may play a role in the binding of FnBPB to the fibrinogen γ-chain were identified and mapped on the 3D model described in Chapter 4. Residues N312 and F314 are in the same position as residues in ClfA and FnBPA that are known to be involved in ligand-binding by dock, lock and latch. These residues were altered by site-directed mutagenesis and are indicated in the amino acid sequence shown in Figure 5.3 and highlighted in pink in the 3D model shown in Figure 5.6. To determine if FnBPB has a second binding

site for fibrinogen in an analogous fashion to ClfA, residues S349 and Y449 were also altered. These residues are indicated in the amino acid sequence shown in Figure 5.3 and highlighted in pink in the 3D model shown in Figure 5.7. They occupy the same position as I408 and Y512, respectively in the N3 subdomain of ClfA where they form part of the epitope for a function-blocking antibody and a second fibrinogen-binding site. The substitution of these residues in ClfA caused a reduction in affinity for fibrinogen but did not affect the affinity of ClfA for the γ-chain peptide.

Plasmid pQE30 $FnBPB_{163-480}$ DNA was used as a template for site-directed mutagenesis by the Quickchange method (see Section 2.6.7). DNA was amplified using primers containing the relevant mutation, the product digested with *Dpn*I to remove parental methylated DNA and transformed into *E.coli*. Recombinant protein was purified as described in Chapter 4 (Section 4.2.2) and analysed by SDS-PAGE. The gel in Figure 5.8 shows that the proteins were of a similar size, had been purified to homogeneity and were intact.

5.2.6 Binding of $rFnBPB_{163-480}$ N312A/F314A to immobilised fibrinogen

To investigate the role in fibrinogen binding of FnBPB trench residues N312 and F314, the interaction between $rFnBPB_{163-480}$ N312A/F314A and fibrinogen was analysed by SPR. Figure 5.9A shows a representative sensorgram obtained from SPR experiments in which increasing concentrations of $rFnBPB_{163-480}$ N312A/F314A, ranging from 0.15μM to 10μM, were passed over the surface of fibrinogen-coated chips. The same fibrinogen-coated chips were used in the SPR experiments described above and in Chapter 4. While some interaction between the double alanine-substituted mutant and fibrinogen is observed, it is apparent that this differs significantly from that of the wild type protein which is described Chapter 4 (Figure 4.14). It appears that the substitution of residues N312 and F316 destabilizes the FnBPB-fibrinogen interaction.

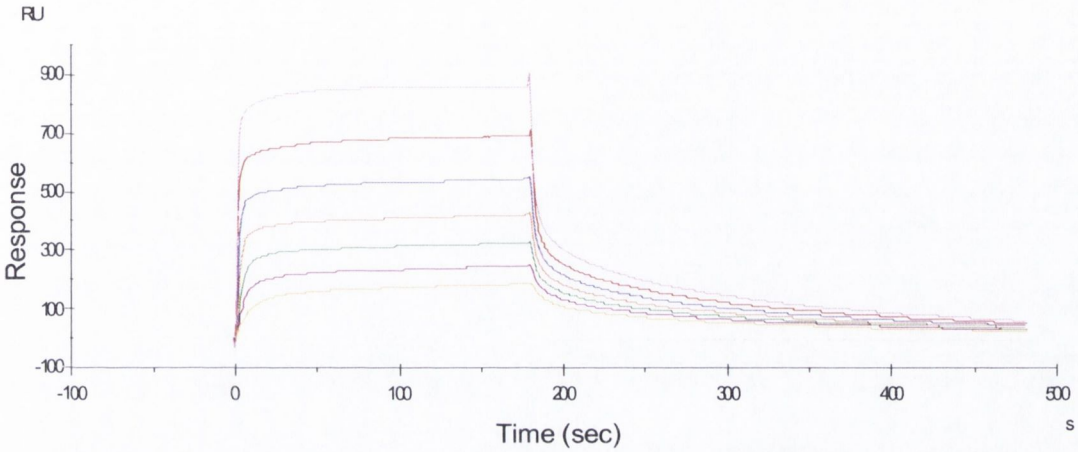

Figure 5.2 Surface plasmon resonance analysis of rFnBPB $_{37-480}$ binding to fibrinogen

Human fibrinogen was immobilised onto the surface of a dextran chip. $rFnBPB_{37-480}$ was passed over the surface in concentrations ranging from 0.15μM (lower-most trace) to 10μM (upper-most trace). The sensorgram has been corrected for the response obtained when $rFnBPB_{37-480}$ was passed over uncoated chips and is representative of 3 independent experiments.

Table 5.1 Rate constants for the interaction of $rFnBPB_{37-480}$ and $rFnBPB_{163-480}$ with fibrinogen

Protein	FnBPB subdomains	Association rate constant (K_a) (M)	Dissociation rate constant (K_d) (M)	Equilibrium dissociation constant (K_D) (μM)
$rFnBPB_{37-480}$	N1N2N3	5.066×10^4	7.146×10^3	2
$rFnBPB_{163-480}$	N2N3	2.417×10^4	7.675×10^3	2

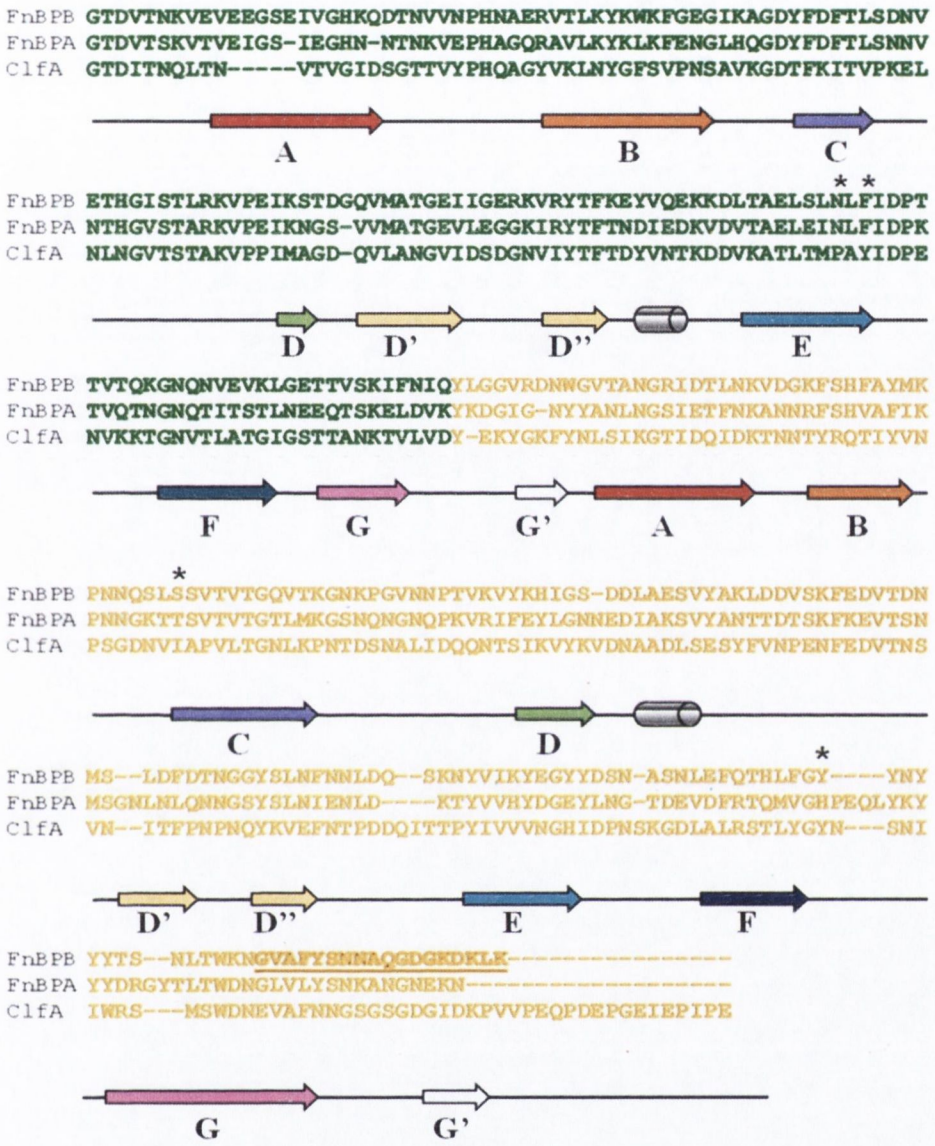

Figure 5.3 Amino acid sequence alignment of the N2N3 subdomains of FnBPB (top), FnBPA (middle) and ClfA (bottom) N2 subdoamin residues are shown in green and N3 subdoamin residues are shown in yellow. The secondary structure elements are represented as arrows below the text. Residues in the N3 subdomain of FnBPB that are predicted to comprise the latching peptide are underlined. FnBPB residues targeted for site-directed mutagenesis are indicated with an asterisk.

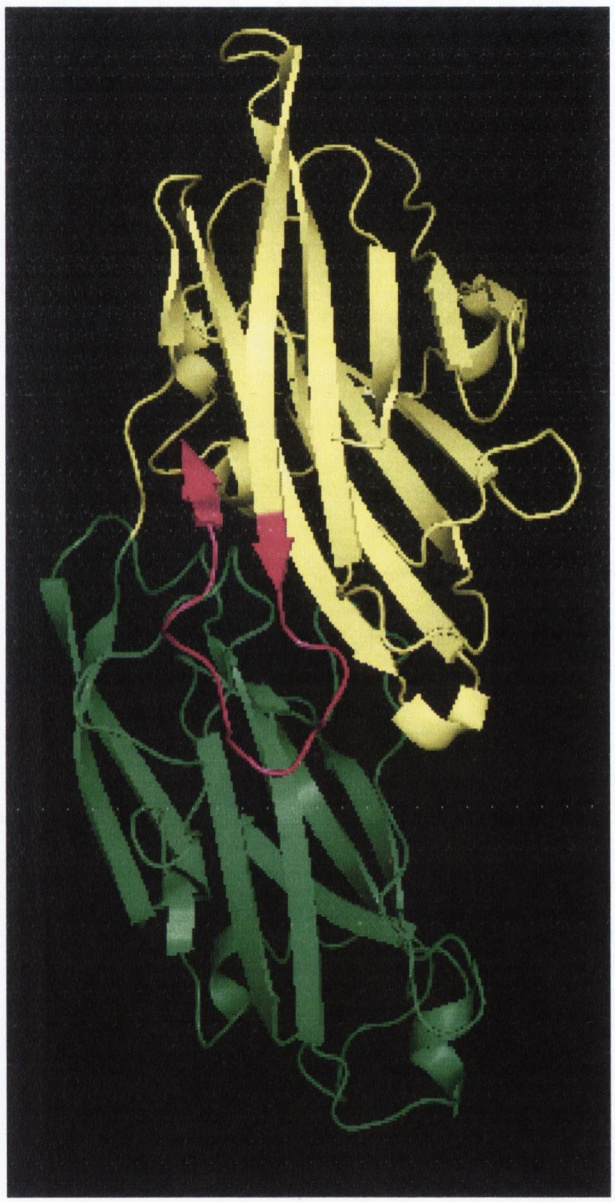

Figure 5.4 3D structural model of N2N3 of FnBPB

The ligand-binding trench is predicted to form between the N2 (green) and N3 (yellow) subdomains. C-terminal residues that are predicted to form the latching peptide are shown in pink.

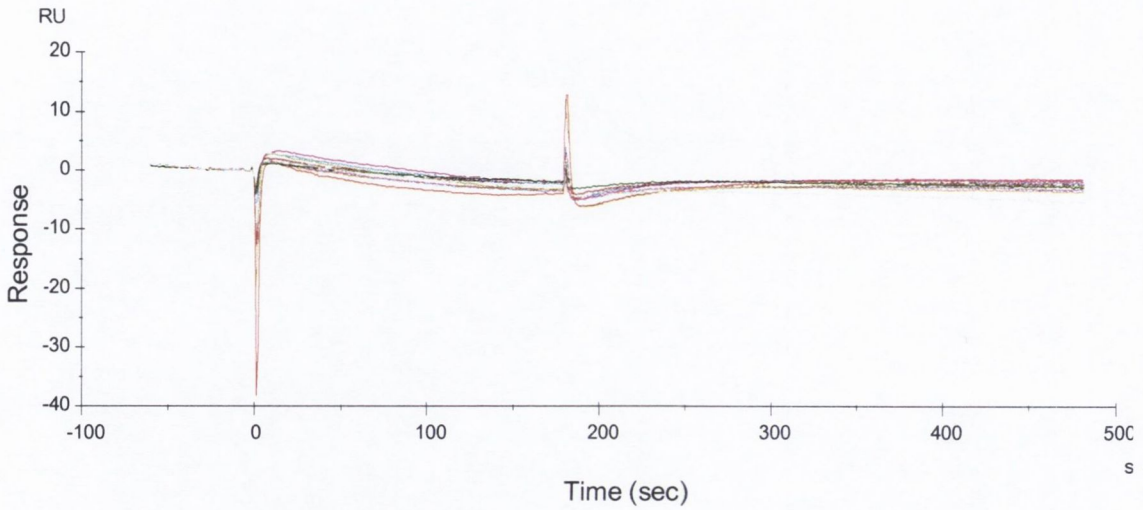

Figure 5.5 Surface plasmon resonance analysis of rFnBPB$_{163-466}$ binding to fibrinogen

Human fibrinogen was immobilised onto the surface of a dextran chip . rFnBPB$_{163-466}$ was passed over the surface in concentrations ranging from 0.15μM (lower-most trace) to 10μM (upper-most trace). The representative sensorgram has been corrected for the response obtained when recombinant FnBPB proteins were passed over uncoated chips.

Figure 5.6 Residues N312 and F314 of FnBPB

The ligand-binding trench is predicted to form between the N2 (green) and N3 (yellow) subdomains of FnBPB. Residues N312 and F314 which were selected for alteration by site-directed mutagenesis are shown in pink ball and stick format in (**A**) and are enlarged in (**B**)

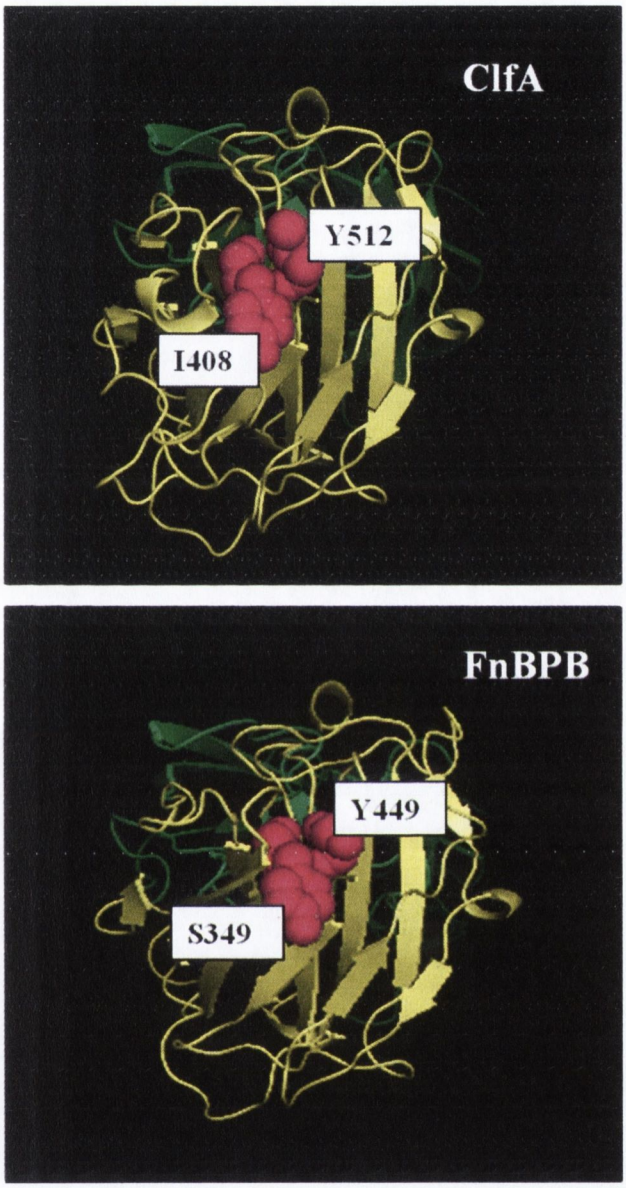

Figure 5.7 Ribbon models showing the top view of the N3 subdomains of ClfA and FnBPB

Residues I408 and Y512 are shown in pink spacefill and are important for fibrinogen binding by ClfA (A). The equivalent residues in FnBPB (B), are S349 and Y449 (pink space fill).

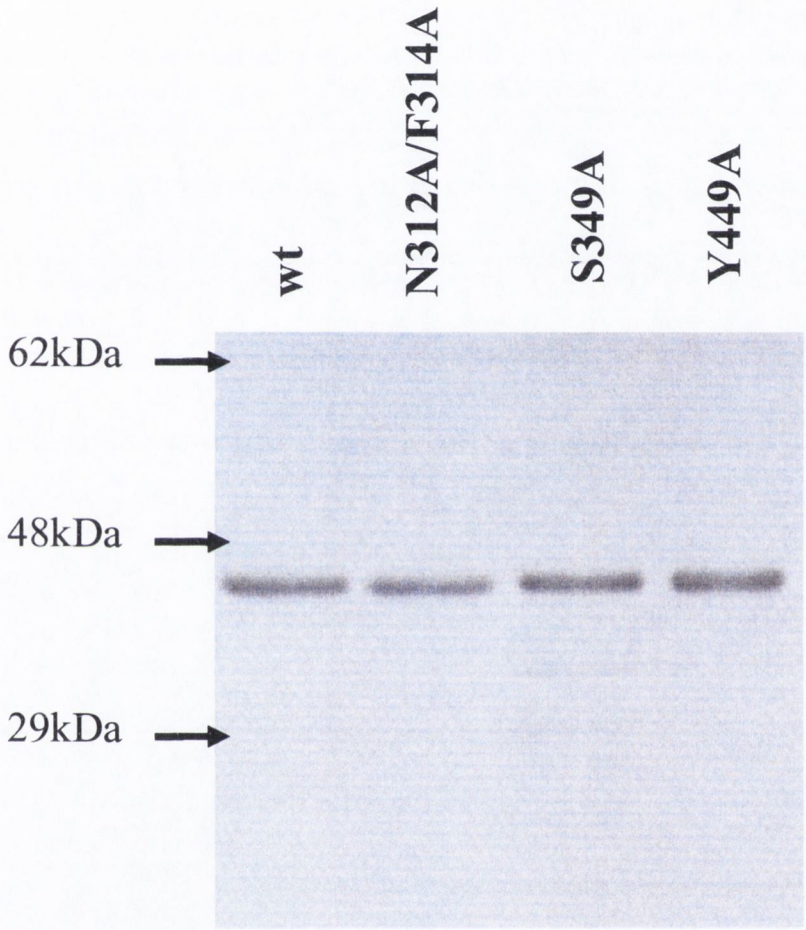

Figure 5.8 SDS-PAGE analysis of rFnBPB proteins

Equal amounts (5μM) of $rFnBPB_{163-480}$ wild type (wt) and alanine substituted variant proteins were analysed by SDS-PAGE and stained with Coomassie blue.

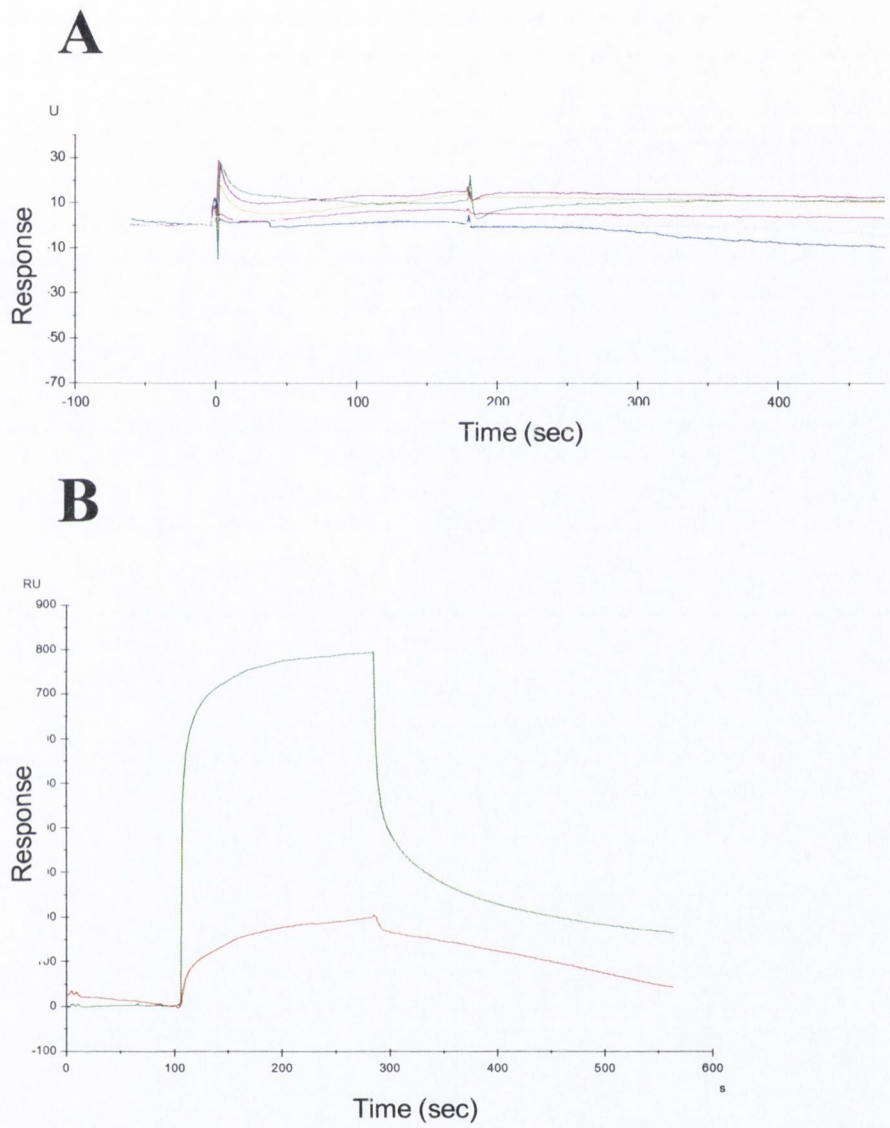

Figure 5.9 Surface plasmon resonance analysis of rFnBPB$_{163-480}$ N312A/F314A binding to fibrinogen

(**A**) rFnBPB$_{163-480}$ N312A/F314A ranging in concentration from 0.15μM to 10μM were passed over the surface of a fibrinogen coated chip. (**B**) Equal amounts (5μM) rFnBPB$_{163-480}$ N312A/F314A (Red) and the wild type protein (Green) were passed over the surface of the same fibrinogen chip. Each sensorgram is representative of three independent experiments and has been corrected for the response obtained when recombinant FnBPB proteins were passed over uncoated chips.

Consequently, no reliable kinetic parameters could be obtained when this sensorgram was analysed using the BIAevaluation software.

To investigate further how the N312A and F314A substitutions affected ligand-binding, equal concentrations (5μM) of $rFnBPB_{163-480}$ N312A/F314A and wild type $rFnBPB_{163-480}$ were passed over the surface of a fibrinogen-coated chip. Binding was compared and the sensorgram profiles obtained (Figure 5.9B). The mutant had greatly reduced binding to fibrinogen. The maximum binding level reached was 190RU compared the wild-type protein which reached a maximum of 800RU. These results indicate that residues N312 and F314 of the A domain play an important role in the interaction of FnBPB with fibrinogen. These residues are predicted to be located within the ligand-bindng trench and may therefore play an important role in "docking" step of fibrinogen binding.

5.2.7 Binding of $rFnBPB_{163-480}$ Y324A and S224A to immobilised fibrinogen

Residues S224 and Y324 correspond to the position of residues I408 and Y512 of ClfA which form part of the second binding site for fibrinogen. To explore the possibility of a second binding site for fibrinogen in FnBPB, the binding of $rFnBPB_{163-480}$ Y324A and $rFnBPB_{163-480}$ S224 to fibrinogen was analysed by SPR. Representative sensorgrams are shown in Figure 5.10. The affinity (K_D) of $rFnBPB_{163-480}$ Y324A and $rFnBPB_{163-480}$ S224 for fibrinogen was 2.6μM and 4μM, respectively. These K_Ds are very similar to the K_D of the wild type protein (2μM) indicating that residues Y324 and S224 of FnBPB play no role in fibrinogen binding.

5.2.8 Binding of $rFnBPB_{163-480}$ to the fibrinogen γ-chain peptide

It has been reported that ClfA has a >100 fold higher affinity for whole fibrinogen than for a synthetic peptide corresponding to the C-terminal 17 amino acids of the fibrinogen γ-chain peptide (Geoghegan,

2008). This is consistent with the presence of a second binding site for ClfA in fibrinogen. The overall K_D is a combination of the two fibrinogen-binding sites. To investigate the possibility of a second binding site for FnBPB in fibrinogen, the interaction between $rFnBPB_{163-480}$ and a recombinant fibrinogen γ-chain peptide was analysed. Recombinant GST and a 17-mer C-terminal fibrinogen γ-chain peptide fused to a GST affinity tag were kind gifts from Dr. Joan Geoghegan, Trinity College Dublin. The ability of $rFnBPB_{163-480}$ to bind whole fibrinogen and the fibrinogen γ-chain peptide was compared in a solid-phase binding ELISA-types assay as described in Chapter 4 (Section 4.2.5). In this assay, recombinant GST was used as a negative control. This experiment showed that there is no discernable difference in the affinity of $rFnBPB_{163-480}$ for immobilised fibrinogen and for immobilised rGST γ-chain (Figure 5.11). Since no detectable binding was measured between $rFnBPB_{163-480}$ and rGST, these results suggest that the 17 C-terminal residues of the fibrinogen γ-chain contain the sole binding site for FnPB in fibrinogen.

To confirm the results of the solid-phase binding assays, the interaction between $rFnBPB_{163-480}$ and rGST γ-chain was analysed by SPR. rGST γ-chain was immobilised onto the surface of a dextran chip using amine coupling. Increasing concentrations (0.15μM to 10μM) of $rFnBPB_{163-480}$ were passed over the surface of the rGST γ-chain-coated chip. A representative sensorgram is shown in Figure 5.12. The affinity (K_D) for rGST γ-chain was calculated to be 3.3μM which is very similar to the K_D for the interaction of FnBPB with fibrinogen (Chapter 4). The kinetic constants calculated for the interactions of $rFnBPB_{163-480}$ with whole fibrinogen and rGST γ-chain are listed in Table 5.2 and indicate that the mechanism of binding is the same in each case. These results are in agreement with the results of the ELISA experiments and demonstrate that FnBPB binds to a single site in fibrinogen, the 17 C-terminal residues of the γ-chain.

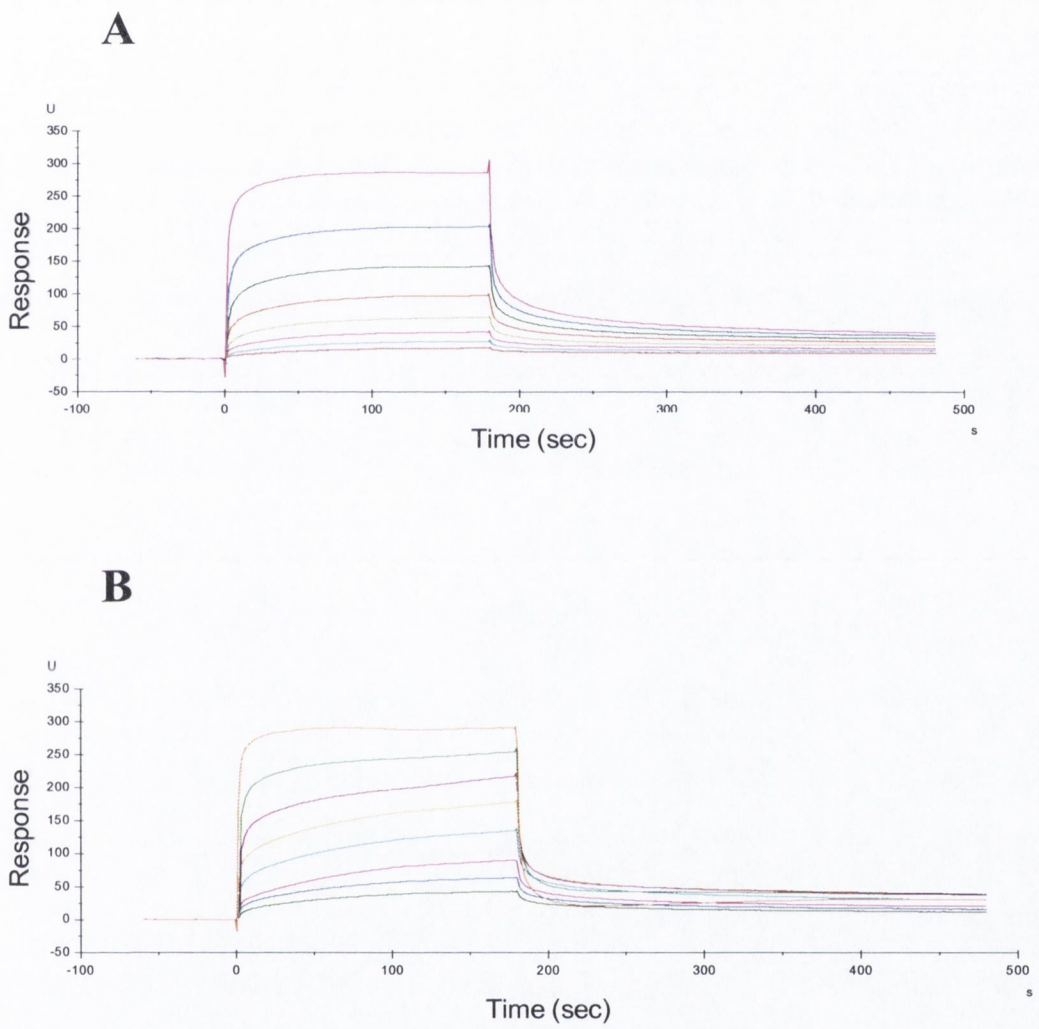

Figure 5.10 Surface plasmoon resonance analysis of rFnBPB$_{163-480}$S349A and rFnBPB$_{163-480}$ Y449 binding to fibrinogen

Human fibrinogen was immobilised onto the surface of a dextran chip. (**A**) rFnBPB163-480 S349A or (**B**) rFnBPB163-480 Y449A was passed over the surface in concentrations ranging from 0.15μM (lower-most traces) to 10μM (upper-most traces). Each sensorgram is representative of three independent experiments and has been corrected for the response obtained when recombinant FnBPB proteins were passed over uncoated chips.

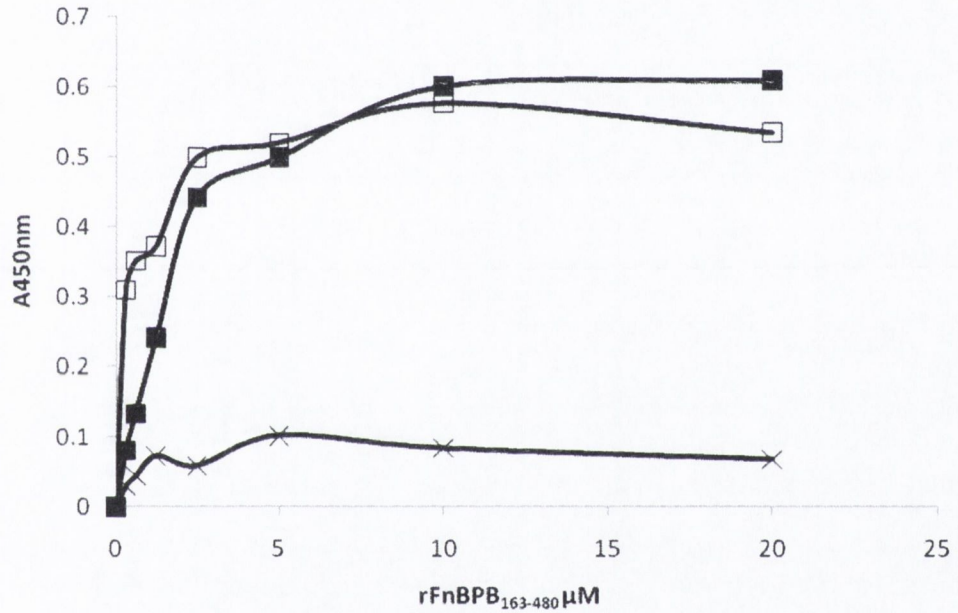

Figure 5.11 Binding of rFnBPB$_{163-480}$ to immobilised fibrinogen and rGST γ-chain

Microtitre plates were coated with an equal concentration (20 μg/ml) of human fibrinogen (□), rGST γ-chain (■) or rGST (X). Increasing concentrations of rFnBPB$_{163-480}$ were added and incubated for 2h at 37°C. Bound protein was detected with mouse anti-hexahistidine monoclonal antibody 7E8 followed by development with TMB substrate. Data points represent the mean of triplicate wells. The graph is representative of three independent experiments.

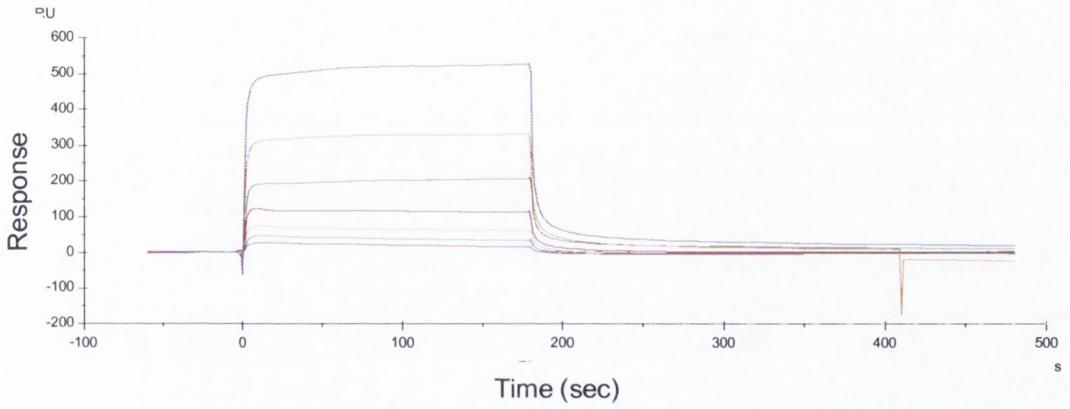

Figure 5.12 Surface plasmon resonance analysis of rFnBPB $_{37-480}$ binding to rGST γ –chain

rGST γ-chain was immobilised onto the surface of a dextran chip. rFnBPB$_{163-480}$ was passed over the surface in concentrations ranging from 0.15μM (lower-most trace) to 10μM (upper-most trace). The sensorgram is representative of three independent experiments and has been corrected for the response obtained when rFnBPB$_{37-480}$ was passed over uncoated chips.

Table 5.2 Rate constants for the interaction of rFnBPB$_{163-480}$ with whole fibrinogen and recombinant γ-chain peptide

Ligand	Association rate constant (K_a) (M)	Dissociation rate constant (K_d) (M)	Equilibrium dissociation constant (K_D) (μM)
Whole fibrinogen	2.417×10^4	7.675×10^3	2
rGST γ-chain	1.196×10^4	4.103×10^3	3.3

5.2.9 Effect of divalent cations on the interaction between FnBPB and the fibrinogen γ-chain.

Previous studies with ClfA indicated that the physiological concentration of Ca^{2+} ions (~ 2.5mM) inhibits the interaction between ClfA and fibrinogen. Here, the effect of Ca^{2+} ions on the interaction between $rFnBPB_{163-480}$ and fibrinogen was analysed by SPR. Since fibrinogen is known to be a Ca^{2+} binding protein it was decided to use the rGST γ-chain protein as the ligand and to assume that the observed effects of metal ions would reflect interactions between fibrinogen and FnBPB. For these experiments, 1μM samples of $rFnBPB_{163-480}$ were incubated with equal concentrations of $CaCl_2$, $MgCl_2$ or $NiCl_2$ ranging from 0.5mM to 25mM and passed over the surface of a rGST γ-chain-coated chip. The maximum binding level (RU) reached by each sample was calculated as a percentage of the maximum binding level reached by a cation-free control sample of $rFnBPB_{163-480}$ (Figure 5.13). The presence of Ca^{2+} ions inhibited the binding of $rFnBPB_{163-480}$ in a dose-dependent manner, whereas the presence of Mg^{2+} or Ni^{2+} ions had no effect at similar concentrations. The binding of $rFnBPB_{163-480}$ to rGST γ-chain was inhibited by fifty percent at a Ca^{2+} concentration of between 2 mM. This is similar to the concentration of Ca^{2+} that is present in normal human sera. These data suggest that like ClfA, Ca^{2+} ions bind to an inhibitory site within the A domain of FnBPB.

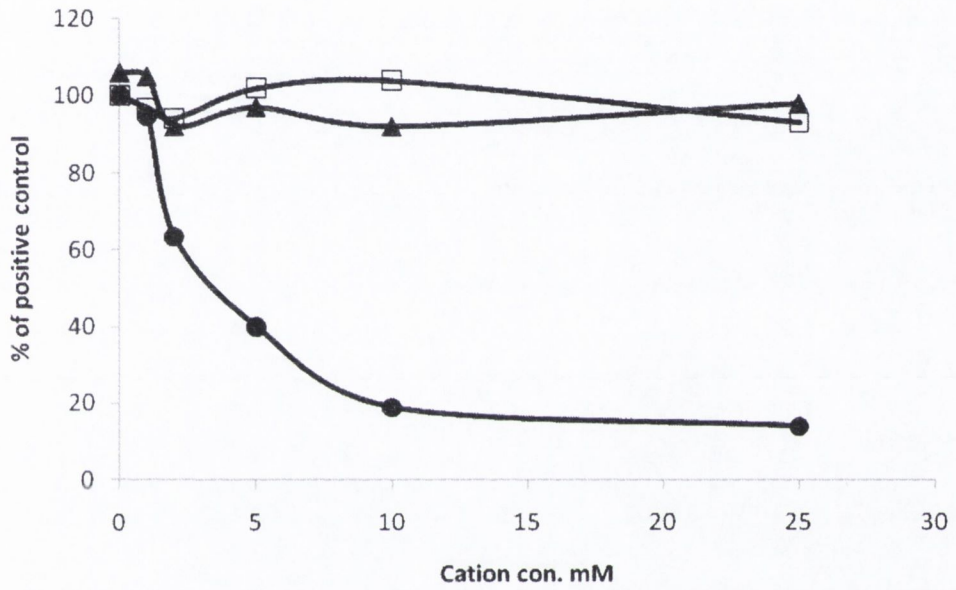

Figure 5.13 Inhibition of rFnBPB$_{163-480}$ binding to fibrinogen by Ca^{2+} ions

1μM of rFnBPB163-480 was incubated with increasing concentrations of $CaCl_2$(●), $MgCl_2$ (□) or $NiCl_2$ (▲) at room temperature for 1h before being passed over the surface of a rGST γ-chain coated chip. Maximum binding levels (RU) are expressed as a percentage of a cation-free rFnBPB$_{163-480}$ control sample. Data points represent the mean of triplicate wells. The graph is representative of three independent experiments.

5.3 Discussion

The N-terminal A domains of the *S. aureus* MSCRAMMs ClfA, FnBPA and FnBPB each promote binding to the C-terminus of the γ-chain of fibrinogen. These A domains share a similar structural organization and are predicted to bind fibrinogen by a similar mechanism. The A domains of ClfA and FnBPA have been characterised thoroughly and share 25% and 48% sequence similarity with the A domain of FnBPB, respectively. This study set out to analyse fibrinogen-binding by the A domain of FnBPB based on studies of ClfA and FnBPA.

In Chapter 4, the N2N3 subdomain of $FnBPB_{(8325\text{-}4)}$ which spans residues 163-480 was found to be sufficient for binding to immobilised fibrinogen. Here, a recombinant N1N2N3 construct spanning residues 37-480 was created to assess any function of N1 in ligand-binding. Fibrinogen binding by $rFnBPB_{37\text{-}480}$ and $rFnBPB_{163\text{-}480}$ was compared by SPR analysis. Each protein bound fibrinogen with an identical K_D indicating that the N1 subdomain of FnBPB does not have any role in fibrinogen-binding. This is in accordance with A domains of ClfA and FnBPA, the N2N3 subdomains of which are both sufficient for binding to fibrinogen (Keane *et al.*, 2007b, Deivanayagam *et al.*, 2002). The binding site for fibrinogen in $FnBPB_{(8325\text{-}4)}$ has thus been localised to residues 163-480 encompassing the N2N3 subdomain of FnBPB.

The 3D structures of the N2N3 subdomains of staphylococcal surface proteins SdrG and ClfA has greatly increased our understanding of the mechanisms by which these proteins can bind to peptide ligands. A dynamic mechanism has been proposed called dock, lock and latch whereby the fibrinogen ligand docks into a hydrophobic trench situated between the N2 and N3 subdomains of region A. A flexible linker region or hinge then folds over the fibrinogen peptide to lock the ligand in place. Upon locking, the C-terminal β-strand of N3 slots between two β-strands of N2 in a β-

strand complementation which forms the latching mechanism. Sequence analysis has indicated that structurally related ligand-binding regions from the A domains of S. aureus ClfA, FnBPA and FnBPB share conserved motifs which include a potential latching peptide (Ponnuraj *et al.*, 2003). It has been proposed that the dock, lock and latch mechanism of ligand-binding is a common to these proteins.

A 3D molecular model of the N2N3 domains of FnBPB based on the known structure of ClfA facilitated an analysis of the binding site for fibrinogen. The C-terminal residues 463-480 are predicted to form the latching peptide that would be critical for the binding of fibrinogen by dock, lock and latch. This hypothesis was tested by constructing a truncate of the N2N3 protein ($rFnBPB_{163-463}$) which lacked the predicted latching peptide. $rFnBPB_{163-463}$ did not bind detectably to fibrinogen by SPR. This indicates that, like ClfA and FnBPA, the C-terminal residues of the N3 subdomain are crucial for the interaction of FnBPB with fibrinogen and provides evidence for a dock, lock and latch mechanism of fibrinogen-binding.

To define further the precise fibrinogen-binding site in FnBPB, amino acids were chosen for alteration due to their being in the equivalent positions as residues previously tested for their importance in fibrinogen-binding by ClfA and FnBPA. Residues N312 and F314 of FnBPB are predicted to line the putative ligand-binding trench in positions equivalent to P336 and Y338 of ClfA and N304 and F306 of FnBPA, respectively. The substitution of residues N312 and F314 to alanines had drastic consequences on the binding of $rFnBPB_{163-480}$ to fibrinogen indicating that these residues play an important role in the fibrinogen binding mechanism. It is proposed that residues N312 and F314 of FnBPB are involved in vital interactions with the fibrinogen ligand within the ligand binding trench. This is further evidence that fibrinogen binds to ClfA, FnBPA and FnBPB in a similar manner. Taken together these data highlight the structural similarities

between the A domains of ClfA, FnBPA and FnBPB which is consistent with the molecular model of the A domain of FnBPB created in this study. This lends support to the use of such models in the understanding of the mechanisms by which staphylococcal MSCRAMMs bind to their ligands.

The interaction between the A domain of ClfA and the γ-chain of fibrinogen has been studied in detail. This interaction is inhibited by minimolar concentrations of Ca^{2+} ions which bind to the A domain of ClfA and induce a conformational change that is incompatible with binding to the C-terminus of the γ-chain of fibrinogen (O'Connell *et al.*, 1998). Since ClfA and FnBPB are predicted to bind to the fibrinogen γ-chain in a similar manner, it was proposed that A domain of FnBPB also contains an inhibitory binding site for Ca^{2+} ions. To test this hypothesis the binding of $rFnBPB_{163-480}$ to rGST γ-chain in the presence of Ca^{2+} was analysed by SPR. As with ClfA, the concentration of Ca^{2+} present in normal human sera inhibited the binding of $rFnBPB_{163-480}$ to the fibrinogen γ-chain peptide. It was suggested previously that Ca^{2+} regulates the fibrinogen-binding function of a subset of ClfA molecules on the cell surface of *S. aureus* during the stationary phase of growth (O'Connell *et al.*, 1997). Since *S. aureus* FnBPs are expressed exclusively during the exponential phase of growth, it is tempting to speculate that Ca^{2+}-dependent regulation of FnBP activity prevents all of the fibrinogen receptors on *S. aureus* cells from being occupied by soluble fibrinogen during the exponential phase. This may allow *S .aureus* cells to adhere to solid-phase fibrinogen or fibrin clots during the early growth phase. In addition, this Ca^{2+}- dependent process may allow cells to detach from the vegetations and spread.

ClfA interacts with the extreme C-terminus of the γ-chain of fibrinogen by a variation of the dock, lock and latch mechanism (Ponnuraj *et al.*, 2003, Ganesh *et al.*, 2008). A second binding site at the top of the N3 subdomain of ClfA has been identified which interacts with another site in

fibrinogen. The presence of a second fibrinogen binding site explains why ClfA has a higher affinity for whole fibrinogen than for the γ-chain peptide. Given the structural similarities between the A domains of ClfA and FnBPB and the fact that both proteins bind to the fibrinogen γ-chain, it was important to explore the possibility of a second binding site for fibrinogen in the A domain of FnBPB. Residues S224 and Y324 of FnBPB were selected for mutagenesis because their predicted positions corresponded to the position of residues which are contained within the second fibrinogen-binding site in of ClfA and play an important role in fibrinogen-binding. Substitution of S224 or Y324 caused no significant reduction in the affinity of $rFnBPB_{163-480}$ for fibrinogen indicating that these residues play no role in fibrinogen binding. This suggests that, unlike ClfA, the N3 subdomain of FnBPB does not contain a second binding site for fibrinogen. Furthermore, $rFnBPB_{163-480}$ bound to immobilised fibrinogen and rGST γ-chain with similar affinities. This demonstrates that the only binding site for FnBPB in fibrinogen is in the extreme C-terminus of the γ-chain. Taken together, these results illustrate important differences between the interactions of ClfA and FnBPB with fibrinogen.

Chapter 6

Analysis of fibronectin binding by the A domain of FnBPB

6.1 Introduction

Bacterial colonization requires the attachment of the colonizing organism to molecules and tissues of the host. *S. aureus* has evolved a wide range of surface proteins known as MSCRAMMs which enable the bacterium to bind specifically to selected components of the host plasma and extracellular matrix (ECM). Fibronectin is a large, ubiquitous glycoprotein that is present in body fluids, on the surface of cells and in the cellular substratum or ECM. The protein has a modular structure and is composed of type 1, 2 and type 3 (F1, F2 and F3) modules (Figure 1.10). It is now over thirty years since Kuusela *et al.*, (1978) first reported that *S. aureus* could bind to fibronectin. Since then, much research has focused on the fibronectin-binding MSCRAMMs of *S. aureus*, the FnBPs. These proteins, which are the archetypal bacterial fibronectin-binding proteins, have been implicated as important mediators in *S. aureus* endocarditis and septic arthritis (Que *et al.*, 2005, Palmqvist *et al.*, 2005).

S. aureus expresses two fibronectin-binding proteins on its cell surface, FnBPA and FnBPB. Both proteins are multifunctional MSCRAMMs that promote adhesion to fibrinogen, elastin and fibronectin. Both proteins contain an N-terminal fibrinogen and elastin-binding A domain which is predicted to fold into three individual subdomains N1, N2 and N3 (Ponnuraj *et al.*, 2003, Deivanayagam *et al.*, 2002). The A domains of FnBPA and FnBPB have low sequence identity (~48 %) and are antigenically distinct (Loughman, 2006). Despite this diversity, the N2N3 subdomain of each protein is sufficient to promote ligand-binding and is believed to bind fibrinogen and elastin by the dock-lock-latch mechanism (Keane *et al.*, 2007b; Chapter 5). Each FnBP A-domain is followed by an intrinsically disordered region containing 11 (FnBPA) or 10 (FnBPB) non-identical fibronectin-binding repeats (FnBRs) (Meenan *et al.*, 2007). The FnBR amino acid sequences are well conserved in FnBPA, FnBPB and in

the fibronectin-binding surface proteins expressed by other gram-positive cocci such as *Streptococcus dysgalactiae* and *Streptococcus pyogenes* (Schwarz-linek *et al.*, 2006). FnBRs target specifically the N-terminal domain of fibronectin which comprises five F1 modules (Schwarz-Linek *et al.*, 2003, Meenan *et al.*, 2007). Studies using synthetic peptides have demonstrated that some FnBRs have a high affinity for fibronectin, whilst others have a much lower affinity (Meenan *et al.*, 2007). It has been proposed that each FnBR of *S. aureus* FnBPA binds a string of 3-4 F1 modules in the N-terminal domain through a variation of the tandem β-zipper mechanism. This mechanism was first described for the fibronectin-binding domains of FnBP from *S. dysgalactiae* (Schwarz-Linek *et al.*, 2003) (Figure 1.12). Recently, the crystal structures of FnBR-1 and FnBR-5 of *S. aureus* FnBPA, each in complex with four type I modules of fibronectin, have been solved. These structures revealed the antiparallel orientation of the binding partners and confirmed the tandem β-zipper mechanism of binding (Bingham *et al.*, 2008) (Figure 1.13).

The expression of FnBPs not only mediates *S. aureus* adhesion to host proteins but also triggers efficient internalization of *S. aureus* into non-phagocytic host cells. The FnBPs are essential for invasion of several eukaryotic cell types by *S. aureus* (Sinha *et al.*, 1999, Grundmeier *et al.*, 2004, Dziewanowska *et al.*, 1999). Heterologous expression of FnBPs in non-invasive gram-positive bacteria such as *L. lactis* or *S. carnosus*, was found to be sufficient to induce uptake by host cells (Sinha *et al.*, 2000). The binding of fibronectin by FnBPs is crucial for the invasion process in which fibronectin serves as a bridging molecule that links FnBPs, expressed by *S. aureus*, with integrin $\alpha_5\beta_1$, the principal fibronectin receptor on the surface of host cells (Fowler *et al.*, 2000). Subsequently, the bacteria are engulfed by an active cellular process which may provide *S. aureus* with a means of evading the host's immune system and antimicrobials. The FnBP-mediated invasion of endothelial host cells is believed to facilitate *S. aureus*

persistence and the establishment of secondary (metastatic) infections. This was convincingly demonstrated in a study of the role of FnBPA in experimental endocarditis where binding to both fibrinogen and fibronectin were investigated. Binding of fibrinogen was required for initial colonization of thrombi on damaged valves while binding to fibronectin was required for the infection to spread (Que *et al.*, 2001). Recent studies have indicated that the presence of multiple high-affinity FnBRs within FnBPA is required for the rapid uptake of *S. aureus* by endothelial cells. *S. aureus* expressing FnBPA variants with no or fewer FnBRs did not invade endothelial cells *in virto* and were significantly less virulent in a murine sepsis model compared to strains expressing FnBPA with the full complement of repeats (Edwards *et al.*, 2010).

The co-ordinates of FnBPA and FnBPB from *S. aureus* strain 8325-4 were recently redefined (Meenan *et al.*, 2007). The revised N2N3 subdomains span residues 194 to 511 and residues 163 to 480, respectively (Keane *et al.*, 2007b, Meenan *et al.*, 2007). These residues do not include any FnBR sequences. The ligand-binding ability of $rFnBPA_{194\text{-}511}$ was tested previously and the protein was found to promote binding only to fibrinogen and elastin. These results confirmed the absence of any fibronectin-binding motifs in the revised N2N3 subdomain of FnBPA (Keane *et al.*, 2007b). In this study, the ligand-binding ability of $rFnBPB_{163\text{-}480}$ (rN2N3 isotype I) was tested (Chapter 4). Unexpectedly, this protein bound to immobilised fibrinogen, elastin and fibronectin with similar affinities. This raised the possibility that, unlike FnBPA, the A domain of FnBPB contains a novel fibronectin binding motif and may bind fibronectin by a novel mechanism. In this chapter, the mechanism by which $rFnBPB_{163\text{-}480}$ binds fibronectin is investigated. The binding sites for fibronectin in $rFnBPB_{163\text{-}480}$ and for $rFnBPB_{163\text{-}480}$ in fibronectin have been localised. Finally, the ability of the A domain of FnBPB to promote bacterial adhesion to fibronectin and invasion of endothelial cells was examined.

6.2 Results

6.2.1 Testing the purity of commercial fibronectin

The revised fibrinogen and elastin-binding N2N3 subdomain of $FnBPB_{(8325\text{-}4)}$ spans residues 163-480 and does not include any known fibronectin binding motifs. However, when the binding ability of $rFnBPB_{163\text{-}480}$ was tested, the protein was found to bind to immobilised fibronectin dose-dependently and saturably in ELISA-type assays and SPR experiments (Chapter 4). Doubts were cast over the purity of the commercial fibronectin used in these assays with the possibility that contaminating fibrinogen was present. This could account for the binding of $rFnBPB_{163\text{-}480}$. Subsequently, the purity of Calbiochem fibronectin used was examined by ELISA and dot-immunoblotting experments. Various concentrations of Calbiochem fibronectin and Calbiochem fibrinogen were coated onto the wells of a microtitre dish or applied to a nitrocellulouse membrane and then probed with a mouse monoclonal anti-fibrinogen antibody. Bound antibody was detected using rabbit HRP-conjugated anti-mouse antibodies. In each experiment, the anti-fibrinogen antibody bound with high affinity to immobilised fibrinogen but did not react detectably with immobilised fibronectin (Figures 6.1 and 6.2). As a control, nitrocellulouse membranes were stripped of anti-fibrinogen antibody and re-probed with polyclonal anti-fibronectin antibodies for the detection of immobilised fibronectin (Figure 6.2B). These results confirmed that the Calbiochem fibronectin used in this study was free from fibrinogen contamination. This suggested that the results of the fibronectin binding assays described in Chapter 4 were not an artifact.

6.2.2 Binding of $rFnBPB_{163\text{-}463}$ to immobilised fibronectin

Based on the molecular model of FnBPB described in Chapter 4, the C-terminal 17 residues of the N3 subdomain were predicted to form the latching peptide that would be critical for ligand binding by the dock, lock

and latch mechanism. In Chapter 5, a truncate of the FnBPB N2N3 protein ($rFnBPB_{163-463}$) which lacked the predicted latching peptide was constructed and its ability to bind fibrinogen was tested. $rFnBPB_{163-463}$ did not bind to immobilised fibrinogen indicating that the C-terminal residues of the N3 subdomain are crucial for the interaction of FnBPB with fibrinogen and provided evidence for a dock, lock and latch mechanism of fibrinogen-binding.

To establish if the N2N3 subdomain of FnBPB binds fibronectin by the same mechanism, the binding of $rFnBPB_{163-463}$ to fibronectin was analysed by SPR. Figure 6.3 shows a representative sensorgram obtained from SPR experiments in which increasing concentrations of $rFnBPB_{163-463}$, ranging from 0.15 μM to 10 μM, were passed over the surface of fibronectin-coated chips. The same fibronectin-coated chips were used in the SPR experiments involving the wild type protein which are described in Chapter 4. $rFnBPB_{163-463}$ bound dose-dependently to fibronectin with an affinity constant (K_D) of 2μM. This is very similar to the K_D calculated for the wild type protein, $rFnBPB_{163-480}$ (Chapter 4). The kinetic rate constants calculated for the two rFnBPB constructs are listed in Table 6.1 and indicate that the C-terminal residues of the N2N3 subdomain of FnBPB play no role in the fibronectin-binding mechanism. These results suggest that different mechanisms are involved in the binding of the A domain of FnBPB to fibrinogen and fibronectin.

6.2.3 Binding of $rFnBPB_{163-480}$ N312/F314 to immobilised fibronectin

In the 3D model of the A domain of FnBPB residues N312 and F314 occupy the same positions as residues in ClfA and FnBPA that are known to be involved in ligand-binding by dock, lock and latch. As described in Chapter 5, the substitution of N213 and F314 for alanines dramatically reduced the affinity of $rFnBPB_{163-480}$ for fibrinogen. This indicated a vital

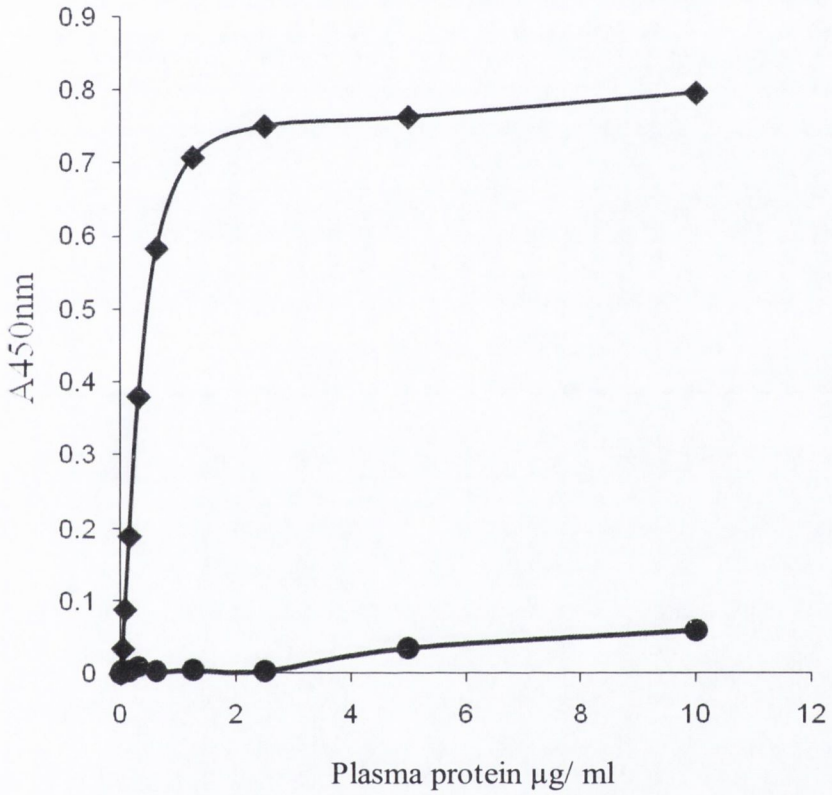

Figure 6.1 Binding of anti-fibrinogen antibodies to immobilised human fibrinogen and fibronectin by ELISA

Microtitre wells were coated Calbiochem human fibrinogen (♦) and fibronectin (●) and probed with mouse monoclonal anti-fibrinogen antibody followed by detection with HRP-conjugated rabbit anti-mouse IgG. Plates were developed with TMB substrate. Data points represent the mean of triplicate wells. The graph is representative of three independent experiments.

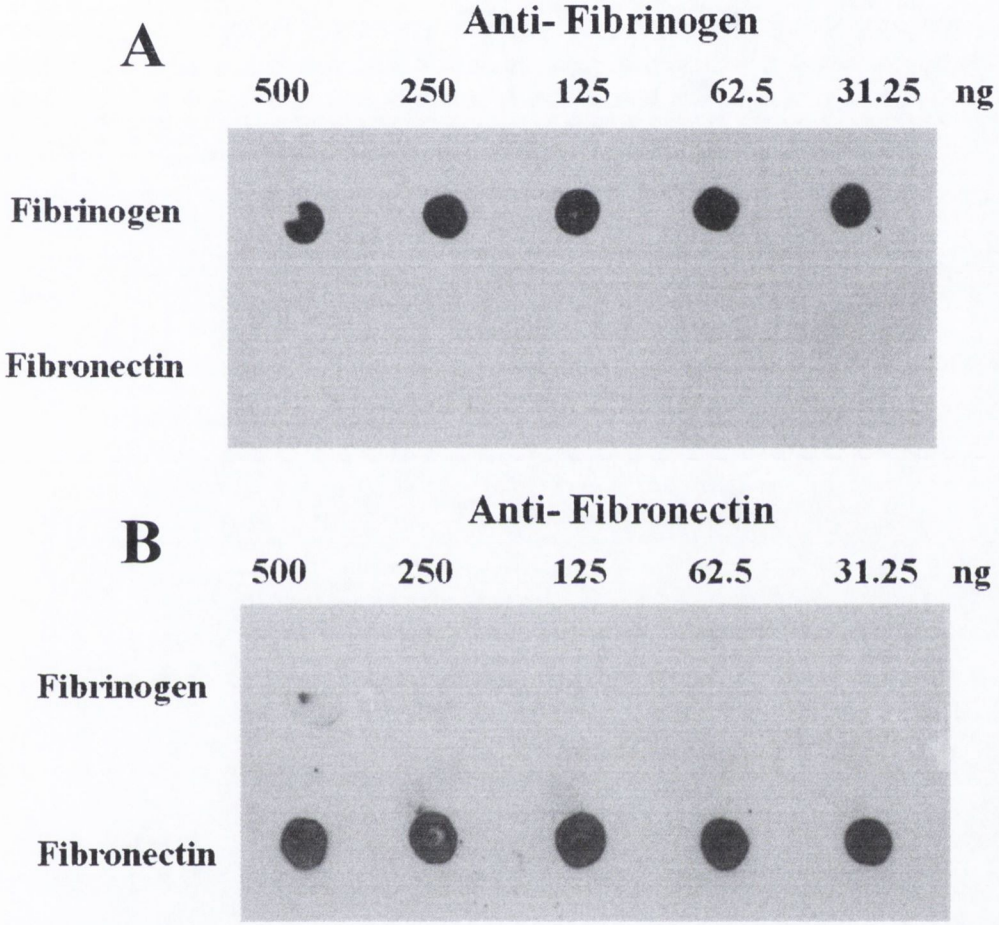

Figure 6.2 Binding of anti-fibrinogen antibodies to immobilised human fibrinogen and fibronectin by dot-immunoblotting
Various concentrations of Calbiochem fibrinogen and Calbiochem fibronectin ranging from 31.25 ng to 500 ng were applied to nitrocellulose membranes and probed with (**A**) a mouse monoclonal anti-fibrinogen antibody or (**B**) rabbit polyclonal anti-fibronectin antibodies. Bound antibody was detected using (**A**) HRP-conjugated rabbit anti-mouse IgG or (**B**) HRP-conjugated goat anti-rabbit IgG. Each blot is representative of three individual experiments.

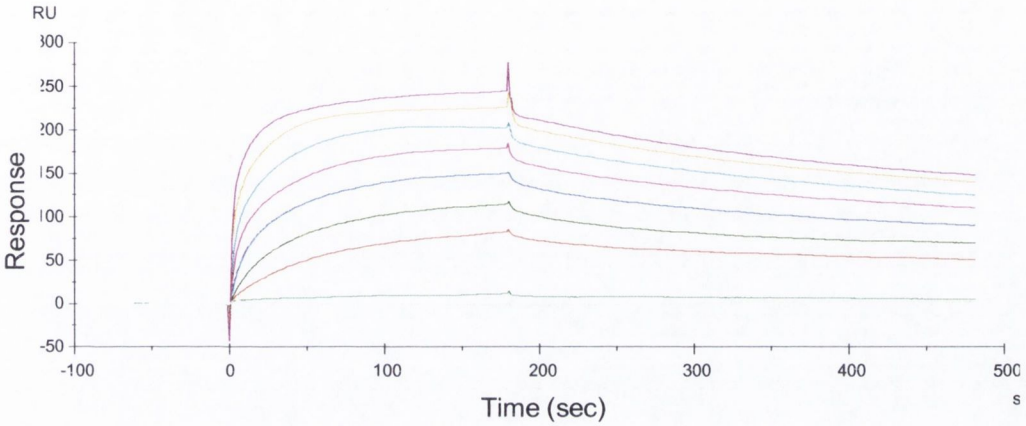

Figure 6.3 Surface plasmon resonance analysis of rFnBPB $_{37-463}$ binding to fibronectin

Human fibronectin was immobilised onto the surface of a dextran chip. rFnBPB$_{163-463}$ was passed over the surface in concentrations ranging from 0.15μM (lower-most trace) to 10μM (upper-most trace). The sensorgrams has been corrected for the response obtained when rFnBPB$_{37-480}$ was passed over uncoated chips and is representative of three independent experiments.

Table 6.1 Rate constants for the interaction of rFnBPB$_{163-480}$ and rFnBPB$_{163-463}$ with fibronectin

Protein	Association rate constant (K_a) (M)	Dissociation rate constant (K_d) (M)	Equillibrium dissociation constant (K_D) (μM)
rFnBPB$_{163-480}$	5.066 x 10^4	7.146 x 10^3	2.5
rFnBPB$_{163-463}$	5.450 x 10^4	4.115 x 10^3	2

role for the predicted ligand-binding trench in the interaction between the A domain of FnBPB and fibrinogen.

In order to determine if the predicted liagnd-binding trench plays a role in the interaction between the A domain of FnBPB and fibronectin, the binding of rFnBPB$_{163-463}$ N312A/F214A to immobilised fibronectin was analysed by SPR. Different concentrations of rFnBPB$_{163-480}$ N312A/F314A ranging from 0.15 μM to 10 μM were passed over the surface of fibronectin-coated chips. The same chips were used in the SPR experiments described above and in Chapter 4. A representative sensorgram obtained for the interaction involving rFnBPB$_{163-480}$N312A/F314A is shown in Figure 6.4A. While some interaction between the double alanine-substituted mutant and fibronectin was observed, it is apparent that this interaction differs significantly from that of the wild type protein which is described Chapter 4. It appears that the alanine-substitution of residues N312 and F316 destabilizes the rN2N3-fibronectin interaction. Consequently, no reliable kinetic parameters could be obtained when this sensorgram was analysed using the BIAevaluation software.

To determine if the N312A and F314A substitutions affected fibronectin-binding, equal amounts (2μM) of rFnBPB$_{163-480}$ N312A/F314A and wild type rFnBPB$_{163-480}$ were passed over the surface of a fibronectin-coated chip. Binding was compared and the sensorgram profiles obtained (Figure 6.4B). The mutant had greatly reduced binding to fibronectin. The maximum binding level reached was 25 RU compared the wild-type protein which reached a maximum of 55 RU. These results indicate that residues N312 and F314 play an important role in the binding of the A domain of FnBPB to fibronectin and suggest that like fibrinogen, fibronectin interacts with the predicted ligand-binding trench.

6.2.4 Purification of recombinant FnBPB N2 and N3 subdomains.

To further localize the fibronectin-binding site in the A domain of FnBPB, individual subdomains N2 and N3 were expressed and purified. DNA encoding FnBPB residues 163-308 (N2) and residues 309-480 (N3) were amplified by PCR from pQE30 rFnBPB$_{163-480}$ DNA (Chapter 4). The PCR products were cloned separately into pQE30 between the *Bam*HI and *Sma*I sites as described in Chapter 4 (Section 4.2.2). The resulting constructs were verified by restriction analysis and by DNA sequencing. The recombinant FnBPB truncated proteins were produced as described in Chapter 4 (Section 4.2.2) and analysed by SDS-PAGE (Figure 6.5). The gel indicates that rFnBPB$_{163-308}$ and rFnBPB$_{309-480}$ were purified to homogeneity, were intact and migrated with an apparent molecular weight that is slightly higher than their molecular masses of 17.8kDA and 20.7kDA, respectively.

6.2.5 Binding of rFnBPB$_{163-308}$ and rFnBPB$_{309-480}$ to immobilised fibronectin

In order to localize the fibronectin-binding site in the N2N3 subdomain of FnBPB, the recombinant FnBPB N2 subdomain (rFnBPB$_{163-308}$) and N3 subdomain (rFnBPB$_{309-480}$) were analysed for binding to fibronectin by SPR. SPR experiments were carried out using the same fibronectin-coated chips described above and in Chapter 4 and representatives of the sensorgrams obtained are shown in Figure 6.6. Each recombinant protein interacted weakly with fibronectin. rFnBPB$_{309-480}$ bound to immobilised fibronectin with an affinity constant (K_D) of 22.7μM, approximately 10-fold weaker than the affinity constant calculated for the wild type rFnBPB$_{163-480}$ in Chapter 4 (Figure 6.6A). An even weaker reaction was observed with rFnBPB$_{163-308}$ (Figure 6.6B). Consequently, no reliable kinetic parameters could be obtained when this sensorgram was analysed using the BIAevaluation software. These results suggest that both subdomains N2 and N3 play a role in the interaction between the N2N3 region of FnBPB and fibronectin.

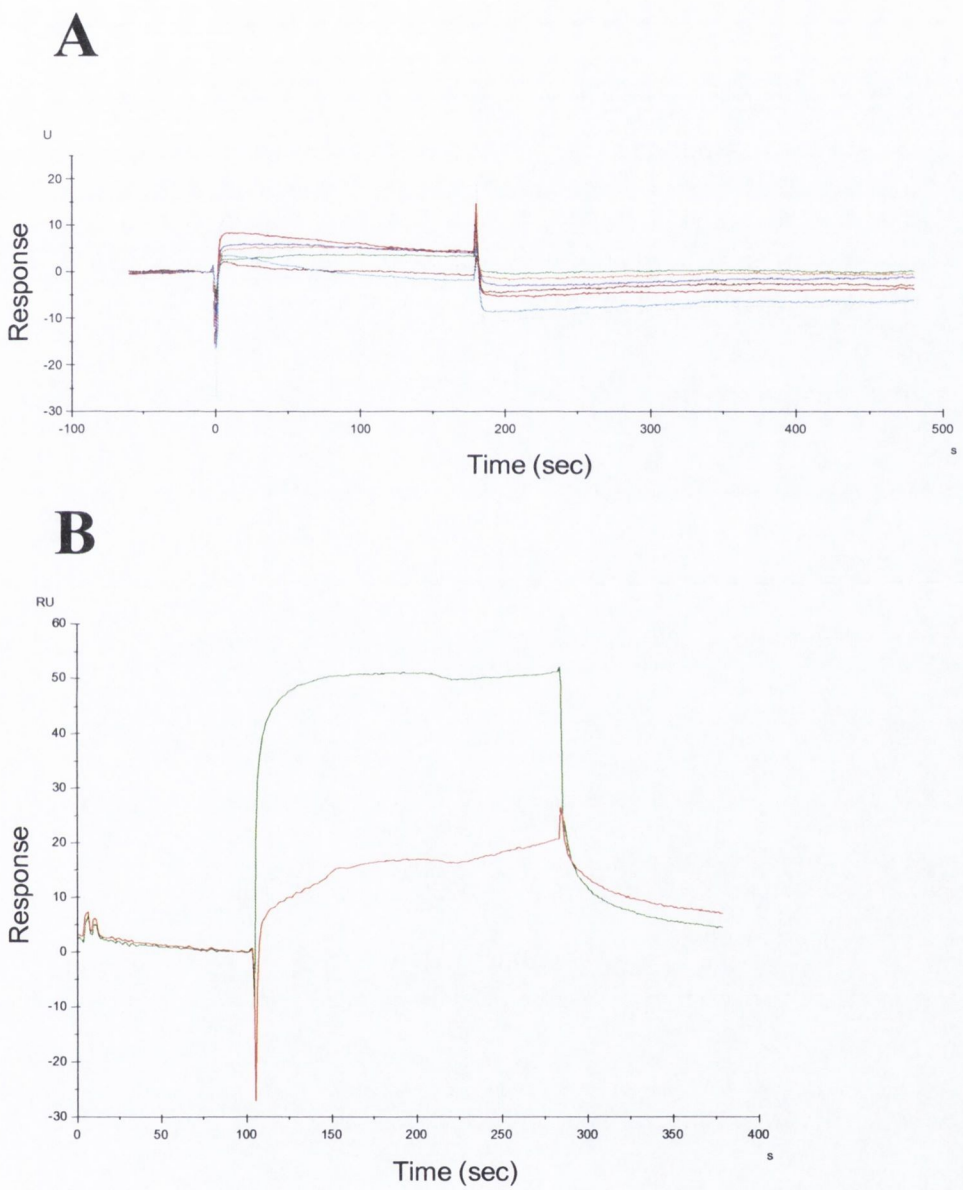

Figure 6.4 Surface plasmon resonance analysis of rFnBPB$_{163-480}$ N312A/F314A binding to fibronectin

(**A**) rFnBPB$_{163-480}$ N312A/F314A ranging in concentration from 0.15μM to 10μM were passed over the surface of a fibronectin-coated chip. (**B**) Equal amounts (2μM) rFnBPB$_{163-480}$ N312A/F314A (Red) and the wild type protein (Green) were passed over the surface of the same fibronectin-coated chip. Each sensorgram has been corrected for the response obtained when recombinant FnBPB proteins were passed over uncoated chips and is representative of three independent experiments.

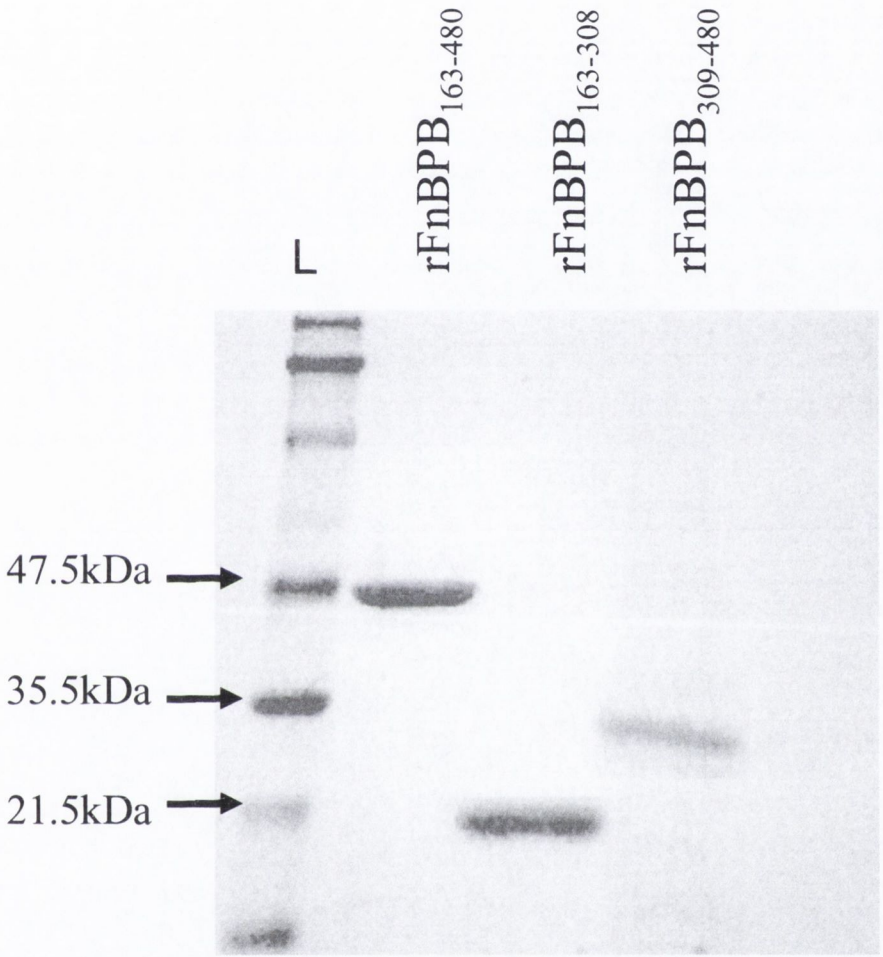

Figure 6.5 SDS-PAGE analysis of rFnBPB subdomains N2 and N3
Equal amounts (5μM) of $rFnBPB_{163-480}$ $rFnBPB_{163-308}$ and $rFnBPB_{309-480}$ were analysed by SDS-PAGE and stained with Coomassie blue. Lane "L" was loaded with 5 μl of a molecular weight marker.

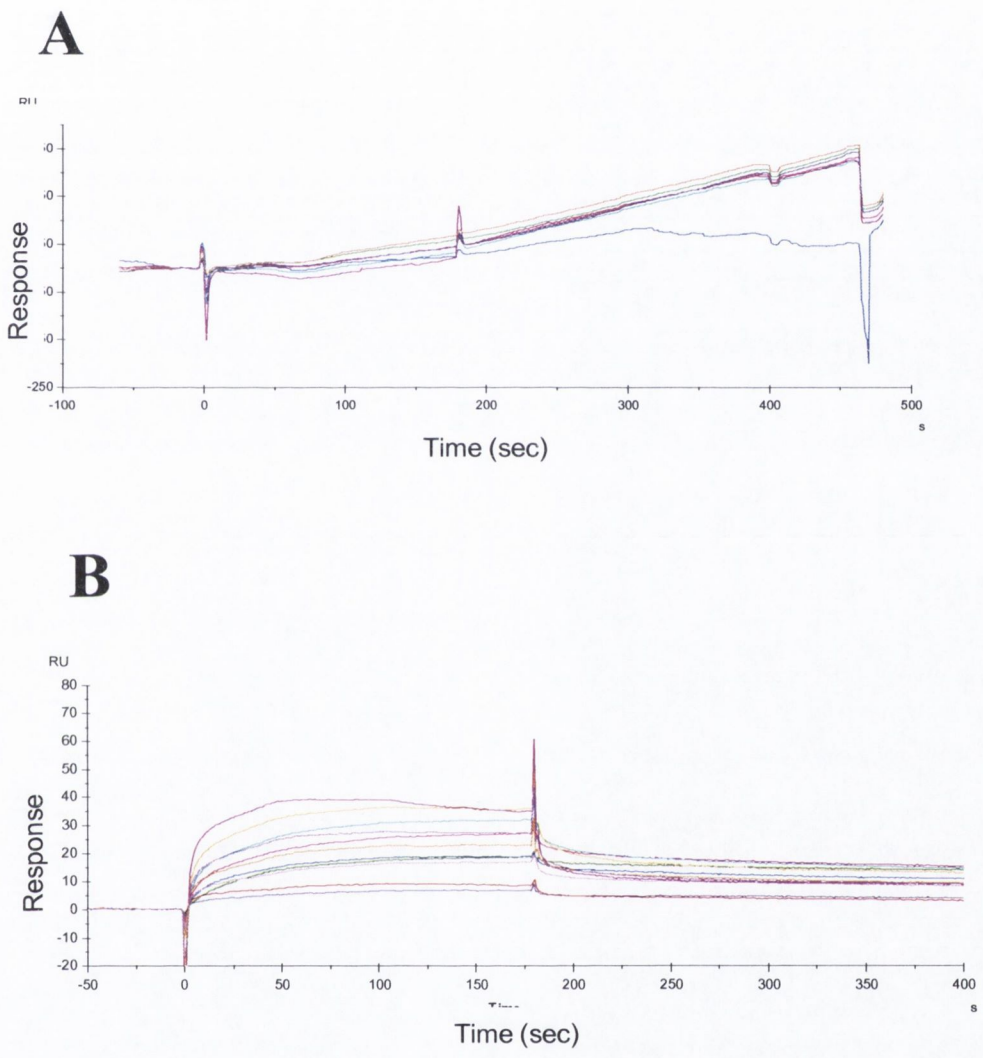

Figure 6.6 Surface plasmon resonance analysis of rFnBPB$_{163-308}$ and rFnBPB$_{309-480}$ binding to fibronectin

Concentrations of (**A**) rFnBPB$_{163-308}$ and (**B**) rFnBPB$_{309-480}$ ranging from 0.15μM to 10μM were passed over the surface of a fibronectin-coated chip. Each sensorgram has been corrected for the response obtained when recombinant FnBPB proteins were passed over uncoated chips and is representative of three independent experiments.

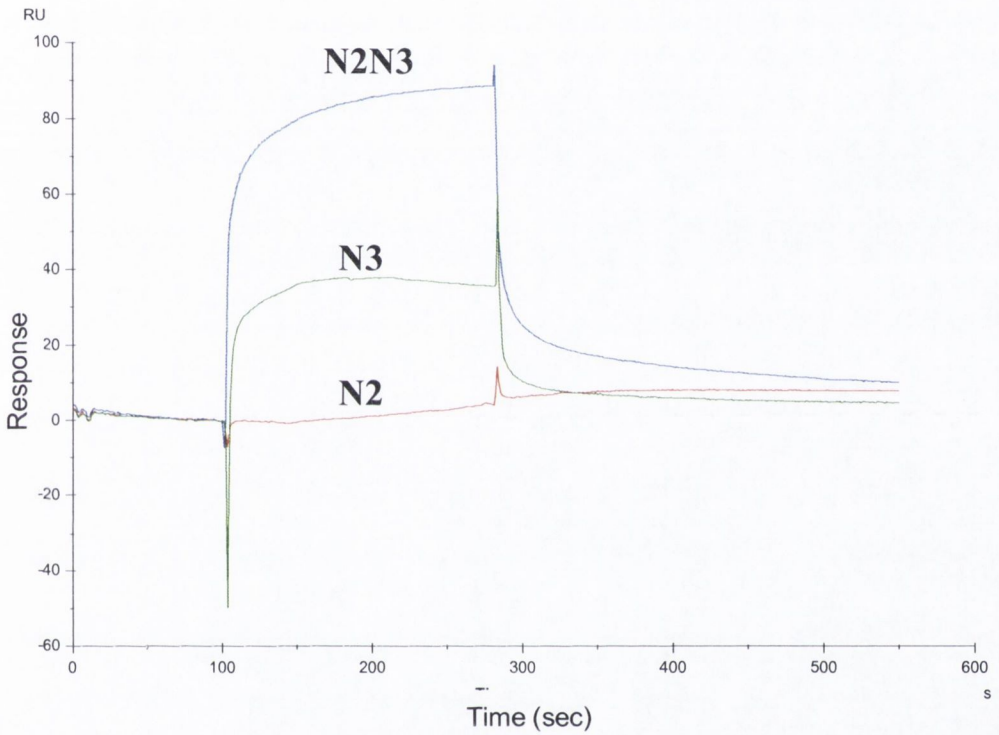

Figure 6.7 Surface plasmon resonance analysis of rFnBPB$_{163-480}$, rFnBPB$_{163-308}$ and rFnBPB$_{309-480}$ binding to fibronectin

Equal amounts (2μM) rFnBPB$_{163-480}$ (blue) , rFnPBB$_{163-308}$ (red) and rFnBPB$_{309-480}$ (green) were passed over the surface of the same fibronectin-coated chip. The sensorgram has been corrected for the response obtained when recombinant FnBPB proteins were passed over uncoated chips and is representative of three independent experiments.

To determine if deletion of individual subdomains affected fibronectin binding by the N2N3 subdomain of FnBPB, equal amounts (2μM) of $rFnBPB_{163-308}$, $rFnBPB_{309-480}$ and wild type $rFnBPB_{163-480}$ were passed over the surface of a fibronectin-coated chip. Binding was compared and the sensorgram profiles obtained (Figure 6.7). Each individual recombinant subdomain had greatly reduced binding to fibronectin when compared to the wild type rN2N3 protein which reached a maximum binding level of 95 RU. However, the reduction in binding was not even. While $rFnBPB_{163-308}$ reached a maximum binding level of 12 RU, $rFnBPB_{309-480}$ reached a significantly higher maximum binding level of 52 RU. These results suggest that while both subdomains N2 and N3 and required for the interaction between the A domain of FnBPB and fibronectin, a greater portion of the fibronectin-bining site is located within the N3 subdomain.

6.2.6 Binding of $rFnBPB_{163-480}$ to immobilised fibronectin fragments

The A domain of FnBPB does not contain any fibronectin-binding motifs that are known to interact with the N-terminal type 1 modules of fibronectin. To localize the binding site in fibronectin for the N2N3 subdomain of FnBPB, the binding of $rFnBPB_{163-480}$ to different fragments of fibronectin was tested by collaborators in the laboratory of Prof. Pietro Spezile, University of Pavia, Italy. A number of functional fibronectin fragments were generated by the steady digestion of human fibronectin with thermolysin. These fragments included: a 29kDa fragment containing the five N-terminal F1 modules (N29), a 45kDa fragment which consists of four F1 modules and two F2 modules (GBD), C-terminal fragments 607-1265 and 1266-1908 which each consist of multiple F3 modules and C-terminal fragment 1913-2477 which contains one F3 module and three F1 modules (Figure 6.8). Equal amounts of fibronectin and fibronectin fragments were dotted onto nitocellulouse memebrane and were then probed with

rFnBPB$_{163-480}$. Bound recombinant protein was detected using rabbit polyclonal anti-rFnBPB163-480 antibodies followed by HRP-conjugated goat anti-rabbit antibodies. rFnBPB$_{163-480}$ bound to whole fibronectin and to the N29 fibronectin fragment with similar affinity (Figure 6.9). By contrast, rFnBPB$_{163-480}$ reacted poorly with fibronectin fragments GBD, 607-1265, 1266-1908 and 1913-2477. Thus the binding site in fibronectin for rFnBPB$_{163-480}$ was localised to the five N-terminal F1 modules of fibronectin.

6.2.7 Construction of plasmids p*fnbB*A::R*clfA* and p*fnbB*

To investigate the biological significance of fibronectin-binding by the A domain of FnBPB, it was important to determine if the A domain alone could promote bacterial adhesion to fibronectin and the subsequent invasion of endothelial cells. This required the bacterial cell surface expression of the N-terminal A domain of FnBPB in the absence of the C-terminal FnBRs. To facilitate this, shuttle plasmid p*fnbB*A::R*clfA* was constructed for the expression of a chimeric protein containing the A domain of FnBPB together with region R and the cell wall anchoring region of *S. aureus* ClfA (Figure 6.10). Region R of ClfA has no known ligand-binding function. It consist of a series of serine-aspartate repeats and its function is to project the ligand-binding A domain of ClfA away from the cell surface allowing interaction with fibrinogen (Hartford *et al.*, 1997)

Shuttle plasmid pCF77 has been described previously (Hartford *et al.*, 1997). It is a pCU1-derived multicopy plasmid which carries the entire *clfA* gene from strain 8325-4 together with 1300bp of upstream sequences containing the promoter region of *clfA* (Figure 6.10). pCF77 DNA was cleaved with *Eco*RI and *Bam*HI to remove DNA encoding the fibrinogen-binding A domain of ClfA and upstream promoter region which is contained within a 3 kb *EcoRI-BamHI* fragment of the plasmid (Figure 6.10A). Primers FnBPB UPR F and FnBPB N3 R2 were designed to amplify 1.9 kb

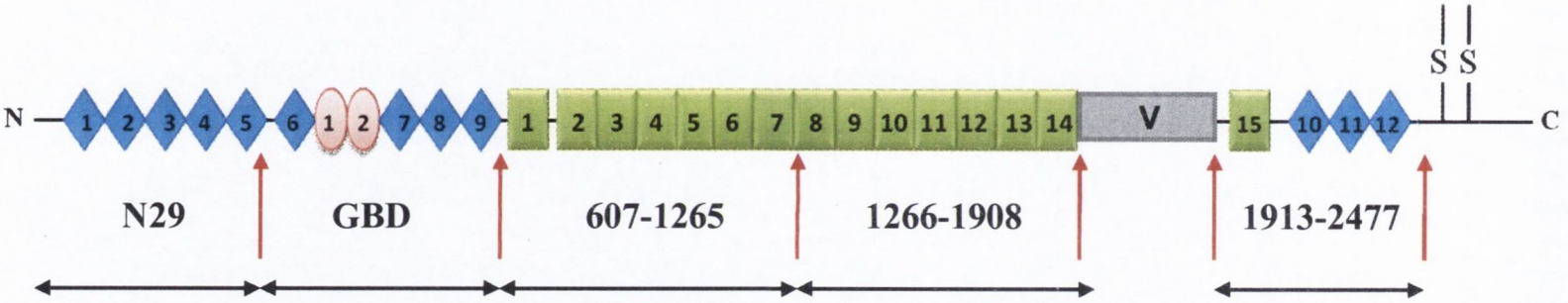

Figure 6.8 Schematic representation of the modular structure of fibronectin

Fibronectin is shown as a monomer and is composed of three different types of protein modules, F1 (blue), F2 (pink) and F3 (green) modules. The variably spliced V region is shown in grey. Thermolysin cut sites are indicated by red arrows. The N-terminal 29 kDa fragment (N29), gelatin-binding fragment (GBD) and fragments 607-1265, 1266-1908 and 1913-2477 were used in this study and are labelled.

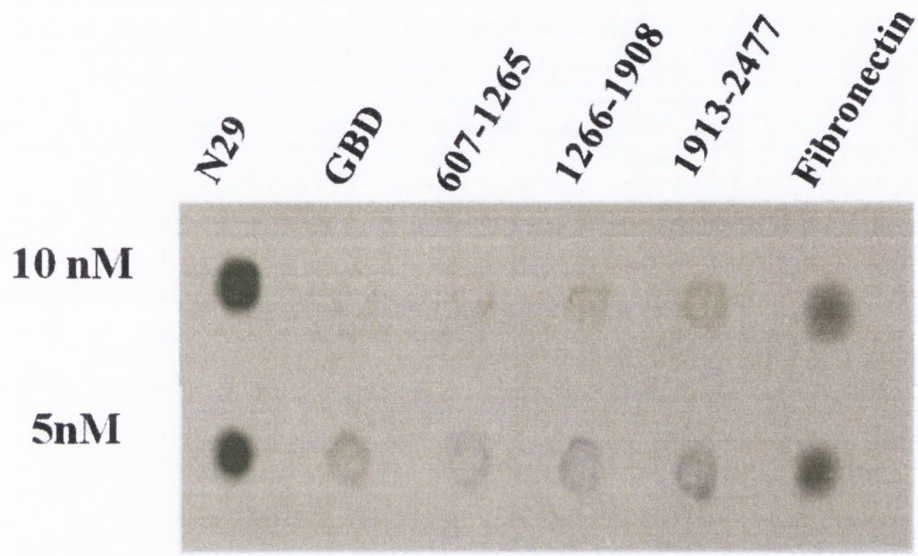

Figure 6.9 Binding of rFnBPB$_{163-480}$ to fibronectin and fibronectin fragments by dot-immunoblotting

Equal concentrations (10nMor 5nM) of whole fibronectin and fibronectin fragments N29, BCD, 607-1265, 1266-1908 and 1913-2477 were applied to nitrocellulose membranes and probed with 1 μg/ml rFnBPB1$_{63-480.}$ Bound recombinant protein was detected using polyclonal anti-rFnBPB antibodies followed by HRP-conjugated goat anti-rabbit IgG.

of *fnbB* DNA from strain 8325-4 genomic DNA which encodes the entire A domain of FnBPB and contains the upstream *fnbB* promoter. The PCR product was cleaved with *Eco*RI and *Bam*HI at restriction sites incorporated into the primers and ligated to pCF77 DNA cleaved with the same enzymes. This generated plasmid p*fnb*BA::R*clf*A for expression of the chimeric FnBPBA::RClfA protein (Figure 6.10B). The 1.9 kb *Eco*RI-*Bam*HI fragment of p*fnbB*A::R*ClfA* contains a *Hind*III restriction site encoding FnBPB A domain residues 388 and 389 which was exploited for the construction of p*fnbB*. Primers FnBPB FnBRs F and FnBPB FnBRs R were designed to amplify DNA encoding FnBPB residues 388-980 using genomic DNA from strain 8325-4 as a template. The PCR product was cleaved with *Hind*III and ligated to p*fnbB*A::R*clfA* DNA cleaved with the same enzyme. This generated plasmid p*fnb*B for expression of full length wild-type FnBPB (Figure 6.10C).

Plasmids p*fnb*BA::R*clf*A and p*fnb*B were sequenced and analysed by restriction mapping. Digestion of pCF77 with *Eco*RI and *Bam*HI produced a 6 kb band and a 3 kb band while digestion of p*fnb*BA::R*clf*A with the same enzymes produced a 6 kb band and a 1.9 kb band (Figure 6.11A). Digestion of p*fnbB* with *Eco*RI and *Hind*III produced three bands of 4.9 kb 1.7 kb and 1.6 kb (Figure 6.11B).

6.2.8 Expression of FnBPB proteins on the surface of *S. epidermidis* cells

Plasmids pCU1, p*fnbB*A::R*clfA* and p*fnbB* were electroporated into *S. epidermidis* strain TU3298 as described in Section 2.10. To demonstrate the cell surface expression of FnBPB and the chimeric FnBPBA-RClfA protein, whole-cell immunoblotting was performed. Cultures of *S. epidermidis* derivatives containing pCU1, p*fnbB*A::R*clfA* and p*fnbB* were grown to exponential phase. Serial dilutions of washed bacterial cells starting at an OD_{600} of 2.0 were spotted onto nitrocellulose membranes and probed using polyclonal rabbit antibodies raised against the A domain of

FnBPB. A representative dot-blot is shown in Figure 6.12. Expression of the chimeric FnBPBA::RClfA protein was at approximately the same level of wild-type FnBPB expressed in *S. epidermidis*. Antibodies did not bind to the *S. epidermidis* cells carrying pCU1. This indicated that equivalent levels of wild-type FnBPB and the chimeric FnBPBA::RClfA protein were expressed on the bacterial cell-surface, allowing direct comparison in functional assays.

6.2.9 Adherence of *S. epidermidis* cells expressing FnBPB proteins to immobilised ligands

The ability of *S. epidermidis* (pCU1), *S. epidermidis* (p*fnbB*A::R*clfA*) and *S. epidermidis* (p*fnbB*) to adhere to immobilised fibrinogen, elastin and fibronectin was tested. Exponential cultures of *S. epidermidis* strains were washed, resuspended to an OD_{600nm} of 2.0 and added to microtitre plates which had been coated with serial dilutions of human fibrinogen, elastin and fibronectin. The expression of full length FnBPB or the chimeric FnBPBA::RClfA protein promoted dose-dependent and saturable adherence of *S. epidermidis* cells to each immobilised ligand. *S. epidermidis* cells containing the empty pCU1 plasmid were used as a negative control in each assay (Figures 6.13 and 6.14). *S. epidermidis* (p*fnbB*) and *S. epidermidis* (p*fnbB*A::R*clfA*) adhered with similar affinities to fibrinogen-coated and elastin-coated wells (Figure 6.13). This demonstrated the functionality of the chimeric protein expressed from p*fnbB*A::R*clfA* which contains the sole binding site for fibrinogen and elastin in FnBPB, the N-terminal A domain. By contrast, the affinity of cells expressing the chimeric FnBPBA::RClfA protein for fibronectin was considerably weaker than that of cells expressing full length FnBPB (Figure 6.14) These results suggest that while the C-terminal FnBRs of FnBPB are necessary for promoting high-affinity bacterial adherence to fibronectin,

Figure 6.10 Construction of plasmids p*fnbB*A::R*clfA* and p*fnbB*

(**A**) Plasmid map of pCF77 .The 4.5 kb *clfA* coding sequence was cloned between the *Eco*RI and *Hind*II sites within the *lac*Z gene of pCU1. DNA encoding the fibrinogen-binding A domain of ClfA and upstream promoter region is contained within a 3kb *EcoRI-BamHI* fragment. (**B**) Plasmid map of p*fnbB*A::R*clfA*. A 1.9 kb fragment of DNA encoding the A domain of FnBPB and upstream promoter region was cloned between the *Eco*RI and *Bam*HI sites of pCF77. (**C**) Plasmid map of p*fnbB*. A 1.7 kb fragment encoding FnBPB residues 389-980 was cloned into the *HindI*II site of p*fnbB*A::R*clfA*. The *bla* gene confers ampicillin resistance in *E. coli* while the *cat* gene confers chloramphenicol resistance in *S. epidermidis*.

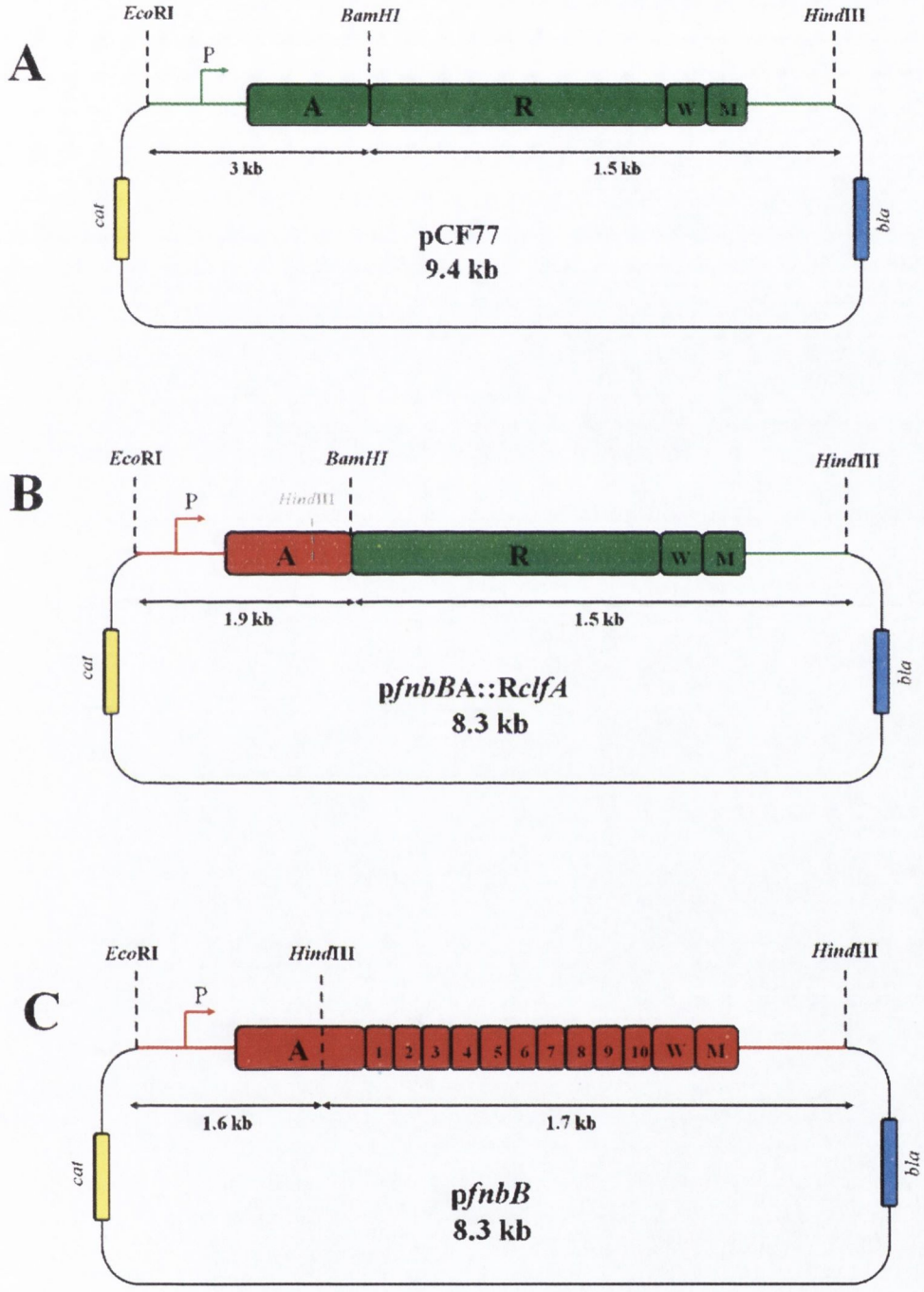
A
EcoRI
BamHI
HindIII
P
A
R
W
M
3 kb
1.5 kb
cat
bla
pCF77
9.4 kb
B
EcoRI
BamHI
HindIII
HindIII
P
A
R
W
M
1.9 kb
1.5 kb
cat
bla
pfnbBA::RclfA
8.3 kb
C
EcoRI
HindIII
HindIII
P
A
1
2
3
4
5
6
7
8
9
10
W
M
1.6 kb
1.7 kb
cat
bla
pfnbB
8.3 kb

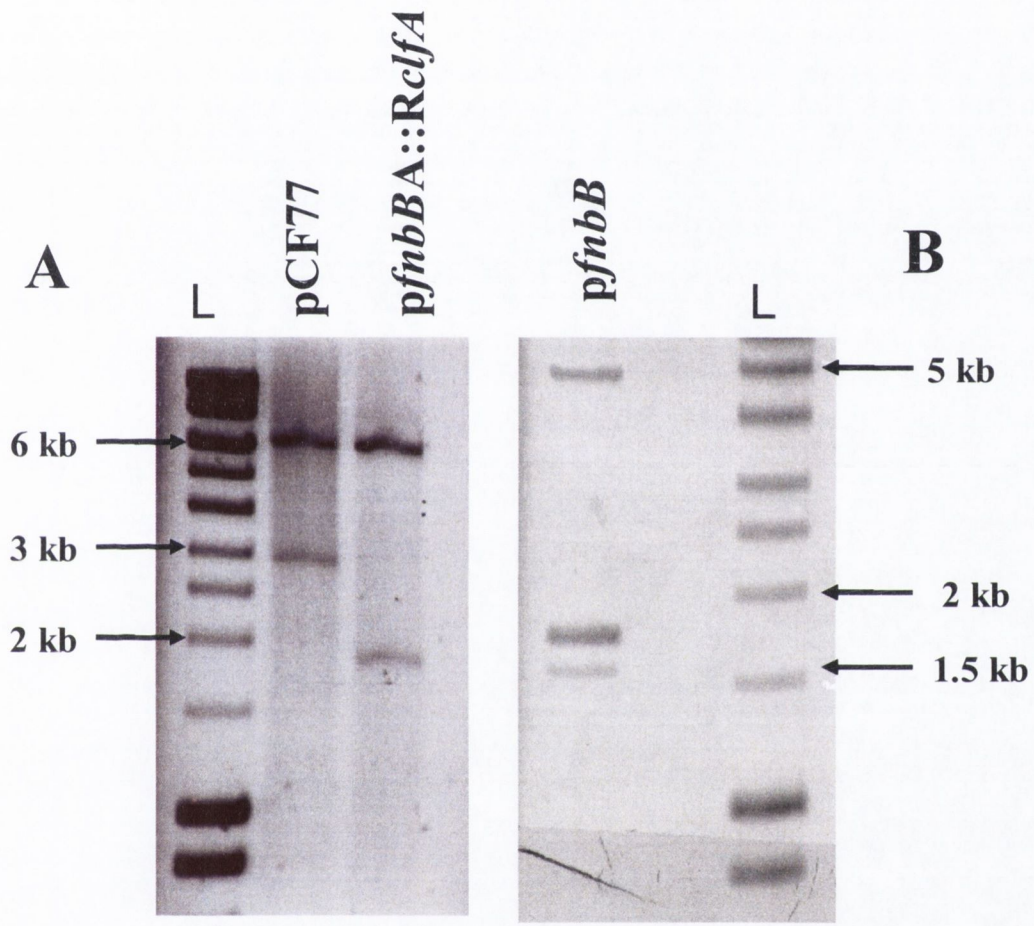

Figure 6.11 Restriction analysis of pCU1-derived plasmids

Agarose gel of restriction digests of (**A**) pCF77 and p*fnbB*A::R*clfA* with *Eco*RI and *Bam*HI (**B**) p*fnbB* with *Hind*III. Lanes "L" were loaded with 5 μl of a 1 kb DNA ladder.

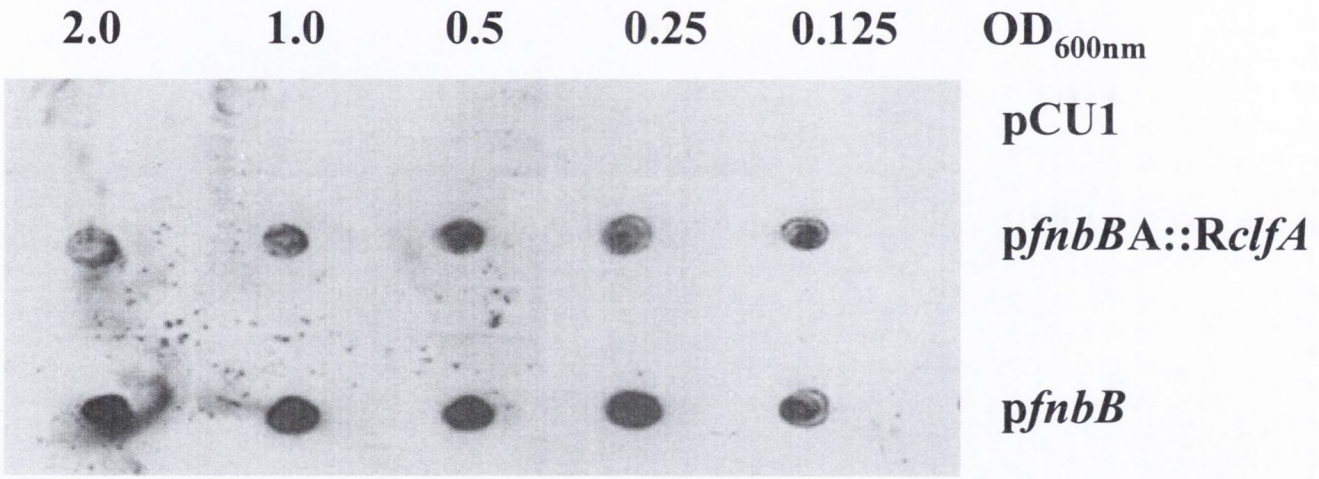

Figure 6.12 Expression of FnBPBA::RClfA and FnBPB from *S. epidermidis*

S. epidermidis (pCU1), *S. epidermidis* (p*fnbB*A::R*clfA*) and *S. epidermidis* (p*fnbB*) cells were grown to exponential phase, washed and doubling dilutions (OD_{600nm} = 0.125 to 2.0) were dotted onto a nitrocellulose membrane. Membranes were probed with rabbit polyclonal anti-FnBPB A domain antibody and HRP-conjugated goat anti-rabbit antibodies. Membranes were developed by chemiluminescence and exposed on autoradiographic film. The blot is representative of three independent experiments.

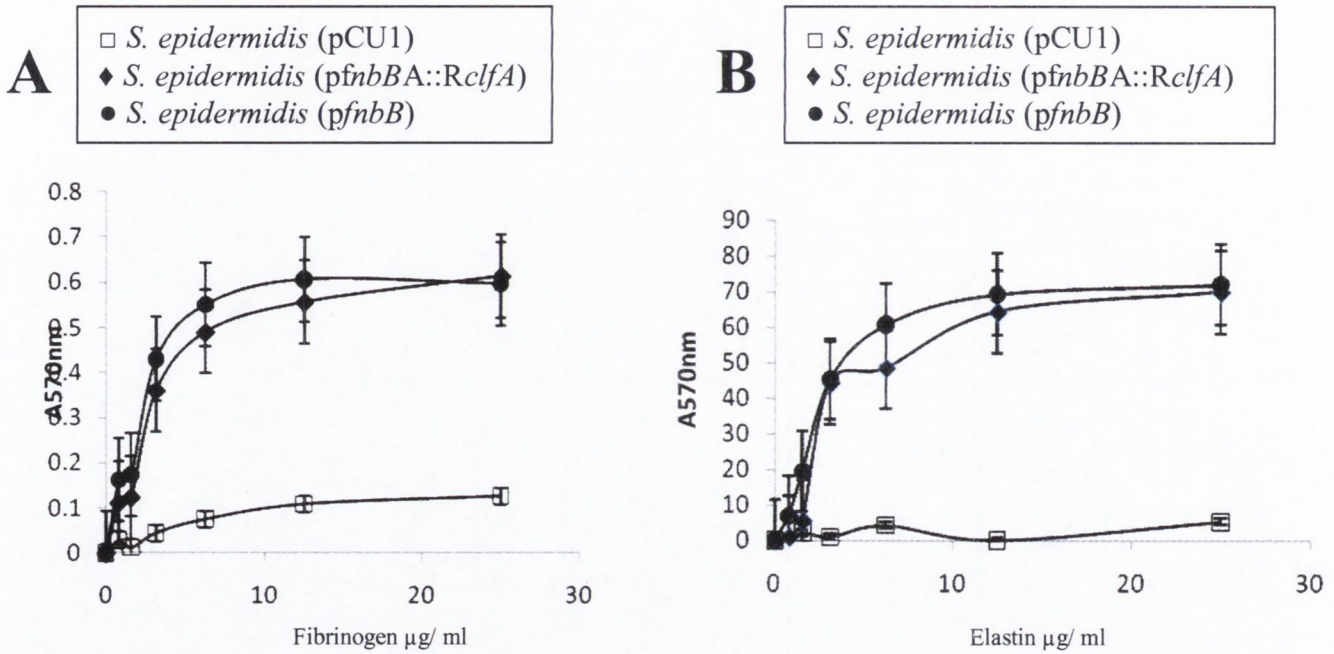

Figure 6.13 Adherence of *S. epidermidis* strains expressing full length FnBPB or chimeric FnBPBA::RClfA to immobilised fibrinogen and elastin

S.epidermidis (pCU1), *S. epidermidis* (p*fnbB*A::R*clfA*) and *S. epidermidis* (p*fnbB)* were grown to exponential phase. Washed cell suspensions were added to ligand-coated microtitre wells and allowed to adhere. Bacterial adherence to fibrinogen (**A**) was measured by staining with crystal violet while elastin adherence (**B**) was measured using SYTO-13 fluorescent dye. Data points represent the mean of triplicate wells and error bars indicate the standard error. Each graph is representative of three independent experiments.

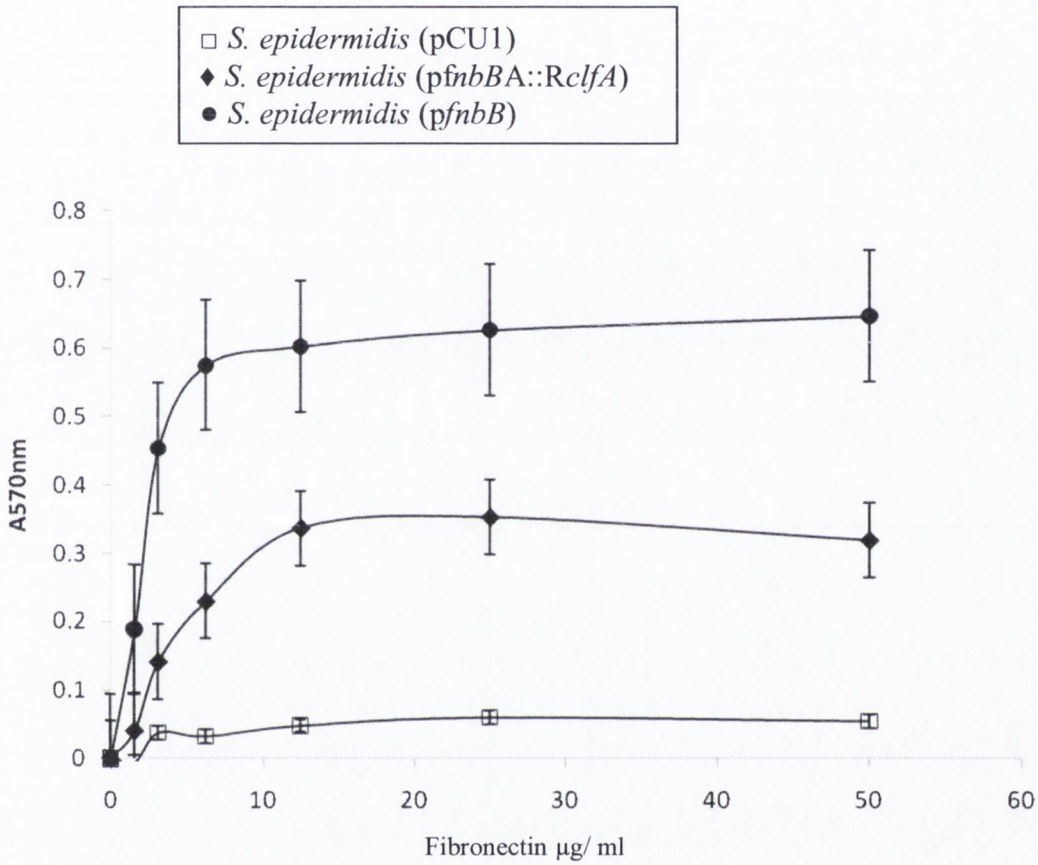

Figure 6.14 Adherence of *S. epidermidis* strains expressing full length FnBPB or chimeric FnBPBA::RClfA to immobilised fibronectin

S. epidermidis (pCU1), *S. epidermidis* (p*fnbB*A::R*clfA*) and *S. epidermidis* (p*fnbB)* were grown to exponential phase. Washed cell suspensions were added to fibronectin-coated microtitre wells and allowed to adhere. Bacterial adherence was measure by staining with crystal violet. Data points represent the mean of triplicate wells and error bars indicate the standard error. This graph is representative of three independent experiments.

low-affinity adherence is achieved by expression of the A domain of FnBPB alone.

6.2.10 Adherence to and invasion of endothelial cells by *S. epidermidis* cells expressing FnBPB constructs

To further investigate the biological significance of fibronectin-binding by the A domain of FnBPB, the ability of *S. epidermidis* cells expressing either full length FnBPB or the chimeric FnBPBA::RClfA protein to adhere to and invade endothelial cells was tested and compared. Endothelial cell adherence and invasion assays were carried out under the supervision of Dr. Ruth Massey, University of Bath, as described in Section 2.16 and previously (Edwards *et al.*, 2010). *S. epidermidis* strains carrying pCU1, p*fnbB* or p*fnbB*A::R*clfA* were grown to exponential phase, washed and incubated with coverslips containing a monolayer of cultured endothelial cells. The initial adherence event and the subsequent uptake process were examined by parallel assays of attachment and invasion combined, and invasion alone. To measure the total number of bacteria associated with the cells (adherent and internalised), coverslips were washed, treated with Triton X-100 and agitated by pipetting to fully lyse the endothelial cells. Colony forming units (CFU) were enumerated by serial dilution and plating onto TSA agar plates. At each time point, similar numbers of *S. epidermidis* (pCU1), *S.epidermidis* (p*fnbB*) and *S. epidermidis* (p*fnbB*A::R*clfA*) cells were associated with the endothelial cells (Figure 6.15A). These results suggest that factors, other than the ability to bind fibronectin, promoted by the expression of FnBPs, promotes endothelial-cell association by *S.epidermidis* cells.

For invasion assays, coverslips were treated with gentamicin to allow killing of bacteria that were unable to invade the endothelial cells before being washed, lysed and plated as described above. At each time point, the number of *S. epidermidis* (p*fnbB*) cells internalised was

approximately 20-fold higher compared to *S. epidermidis* (pCU1) and *S. epidermidis* (p*fnbB*A::R*clfA*) cells (Figure 6.15B). These results indicate that the FnBRs of FnBPB play a crucial role in FnBPB-mediated internalization into endothelial cells and that the A domain of FnBPB alone is not sufficient to promote endothelial cell invasion.

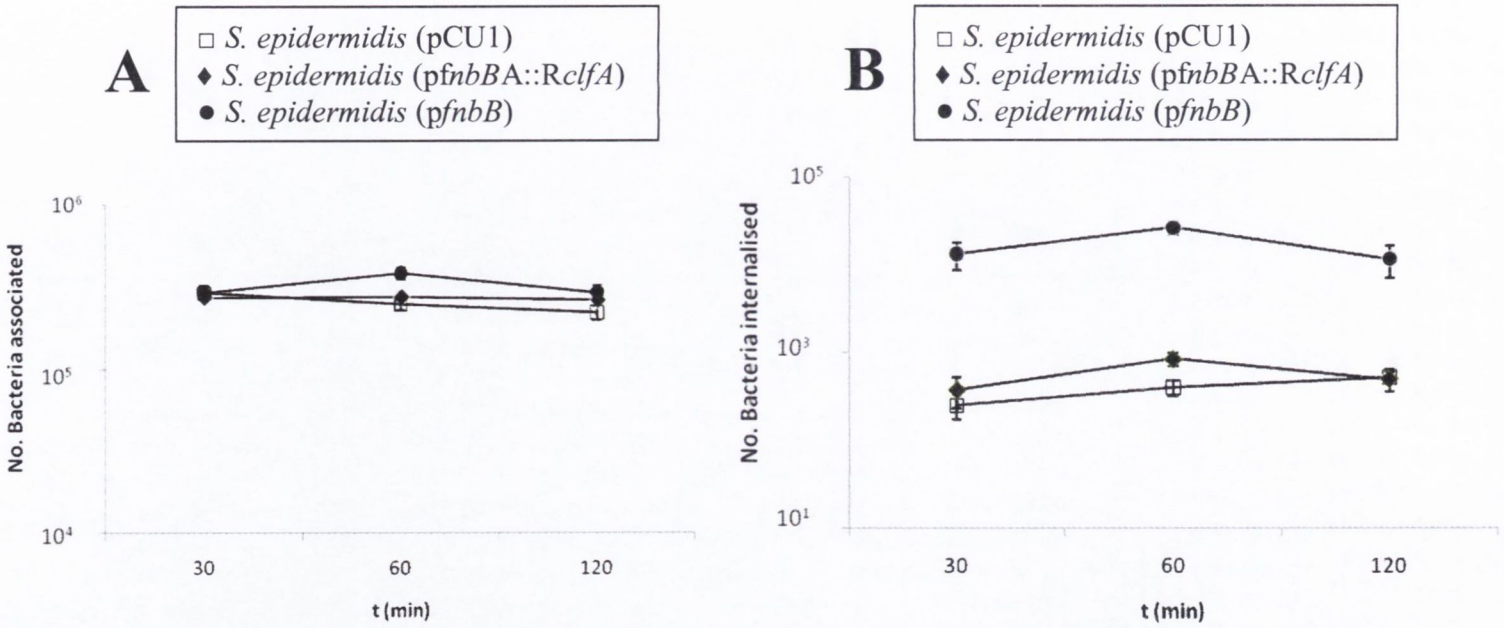

Figure 6.15 Endothelial cell association and invasion by *S. epidermidis* strains expressing full legnth FnBPB or chimeric FnBPBA::RClfA

S. epidermidis (pCU1), *S. epidermidis* (p*fnbB*A::R*clfA*) and *S. epidermidis* (p*fnbB*) were grown to exponential phase washed and incubated with coverslips containing a monolayer of cultured endothelial cells. To measure the total number of bacteria associated with the cells (adherent and internalized) (**A**) coverslips were washed, treated with Triton X-100 and agitated by pipetting to fully lyse the endothelial cells. CFU were enumerated by serial dilution and plating onto TSA agar plates. For invasion assays (**B**) coverslips were treated with gentamicin to allow killing of bacteria that were unable to invade the endothelial cells before being washed, lysed and plated for CFU. Data points represent the mean of triplicate plates and error bars indicate the standard error. Each graph is representative of three independent experiments.

6.3 Discussion

FnBPA and FnBPB of *S. aureus* are multifunctional MSCRAMMs which were first described for their ability to promote adhesion to fibronectin. The C-terminal region of each protein contains a series of highly conserved and tandemly repeated fibronectin-binding repeats (FnBRs) which interact specifically with the N-terminal type 1 modules of fibronectin through a tandem β-zipper mechanism (Bingham *et al.*, 2008)

The binding of fibronectin by *S. aureus* FnBPs is critical for the invasion of the bacterium into non-phagocytic host cells. Fibronectin acts as a molecular bride linking the bacterial cell to the host-cell integrin $\alpha_5\beta_1$ (Fowler *et al.*, 2000). The subsequent internalization of *S. aureus* is believed to protect the bacterium from the host immune system and promote its spread from the site of infection to other tissues and organs of the host. Indeed, FnBP-mediated invasion of endothelial and epithelial cells has been implicated as an important virulence factor in animal models of endocarditis (Que *et al.*, 2005, Que *et al.*, 2001).

Located proximal to the FnBRs of FnBPA and FnBPB are the N-terminal fibrinogen and elastin-binding A domains. The amino acid sequences of the A domains are more diverse than those of the FnBRs sharing only 48% sequence identity. Each A domain is subdivided into subdomains N1, N2 and N3 and the minimum binding site for fibrinogen and elastin in each protein is contained within the N2N3 subdomain. The revised co-ordinates for the N2N3 subdomains of FnBPA and FnBPB span residues 194-511 and 163-480, respectively and do not contain any known fibronectin-binding motifs. Accordingly, rFnBPA$_{194\text{-}511}$ bound only fibrinogen and elastin and did not bind fibronectin. By contrast, rFnBPB$_{163\text{-}480}$ was found to bind to immobilised fibrinogen, elastin and fibronectin with similar affinity. Based on these findings it was decided that the mechanism

by which the A domain of FnBPB binds fibronectin and the biological significance of this interaction warranted further investigation.

The dock, lock and latch mechanism of fibrinogen binding by the A domain of FnBPB was analysed in Chapter 5. To establish if $rFnBPB_{163-480}$ binds to fibronectin by the same mechanism, recombinant FnBPB N2N3 subdomain mutants that are defective in fibrinogen-binding were tested for their ability to bind fibronectin. The truncated protein $rFnBPB_{163-463}$ lacks the C-terminal 17 residues of the N3 subdomain which are crucial for fibrinogen-binding. These residues are predicted to form the latching peptide which plays an important role in the "locking" step of the dock-lock-latch mechanism of ligand-binding. $rFnBPB_{163-463}$ was found to bind immobilised fibronectin with an affinity K_D similar to that calculated previously for the full length protein, $rFnBPB_{163-480}$. This indicated that the predicted latching peptide plays no role in the interaction between the A domain of FnBPB and fibronectin. It was thus concluded that the N2N3 subdomain of FnBPB binds fibrinogen and fibronectin by different mechanisms.

In Chapter 5, the substitution of residues N312 and F314 for alanine reduced significantly the affinity of $rFnBPB_{163-480}$ for fibrinogen. In the 3D model of N2N3 subdomain of FnBPB, residues N312 and F314 line the predicted ligand-binding trench which plays an important role in the "docking" step of the dock,lock and latch mechanism of ligand-binding. In this chapter it was demonstrated that the substitution of residues N312 and F314 for alanines also reduced to ability of $rFnBPB_{163-480}$ to bind fibronectin. This suggested that the predicted ligand-binding trench plays a key role in the mechanism by which the A domain of FnBPB binds fibronectin. To further localize the fibronectin-binding site, individual subdomains rN2 and rN3 were tested for their ability to bind fibronectin. Each truncated protein showed a reduced affinity for fibronectin compared

to the wild type rN2N3 construct. This suggested that each subdomain plays an important role in the fibronectin-binding mechanism. These results are consistent with the above proposal that fibronectin interacts with a ligand binding trench which comprises N2 and N3 subdomain residues. Taken together, these results indicate that the overall conformation of the N2N3 subdomain of FnBPB is critical for the fibronectin-binding mechanism. The recombinant N3 protein appeared to have a higher affinity for fibronectin than the recombinant N2 protein. It may therefore be postulated that a greater portion of the fibronectin-binding site in the A domain of FnBPB is contained within subdomain N3.

The binding site in fibronectin for *S. aureus* FnBPs is located in the N-terminus (Kuusela *et al.*, 1984). However, another binding site in the C-terminal gelatin-binding domain (GBD) has also been reported (Sakata *et al.*, 1994, Bozzini *et al.*, 1992). The C-terminal FnBRs of *S. aureus* FnBPA and FnBPB promote binding to the N-terminal F1 modules of fibronectin through a tandem β-zipper mechanism. FnBPB from strain 8325-4 contains 10 FnBRs, the first of which lies outside the boundary of the revised A domain, which spans residues 37-480. In Chapter 4 it was found that $rFnBPB_{163\text{-}480}$ bound to immobilised fibronectin suggesting that the A domain of FnBPB contains a novel fibronectin-binding motif that may promote binding to a region of fibronectin other than the N-terminus. To localize the binding site in fibronectin for the N2N3 subdomain of FnBPB, the binding of $rFnBPB_{163\text{-}480}$ to different fragments of fibronectin was tested. $rFnBPB_{163\text{-}480}$ bound with similar affinity to whole fibronectin and to an N-terminal fragment of fibronectin containing F1 modules 1 to 5. This is the same region of fibronectin to which the FnBRs of FnBPA and FnBPB bind. These findings indicate that the A domain of FnBPB contains a novel motif which interacts with the N-terminal type 1 modules of fibronectin through a novel mechanism.

To explore the biological significance of the interaction between the A domain of FnBPB and fibronectin, the ability of the A domain, in isolation from the FnBRs, to promote bacterial adhesion to fibronectin was examined. This was facilitated by the construction of a chimeric FnBPBA-RClfA protein containing the A domain of FnBPB and the stalk and cell wall anchoring region of ClfA. The expression of the chimeric FnBPB-ClfA protein on the surface of *S. epidermidis* cells promoted dose-dependent and saturable adhesion to fibrinogen, elastin and fibronectin. This supports the work undertaken with recombinant protein and shows once again that the A domain of FnBPB contains a binding site for fibronectin. The affinity for fibronectin of *S.epidermidis* cells expressing the chimeric FnBPB-ClfA protein was significantly weaker than that of cells expressing full length wild-type FnBPB with its full complement of FnBRs. This suggests that the A domain of FnBPB promotes low-affinity adhesion of bacterial cells to fibronectin

The binding of FnBPs to the N-terminal type 1 modules of fibronectin promotes the uptake of *S. aureus* by human endothelial cells. Since the binding site for the A domain of FnBPB was localised to the N-terminus of fibronectin, it was important to determine if expression of the A domain alone could promote bacterial invasion of endothelial cells. In vitro assays revealed that the FnBRs of FnBPB are a crucial requirement for FnBPB-mediated invasion. While expression of the A domain of FnBPB alone promoted low-affinity adhesion of *S. epidermidis* to fibronectin, it did not trigger the subsequent uptake of *S. epidermidis* cells by endothelial cells. This is consistent with a recent study which indicated that the affinity of bacterial cells for fibronectin is indicative of the potential to trigger the invasion process (Edwards *et al.*, 2010). The efficiency of FnBPB to promote endothelial cell invasion in the absence of the N-terminal A domain was not tested in this study. Consequently, the results from this chapter to not exclude the possibility that fibronectin-binding by the A domain

contributes to some extent to the overall process of FnBPB-mediated invasion of endothelial cells. It is also possible that the A domain of FnBPB plays a role in other fibronectin-binding mediated processes *in vivo* such as platelet activation. Therefore, the precise biological consequences of fibronectin-binding by the A domain of FnBPB requires further investigation.

To conclude, the N2N3 subdomain of FnBPB contains a novel fibronectin-binding site which promotes binding to the N-terminal type 1 modules of fibronectin by a novel meachanism. It is postulated that the N-terminus of fibronectin interacts with a hydrophobic ligand-binding trench that is predicted to lie between subdomains N2 and N3 of FnBPB. Expression of the A domain of FnBPB alone promotes low-affinity adhesion of bacterial cells to immobilised fibronectin but does not promote bacterial invasion of human endothelial cells. The biological significance of fibronectin-binding by the A domain of FnBPB has yet to be determined.

Chapter 7

Discussion

7.1 Discussion

S. aureus is a complex pathogen with an extraordinary repertoire of virulence factors that allow it to survive extreme conditions in the mammalian host. Cell surface adhesins called MSCRAMMs promote adherence to host tissues as a first step in the development of *S. aureus* infections. Many *S. aureus* MSCRAMMs are multifunctional. Redundancy also occurs with different MSCRAMMs performing similar functions. This is typified by the fibronectin-binding proteins FnBPA and FnBPB which both mediate adhesion to fibrinogen, elastin and fibronectin.

FnBPA and FnBPB are encoded by the two closely linked genes, *fnbA* and *fnbB*. It has been reported that the *fnbA* and *fnbB* genes from 50 different strains, representing the major MRSA clones found in Europe, have undergone greater sequence divergence than genes encoding other surface proteins such as *clfA* and *clfB* (Kuhn *et al.*, 2006). Analysis of the *fnb* genes from published genome sequences showed that divergence was confined to the region encoding the N-terminal fibrinogen and elastin-binding A domains while the C-terminal fibronectin-binding motifs were highly conserved. Seven isotypes of FnBPA were identified based on divergence in the minimal ligand-binding N2N3 subdomain (Loughman *et al.*, 2008). Each recombinant isotype was found to retain ligand-binding function but was antigenically distinct. Given the functional, organisational and sequence similarity between FnBPA and FnBPB, these findings prompted an investigation of the divergence in the A domain of FnBPB and to determine if variation in this region of the protein is widespread amongst *S. aureus* strains.

7.1.1 FnBPB isotypes

In this study, the *fnbB* gene sequences from sequenced *S. aureus* genomes and from strain P1 were compared by pairwise alignments. Four FnBPB variants (isotypes I-IV) were identified based on divergence in the N2N3 subdomains, which are 66-76% identical to one another. In order to determine the distribution of FnBPB isotypes I-IV and to identify novel isotypes, isotype-specific probes were generated and used to screen *fnbB* DNA from a variety of clonal types using a well characterised strain collection of human origin. Three novel FnBPB isotypes were identified (types V, VI and VII) which are 61.1% - 85% identical to isotypes I-IV. Phylogenetic analysis of FnBPB isotypes indicated that the phylogeny of *fnbB* alleles does not correlate with the core genome as reflected by MLST.

The evolution of *S. aureus* has been predominantly clonal where alleles are 5- to 10-fold more likely to diversify by point mutations than by recombination (Feil *et al.*, 2003). The distribution of *fnbB* (and *fnbA*) alleles amongst different *S. aureus* lineages suggests, however, that recombination has been involved. Horizontal transfer by homologous recombination is likely to be responsible for the dispersal of genes encoding the same isotypes across strains of different phylogenies. Interestingly, the distribution of *fnbA* alleles described in the study by Loughman *et al* does not match the distribution of *fnbB* alleles described here (Loughman *et al.*, 2008). Different combinations of FnBPA and FnBPB isotypes are specified by strains that cluster phylogenetically suggesting that the phylogeny of *fnbB* alleles has evolved independently from that of *fnbA* alleles and has involved separate recombination events despite the genes being closely linked. The gene for coagulase has undergone similar diversification as the *fnb* genes (Watanabe *et al.*, 2009). Recombination within *coa* genes encoding ten major isotypes has created novel subtypes and there is evidence for the same *coa* isotype being expressed by strains with different

genetic backgrounds. This is further evidence for horizontal dissemination of *S. aureus* virulence genes by homologous recombination.

7.1.1.1 Ligand binding

To determine the significance of FnBPB sequence variation, a 3D molecular model of the A domain of FnBPB was generated based on the known structure of ClfA. Like the A domain of ClfA (and FnBPA) it was predicted that the N2N3 subdomain of FnBPB represents the minimal ligand binding region and that ligand binding occurs by a similar mechanism known as dock, lock and latch. Based on this model, it was shown that the majority of variant residues are located on the surface of the protein while residues that are predicted to be involved in ligand-binding by dock, lock and latch are highly conserved. Amino acid sequence variation affected antibody recognition. Polyclonal antibodies against isotype I had reduced affinity for isotypes II-VII while a monoclonal antibody raised against isotype I had little or no affinity for all other isotypes. As with FnBPA isotypes, FnBPB sequence variation has created different epitopes on the A domains that affect immunocross-reactivity. The ligand binding ability of recombinant FnBPB N2N3 subdomain isotypes I-VII was compared by ELISA-based solid phase binding assays and SPR. Each A domain isotype bound to immobilised fibrinogen and elastin with similar affinities indicating that variation in the A domain of FnBPB does not compromise its ligand-binding function. These results suggest that these ligand-binding functions are biologically important and are consistent with the predicted location of variant residues on the surface of the protein and not in regions predicted to be involved in ligand binding. Together, the theoretical 3D model of the A domain of FnBPB and the results of functional assays hinted at the importance of the N2 and N3 domains in ligand binding during dock, lock and latch.

The results of ligand binding assays also confirmed that like the A domains of ClfA and FnBPA, the N2N3 subdomain of FnBPB is sufficient for ligand-binding and that the N1 subdomain is not required. Interestingly, the diversity which occurs in the N2 and N3 subdomains of FnBPA and FnBPB does not occur in the N1 subdomain of either protein. The A domain of both ClfA and another *S. aureus* fibrinogen binding protein, clumping factor B (ClfB), are susceptible to cleavage by aureolysin at a SLAVA / SLAAVA motif located between subdomains N1 and N2 (McAleese *et al.*, 2001). A SLAVA-like motif also occurs in both FnBP proteins with $S_{177}ADVA_{181}$ and $S_{144}TDVTA_{149}$ present in FnBPA and FnBPB , respectively. This may render the A domains similarly susceptible to proteolysis. Indeed the inactivation aureolysin in *S. aureus* 8325-4 correlated with a threshold increase in the amount of cell-bound FnBPs (Karlsson *et al.*, 2001). The function and structure of the N1 subdomains of *S. aureus* fibrinogen-binding MSCRAMMs are not yet known. Preliminary functional studies of ClfA have suggested that subdomain N1 plays a role in the secretion of ClfA to the cell surface (N.McCormack, unpublished data). It may be postulated that the highly conserved N1 subdomains of FnBPA and FnBPB are less readily recognised by the host immune system and serve to protect the ligand-binding N2N3 regions during secretion to the cell surface or during early stages of infection.

7.1.1.2 Biofilm

Another function of the A domains of FnBPA and FnBPB expressed by MRSA strains is to promote biofilm accumulation (O'Neill *et al.*, 2008). While FnBP-mediated biofilm formation involves exclusively the FnBP A domains it is not dependent on their ligand-binding functions. Experiments are currently underway to determine the molecular basis for biofilm accumulation promoted by *S. aureus* FnBPs. Preliminary results reveal that, similar to the *S. aureus* protein SasG, FnBPA and FnBPB-mediated biofilm

accumulation occurs through a process that is dependent on a reductions in pH and the presence of physiological levels of Zn^{2+}. One hypothesis is that, like the B repeats of SasG, the A domains of the FnBPs on the surface of neighboring cells interact in the presence of Zn^{2+} to form homooligomers which promote intracellular adhesion and the subsequent accumulation of biofilm. It would be of interest to compare the level of biofilm accumulation promoted by different isotypes of FnBPA and FnBPB. This could help to localise the region in each FnBP A domain responsible for promoting biofilm accumulation and to identify potential sites for Zn^{2+} binding and oligomerisation.

7.1.2 FnBP expression

While most *S. aureus* strains contain both *fnb* genes, some strains contain only *fnbA* (Peacock *et al.*, 2000). Studies with site-specific *fnbA* and *fnbB* insertion mutants of strain 8325-4 have shown that either FnBPA or FnBPB can mediate adherence to □nternalize fibronectin, but there was no difference in adherence between wild type strains and single *fnb* mutants, indicating functional redundancy (Greene *et al.*, 1995). However, isolates associated with invasive diseases are significantly more likely to have two *fnb* genes suggesting a role for FnBPB in virulence (Peacock *et al.*, 2000). Several studies have indicated distinct differences in the regulation of expression of FnBPA and FnBPB (Wolz *et al.*, 2000, Mitchell *et al.*, 2008, Li *et al.*, 2005). Such regulatory differences may ensure that at least one FnBP protein is expressed on the *S. aureus* cell surface under any given environmental condition to facilitate adhesion to fibronectin and elastin. However, the simultaneous transcription of both *fnbA* and *fnbB* in *S. aureus* strains has been demonstrated (Saravia-Otten *et al.*, 1997, Greene *et al.*, 1996). It may be postulated that combined antigenic variation in both FnBPA and FnBPB expressed on the cell surface is employed by *S. aureus* to thwart the host immune responses during colonization or invasive

infection. Sequence variation amongst FnBP A domains may help *S. aureus* strains to evade the immune response in individuals previously exposed to a strain expressing a different isotypes. It is important to remember that some strains of *S. aureus* lack the gene encoding FnBPB. Colonisation by or exposure to such strains may render a carrier or non-carrier vulnerable to infection by *S. aureus* strains expressing any isotype of FnBPB. Thus, it may be proposed that the expression of a second fibronectin-binding protein, FnBPB, may contribute to the virulence of *S. aureus* by increasing its ability to evade pre-primed anti-FnBP immune responses that are mounted by its host.

It is not fully understood why the FnBPs of *S. aureus* are subject to a greater degree of sequence variation compared the similar fibrinogen-binding MSCRAMMs ClfA and ClfB. It may be due to the importance of these proteins in the early stages of infection. In contrast to FnBPA and FnBPB, ClfA is predominantly expressed in the stationary phase of growth. While ClfB is produced in exponential phase and has been shown to bind fibrinogen and keratin (Walsh *et al.*, 2004, Ni Eidhin *et al.*, 1998) the importance of this protein mainly lies in its role in nasal colonization (Schaffer *et al.*, 2006). Resisting opsonisation by undergoing FnBP sequence variation and antigenic variation would aid in the survival of *S. aureus* during the crucial initial stages of infection, thereby allowing it subsequently to □nternalize into endothelial cells. This would serve to protect the bacterium from the host immune system and allow the spread of infection. A similar observation of antigenic variation with conserved function in the coagulase protein of *S. aureus* has also been proposed as an immune evasion mechanism (Watanabe *et al.*, 2005).

7.1.3 Bovine FnBPs

The study of FnBP variation in *S. aureus* was extended in this study to include bovine *S. aureus* strains. The genome of the bovine strain RF122

contains only the *fnbA* gene and lacks *fnbB*. In this study, *fnbB* DNA was identified in the genomic DNA of 19 bovine *S. aureus* strains indicating that the lack of the *fnbB* gene in strain RF122 is not a common feature of bovine-specific *S. aureus* lineages. It was also found that bovine isolates specify some of the same isotypes of FnBPB and FnBPA as those specified by human isolates. However, some differences were observed in the distribution of isotypes within the human and bovine *S. aureus* populations. For example, the majority of the bovine strains tested were found to specify FnBPA isoype IV while FnBPA isotype II was found to be predominant in human clinical isolates previously (Loughman *et al.*, 2008). It could be postulated that this difference in FnBPA isotype frequency reflects the differences in selective pressures posed by these two distinct host immune systems.

7.1.4 Fibrinogen binding by FnBPB

The A domains of *S. aureus* ClfA, FnBPA and FnBPB each bind fibrinogen at the extreme C-terminus of its γ-chain. Sequence analysis has indicated that the structurally related N2N3 subdomains of ClfA, FnBPA and FnBPB share conserved motifs suggesting that like the A domain of ClfA, the A domains of FnBPA and FnBPB bind fibrinogen by a variation of the dock, lock and latch mechanism. The ClfA-based molecular model of the N2N3 subdomain of FnBPB facilitated an analysis of its fibrinogen-binding mechanism for this study. In this model, the C-terminal seventeen residues of the N3 subdomain comprise the lactching peptide which in ClfA plays a crucial role in fibrinogen binding by dock, lock and latch. To examine the role of the predicted latching peptide, the C-terminal seventeen residues of the rFnBPB N2N3 construct were removed. The truncated protein did not bind detectably to immobilised fibrinogen indicating that similar to ClfA (and FnBPA) the C-terminal A domain residues of FnBPB are crucial for fibrinogen-binding. This is consistent with the molecular

model of FnBPB and provides evidence for a dock, lock and latch mechanism of fibrinogen-binding.

To define further the precise fibrinogen-binding site in FnBPB, amino acid residues were selected for alteration due to their being in the equivalent positions as residues previously identified for their importance in fibrinogen-binding by ClfA and FnBPA. Based on the 3D model of the N2N3 subdomains of FnBPB, residues N312 and F314 are predicted to line the putative ligand-binding trench located between subdomains N2 and N3. The substitution of residues N312 and F316 significantly reduced the affinity of rFnBPB N2N3 protein for fibrinogen. This demonstrates the importance of the FnBPB ligand-binding trench and is further evidence that fibrinogen binds to ClfA, FnBPA and FnBPB in a similar manner. Taken together these data highlight the structural similarities between the A domains of ClfA, FnBPA and FnBPB which is consistent with the molecular model of the A domain of FnBPB created in this study.

7.1.4.1 Role of Ca^{2+}

The interaction between the N2N3 subdomain of ClfA and the γ-chain of fibrinogen has been studied in detail. This interaction is inhibited by minimolar concentrations of Ca^{2+} ions which bind to the A domain of ClfA and induce a conformational change that is incompatible with binding to fibrinogen γ-chain (O'Connell *et al.*, 1998). In this study it was demonstrated that the concentration of Ca^{2+} present in normal human sera also inhibited the binding of rFnBPB N2N3 to the fibrinogen γ-chain peptide. This finding highlights once again the structural similarities between that A domains of *S. aureus* ClfA and FnBPs. In addition to fibrinogen, the A domain of ClfA binds complement factor I. It appears that expression of ClfA allows *S. aureus* to capture and activate factor I resulting ultimately in a reduction in phagocytosis of the bacterium by human neutrophils (Visai *et al.*, 2008, Hair *et al.*, 2010). Given their homology with

the A domain of ClfA, it may be of interest to determine if the A domain isotypes of FnBPA and FnBPB have a similar anti-phagocytic function.

ClfA interacts with the extreme C-terminus of the γ-chain of fibrinogen by a variation of the dock, lock and latch mechanism (Ponnuraj *et al.*, 2003, Ganesh *et al.*, 2008). A second binding site in the N3 subdomain of ClfA has been identified which interacts with another site in the D domain of fibrinogen (Geoghegan, 2008). The presence of a second fibrinogen binding site explains why ClfA has a higher affinity for whole fibrinogen than for the γ-chain peptide. To explore the possibility of a second binding site for fibrinogen in the A domain of FnBPB, residues S224 and Y324 of FnBPB were selected for alteration because their predicted positions corresponded to the position of residues which are contained within the second fibrinogen-binding site in of ClfA and play an important role in fibrinogen-binding. The substitution of S224 or Y324 caused no reduction in the affinity of rFnBPB N2N3 for fibrinogen indicating that these residues play no role in fibrinogen binding. This suggests that, unlike ClfA, the N3 subdomain of FnBPB does not contain a second binding site for fibrinogen. Furthermore, rFnBPB N2N3 bound to immobilised fibrinogen and rGST γ-chain with similar affinities. This indicates that the only binding site for FnBPB in fibrinogen is in the extreme C-terminus of the γ-chain. This result could explain why the affinity (K_D) of rFnBPB N2N3 for fibrinogen calculated in this study was approximately 20-fold weaker than that calculated previously for rClfA N2N3 (Geoghegan, 2008). Taken together, these data illustrate important differences between the interaction of ClfA and FnBPB with fibrinogen. The precise interaction of FnBPB residues with a fibrinogen ligand will only be fully understood with a co-crystalised complex. Until that is achieved, it would be interesting to study the interaction of a series of alanine-substituted fibrinogen γ-chain peptides with rFnBPB N2N3. Recently, a panel of fibrinogen peptides, each containing different alanine substituted residues was used to study the

details of the interaction of this peptide with ClfA (Ganesh *et al.*, 2008). Similar investigations with FnBPB could be carried out to understand the contacts made by residues such as N312 and F316 with fibrinogen.

7.1.5 Fibronectin-binding by FnBPB

The fibrinogen and elastin-binding N-terminal A domains of FnBPA and FnBPB are followed by an intrinsically disordered C-terminal regions containing 11 (FnBPA) or 10 (FnBPB) non-identical fibronectin-binding repeats (FnBRs). FnBRs bind specifically to the N-terminal domain of fibronectin which comprises five F1 modules (Schwarz-Linek *et al.*, 2003, Meenan *et al.*, 2007, Keane *et al.*, 2007b). The co-ordinates of FnBPA and FnBPB from *S. aureus* strain 8325-4 were recently redefined (Meenan *et al.*, 2007). The revised N2N3 subdomains span residues 194 to 511 and residues 163 to 480, respectively, and do not include any FnBR sequences (Meenan *et al.*, 2007, Keane *et al.*, 2007b). The ligand-binding ability of $rFnBPA_{194-511}$ was tested previously and the protein was found to promote binding only to fibrinogen and elastin. These results confirmed the absence of any fibronectin-binding motifs in the revised N2N3 subdomain of FnBPA (Keane *et al.*, 2007). In this study, the ligand-binding ability of $rFnBPB_{163-480}$ was tested. Unexpectedly, this protein bound to immobilised fibronectin. This raised the possibility that, unlike FnBPA, the A domain of FnBPB contains a novel fibronectin binding motif that may bind fibronectin by a novel mechanism. The recombinant FnBPB N2N3 protein bound to fibronectin with the same affinity (K_D) as that which was calculated for its interaction with fibrinogen. Furthermore, the fibronectin-binding phenotype was retained in each of the seven rFnBPB N2N3 isotypes. Taken together these results suggested that the fibronectin-binding function of the A domain of FnBPB is biologically important.

To determine if the A domain of FnBPB binds fibrinogen and fibronectin by the same mechanism, rFnBPB N2N3 mutants that are

defective in fibrinogen-binding were tested for their ability to bind fibronectin. As described above, the predicted latching peptide of rFnBPB N2N3 comprising seventeen C-terminal residues was found to play a crucial role in fibrinogen binding by dock, lock and latch. By contrast, deletion of the predicted latching peptide had no affect on the affinity of rFnBPB N2N3 for fibronectin. This result indicates that the A domain of FnBPB binds fibrinogen and fibronectin by different mechanisms. The substitution of FnBPB residues N312 and F314 to alanines which reduced the affinity of rFnBPB N2N3 for fibrinogen also reduced the affinity of this protein for fibronectin. This suggests that the predicted ligand binding trench of FnBPB plays a key role in both the fibrinogen and fibronectin-binding mechanisms. It would be of interest to determine if the binding sites for fibrinogen and fibronectin overlap within the hydrophobic ligand-binding trench.

To further localise the fibronectin-binding site, recombinant forms of FnBPB subdomains N2 and N3 were tested for their ability to bind fibronectin. Each truncated protein showed a reduced affinity for fibronectin suggesting that each subdomain plays an important role in the fibronectin-binding mechanism. These results are consistent with the proposal that fibronectin interacts with a ligand binding trench comprising N2 and N3 subdomain residues. The N2N3 subdomain of FnBPB and FnBPA are sufficiently similar to accommodate the same region of fibrinogen yet they differ in their affinities for fibronectin. A systematic comparison of the residues of the trench regions of both proteins may identify key residues which would aid in the understanding of fibronectin binding by the N2N3 subdomain of FnBPB.

To localise the binding site in fibronectin for the N2N3 subdomain of FnBPB, the binding of rFnBPB N2N3 to different fragments of fibronectin was tested. The recombinant protein bound with similar affinity to whole fibronectin and to an N-terminal fragment of fibronectin containing

F1 modules 1 to 5. This is the same region of fibronectin with which the C-terminal FnBRs of FnBPA and FnBPB interact. Binding of the N-terminal type 1 modules to the C-terminal FnBRs triggers the uptake of *S. aureus* by human endothelial cells and is believed to facilitate *S. aureus* persistence and the establishment of secondary (metastatic) infections

To explore the biological significance of the interaction between the A domain of FnBPB and fibronectin, the ability of the N-termianl A domain, in isolation from the C-terminal FnBRs, to promote bacterial adhesion to fibronectin and the subsequent invasion of human endothelial cells was examined. This was facilitated by the expression of a chimeric FnBPB-ClfA protein containing the N-terminal A domain of FnBPB and the C-terminal stalk and cell wall anchoring region of ClfA on the surface of *S. epidermidis* cells. Functional assays revealed that the A domain of FnBPB was sufficient to promote bacterial adherence to immobilised fibronectin. However, the affinity for fibronectin of *S.epidermidis* cells expressing the chimeric FnBPB-ClfA protein was significantly weaker than that of cells expressing full length wild-type FnBPB with its full complement of FnBRs

While expression of the A domain of FnBPB promoted low-affinity adhesion of *S. epidermidis* to fibronectin, it did not trigger the subsequent uptake of *S. epidermidis* cells by endothelial cells. This is consistent with a recent study which indicated that the affinity of bacterial cells for fibronectin is indicative of the potential to trigger the invasion process (Edwards *et al.*, 2010). To determine conclusively if the A domain of FnBPB contributes to some extent to the overall process of FnBPB-mediated invasion of endothelial cells, it would be necessary to examine the efficiency of FnBPB to promote endothelial cell invasion in the absence of the N-terminal A domain. Also, it is possible that the A domain of FnBPB plays a role in other fibronectin-binding mediated processes *in vivo* such as platelet activation. While the precise biological consequences of fibronectin-

binding by the A domain of FnBPB requires further investigation, the conserved fibronectin-binding ability of antigenically distinct isotypes of FnBPB may have implications for the N2N3 subdomain of FnBPB as a target for a vaccine or immunotherapeutics.

References

Almeida, R. A., K. R. Matthews, E. Cifrian, A. J. Guidry & S. P. Oliver, (1996) *Staphylococcus aureus* invasion of bovine mammary epithelial cells. *J Dairy Sci* **79**: 1021-1026.

Augustin, J. & F. Gotz, (1990) Transformation of *Staphylococcus epidermidis* and other staphylococcal species with plasmid DNA by electroporation. *FEMS Microbiol Lett* **54**: 203-207.

Augustin, J., R. Rosenstein, B. Wieland, U. Schneider, N. Schnell, G. Engelke, K. D. Entian & F. Gotz, (1992) Genetic analysis of epidermin biosynthetic genes and epidermin-negative mutants of *Staphylococcus epidermidis*. *Eur J Biochem* **204**: 1149-1154.

Baddour, L. M., C. Lowrance, A. Albus, J. H. Lowrance, S. K. Anderson & J. C. Lee, (1992) *Staphylococcus aureus* microcapsule expression attenuates bacterial virulence in a rat model of experimental endocarditis. *J Infect Dis* **165**: 749-753.

Bestebroer, J., M. J. Poppelier, L. H. Ulfman, P. J. Lenting, C. V. Denis, K. P. van Kessel, J. A. van Strijp & C. J. de Haas, (2007) Staphylococcal superantigen-like 5 binds PSGL-1 and inhibits P-selectin-mediated neutrophil rolling. *Blood* **109**: 2936-2943.

Bingham, R. J., E. Rudino-Pinera, N. A. Meenan, U. Schwarz-Linek, J. P. Turkenburg, M. Hook, E. F. Garman & J. R. Potts, (2008) Crystal structures of fibronectin-binding sites from *Staphylococcus aureus* FnBPA in complex with fibronectin domains. *Proc Natl Acad Sci U S A* **105**: 12254-12258.

Biswas, R., L. Voggu, U. K. Simon, P. Hentschel, G. Thumm & F. Gotz, (2006) Activity of the major staphylococcal autolysin Atl. *FEMS Microbiol Lett* **259**: 260-268.

Boden, M. K. & J. I. Flock, (1989) Fibrinogen-binding protein/clumping factor from *Staphylococcus aureus*. *Infect Immun* **57**: 2358-2363.

Bokarewa, M. I., T. Jin & A. Tarkowski, (2006) *Staphylococcus aureus*: Staphylokinase. *Int J Biochem Cell Biol* **38**: 504-509.

Bork, P., A. K. Downing, B. Kieffer & I. D. Campbell, (1996) Structure and distribution of modules in extracellular proteins. *Q Rev Biophys* **29**: 119-167.

Boyd, C. D., A. M. Christiano, R. A. Pierce, C. A. Stolle & S. B. Deak, (1991) Mammalian tropoelastin: multiple domains of the protein define an evolutionarily divergent amino acid sequence. *Matrix* **11**: 235-241.

Bozzini, S., L. Visai, P. Pignatti, T. E. Petersen & P. Speziale, (1992) Multiple binding sites in fibronectin and the staphylococcal fibronectin receptor. *Eur J Biochem* **207**: 327-333.

Casolini, F., L. Visai, D. Joh, P. G. Conaldi, A. Toniolo, M. Hook & P. Speziale, (1998) Antibody response to fibronectin-binding adhesin FnbpA in patients with *Staphylococcus aureus* infections. *Infect Immun* **66**: 5433-5442.

Chavakis, T., K. Wiechmann, K. T. Preissner & M. Herrmann, (2005) *Staphylococcus aureus* interactions with the endothelium: the role of bacterial "secretable expanded repertoire adhesive molecules" (SERAM) in disturbing host defense systems. *Thromb Haemost* **94**: 278-285.

Clarke, S. R., L. G. Harris, R. G. Richards & S. J. Foster, (2002) Analysis of Ebh, a 1.1-megadalton cell wall-associated fibronectin-binding protein of *Staphylococcus aureus*. *Infect Immun* **70**: 6680-6687.

Conrady, D. G., C. C. Brescia, K. Horii, A. A. Weiss, D. J. Hassett & A. B. Herr, (2008) A zinc-dependent adhesion module is responsible for intercellular adhesion in staphylococcal biofilms. *Proc Natl Acad Sci U S A* **105**: 19456-19461.

Cooper, J. E. & E. J. Feil, (2006) The phylogeny of *Staphylococcus aureus* - which genes make the best intra-species markers? *Microbiology* **152**: 1297-1305.

Corrigan, R. M., H. Miajlovic & T. J. Foster, (2009) Surface proteins that promote adherence of *Staphylococcus aureus* to human desquamated nasal epithelial cells. *BMC Microbiol* **9**: 22.

Corrigan, R. M., D. Rigby, P. Handley & T. J. Foster, (2007) The role of *Staphylococcus aureus* surface protein SasG in adherence and biofilm formation. *Microbiology* **153**: 2435-2446.

Cosgrove, S. E., K. C. Carroll & T. M. Perl, (2004) *Staphylococcus aureus* with reduced susceptibility to vancomycin. *Clin Infect Dis* **39**: 539-545.

Cunnion, K. M., H. M. Zhang & M. M. Frank, (2003) Availability of complement bound to *Staphylococcus aureus* to interact with membrane complement receptors influences efficiency of phagocytosis. *Infect Immun* **71**: 656-662.

de Haas, C. J., K. E. Veldkamp, A. Peschel, F. Weerkamp, W. J. Van Wamel, E. C. Heezius, M. J. Poppelier, K. P. Van Kessel & J. A. van Strijp, (2004) Chemotaxis inhibitory protein of *Staphylococcus aureus*, a bacterial antiinflammatory agent. *J Exp Med* **199**: 687-695.

Deisenhofer, J., (1981) Crystallographic refinement and atomic models of a human Fc fragment and its complex with fragment B of protein A from *Staphylococcus aureus* at 2.9- and 2.8-A resolution. *Biochemistry* **20**: 2361-2370.

Deivanayagam, C. C., R. L. Rich, S. Danthuluri, R. T. Owens, J. M. Patti, M. Hook, L. J. DeLucas & S. V. Narayana, (1999) Crystallization and preliminary X-ray analysis of B-domain fragments of a *Staphylococcus aureus* collagen-binding protein. *Acta Crystallogr D Biol Crystallogr* **55**: 525-527.

Deivanayagam, C. C., E. R. Wann, W. Chen, M. Carson, K. R. Rajashankar, M. Hook & S. V. Narayana, (2002) A novel variant of the immunoglobulin fold in surface adhesins of *Staphylococcus aureus*: crystal structure of the fibrinogen-binding MSCRAMM, clumping factor A. *EMBO J* **21**: 6660-6672.

Doery, H. M., B. J. Magnusson, I. M. Cheyne & J. Sulasekharam, (1963) A phospholipase in staphylococcal toxin which hydrolyses sphingomyelin. *Nature* **198**: 1091-1092.

Doolittle, R. F., (1984) Fibrinogen and fibrin. *Annu Rev Biochem* **53**: 195-229.

Downer, R., F. Roche, P. W. Park, R. P. Mecham & T. J. Foster, (2002) The elastin-binding protein of *Staphylococcus aureus* (EbpS) is expressed at the cell surface as an integral membrane protein and not as a cell wall-associated protein. *J Biol Chem* **277**: 243-250.

Dryla, A., D. Gelbmann, A. von Gabain & E. Nagy, (2003) Identification of a novel iron regulated staphylococcal surface protein with haptoglobin-haemoglobin binding activity. *Mol Microbiol* **49**: 37-53.

Dryla, A., S. Prustomersky, D. Gelbmann, M. Hanner, E. Bettinger, B. Kocsis, T. Kustos, T. Henics, A. Meinke & E. Nagy, (2005) Comparison of antibody repertoires against *Staphylococcus aureus* in healthy individuals and in acutely infected patients. *Clin Diagn Lab Immunol* **12**: 387-398.

Dziewanowska, K., J. M. Patti, C. F. Deobald, K. W. Bayles, W. R. Trumble & G. A. Bohach, (1999) Fibronectin binding protein and host cell tyrosine kinase are required for internalization of *Staphylococcus aureus* by epithelial cells. *Infect Immun* **67**: 4673-4678.

Edgell, C. J., C. C. McDonald & J. B. Graham, (1983) Permanent cell line expressing human factor VIII-related antigen established by hybridization. *Proc Natl Acad Sci U S A* **80**: 3734-3737.

Edwards, A.M., Potts, J.R., E. Josefsson & R.C. Massey, (2010) *Staphylococcus aureus* host cell invasion and virulence in sepsis is facilitated by the multiple repeats within FnBPA. *PLoS Pathog* **24**: 6 (6)

Enright, M. C., D. A. Robinson, G. Randle, E. J. Feil, H. Grundmann & B. G. Spratt, (2002) The evolutionary history of methicillin-resistant *Staphylococcus aureus* (MRSA). *Proc Natl Acad Sci U S A* **99**: 7687-7692.

Fazio, M. J., M. G. Mattei, E. Passage, M. L. Chu, D. Black, E. Solomon, J. M. Davidson & J. Uitto, (1991) Human elastin gene: new evidence for localization to the long arm of chromosome 7. *Am J Hum Genet* **48**: 696-703.

Feil, E. J., J. E. Cooper, H. Grundmann, D. A. Robinson, M. C. Enright, T. Berendt, S. J. Peacock, J. M. Smith, M. Murphy, B. G. Spratt, C. E. Moore & N. P. Day, (2003) How clonal is *Staphylococcus aureus*? *J Bacteriol* **185**: 3307-3316.

Feil, E. J. & M. C. Enright, (2004) Analyses of clonality and the evolution of bacterial pathogens. *Curr Opin Microbiol* **7**: 308-313.

Feil, E. J. & B. G. Spratt, (2001) Recombination and the population structures of bacterial pathogens. *Annu Rev Microbiol* **55**: 561-590.

ffrench-Constant, C., (1995) Alternative splicing of fibronectin--many different proteins but few different functions. *Exp Cell Res* **221**: 261-271.

Fitzgerald, J. R., P. J. Hartigan, W. J. Meaney & C. J. Smyth, (2000) Molecular population and virulence factor analysis of *Staphylococcus aureus* from bovine intramammary infection. *J Appl Microbiol* **88**: 1028-1037.

Fitzgerald, J. R., A. Loughman, F. Keane, M. Brennan, M. Knobel, J. Higgins, L. Visai, P. Speziale, D. Cox & T. J. Foster, (2006) Fibronectin-binding proteins of *Staphylococcus aureus* mediate

activation of human platelets via fibrinogen and fibronectin bridges to integrin GPIIb/IIIa and IgG binding to the FcgammaRIIa receptor. *Mol Microbiol* **59**: 212-230.

Flock, J. I., S. A. Hienz, A. Heimdahl & T. Schennings, (1996) Reconsideration of the role of fibronectin binding in endocarditis caused by *Staphylococcus aureus*. *Infect Immun* **64**: 1876-1878.

Forsgren, A. & K. Nordstrom, (1974) Protein A from *Staphylococcus aureus*: the biological significance of its reaction with IgG. *Ann N Y Acad Sci* **236**: 252-266.

Fowler, T., E. R. Wann, D. Joh, S. Johansson, T. J. Foster & M. Hook, (2000) Cellular invasion by *Staphylococcus aureus* involves a fibronectin bridge between the bacterial fibronectin-binding MSCRAMMs and host cell beta1 integrins. *Eur J Cell Biol* **79**: 672-679.

Friedrich, R., P. Panizzi, P. Fuentes-Prior, K. Richter, I. Verhamme, P. J. Anderson, S. Kawabata, R. Huber, W. Bode & P. E. Bock, (2003) Staphylocoagulase is a prototype for the mechanism of cofactor-induced zymogen activation. *Nature* **425**: 535-539.

Fujita, T., (2002) Evolution of the lectin-complement pathway and its role in innate immunity. *Nat Rev Immunol* **2**: 346-353.

Ganesh, V. K., J. J. Rivera, E. Smeds, Y. P. Ko, M. G. Bowden, E. R. Wann, S. Gurusiddappa, J. R. Fitzgerald & M. Hook, (2008) A structural model of the *Staphylococcus aureus* ClfA-fibrinogen interaction opens new avenues for the design of anti-staphylococcal therapeutics. *PLoS Pathog* **4**: e1000226.

Geoghegan, J., (2008) Molecular Analysis of Fibrinogen Binding Proteins of Staphylococci. In: Microbiology. Trinity College Dublin, pp.

Geoghegan, J.A., R.M. Corrigan, D.T. Gruszka, P. Speziale, J.P. O'Gara, J.R. Potts & T.J. Foster (2010) Role of surface protein SasG in

biofilm formation by *Staphylococcus aureus*. *J Bacteriol* **21**:5663-5673

George, E. L., E. N. Georges-Labouesse, R. S. Patel-King, H. Rayburn & R. O. Hynes, (1993) Defects in mesoderm, neural tube and vascular development in mouse embryos lacking fibronectin. *Development* **119**: 1079-1091.

Gillaspy, A. F., C. Y. Lee, S. Sau, A. L. Cheung & M. S. Smeltzer, (1998) Factors affecting the collagen binding capacity of *Staphylococcus aureus*. *Infect Immun* **66**: 3170-3178.

Gillaspy, A. F., J. M. Patti & M. S. Smeltzer, (1997) Transcriptional regulation of the *Staphylococcus aureus* collagen adhesion gene, cna. *Infect Immun* **65**: 1536-1540.

Goodyear, C. S. & G. J. Silverman, (2003) Death by a B cell superantigen: In vivo VH-targeted apoptotic supraclonal B cell deletion by a Staphylococcal Toxin. *J Exp Med* **197**: 1125-1139.

Goodyear, C. S. & G. J. Silverman, (2004) Staphylococcal toxin induced preferential and prolonged in vivo deletion of innate-like B lymphocytes. *Proc Natl Acad Sci U S A* **101**: 11392-11397.

Gouda, H., H. Torigoe, A. Saito, M. Sato, Y. Arata & I. Shimada, (1992) Three-dimensional solution structure of the B domain of staphylococcal protein A: comparisons of the solution and crystal structures. *Biochemistry* **31**: 9665-9672.

Greene, C., P. E. Vaudaux, P. Francois, R. A. Proctor, D. McDevitt & T. J. Foster, (1996) A low-fibronectin-binding mutant of *Staphylococcus aureus* 879R4S has Tn918 inserted into its single fnb gene. *Microbiology* **142 (Pt 8)**: 2153-2160.

Grundmeier, M., M. Hussain, P. Becker, C. Heilmann, G. Peters & B. Sinha, (2004) Truncation of fibronectin-binding proteins in *Staphylococcus aureus* strain Newman leads to deficient adherence and host cell

Ito, T., K. Okuma, X. X. Ma, H. Yuzawa & K. Hiramatsu, (2003) Insights on antibiotic resistance of *Staphylococcus aureus* from its whole genome: genomic island SCC. *Drug Resist Updat* **6**: 41-52.

Jevons, M. P., (1961) "Celbenin"- resistant staphylococci. *Br Med J* **124**: 124-125.

Jin, T., M. Bokarewa, T. Foster, J. Mitchell, J. Higgins & A. Tarkowski, (2004) *Staphylococcus aureus* resists human defensins by production of staphylokinase, a novel bacterial evasion mechanism. *J Immunol* **172**: 1169-1176.

Jonsson, K., C. Signas, H. P. Muller & M. Lindberg, (1991) Two different genes encode fibronectin binding proteins in *Staphylococcus aureus*. The complete nucleotide sequence and characterization of the second gene. *Eur J Biochem* **202**: 1041-1048.

Josefsson, E., K. W. McCrea, D. Ni Eidhin, D. O'Connell, J. Cox, M. Hook & T. J. Foster, (1998) Three new members of the serine-aspartate repeat protein multigene family of *Staphylococcus aureus*. *Microbiology* **144 (Pt 12)**: 3387-3395.

Kaneko, J. & Y. Kamio, (2004) Bacterial two-component and hetero-heptameric pore-forming cytolytic toxins: structures, pore-forming mechanism, and organization of the genes. *Biosci Biotechnol Biochem* **68**: 981-1003.

Karlsson, A., P. Saravia-Otten, K. Tegmark, E. Morfeldt & S. Arvidson, (2001) Decreased amounts of cell wall-associated protein A and fibronectin-binding proteins in *Staphylococcus aureus* sarA mutants due to up-regulation of extracellular proteases. *Infect Immun* **69**: 4742-4748.

Keane, F. M., A. W. Clarke, T. J. Foster & A. S. Weiss, (2007a) The N-terminal A domain of *Staphylococcus aureus* fibronectin-binding protein A binds to tropoelastin. *Biochemistry* **46**: 7226-7232.

Keane, F. M., A. Loughman, V. Valtulina, M. Brennan, P. Speziale & T. J. Foster, (2007b) Fibrinogen and elastin bind to the same region within the A domain of fibronectin binding protein A, an MSCRAMM of *Staphylococcus aureus*. *Mol Microbiol* **63**: 711-723.

Kintarak, S., S. A. Whawell, P. M. Speight, S. Packer & S. P. Nair, (2004) Internalization of *Staphylococcus aureus* by human keratinocytes. *Infect Immun* **72**: 5668-5675.

Kuhn, G., P. Francioli & D. S. Blanc, (2006) Evidence for clonal evolution among highly polymorphic genes in methicillin-resistant *Staphylococcus aureus*. *J Bacteriol* **188**: 169-178.

Kuroda, M., T. Ohta, I. Uchiyama, T. Baba, H. Yuzawa, I. Kobayashi, L. Cui, A. Oguchi, K. Aoki, Y. Nagai, J. Lian, T. Ito, M. Kanamori, H. Matsumaru, A. Maruyama, H. Murakami, A. Hosoyama, Y. Mizutani-Ui, N. K. Takahashi, T. Sawano, R. Inoue, C. Kaito, K. Sekimizu, H. Hirakawa, S. Kuhara, S. Goto, J. Yabuzaki, M. Kanehisa, A. Yamashita, K. Oshima, K. Furuya, C. Yoshino, T. Shiba, M. Hattori, N. Ogasawara, H. Hayashi & K. Hiramatsu, (2001) Whole genome sequencing of meticillin-resistant *Staphylococcus aureus*. *Lancet* **357**: 1225-1240.

Kuroda, M., Y. Tanaka, R. Aoki, D. Shu, K. Tsumoto & T. Ohta, (2008) *Staphylococcus aureus* giant protein Ebh is involved in tolerance to transient hyperosmotic pressure. *Biochem Biophys Res Commun* **374**: 237-241.

Kuusela, P., T. Vartio, M. Vuento & E. B. Myhre, (1984) Binding sites for streptococci and staphylococci in fibronectin. *Infect Immun* **45**: 433-436.

Kuypers, J. M. & R. A. Proctor, (1989) Reduced adherence to traumatized rat heart valves by a low-fibronectin-binding mutant of *Staphylococcus aureus*. *Infect Immun* **57**: 2306-2312.

Laemmli, U. K., (1970) Cleavage of structural proteins during the assembly of the head of bacteriophage T4. *Nature* **227**: 680-685.

Lee, J. C., J. S. Park, S. E. Shepherd, V. Carey & A. Fattom, (1997) Protective efficacy of antibodies to the *Staphylococcus aureus* type 5 capsular polysaccharide in a modified model of endocarditis in rats. *Infect Immun* **65**: 4146-4151.

Lee, L. Y., X. Liang, M. Hook & E. L. Brown, (2004) Identification and characterization of the C3 binding domain of the *Staphylococcus aureus* extracellular fibrinogen-binding protein (Efb). *J Biol Chem* **279**: 50710-50716.

Li, D., A. Renzoni, T. Estoppey, C. Bisognano, P. Francois, W. L. Kelley, D. P. Lew, J. Schrenzel & P. Vaudaux, (2005) Induction of fibronectin adhesins in quinolone-resistant *Staphylococcus aureus* by subinhibitory levels of ciprofloxacin or by sigma B transcription factor activity is mediated by two separate pathways. *Antimicrob Agents Chemother* **49**: 916-924.

Lindsay, J. A. & M. T. Holden, (2004) *Staphylococcus aureus*: superbug, super genome? *Trends Microbiol* **12**: 378-385.

Loughman, A., (2006) Platelet activation by *Staphylococcus aureus*. In.: Trinity College Dublin, pp.

Loughman, A., J. R. Fitzgerald, M. P. Brennan, J. Higgins, R. Downer, D. Cox & T. J. Foster, (2005) Roles for fibrinogen, immunoglobulin and complement in platelet activation promoted by *Staphylococcus aureus* clumping factor A. *Mol Microbiol* **57**: 804-818.

Loughman, A., T. Sweeney, F. M. Keane, G. Pietrocola, P. Speziale & T. J. Foster, (2008) Sequence diversity in the A domain of *Staphylococcus aureus* fibronectin-binding protein A. *BMC Microbiol* **8**: 74.

Lowy, F. D., (1998) *Staphylococcus aureus* infections. *N Engl J Med* **339**: 520-532.

Ludwig, W., E. Seewaldt, R. Kilpper-Balz, K. H. Schleifer, L. Magrum, C. R. Woese, G. E. Fox & E. Stackebrandt, (1985) The phylogenetic position of Streptococcus and Enterococcus. *J Gen Microbiol* **131**: 543-551.

Luong, T. T. & C. Y. Lee, (2002) Overproduction of type 8 capsular polysaccharide augments *Staphylococcus aureus* virulence. *Infect Immun* **70**: 3389-3395.

Mack, D., P. Becker, I. Chatterjee, S. Dobinsky, J. K. Knobloch, G. Peters, H. Rohde & M. Herrmann, (2004) Mechanisms of biofilm formation in *Staphylococcus epidermidis* and *Staphylococcus aureus*: functional molecules, regulatory circuits, and adaptive responses. *Int J Med Microbiol* **294**: 203-212.

Massey, R. C., M. N. Kantzanou, T. Fowler, N. P. Day, K. Schofield, E. R. Wann, A. R. Berendt, M. Hook & S. J. Peacock, (2001) Fibronectin-binding protein A of *Staphylococcus aureus* has multiple, substituting, binding regions that mediate adherence to fibronectin and invasion of endothelial cells. *Cell Microbiol* **3**: 839-851.

Mazmanian, S. K., H. Ton-That & O. Schneewind, (2001) Sortase-catalysed anchoring of surface proteins to the cell wall of *Staphylococcus aureus*. *Mol Microbiol* **40**: 1049-1057.

Mazmanian, S. K., H. Ton-That, K. Su & O. Schneewind, (2002) An iron-regulated sortase anchors a class of surface protein during *Staphylococcus aureus* pathogenesis. *Proc Natl Acad Sci U S A* **99**: 2293-2298.

McAleese, F. M., E. J. Walsh, M. Sieprawska, J. Potempa & T. J. Foster, (2001) Loss of clumping factor B fibrinogen binding activity by *Staphylococcus aureus* involves cessation of transcription, shedding and cleavage by metalloprotease. *J Biol Chem* **276**: 29969-29978.

McDevitt, D. & T. J. Foster, (1995) Variation in the size of the repeat region of the fibrinogen receptor (clumping factor) of *Staphylococcus aureus* strains. *Microbiology* **141 (Pt 4)**: 937-943.

McDevitt, D., P. Francois, P. Vaudaux & T. J. Foster, (1994) Molecular characterization of the clumping factor (fibrinogen receptor) of *Staphylococcus aureus*. *Mol Microbiol* **11**: 237-248.

McDevitt, D., T. Nanavaty, K. House-Pompeo, E. Bell, N. Turner, L. McIntire, T. Foster & M. Hook, (1997) Characterization of the interaction between the *Staphylococcus aureus* clumping factor (ClfA) and fibrinogen. *Eur J Biochem* **247**: 416-424.

McDevitt, D., P. Vaudaux & T. J. Foster, (1992) Genetic evidence that bound coagulase of *Staphylococcus aureus* is not clumping factor. *Infect Immun* **60**: 1514-1523.

Meenan, N. A., L. Visai, V. Valtulina, U. Schwarz-Linek, N. C. Norris, S. Gurusiddappa, M. Hook, P. Speziale & J. R. Potts, (2007) The tandem beta-zipper model defines high affinity fibronectin-binding repeats within *Staphylococcus aureus* FnBPA. *J Biol Chem* **282**: 25893-25902.

Miajlovic, H., A. Loughman, M. Brennan, D. Cox & T. J. Foster, (2007) Both complement- and fibrinogen-dependent mechanisms contribute to platelet aggregation mediated by *Staphylococcus aureus* clumping factor B. *Infect Immun* **75**: 3335-3343.

Mitchell, G., C. A. Lamontagne, E. Brouillette, G. Grondin, B. G. Talbot, M. Grandbois & F. Malouin, (2008) *Staphylococcus aureus* SigB activity promotes a strong fibronectin-bacterium interaction which may sustain host tissue colonization by small-colony variants isolated from cystic fibrosis patients. *Mol Microbiol* **70**: 1540-1555.

Mongodin, E., O. Bajolet, J. Cutrona, N. Bonnet, F. Dupuit, E. Puchelle & S. de Bentzmann, (2002) Fibronectin-binding proteins of

Staphylococcus aureus are involved in adherence to human airway epithelium. *Infect Immun* **70**: 620-630.

Montoya, M. & E. Gouaux, (2003) Beta-barrel membrane protein folding and structure viewed through the lens of alpha-hemolysin. *Biochim Biophys Acta* **1609**: 19-27.

Moreillon, P., J. M. Entenza, P. Francioli, D. McDevitt, T. J. Foster, P. Francois & P. Vaudaux, (1995) Role of *Staphylococcus aureus* coagulase and clumping factor in pathogenesis of experimental endocarditis. *Infect Immun* **63**: 4738-4743.

Much, M., (1908) Uber eine Vorstufe des Fibrinfermentes in Kulturen von *Staphylococcus aureus*. *Biochem. Z.* **14**: 143-155.

Ni Eidhin, D., S. Perkins, P. Francois, P. Vaudaux, M. Hook & T. J. Foster, (1998) Clumping factor B (ClfB), a new surface-located fibrinogen-binding adhesin of *Staphylococcus aureus*. *Mol Microbiol* **30**: 245-257.

Nilsson, I. M., J. M. Patti, T. Bremell, M. Hook & A. Tarkowski, (1998) Vaccination with a recombinant fragment of collagen adhesin provides protection against *Staphylococcus aureus*-mediated septic death. *J Clin Invest* **101**: 2640-2649.

O'Connell, D. P., T. Nanavaty, D. McDevitt, S. Gurusiddappa, M. Hook & T. J. Foster, (1998) The fibrinogen-binding MSCRAMM (clumping factor) of *Staphylococcus aureus* has a Ca2+-dependent inhibitory site. *J Biol Chem* **273**: 6821-6829.

O'Neill, E., H. Humphreys & J. P. O'Gara, (2009) Carriage of both the fnbA and fnbB genes and growth at 37 degrees C promote FnBP-mediated biofilm development in meticillin-resistant *Staphylococcus aureus* clinical isolates. *J Med Microbiol* **58**: 399-402.

O'Neill, E., C. Pozzi, P. Houston, H. Humphreys, D. A. Robinson, A. Loughman, T. J. Foster & J. P. O'Gara, (2008) A novel *Staphylococcus aureus* biofilm phenotype mediated by the

fibronectin-binding proteins, FnBPA and FnBPB. *J Bacteriol* **190**: 3835-3850.

O'Riordan, K. & J. C. Lee, (2004) *Staphylococcus aureus* capsular polysaccharides. *Clin Microbiol Rev* **17**: 218-234.

Palma, M., A. Haggar & J. I. Flock, (1999) Adherence of *Staphylococcus aureus* is enhanced by an endogenous secreted protein with broad binding activity. *J Bacteriol* **181**: 2840-2845.

Palma, M., O. Shannon, H. C. Quezada, A. Berg & J. I. Flock, (2001) Extracellular fibrinogen-binding protein, Efb, from *Staphylococcus aureus* blocks platelet aggregation due to its binding to the alpha-chain. *J Biol Chem* **276**: 31691-31697.

Palmqvist, N., J. M. Patti, A. Tarkowski & E. Josefsson, (2004) Expression of staphylococcal clumping factor A impedes macrophage phagocytosis. *Microbes Infect* **6**: 188-195.

Palmqvist, N., G. J. Silverman, E. Josefsson & A. Tarkowski, (2005) Bacterial cell wall-expressed protein A triggers supraclonal B-cell responses upon in vivo infection with *Staphylococcus aureus*. *Microbes Infect* **7**: 1501-1511.

Pankov, R. & K. M. Yamada, (2002) Fibronectin at a glance. *J Cell Sci* **115**: 3861-3863.

Parks, W. C., H. Secrist, L. C. Wu & R. P. Mecham, (1988) Developmental regulation of tropoelastin isoforms. *J Biol Chem* **263**: 4416-4423.

Patti, J. M., H. Jonsson, B. Guss, L. M. Switalski, K. Wiberg, M. Lindberg & M. Hook, (1992) Molecular characterization and expression of a gene encoding a *Staphylococcus aureus* collagen adhesin. *J Biol Chem* **267**: 4766-4772.

Peacock, S. J., N. P. Day, M. G. Thomas, A. R. Berendt & T. J. Foster, (2000) Clinical isolates of *Staphylococcus aureus* exhibit diversity in fnb genes and adhesion to human fibronectin. *J Infect* **41**: 23-31.

Peacock, S. J., C. E. Moore, A. Justice, M. Kantzanou, L. Story, K. Mackie, G. O'Neill & N. P. Day, (2002) Virulent combinations of adhesin and toxin genes in natural populations of *Staphylococcus aureus*. *Infect Immun* **70**: 4987-4996.

Ponnuraj, K., M. G. Bowden, S. Davis, S. Gurusiddappa, D. Moore, D. Choe, Y. Xu, M. Hook & S. V. Narayana, (2003) A "dock, lock, and latch" structural model for a staphylococcal adhesin binding to fibrinogen. *Cell* **115**: 217-228.

Postma, B., M. J. Poppelier, J. C. van Galen, E. R. Prossnitz, J. A. van Strijp, C. J. de Haas & K. P. van Kessel, (2004) Chemotaxis inhibitory protein of *Staphylococcus aureus* binds specifically to the C5a and formylated peptide receptor. *J Immunol* **172**: 6994-7001.

Potts, J. R. & I. D. Campbell, (1994) Fibronectin structure and assembly. *Curr Opin Cell Biol* **6**: 648-655.

Prevost, G., T. Bouakham, Y. Piemont & H. Monteil, (1995) Characterisation of a synergohymenotropic toxin produced by Staphylococcus intermedius. *FEBS Lett* **376**: 135-140.

Proft, T. & J. D. Fraser, (2003) Bacterial superantigens. *Clin Exp Immunol* **133**: 299-306.

Que, Y. A., P. Francois, J. A. Haefliger, J. M. Entenza, P. Vaudaux & P. Moreillon, (2001) Reassessing the role of *Staphylococcus aureus* clumping factor and fibronectin-binding protein by expression in *Lactococcus lactis*. *Infect Immun* **69**: 6296-6302.

Que, Y. A., J. A. Haefliger, L. Piroth, P. Francois, E. Widmer, J. M. Entenza, B. Sinha, M. Herrmann, P. Francioli, P. Vaudaux & P. Moreillon, (2005) Fibrinogen and fibronectin binding cooperate for valve infection and invasion in *Staphylococcus aureus* experimental endocarditis. *J Exp Med* **201**: 1627-1635.

Raibaud, S., U. Schwarz-Linek, J. H. Kim, H. T. Jenkins, E. R. Baines, S. Gurusiddappa, M. Hook & J. R. Potts, (2005) Borrelia burgdorferi

binds fibronectin through a tandem beta-zipper, a common mechanism of fibronectin binding in staphylococci, streptococci, and spirochetes. *J Biol Chem* **280**: 18803-18809.

Rice, K., M. Huesca, D. Vaz & M. J. McGavin, (2001) Variance in fibronectin binding and fnb locus polymorphisms in *Staphylococcus aureus*: identification of antigenic variation in a fibronectin binding protein adhesin of the epidemic CMRSA-1 strain of methicillin-resistant *S. aureus*. *Infect Immun* **69**: 3791-3799.

Risley, A. L., A. Loughman, C. Cywes-Bentley, T. J. Foster & J. C. Lee, (2007) Capsular polysaccharide masks clumping factor A-mediated adherence of *Staphylococcus aureus* to fibrinogen and platelets. *J Infect Dis* **196**: 919-927.

Robinson, D. A. & M. C. Enright, (2004) Multilocus sequence typing and the evolution of methicillin-resistant *Staphylococcus aureus*. *Clin Microbiol Infect* **10**: 92-97.

Roche, F. M., R. Downer, F. Keane, P. Speziale, P. W. Park & T. J. Foster, (2004) The N-terminal A domain of fibronectin-binding proteins A and B promotes adhesion of *Staphylococcus aureus* to elastin. *J Biol Chem* **279**: 38433-38440.

Roche, F. M., R. Massey, S. J. Peacock, N. P. Day, L. Visai, P. Speziale, A. Lam, M. Pallen & T. J. Foster, (2003a) Characterization of novel LPXTG-containing proteins of *Staphylococcus aureus* identified from genome sequences. *Microbiology* **149**: 643-654.

Roche, F. M., M. Meehan & T. J. Foster, (2003b) The *Staphylococcus aureus* surface protein SasG and its homologues promote bacterial adherence to human desquamated nasal epithelial cells. *Microbiology* **149**: 2759-2767.

Roghmann, M., K. L. Taylor, A. Gupte, M. Zhan, J. A. Johnson, A. Cross, R. Edelman & A. I. Fattom, (2005) Epidemiology of capsular and

surface polysaccharide in *Staphylococcus aureus* infections complicated by bacteraemia. *J Hosp Infect* **59**: 27-32.

Rooijakkers, S. H., M. Ruyken, A. Roos, M. R. Daha, J. S. Presanis, R. B. Sim, W. J. van Wamel, K. P. van Kessel & J. A. van Strijp, (2005) Immune evasion by a staphylococcal complement inhibitor that acts on C3 convertases. *Nat Immunol* **6**: 920-927.

Rus, H., C. Cudrici & F. Niculescu, (2005) The role of the complement system in innate immunity. *Immunol Res* **33**: 103-112.

Sabat, A., D. C. Melles, G. Martirosian, H. Grundmann, A. van Belkum & W. Hryniewicz, (2006) Distribution of the serine-aspartate repeat protein-encoding sdr genes among nasal-carriage and invasive *Staphylococcus aureus* strains. *J Clin Microbiol* **44**: 1135-1138.

Sakata, N., E. Jakab & T. Wadstrom, (1994) Human plasma fibronectin possesses second binding site(s) to *Staphylococcus aureus* on its C-terminal region. *J Biochem* **115**: 843-848.

Sakharov, D. V., H. R. Lijnen & D. C. Rijken, (1996) Interactions between staphylokinase, plasmin(ogen), and fibrin. Staphylokinase discriminates between free plasminogen and plasminogen bound to partially degraded fibrin. *J Biol Chem* **271**: 27912-27918.

Saravia-Otten, P., H. P. Muller & S. Arvidson, (1997) Transcription of *Staphylococcus aureus* fibronectin binding protein genes is negatively regulated by agr and an agr-independent mechanism. *J Bacteriol* **179**: 5259-5263.

Schroder, A., R. Kland, A. Peschel, C. von Eiff & M. Aepfelbacher, (2006a) Live cell imaging of phagosome maturation in *Staphylococcus aureus* infected human endothelial cells: small colony variants are able to survive in lysosomes. *Med Microbiol Immunol* **195**: 185-194.

Schroder, A., B. Schroder, B. Roppenser, S. Linder, B. Sinha, R. Fassler & M. Aepfelbacher, (2006b) *Staphylococcus aureus* fibronectin

binding protein-A induces motile attachment sites and complex actin remodeling in living endothelial cells. *Mol Biol Cell* **17**: 5198-5210.

Schroeder, K., M. Jularic, S. M. Horsburgh, N. Hirschhausen, C. Neumann, A. Bertling, A. Schulte, S. Foster, B. E. Kehrel, G. Peters & C. Heilmann, (2009) Molecular characterization of a novel *Staphylococcus aureus* surface protein (SasC) involved in cell aggregation and biofilm accumulation. *PLoS One* **4**: e7567.

Schwarz-Linek, U., M. Hook & J. R. Potts, (2006) Fibronectin-binding proteins of gram-positive cocci. *Microbes Infect* **8**: 2291-2298.

Schwarz-Linek, U., J. M. Werner, A. R. Pickford, S. Gurusiddappa, J. H. Kim, E. S. Pilka, J. A. Briggs, T. S. Gough, M. Hook, I. D. Campbell & J. R. Potts, (2003) Pathogenic bacteria attach to human fibronectin through a tandem beta-zipper. *Nature* **423**: 177-181.

Schwarzbauer, J. E., J. W. Tamkun, I. R. Lemischka & R. O. Hynes, (1983) Three different fibronectin mRNAs arise by alternative splicing within the coding region. *Cell* **35**: 421-431.

Shannon, O. & J. I. Flock, (2004) Extracellular fibrinogen binding protein, Efb, from *Staphylococcus aureus* binds to platelets and inhibits platelet aggregation. *Thromb Haemost* **91**: 779-789.

Sherertz, R. J., W. A. Carruth, A. A. Hampton, M. P. Byron & D. D. Solomon, (1993) Efficacy of antibiotic-coated catheters in preventing subcutaneous *Staphylococcus aureus* infection in rabbits. *J Infect Dis* **167**: 98-106.

Siboo, I. R., H. F. Chambers & P. M. Sullam, (2005) Role of SraP, a Serine-Rich Surface Protein of *Staphylococcus aureus*, in binding to human platelets. *Infect Immun* **73**: 2273-2280.

Signas, C., G. Raucci, K. Jonsson, P. E. Lindgren, G. M. Anantharamaiah, M. Hook & M. Lindberg, (1989) Nucleotide sequence of the gene for a fibronectin-binding protein from *Staphylococcus aureus*: use of

this peptide sequence in the synthesis of biologically active peptides. *Proc Natl Acad Sci U S A* **86**: 699-703.

Sinha, B., P. Francois, Y. A. Que, M. Hussain, C. Heilmann, P. Moreillon, D. Lew, K. H. Krause, G. Peters & M. Herrmann, (2000) Heterologously expressed *Staphylococcus aureus* fibronectin-binding proteins are sufficient for invasion of host cells. *Infect Immun* **68**: 6871-6878.

Sinha, B., P. P. Francois, O. Nusse, M. Foti, O. M. Hartford, P. Vaudaux, T. J. Foster, D. P. Lew, M. Herrmann & K. H. Krause, (1999) Fibronectin-binding protein acts as *Staphylococcus aureus* invasin via fibronectin bridging to integrin alpha5beta1. *Cell Microbiol* **1**: 101-117.

Smyth, D. S., E. J. Feil, W. J. Meaney, P. J. Hartigan, T. Tollersrud, J. R. Fitzgerald, M. C. Enright & C. J. Smyth, (2009) Molecular genetic typing reveals further insights into the diversity of animal-associated *Staphylococcus aureus*. *J Med Microbiol* **58**: 1343-1353.

Stranger-Jones, Y. K., T. Bae & O. Schneewind, (2006) Vaccine assembly from surface proteins of *Staphylococcus aureus*. *Proc Natl Acad Sci U S A* **103**: 16942-16947.

Symersky, J., J. M. Patti, M. Carson, K. House-Pompeo, M. Teale, D. Moore, L. Jin, A. Schneider, L. J. DeLucas, M. Hook & S. V. Narayana, (1997) Structure of the collagen-binding domain from a *Staphylococcus aureus* adhesin. *Nat Struct Biol* **4**: 833-838.

Tamura, K., J. Dudley, M. Nei & S. Kumar, (2007) MEGA4: Molecular Evolutionary Genetics Analysis (MEGA) software version 4.0. *Mol Biol Evol* **24**: 1596-1599.

Thakker, M., J. S. Park, V. Carey & J. C. Lee, (1998) *Staphylococcus aureus* serotype 5 capsular polysaccharide is antiphagocytic and enhances bacterial virulence in a murine bacteremia model. *Infect Immun* **66**: 5183-5189.

Ton-That, H., S. K. Mazmanian, K. F. Faull & O. Schneewind, (2000) Anchoring of surface proteins to the cell wall of *Staphylococcus aureus*. Sortase catalyzed in vitro transpeptidation reaction using LPXTG peptide and NH(2)-Gly(3) substrates. *J Biol Chem* **275**: 9876-9881.

Trindade, P. A., J. A. McCulloch, G. A. Oliveira & E. M. Mamizuka, (2003) Molecular techniques for MRSA typing: current issues and perspectives. *Braz J Infect Dis* **7**: 32-43.

Tung, H., B. Guss, U. Hellman, L. Persson, K. Rubin & C. Ryden, (2000) A bone sialoprotein-binding protein from *Staphylococcus aureus*: a member of the staphylococcal Sdr family. *Biochem J* **345 Pt 3**: 611-619.

Upadhyay, A., J. D. Burman, E. A. Clark, E. Leung, D. E. Isenman, J. M. van den Elsen & S. Bagby, (2008) Structure-function analysis of the C3 binding region of *Staphylococcus aureus* immune subversion protein Sbi. *J Biol Chem* **283**: 22113-22120.

Vandenesch, F., J. Kornblum & R. P. Novick, (1991) A temporal signal, independent of agr, is required for hla but not spa transcription in *Staphylococcus aureus*. *J Bacteriol* **173**: 6313-6320.

von Eiff, C., K. Becker, K. Machka, H. Stammer & G. Peters, (2001) Nasal carriage as a source of *Staphylococcus aureus* bacteremia. Study Group. *N Engl J Med* **344**: 11-16.

Vrhovski, B. & A. S. Weiss, (1998) Biochemistry of tropoelastin. *Eur J Biochem* **258**: 1-18.

Vuong, C., J. M. Voyich, E. R. Fischer, K. R. Braughton, A. R. Whitney, F. R. DeLeo & M. Otto, (2004) Polysaccharide intercellular adhesin (PIA) protects *Staphylococcus epidermidis* against major components of the human innate immune system. *Cell Microbiol* **6**: 269-275.

Walev, I., P. Vollmer, M. Palmer, S. Bhakdi & S. Rose-John, (1996) Pore-forming toxins trigger shedding of receptors for interleukin 6 and lipopolysaccharide. *Proc Natl Acad Sci U S A* **93**: 7882-7887.

Walsh, E. J., L. M. O'Brien, X. Liang, M. Hook & T. J. Foster, (2004) Clumping factor B, a fibrinogen-binding MSCRAMM (microbial surface components recognizing adhesive matrix molecules) adhesin of *Staphylococcus aureus*, also binds to the tail region of type I cytokeratin 10. *J Biol Chem* **279**: 50691-50699.

Wann, E. R., S. Gurusiddappa & M. Hook, (2000) The fibronectin-binding MSCRAMM FnbpA of *Staphylococcus aureus* is a bifunctional protein that also binds to fibrinogen. *J Biol Chem* **275**: 13863-13871.

Watanabe, S., T. Ito, T. Sasaki, S. Li, I. Uchiyama, K. Kishii, K. Kikuchi, R. L. Skov & K. Hiramatsu, (2009) Genetic diversity of staphylocoagulase genes (coa): insight into the evolution of variable chromosomal virulence factors in *Staphylococcus aureus*. *PLoS One* **4**: e5714.

Watanabe, S., T. Ito, F. Takeuchi, M. Endo, E. Okuno & K. Hiramatsu, (2005) Structural comparison of ten serotypes of staphylocoagulases in *Staphylococcus aureus*. *J Bacteriol* **187**: 3698-3707.

Wertheim, H. F., M. C. Vos, A. Ott, A. van Belkum, A. Voss, J. A. Kluytmans, P. H. van Keulen, C. M. Vandenbroucke-Grauls, M. H. Meester & H. A. Verbrugh, (2004) Risk and outcome of nosocomial *Staphylococcus aureus* bacteraemia in nasal carriers versus non-carriers. *Lancet* **364**: 703-705.

Wolz, C., P. Pohlmann-Dietze, A. Steinhuber, Y. T. Chien, A. Manna, W. van Wamel & A. Cheung, (2000) Agr-independent regulation of fibronectin-binding protein(s) by the regulatory locus sar in *Staphylococcus aureus*. *Mol Microbiol* **36**: 230-243.

Zhang, S., J. J. Iandolo & G. C. Stewart, (1998) The enterotoxin D plasmid of *Staphylococcus aureus* encodes a second enterotoxin determinant (sej). *FEMS Microbiol Lett* **168**: 227-233.